

This item was submitted to Loughborough University as a PhD thesis by the author and is made available in the Institutional Repository (<https://dspace.lboro.ac.uk/>) under the following Creative Commons Licence conditions.



For the full text of this licence, please go to:  
<http://creativecommons.org/licenses/by-nc-nd/2.5/>

BLLID NO: - D68734/86

LOUGHBOROUGH  
UNIVERSITY OF TECHNOLOGY  
LIBRARY

AUTHOR/FILING TITLE

WILLIAMS, P W

ACCESSION/COPY NO.

010 644/01

VOL. NO.

CLASS MARK

**FOR REFERENCE ONLY**

**FOR REFERENCE ONLY**

001 0644 01



POLYMER BLEND MISCIBILITY

by

P. W. WILLIAMS

Supervisor: Professor R. E. Wetton

A Doctoral Thesis submitted in partial fulfilment of the  
requirements for the award of the degree of  
Doctor of Philosophy  
of Loughborough University of Technology

December 1985

Department of Chemistry

© PETER WYNNE WILLIAMS, 1985.

Loughborough University  
of T.  
May 1986  
010644/01

## ACKNOWLEDGEMENTS

I would like to thank my supervisor, Professor R. E. Wetton, for initiating this work and providing constructive assistance throughout. Thanks are also due to the S.E.R.C. for the provision of a research grant and to Professor F. Wilkinson for the use of the facilities in the Chemistry Department. Finally, I must pay tribute to Mrs. S. Dart for the speed, accuracy and professionalism of her typing of this thesis.

ORIGINALITY

All the work presented in this thesis was undertaken by the author, except where otherwise acknowledged, and has not previously been presented for a degree at any other institution.

ABSTRACT

A number of quasi-binary homopolymer blends have been investigated with regard to their miscibility. The blends consisted of poly(epichlorohydrin) (PEPC) mixed with a range of poly(methacrylate) polymers:- poly(methyl methacrylate); poly(ethoxy ethyl methacrylate); poly(tetrahydrofurfuryl methacrylate) and poly(glycidyl methacrylate) (PGMA). It was found that the state of mixing of the systems varied with the structure of the ester side chain, embracing a number of miscibility states. It has been postulated that the observed miscibility in the system PGMA/PEPC is due to the presence of a small specific interaction between the species.

A second category of blend investigated comprised of a homopolymer (PEPC) and a random copolymer. In two cases the copolymers (styrene-co-methacrylonitrile; methyl methacrylate-co-methacrylonitrile) were chosen such that the cohesive energy density of PEPC lay between those of the comonomers. This led to the observation of a number of miscibility states for the systems, depending upon the copolymer composition. Analysis of these systems and similar examples in the literature was conducted using the mean-field approach. A reasonable accord between theory and experiment was found when the role of both specific interactions and free-volume terms was negligible.

A third type of copolymer (glycidyl methacrylate-co-methyl methacrylate) was found to be only partially miscible with PEPC. This was due to the small GMA/PEPC interaction and the tendency of the copolymer to diverge from the copolymerisation equation at high GMA concentrations.

The experimental probe for miscibility has been the glass transition temperature. This was determined using Differential Thermal Analysis, Dynamic Mechanical Thermal Analysis and to a lesser extent, Dielectric Relaxation.

The phenomenon of partial miscibility, in which phase composition varies with overall blend composition, has been discussed. It has been postulated that this widely observed behaviour is due to a non-equilibrium phase separation process. The inadequacy of existing relationships in describing the variation of the glass transition temperature of a miscible blend with composition has been highlighted. Furthermore, the importance of the transition width as an indicator of miscibility has been stressed.



v

C O N T E N T S

	<u>PAGE</u>
ACKNOWLEDGEMENTS ... ..	i
ORIGINALITY ... ..	ii
ABSTRACT ... ..	iii
CONTENTS ... ..	v

CHAPTER 1 - INTRODUCTION

1.1 WHY BLEND POLYMERS? ... ..	1
1.2 DEFINITIONS OF MISCIBILITY ... ..	2
1.3 THERMODYNAMICS OF POLYMER BLENDS ... ..	4
1.4 IMMISCIBLE AND PARTIALLY MISCIBLE POLYMER MIXTURES ... ..	7
1.5 SUMMARY OF THE WORK UNDERTAKEN IN THIS STUDY	8

CHAPTER 2 - THEORY AND SELECTIVE REVIEW OF THE LITERATURE  
ON POLYMER BLENDS

2.1 FLORY-HUGGINS THEORY OF POLYMER/POLYMER THERMODYNAMICS ... ..	10
2.1.1 The Entropy of Mixing ... ..	11
2.1.2 The Enthalpy of Mixing ... ..	15
2.1.3 Free Energy of Mixing ... ..	16

	<u>PAGE</u>
2.1.4	Chemical Potential ... .. 17
2.1.5	Simplifications Inherent in the Lattice Theory ... .. 18
2.1.6	Modifications of the Lattice Theory ... 19
2.1.7	Phase Equilibrium in Binary Polymer Blends... .. 20
2.1.8	Multicomponent Polymer Mixtures .. ... 24
2.1.9	Lattice Theory and Lower Critical Miscibility ... .. 26
2.2	EQUATION OF STATE THEORIES ... .. 27
2.2.1	The Partition Function and Characteristic Parameters ... .. 27
2.2.2	The Free Energy of Mixing ... .. 31
2.2.3	Phase Boundaries... .. 32
2.2.4	Implications of Equation of State Theory for Polymer-Polymer Miscibility .. ... 32
2.2.5	Comparison of Calculated and Measured Phase Boundaries Using Flory's Equation of State Theory ... .. 34
2.3	THERMODYNAMIC THEORIES OF THE MISCIBILITY BEHAVIOUR OF RANDOM COPOLYMER MIXTURES ... .. 38
2.3.1	Copolymer/Homopolymer Systems ... .. 39
2.3.2	Phase-Separation .. ... 41
2.4	MISCIBILITY PREDICTION USING SOLUBILITY PARAMETERS 42

	<u>PAGE</u>
2.5 THE GLASS TRANSITION TEMPERATURE ... ..	46
2.5.1 Definition of the Glass Transition Temperature .. ... ..	46
2.5.2 Kinetic Theories .. ... ..	48
2.5.3 Thermodynamic Theories.. ... ..	52
2.5.4 Factors Which Influence the Glass Transition Temperature.. ... ..	54
2.6 DIELECTRIC RELAXATION ... ..	63
2.6.1 Polarization.. ... ..	63
2.6.2 Dielectric Dispersion .. ... ..	64
2.6.3 Influence of Temperature on Dielectric Relaxation ... ..	67
2.6.4 Dielectric Relaxation Process ... ..	68
2.6.5 Maxwell-Wagner-Sillars Interfacial Polarization.. ... ..	69
2.6.6 Dielectric Relaxation in Polymer Mixtures	69
2.7 MECHANICAL PROPERTIES OF POLYMERS ... ..	72
2.7.1 Dynamic Mechanical Analysis.. ... ..	72
2.7.2 Factors Which Influence Dynamic Mechanical Behaviour ... ..	75
2.8 COPOLYMERISATION ... ..	78
2.8.1 Composition of Random Copolymers.. ... ..	78
2.8.2 Determination of Sequence Length Distribution in Random Copolymers ... ..	81

CHAPTER 3 - EXPERIMENTAL DETAILS

3.1	PREPARATION OF HOMOPOLYMERS AND COPOLYMERS ...	84
3.1.1	Solution Polymerisation ... ..	84
3.1.2	Bulk Polymerisation ... ..	84
3.2	PURIFICATION OF HOMOPOLYMERS AND COPOLYMERS ..	86
3.2.1	Fractionation of Poly(Glycidyl Methacrylate) ... ..	86
3.3	CHARACTERISATION OF HOMOPOLYMERS AND COPOLYMERS	89
3.3.1	Gel Permeation Chromatography ... ..	89
3.3.2	Nuclear Magnetic Resonance ... ..	90
3.3.3	Elemental Analysis ... ..	91
3.4	PREPARATION OF POLYMER BLENDS ... ..	91
3.5	TECHNIQUES USED TO DETERMINE MISCIBILITY ...	92
3.5.1	Optical Microscopy ... ..	92
3.5.2	Differential Thermal Analysis ... ..	93
3.5.3	Dynamic Mechanical Thermal Analysis ..	94
3.5.4	Dielectric Relaxation.. ... ..	96

CHAPTER 4 - RESULTS FOR HOMOPOLYMER/HOMOPOLYMER BLENDS

4.1	POLY(METHYL METHACRYLATE) (PMMA)/POLY (EPICHLOROHYDRIN) (PEPC) ... ..	98
-----	---	----

	<u>PAGE</u>
4.1.1	Characterisation of Polymers ... .. 98
4.1.2	Optical Properties ... .. 98
4.1.3	Thermal Analysis Data ... .. 98
4.1.4	Dynamic Mechanical Data ... .. 98
4.2	POLY(ETHOXY ETHYL METHACRYLATE) (PEEMA)/ POLY(EPOCHLOROXYDRIN) ... .. 100
4.2.1	Characterisation of PEEMA .. ... 100
4.2.2	Optical Properties of PEEMA/PEPC ... 100
4.2.3	Thermal Analysis ... .. 100
4.2.4	Dynamic Mechanical Behaviour of PEEMA/PEPC .. ... 101
4.3	POLY(TETRAHYDROFURFURYL METHACRYLATE)/POLY (EPOCHLOROXYDRIN) ... .. 102
4.3.1	Characterisation of PTHFMA ... .. 102
4.3.2	Optical Properties of PTHFMA/PEPC ... 102
4.3.3	Thermal Analysis of Blends ... .. 102
4.3.4	Dynamic Mechanical Behaviour of PTHFMA/PEPC ... .. 103
4.4	POLY(GLYCIDYL METHACRYLATE) (PGMA)/POLY (EPOCHLOROXYDRIN) ... .. 103
4.4.1	Characterisation and Fractionation of PGMA ... .. 103
4.4.2	Optical Properties ... .. 105
4.4.3	Thermal Analysis Data ... .. 105
4.4.4	Dynamic Mechanical Results ... .. 105

CHAPTER 5 - RESULTS FOR RANDOM COPOLYMER/HOMOPOLYMERBLENDS

5.1	GLYCIDYL METHACRYLATE-CO-METHYL METHACRYLATE/ POLY(EPICHLOORHYDRIN) BLENDS ... ..	108
5.1.1	Characterisation of Copolymers ... ..	108
5.1.2	Optical Properties of GMA-co-MMA/PEPC Blends ... ..	110
5.1.3	Thermal Analysis of GMA-co-MMA/PEPC Blends ... ..	110
5.1.4	Dynamic Mechanical Results ... ..	112
5.2	STYRENE-CO-METHACRYLONITRILE/POLY(EPICHLOORHYDRIN) BLENDS .. ..	113
5.2.1	Characterisation of Copolymers ... ..	113
5.2.2	Optical Properties of Blends .. ..	115
5.2.3	Thermal Analysis Data ... ..	115
5.2.4	Dynamic Mechanical Results ... ..	118
5.2.5	Dielectric Measurements on Selected SM/PEPC Blends ... ..	119
5.3	METHYL METHACRYLATE-CO-METHACRYLONITRILE/POLY (EPICHLOORHYDRIN) BLENDS ... ..	120
5.3.1	Characterisation of Copolymers ... ..	120
5.3.2	Optical Properties of Blends .. ..	122
5.3.3	Thermal Analysis Data ... ..	122
5.3.4	Dynamic Mechanical Results ... ..	124
5.3.5	Dielectric Measurements on Selected MA/PEPC Blends.. ... ..	124

	<u>PAGE</u>
<b>CHAPTER 6 - <u>DISCUSSION OF HOMOPOLYMER/HOMOPOLYMER BLENDS</u></b>	
6.1 THE INFLUENCE OF SOLVENT ON THE MISCIBILITY OF BLENDS CAST FROM SOLUTION ... ..	126
6.2 POLY(METHYL METHACRYLATE)/POLY (EPICHLOROHYDRIN) BLENDS ... ..	127
6.3 POLY(ETHOXY ETHYL METHACRYLATE)/POLY (EPICHLOROHYDRIN) BLENDS ... ..	129
6.4 POLY(TETRAHYDROFURFURYL METHACRYLATE)/ POLY(EPICHLOROHYDRIN) BLENDS ... ..	132
6.5 POLY(GLYCIDYL METHACRYLATE)/POLY (EPICHLOROHYDRIN) BLENDS ... ..	138
6.6 SUMMARY ... ..	144
 <b>CHAPTER 7 - <u>DISCUSSION OF HOMOPOLYMER/COPOLYMER BLENDS</u></b>	
7.1 COPOLYMER PREPARATION ... ..	150
7.2 GLYCIDYL METHACRYLATE-CO-METHYL METHACRYLATE/ POLY(EPICHLOROHYDRIN) BLENDS ... ..	153
7.3 STYRENE-CO-METHACRYLONITRILE/POLY (EPICHLOROHYDRIN) BLENDS ... ..	163
7.4 METHYL METHACRYLATE-CO-METHACRYLONITRILE/ POLY(EPICHLOROHYDRIN) BLENDS ... ..	173
7.5 GENERAL ASPECTS OF THE BEHAVIOUR OF COPOLYMER/ HOMOPOLYMER BLENDS ... ..	180
7.6 SUMMARY ... ..	185

LIST OF TABLES

	<u>PAGE</u>
3.1	Solution Polymerisations ... .. 85
3.2	Bulk Polymerisation ... .. 87
3.3	Repeat Unit Structures of Homopolymers Used ... 88
4.1	G.P.C. Results for PEPC and PMMA ... .. 99
4.2	G.P.C. Results for PGMA and Its Fractions.. ... 104
5.1	Details of Composition and Molecular Weight for GMA-co-MMA Random Copolymers ... .. 109
5.2	Details of Sequence Length Distribution in GMA-co-MMA Copolymers ... .. 111
5.3	Details of SM Copolymer Compositions and Molecular Weights ... .. 114
5.4	Sequence Length Distribution of SM Copolymers .. 116
5.5	Sequence Length Distribution of SM Copolymers .. 117
5.6	Molecular Weights and Compositions of MA Copolymers .. .. 121
5.7	Sequence Length Distribution of MA Copolymers... 123
6.1	Homopolymer Solubility Parameters ... .. 145
6.2	Dipole Moments of Molecules Corresponding to Homopolymer Repeat Units or Parts Thereof ... 146



	<u>PAGE</u>
7.1 Reactivity Ratios for Methacrylonitrile Copolymers ... ..	152
7.2 Examples of Systems in Which the Homopolymer Interacts Favourably with One Copolymer Segment Type ... ..	160
7.3 Calculated Degree of Polymerisation Tolerable for Miscibility in Measured 2 Phase Systems ... ..	164
7.4 Random Copolymers of Various Halogenated Styrenes Whose Blends with PPO Have Been Reported ... ..	174

CHAPTER 1

INTRODUCTION

## 1.1 WHY BLEND POLYMERS?

A polymer blend is quite simply a mixture of two or more polymeric components which are not chemically bonded to each other. There are two main reasons for blending polymers together. The first is property modification of a given polymer to extend its range of application or to tailor its properties to fit a specific requirement. Indeed, depending upon the level of mixing of the components in a binary mixture, the blend can have properties which suit it to areas of application beyond consideration of either individual constituent. A well known example is that of poly(vinyl chloride) (PVC) which forms a miscible blend in all proportions with copolymers of butadiene and acrylonitrile<sup>(1,2)</sup> (NBR). The addition of nitrile rubber to PVC results in a permanently plasticized PVC. The advantages of NBR over conventional low molecular weight plasticizers are its permanence, superior solvent resistance and resistance to biological degradation. At the other end of the composition scale the addition of plasticized PVC to nitrile rubber, followed by vulcanization, results in improved ozone and sunlight resistance, flex cracking and chemical resistance. There is however a decrease in tensile strength and abrasion resistance. It is apparent that a balance needs to be struck between these property gains and losses by adjusting composition to fit the particular requirement.

The second reason for blending is to reduce costs. This is best illustrated by the miscible blend of poly(2,6-dimethyl-1,4-phenylene oxide) (PPO) with poly(styrene) which is marketed under the trade name of Noryl<sup>(3)</sup>. PPO has a high glass transition temperature (210°C)

and consequently has attracted attention because of superior heat distortion characteristics. Heat distortion temperatures are generally 10-15° below the glass transition temperature. However, because of the high monomer cost and difficult polymerisation procedure its price is prohibitive for many applications. Blending with the much cheaper poly(styrene) ( $T_g = 100^\circ\text{C}$ ) allows the production of a range of products which link price and performance. It is also significantly cheaper to produce a new material by mixing existing polymers than it is to develop new monomers possibly requiring new polymerisation processes.

In practice the two reasons given for blending are not treated independently, each being an intrinsic element in the development strategy for new materials. The mixing of polymers can be seen as an extension of the well established procedures for the modification of polymers. These include the addition of low molecular weight materials as plasticizers, anti-oxidants and processing aids; the incorporation of fillers such as carbon black, mica and glass fibre; and copolymerisation to form random copolymers. A recent review of miscible blend applications has been presented by Robeson<sup>(32)</sup>.

## 1.2 DEFINITIONS OF MISCIBILITY

In the above section the commercial examples of polymer blends were termed miscible. The question which arises is what level of homogeneity does this term imply? In the vast majority of cases cited in the literature miscibility is defined in terms of the behaviour of a macroscopic property, usually the glass transition temperature. The appearance of a single sharp glass transition temperature at a position intermediate between those of the pure components is usually taken to imply miscibility. At the other

extreme a blend exhibiting essentially the glass transition behaviour of the unmixed components is defined as being immiscible. In particular cases behaviour is often observed which lies somewhere between these two extremes. This can be manifested for example by the appearance of two glass transitions lying not at the pure component positions, or by a single very broad transition. Intermediate behaviour such as this is said to characterise partially miscible blends.

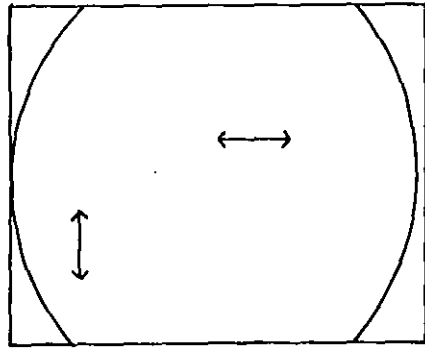
The level of homogeneity implied by the observation of a single, sharp glass transition temperature leads us to the question of what size does a domain have to be to exhibit a glass transition? A domain size is the average length in which only one component exists. Kaplan<sup>(4)</sup> has introduced the notion of a miscibility number  $N$ , such that in general

$$N = \frac{\text{Experimental probe size}}{\text{Domain size}} \quad (1.1)$$

In the present example where miscibility is defined in terms of glass transition behaviour the experimental probe size is the segmental length associated with the  $T_g$  relaxation process. When  $N$  tends towards infinity one has a miscible system, a value of about one indicates partial miscibility and a value of zero indicates immiscibility. Using dynamic mechanical data to study  $T_g$  and electron microscopy to measure phase size the data of Sperling *et al.*<sup>(5)</sup> and Matsuo *et al.*<sup>(6)</sup> seems to indicate that the segmental length associated with the glass transition is of the order of  $150 \text{ \AA}$ <sup>(4)</sup>. Obviously using a technique with a smaller experimental probe size will lead to a more rigorous definition of miscibility, whilst the converse is equally true. The situation is illustrated in Figure (1.1).

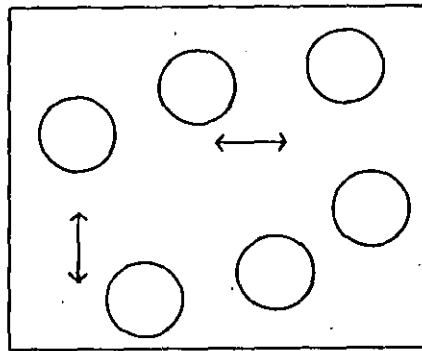
A widely used but more coarse criterion than a single sharp

Figure(1.1)  
Variation of Miscibility Number with Domain Size



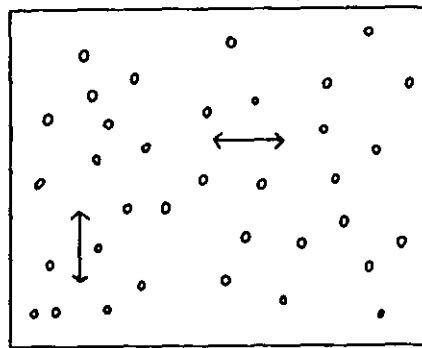
Immiscible

$$N \rightarrow 0$$



Partially Miscible

$$N \rightarrow 1$$



Miscible

$$N \rightarrow \infty$$

$\longleftrightarrow$  Probe Size

glass transition temperature is that of optical clarity. Miscible amorphous polymer mixtures are transparent whilst immiscible blends are usually translucent or opaque. The probe size in this technique is the wavelength of visible light. Rosen<sup>(7)</sup> has suggested that domains smaller than about  $1,000 \text{ \AA}$  will not influence optical clarity. Erroneous conclusions about blend miscibility can also be reached if the refractive indices of the two components are similar. Bohn<sup>(8)</sup> has indicated that for transparency a difference of no more than 0.01 can be tolerated. Optical clarity is a necessary but not sufficient criterion for blend miscibility of amorphous constituents, and so any inferences drawn from such observations must be verified by another technique.

This brief discussion highlights the difficulties in assigning absolute definitions of miscibility to polymer blends, which results from the long chain nature of macromolecules. The definition of miscibility for low molecular weight liquids of intimate mixing on the molecular level is neither appropriate nor attainable.

In the literature the term miscibility is often used interchangeably with the word compatibility to indicate single phase behaviour. However, confusion has arisen due to the assignment of compatibility to multi-phase blends<sup>(9)</sup>, particularly in the context of materials science. Here it indicates good adhesion between phases or ease of blending. Consequently miscibility is the preferred term in this work.

### 1.3 THERMODYNAMICS OF POLYMER BLENDS

Thermodynamics provides the most effective tool to study the factors which determine the state of mixing of a polymer blend. The use of thermodynamics pre-supposes that the mixture is at

equilibrium, a state which is difficult to define with any precision in polymeric materials. Olabisi *et al.*<sup>(10)</sup> have advanced the usage of the established criteria of reproducibility, uniformity and stability dependent only upon thermodynamic variables to define a true equilibrium phase. However as with the definition of miscibility, the establishment of these criteria depends upon the method of examination. Nevertheless a great deal of attention needs to be paid to the method of blend preparation used and the thermal history of the blend to ensure that equilibrium is approached. The non-equilibrium characteristics of the glassy state mean that thermodynamic discussions are limited to temperatures above  $T_g$ .

It is often stated that the requirement for miscibility is a negative Gibbs free energy of mixing. This is however a necessary but not sufficient criterion. As pointed out by Koningsveld<sup>(11)</sup>, it is the shape of the free energy of mixing as a function of composition which determines the state of mixing. Mixtures with a negative free energy of mixing can be unstable relative to some intermediate composition. This will lead to phase separation (partial miscibility) in order to reduce the value of the free energy still further.

The relation between the free energy, enthalpy and entropy of mixing is given by

$$\Delta G_m = \Delta H_m - T\Delta S_m \quad (1.2)$$

where as a first approximation  $\Delta S_m$  is taken to represent only combinatorial terms. The reason why the number of immiscible blends far outweighs the number of miscible blends can readily be understood by examination of the entropy of mixing term.  $\Delta S_m$  decreases rapidly as the degree of polymerisation of the components rises. This reflects



the declining number of excess conformations available in the mixture compared with the pure component states as chain length rises. In high polymers ( $\bar{M}_w \gg 10^5$ )  $\Delta S_m$  becomes negligible and the enthalpy of mixing term becomes the determinant of miscibility. It is for this reason that miscibility in many blend pairs has been identified as resulting from a negative enthalpy of mixing. This has been attributed in many cases to the presence of a specific interaction such as hydrogen bonding between the two component repeat units. Evidence has been presented for this case using techniques such as fourier transform infra-red<sup>(12)</sup>, analogue calorimetry<sup>(13)</sup> and inverse gas chromatography<sup>(14)</sup>.

Miscibility has so far been presented as a 'Yes' or 'No' situation for a particular mixture. However it would be more accurate to define miscibility over particular temperature ranges. This is because many polymer mixtures exhibit phase separation behaviour. In small molecules, oligomeric and polymer/solvent mixtures phase separation, when it occurs, is as a result of decreasing the temperature of the mixture. In polymer mixtures it has been observed that the reverse is the normal mode of the phase separation behaviour. That is a mixture can pass from the homogeneous to the heterogeneous state on raising temperature.

The Flory-Huggins<sup>(16-20)</sup> expression for the free energy of mixing of polymer-solvent systems has been extended to embrace polymer-polymer mixtures. However the theory cannot predict the observed phase separation behaviour. The Flory<sup>(21-24)</sup> equation of state theory remedies this deficiency, but, without fitting the expressions to measured phase boundaries using a number of empirical correction parameters, can only describe behaviour semi-qualitatively. The Flory approach however does indicate that whilst specific interactions are usually

the driving force for miscibility, the difference between the equation of state parameters of the components can have an influence.

Measurement of phase boundaries in polymer blends<sup>(25,26)</sup> has indicated that their shape and position in the temperature plane is quite sensitive to changes in molecular weight and polydispersity.

#### 1.4 IMMISCIBLE AND PARTIALLY MISCIBLE POLYMER MIXTURES

Whilst miscible polymer blends have aroused much academic interest, the vast majority of multicomponent polymer systems available commercially are two-phase. In addition to simple mixtures, graft and block copolymers and interpenetrating networks can be included in this category.

One of the most common areas in which incorporation of a second material to form a virtually discrete phase is used is in the area of impact modification. For example, poly(styrene) can be modified by the addition of poly(butadiene), however it has been found that simply melt mixing the two polymers does not lead to substantial impact improvement. This has been solved by the development of an *in situ* polymerisation technique<sup>(27,28)</sup> resulting in a disperse, lightly cross-linked rubber phase of optimum size grafted on to a polystyrene matrix. Similar impact modification has been achieved with poly(vinyl chloride)<sup>(29)</sup>, poly(methyl methacrylate), and styrene-acrylonitrile copolymers.

A large number of poly(olefin) blends<sup>(30)</sup> have been described, such as poly(isobutylene) with high or low density poly(ethylene), where addition of the first component improves such properties as impact strength, flexibility and filler acceptance. There are at least an equal number of examples where immiscible blends of elastomers<sup>(31)</sup> have provided significant property and/or cost advantages.

The utility of multi-phase materials depends on the interfacial

adhesion. The degree of adhesion in simple mixtures will depend on the level of miscibility such that completely immiscible blends have no adhesion. This problem can be overcome by grafting the disperse phase onto the matrix phase or by using compatibilizing agents. The latter are usually diblock copolymers where one block has a preference for the matrix phase whilst the other tends towards the disperse phase. Consequently the copolymers tend to be situated in the interfacial region and improve adhesion. Diblock and triblock copolymers have also been used in their own right as thermoplastic elastomers, containing a soft block (matrix phase) and a hard block (disperse phase). General reviews of multiphase polymer systems have been given by Battaerd<sup>(33)</sup> and Eastmond<sup>(34)</sup>.

#### 1.5 SUMMARY OF THE WORK UNDERTAKEN IN THIS STUDY

The research has concentrated upon the investigation of new polymer blends of various types. Homopolymer/homopolymer blends comprising of poly(epichlorohydrin) and one of a range of methacrylate homopolymers were examined in the first instance. The availability of a wide range of methacrylate monomers allowed the investigation of the influence of molecular structure on the interaction of this component with poly(epichlorohydrin) as determined by the miscibility behaviour exhibited. Having identified a miscible blend a range of copolymers were prepared consisting of one segment which was miscible with poly(epichlorohydrin) and another segment which was immiscible. Miscibility of these copolymers with the same elastomer was then monitored as a function of copolymer composition.

The major determinant of blend homogeneity in the above systems was whether a specific interaction of sufficient strength existed between the dissimilar segments. The final category of blends consisted

of a random copolymer mixed with a homopolymer. However, in this instance the components were selected such that the three different segmental interactions present were all unfavourable. Nevertheless as a result of the negative contribution of the segmental interaction between the unlike copolymer segments to the overall blend interaction, it was found that immiscibility need not result. Careful selection of the components led to a variety of miscibility states within the same system as copolymer composition was varied.

CHAPTER 2

THEORY AND SELECTIVE REVIEW OF THE LITERATURE  
ON POLYMER BLENDS

## 2.1 FLORY-HUGGINS THEORY OF POLYMER/POLYMER THERMODYNAMICS

The inherent state of mixing of a polymer blend whether miscible, partially miscible or immiscible is determined by the thermodynamics of interaction between the blend components. Specifically the state of mixing depends upon the shape and sign of the free energy of mixing vs. composition function. Phase rule theory states that at equilibrium the free energy is minimal, thus a system will behave in a manner that best satisfies this condition. The purpose of the theories proposed to describe polymer blend thermodynamics has been to allow the prediction of the state of mixing of a blend given some knowledge of the properties of the pure components. Consequently the applicability of a theory can be judged by comparison with experimental data.

The theory developed to describe the thermodynamics of polymer blends<sup>(35,36)</sup> is an extension of the theory relating to polymer/solvent systems. The most obvious feature of a polymer/solvent system (compared with a mixture of small molecules) is the disparity in size between the two components. Using his equation of state van der Waal's<sup>(37)</sup> gave a qualitative description of the partial miscibility of such solutions and noted that appreciable differences between the molecular sizes of the constituents would cause the co-existence curve to shift towards the axis representing the solvent. The major breakthrough in putting phase-rule theory on a quantitative basis was made simultaneously and independently by Flory<sup>(16-18)</sup> and Huggins<sup>(19,20)</sup> who invoked a lattice model to calculate the free energy of mixing for polymer/solvent systems. It is intended here to provide an outline

of the theory as it applies to a two-component polymer blend where both species are monodisperse. The resulting expressions are then extended to account for polydispersity.

### 2.1.1 The Entropy of Mixing

The blend is taken to consist of two polymers, 1 and 2, each chain of which is made up of a number of segments  $x_1$  and  $x_2$ . The segment size is the same for each component and thus  $x_1$  and  $x_2$  can be defined as the ratio of the molar volumes ( $\tilde{V}_i$ ) of the two polymers to a reference volume  $V_r$  ( $x_1 = \tilde{V}_1/V_r$ ;  $x_2 = \tilde{V}_2/V_r$ ).

We require an expression from which we can compute the number of ways in which the polymers can be arranged in a lattice consisting of  $n_0$  cells, each cell having the same volume as a segment.  $n_0$  is consequently equal to the total number of segments,

$$n_0 = n_1 x_1 + n_2 x_2 \quad (2.1)$$

where  $n_1$  and  $n_2$  refer to the number of chains of polymer 1 and 2 respectively. Consider placing  $n_2 x_2$  segments of polymer 2 in the lattice given that  $i_2$  molecules of polymer 2 have previously been placed randomly. There remains a total of  $n_0 - i_2 x_2$  vacant cells in which to place the first segment of the  $(i_2 + 1)^{\text{th}}$  molecule. If  $Z$  (the lattice co-ordination number) represents the number of cells immediately adjacent to a given cell there will be  $Z$  sites in which to place the second segment assuming that all the sites are vacant. The probability of vacancy is  $(1 - f_{i_2})$  where  $f_{i_2}$  is the probability that a site adjacent to one in which a segment has been placed is occupied. Consequently the number of cells available for the second segment is  $Z(1 - f_{i_2})$ . For each successive segment

the expected number of vacant cells will be  $(Z - 1)(1 - f_{i_2})$ . Assuming that segments occupy cells sequentially along the chain, the expected number of continuous cells available to the molecule is,

$$v_{i_2 + 1} = \frac{1}{2}(n_0 - i_2 x_2) Z(Z - 1)^{x_2 - 2} (1 - f_{i_2})^{x_2 - 1} \quad (2.2)$$

The number of ways  $\Omega_2$  in which  $n_2$  sets of  $x_2$  consecutively adjacent cells may be chosen is given by,

$$\frac{1}{n_2!} \prod_{i_2 = 1}^{n_2} v_{i_2} = \Omega_2 \quad (2.3)$$

The factor of  $1/n_2!$  is introduced to eliminate those cases where the sets of cells chosen for occupation are identical but are filled in a different order, whilst the factor of  $\frac{1}{2}$  enters equation (2.2) as the chain ends are indistinguishable. The probability  $f_i$  is not exactly equal to the average probability of occupation of a cell selected at random ( $\bar{f}_{i_2}$ ) as  $f_{i_2}$  assumes the vacancy of an adjoining cell. However  $f_{i_2}$  will approach  $\bar{f}_{i_2}$  for sufficiently larger values of  $Z$ , so one may write

$$(1 - \bar{f}_{i_2}) = (1 - f_{i_2}) = (n_0 - x_2 i_2)/n_0 \quad (2.4)$$

Substituting for  $(1 - f_{i_2})$  into eqn. (2.2) and replacing the  $Z$  term by  $(Z - 1)$  one obtains

$$v_{i_2 + 1} = \frac{1}{2}(n_0 - x_2 i_2)^{x_2} [(Z - 1)/n_0]^{x_2 - 1} \quad (2.5)$$



Substitution of eqn. (2.5) into eqn. (2.3) gives the total number of ways in which  $n_2$  identical polymer molecules can be arranged in a lattice of  $n_0$  cells

$$\Omega_2 = \frac{1}{n_2!} \prod_{i_2=0}^{n_2-1} \frac{1}{2} (n_0 - x_2 i_2)^{x_2} [(Z-1)/n_0]^{x_2-1} \quad (2.6)$$

It is now necessary to calculate the number of ways in which the segments of polymer 1 can be introduced into the remaining vacant sites. The probability of a vacant cell is given by

$$1 - \bar{g}_{i_1} \approx 1 - g_{i_1} = (n_0 - (x_2 n_2 + i_1 x_1))/n_0 \quad (2.7)$$

the reasoning behind this expression being analogous to that used to derive eqn. (2.4). Using eqn. (2.7) one obtains expressions for  $v_{i_1+1}$  and  $\Omega_1$  viz

$$v_{i_1+1} = \frac{1}{2} (n_0 - (x_2 n_2 + i_1 x_1))^{x_1} [(Z-1)/n_0]^{x_1-1} \quad (2.8)$$

$$\Omega_1 = \frac{1}{n_1!} \prod_{i_1=0}^{n_1-1} \frac{1}{2} (n_0 - (x_2 n_2 + i_1 x_1))^{x_1} [(Z-1)/n_0]^{x_1-1} \quad (2.9)$$

The configurational entropy of mixing pure, perfectly ordered polymer 1 with pure, perfectly ordered polymer 2 is given by the Boltzmann relation

$$S_c = k \ln \Omega_1 \Omega_2 \quad (2.10)$$

where  $k$  is the Boltzmann constant

Substituting for  $\Omega_1$  and  $\Omega_2$  from eqns. (2.6) and (2.9) and application of Stirlings approximation for a logarithmic factorial ( $\ln n! = n \ln n - n$ ) one obtains

$$\frac{S_c}{k} = -n_1 \ln n_1 - n_2 \ln n_2 + (n_1 + n_2) + n_2(x_2 - 1) \ln[(Z - 1)/n_0] + n_1(x_1 - 1) \ln[(Z - 1)/n_0] + n_1 \ln n_0 + n_2 \ln n_0 - n_1 x_1 - n_2 x_2 \quad (2.11)$$

The entropy of polymer 1 ( $S_1$ ) in a lattice of  $n_1 x_1$  cells can be determined by replacing  $n_0$  by  $n_1 x_1 + n_2 x_2$  in eqn. (2.11) and setting  $n_2$  equal to zero. The entropy of polymer 2 ( $S_2$ ) can be calculated similarly. The combinatorial entropy of mixing polymers 1 and 2 is defined as

$$\frac{\Delta S_m}{k} = \frac{1}{k} [S_c - (S_1 + S_2)] \quad (2.12)$$

Substitution for  $S_c$ ,  $S_1$  and  $S_2$  yields

$$-\frac{\Delta S_m}{k} = n_1 \ln(n_1 x_1 / n_0) + n_2 \ln(n_2 x_2 / n_0) \quad (2.13)$$

The volume fractions of polymers 1 and 2 in the mixture are defined as

$$n_1 x_1 / n_0 = \phi_1 \quad n_2 x_2 / n_0 = \phi_2 \quad (2.14)$$

Substitution for volume fractions into equation (2.13) and division

by Avogadro's number results in the familiar expression

$$-\frac{\Delta S_m}{k} = (m_1 \ln \phi_1 + m_2 \ln \phi_2) \quad (2.15)$$

where  $m_i$  refers to the number of moles of species  $i$ . Eqn. (2.15) is similar to the expression derived by Flory for a polymer solvent system except that a lattice cell is defined differently and in a solvent system  $x_1$  is usually taken to be unity.

### 2.1.2 The Enthalpy of Mixing

The enthalpy of mixing is derived in a manner identical to that used for solutions of small molecules. The energy change involved in replacing like segments, in adjacent sites to a reference segment, by unlike segments is calculated. The energy of interaction between like segments is denoted by  $\epsilon_{11}$  and  $\epsilon_{22}$  for polymers 1 and 2 respectively whilst the interaction between unlike segments is represented by  $\epsilon_{12}$ . Each segment of polymer 1 is surrounded by  $(Z - 2)$  segments of different chains, except for end segments which have  $(Z - 1)$  neighbours. The total number of contacts per molecule of polymer 1 is thus  $(Z - 2)x + 2$  which approximates to  $Zx$  for large  $Z$ . In the mixture there are on average  $(Zn_1x_1/n_0)$  segments of polymer 1 and  $(Zn_2x_2/n_0)$  segments of polymer 2 surrounding each segment of polymer 1 in the mixture. The energy change for the formation of an unlike pair is

$$\Delta\epsilon_{12} = \epsilon_{12} - \frac{1}{2}(\epsilon_{11} + \epsilon_{22}) \quad (2.16)$$

The enthalpy of mixing  $\Delta H_m$  is the difference between the total enthalpy of the mixture and the combined enthalpy of the pure components prior to mixing. It can also be thought of in terms of equation (2.16) as

$$\Delta H_m = \Delta \epsilon_{12} p_{12} \quad (2.17)$$

where  $p_{12}$  is the average number of contacts between unlike segments at a particular composition.  $p_{12}$  is given by the product of the total number of contacts of molecules of polymer 1 and the concentration of polymer 2 (in terms of the volume fraction)

$$p_{12} = Z x_1 n_1 \phi_2 \quad (2.18)$$

$$\frac{\Delta H_m}{N_A} = Z m_1 x_1 \phi_2 \Delta \epsilon_{12} \quad (2.19)$$

Equation (2.19) is the well known Van Laar expression for the heat of mixing in any two component system. It is usually written in terms of the interaction parameter ( $\chi$ ) which is defined as the interaction energy between a segment of polymer 1 and a segment of polymer 2, divided by  $kT$ .

$$\frac{\Delta H_m}{N_A} = kT \chi m_1 x_1 \phi_2 \quad (2.20)$$

or 
$$\frac{\Delta H_m}{RT} = \chi m_1 x_1 \phi_2 \quad (2.21)$$

where 
$$\chi = Z \Delta \epsilon_{12} / kT \quad (2.22)$$

### 2.1.3 Free Energy of Mixing

The Gibbs free energy of mixing is defined by the familiar expression

$$\Delta G_m = \Delta H_m - T \Delta S_m \quad (2.23)$$

Substituting for  $\Delta H_m$  and  $\Delta S_m$  from equations (2.15) and (2.20) one obtains for the free energy of mixing two monodisperse polymers,

$$\Delta G_m = RT(m_1 \ln \phi_1 + m_2 \ln \phi_2 + \chi m_1 x_1 \phi_2) \quad (2.24)$$

If the two polymers are polydisperse equation (2.24) can be generalised to

$$\frac{\Delta G_\phi}{RT} = \sum_i \phi_{1,i} x_{1,i}^{-1} \ln \phi_{1,i} + \sum_j \phi_{2,j} x_{2,j}^{-1} \ln \phi_{2,j} + \sum_i \phi_{1,i} \sum_j \phi_{2,j} \chi \quad (2.25)$$

where  $\Delta G_\phi$  is the free energy of mixing polymers 1 and 2 per mole of lattice sites.

#### 2.1.4 Chemical Potential

The chemical potential or partial molar free energy of a species  $i$  in solution ( $\kappa_i$ ) relative to its chemical potential in the pure state ( $\kappa_i^0$ ) is defined as the first derivative of  $\Delta G_m$  with respect to the concentration of species  $i$ .

$$\kappa_i - \kappa_i^0 = \Delta \kappa_i = \left( \frac{\delta \Delta G_m}{\delta m_i} \right)_{T,P,m_j} \quad (2.26)$$

Differentiating eqn. (2.24) with respect to  $m_1$  one obtains the chemical potential of polymer 1 in the mixture

$$\frac{\Delta \kappa_1}{RT} = \ln \phi_1 + (1 - x_1/x_2) \phi_2 + \chi x_1 \phi_2^2 \quad (2.27)$$

Similarly the chemical potential of polymer 2 is given by

$$\frac{\Delta u_2}{RT} = \ln \phi_2 + (1 - x_2/x_1) \phi_1 + \chi x_2 \phi_1^2 \quad (2.28)$$

*Simplifications!*

### 2.1.5 Simplifications Inherent in the Lattice Theory

The approximations and limitations of the lattice treatment have been discussed at length by Flory<sup>(18)</sup> in his treatment of polymer/solvent systems. To a large extent these simplifications are equally applicable to polymer blends and are briefly summarised below.

The assumption of greatest consequence is the acceptance of a single lattice to characterise polymer 1, polymer 2 and all intermediate mixtures. In the overwhelming majority of cases this assumption cannot be justified due to the different spatial requirements of the two chain segments. Consequently the theory has a fundamental mismatch with reality.

The entropy calculation only takes into account the combinatorial entropy of mixing. Interactions between unlike segments will produce some deviation from random mixing and thus  $\Delta S_m$  will be an overestimate of the true entropy. Maron and Guggenheim<sup>(38,39)</sup> circumvented this problem, whilst retaining the combinatorial entropy of mixing, by redefining the interaction parameter so that it contained entropic as well as enthalpic terms. Furthermore, only interactions between nearest neighbours were considered, in the calculation of  $\Delta H_m$ .

The model is not applicable to very dilute solutions as the condition of a random distribution of segments of species 1 amongst segments of species 2 is breached. At high dilutions the blend would consist of small clusters of segments of polymer 1 separated by comparatively large regions of the almost pure polymer 2.

There are a number of mathematical simplifications, most importantly in the calculation of  $\bar{f}_i$  and  $v_i$ . However refinement of the appropriate

expressions<sup>(19,40-42)</sup> has resulted in the complication of equations without improving the agreement with experiment.

### 2.1.6 Modifications of the Lattice Theory

Both polymer/solvent and polymer/polymer solutions have long been shown to be inadequately described by the simple Flory-Huggins expression (eqn. (2.24)) when its predictions have been quantitatively compared with experiment. The definition of the interaction parameter (eqn. (2.22)) implies its dependence on temperature alone. However there is a wealth of literature observing a dependence on concentration and molecular weight in  $\chi$ <sup>(43,44)</sup> as well as temperature. This has led to the formulation of a number of empirical expressions for  $\chi$ . Tompa<sup>(36)</sup> suggested a relation for  $\chi$  of the form

$$\chi = \chi_1 + \chi_2 \phi_2 + \chi_3 \phi_2^2 + \dots \quad (2.29)$$

where the temperature dependence of  $\chi$  can be restricted to  $\chi_1$ .

Similarly Koningsveld<sup>(11)</sup> advanced a relation for  $\chi$  (which he termed  $g$ ), which can be represented as

$$g = \sum_{k=0}^n g_k \phi^k \quad k = 0, 1, 2, \dots, n \quad (2.30)$$

where any coefficient  $g_k$  can be written as a function of temperature

$$g_k = g_{k,1} + g_{k,2}/T + g_{k,3} T + g_{k,4} \ln T \quad (2.31)$$

The  $g_{k,i}$  have been shown in some instances to depend on measurable physical quantities such as the molecular weight. However, no generally

acceptable molecular interpretations of  $g_{k,i}$  exist and these coefficients remain empirical.

### 2.1.7 Phase Equilibria in Binary Polymer Blends

In general in any system in stable equilibrium the free energy is a minimum at constant temperature and pressure. In a two component polymer system at equilibrium (neglecting for the present the influence of the glass transition) therefore the system can be characterised by the fact that the free energy of mixing  $\Delta G_m$  is also a minimum. Consequently the equilibrium state of mixing of such a polymer blend at constant temperature and pressure can be determined by inspection of  $\Delta G_m$  as a function of blend composition.

A binary polymeric mixture has an enthalpy of mixing which differs little from that of the equivalent monomeric mixture. However, the entropy of mixing decreases rapidly with increasing chain length and for two high polymers has a negligible contribution to the free energy of mixing. Therefore a small positive enthalpy of mixing is often enough to make the free energy of mixing positive and cause phase separation.

At constant temperature and pressure a binary polymer mixture will be completely miscible if  $\Delta G_m$  is concave upwards over the whole composition range (Fig. (2.1)). For example, for a stable mixture of composition  $\phi_2$  to separate into 2 phases whose compositions are denoted by  $\phi_{2a}$  and  $\phi_{2b}$  this could only occur with an increase in  $\Delta G_m$ . This holds at all compositions as any chord will lie above the curve. The intercepts of the tangent at a point define the chemical potentials of the pure components.

$$\text{As } \Delta G_m = \phi_1 \Delta \mu_1 + \phi_2 \Delta \mu_2 \quad (2.32)$$



$\Delta G_m$  vs. Composition for a Miscible and a Partially Miscible Blend

Figure (2.1)

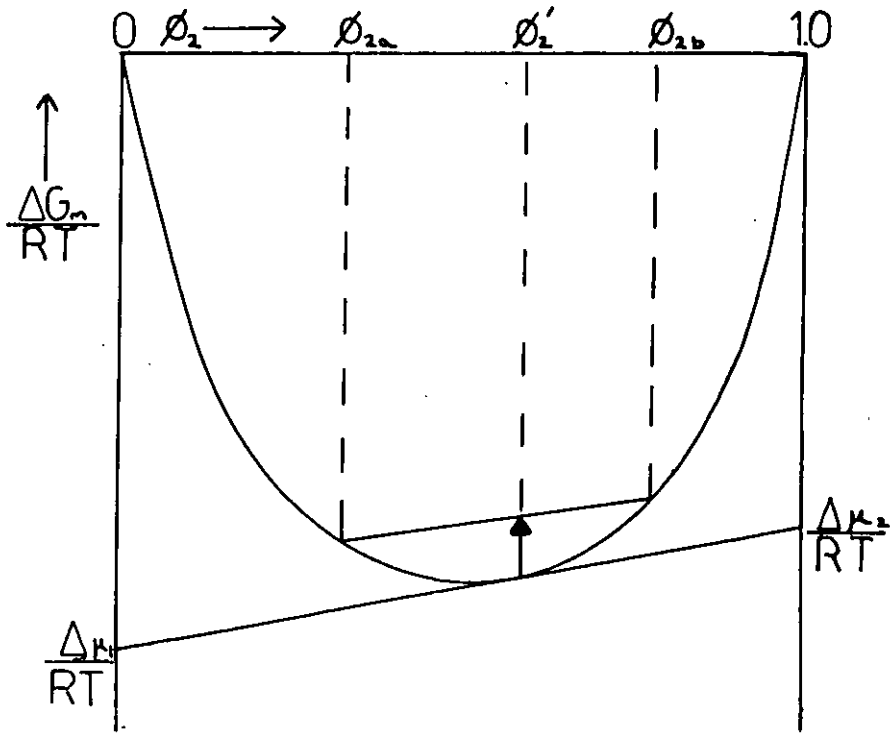
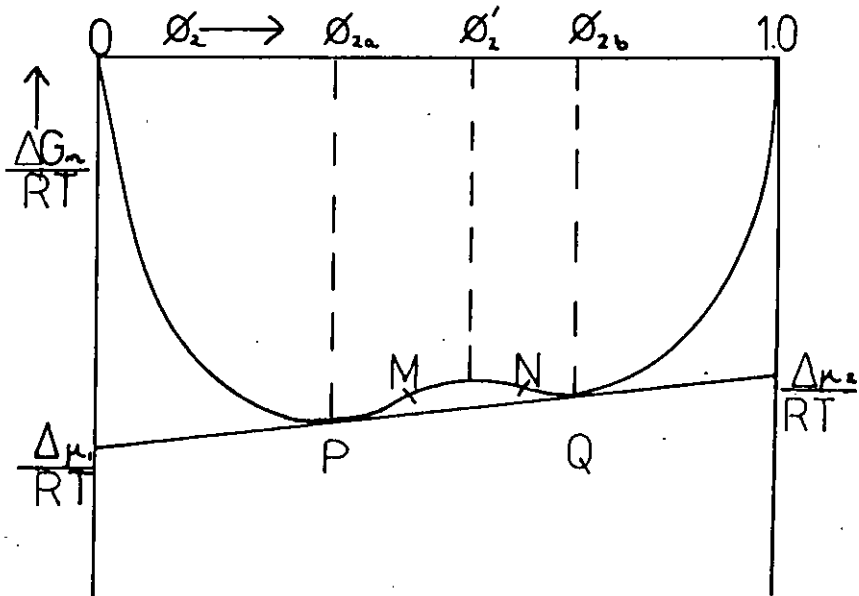


Figure (2.2)



$$\frac{\delta \Delta G_m}{\delta \phi_2} = \Delta \mu_2 - \Delta \mu_1 \quad (2.33)$$

which is the chemical potential change of the mixture.

Phase separation will only occur if  $\Delta G_m(\phi_2)$  exhibits negative curvature. This situation is described in Figure (2.2), a mixture of composition  $\phi_2^i$  will phase separate into two phases of compositions  $\phi_{2a}$  and  $\phi_{2b}$  thereby decreasing  $\Delta G_m$  for the system. The double tangent defines the compositions of the two phases in which the chemical potentials of the two components are equivalent

$$\Delta \mu_{2a} = \Delta \mu_{2b} \quad \Delta \mu_{1a} = \Delta \mu_{1b} \quad (2.34)$$

All mixtures with overall compositions between  $\phi_{2a}$  and  $\phi_{2b}$  will phase separate into these two phases. The curve shown in Figure (2.2) has two points of inflection at compositions denoted by M and N. Compositions between M and N will phase separate spontaneously as the slightest concentration fluctuation will decrease  $\Delta G_m$  and will initiate further separation until the stable situation at points P and Q has been attained. This mechanism of phase separation is called spinodal decomposition. Overall compositions lying between PM and NQ are termed metastable because the system is stable to small concentration fluctuations due to the positive curvature of  $\Delta G_m(\phi_2)$ . Phase separation occurs via large concentration fluctuations which lead to the formation of nuclei rich in concentration of one of the components. These nuclei then grow by a process of diffusion and the phase separation mechanism is thus termed nucleation and growth.

The two  $\Delta G_m(\phi_2)$  curves shown in Figures (1)-(2) could represent the same binary mixture at different temperatures and/or pressures.

Assuming that ambient pressure is maintained, varying temperature can result in a family of  $\Delta G_m(\phi_2)$  curves as shown in Figures (2.3) and (2.4). The locus of tangent points is known as the binodal (in a binary system) or cloud-point curve and is the boundary between stable and meta-stable regions. The locus of inflection points is termed the spinodal and separates the meta-stable and unstable regions. These two curves have a common horizontal tangent at the critical point which is located at the extreme of the binodal and spinodal in truly binary systems. The spinodal, being the locus of the inflection points is characterised by the condition that

$$\left( \frac{\delta^2 \Delta G_m}{\delta \phi_2^2} \right)_{P,T} = 0 = \left( \frac{\delta \Delta \mu_2}{\delta \phi_2} \right)_{P,T} = \left( \frac{\delta \Delta \mu_1}{\delta \phi_1} \right)_{P,T} \quad (2.35)$$

Applying this condition to eqn. (2.27) one obtains

$$2(\chi)_{SP} = \left[ \frac{1}{x_1(\phi_1)_{SP}} + \frac{1}{x_2(\phi_2)_{SP}} \right] \quad (2.36)$$

The equations for the binodal are calculated by applying the condition of equivalence of the chemical potentials of the two components in both phases.

$$\ln \phi_{1a} + (1 - x_1/x_2)\phi_{2a} + \chi x_1 \phi_{2a}^2 = \ln \phi_{1b} + (1 - x_1/x_2)\phi_{2b} + \chi x_1 \phi_{2b}^2 \quad (2.37)$$

$$\ln \phi_{2a} + (1 - x_1/x_2)\phi_{1a} + \chi x_2 \phi_{2a}^2 = \ln \phi_{2b} + (1 - x_1/x_2)\phi_{1b} + \chi x_2 \phi_{2b}^2 \quad (2.38)$$

Figure (2.3)

Temperature Dependence of  $\Delta G_m$  in a Blend Showing U.C.S.T. Behaviour

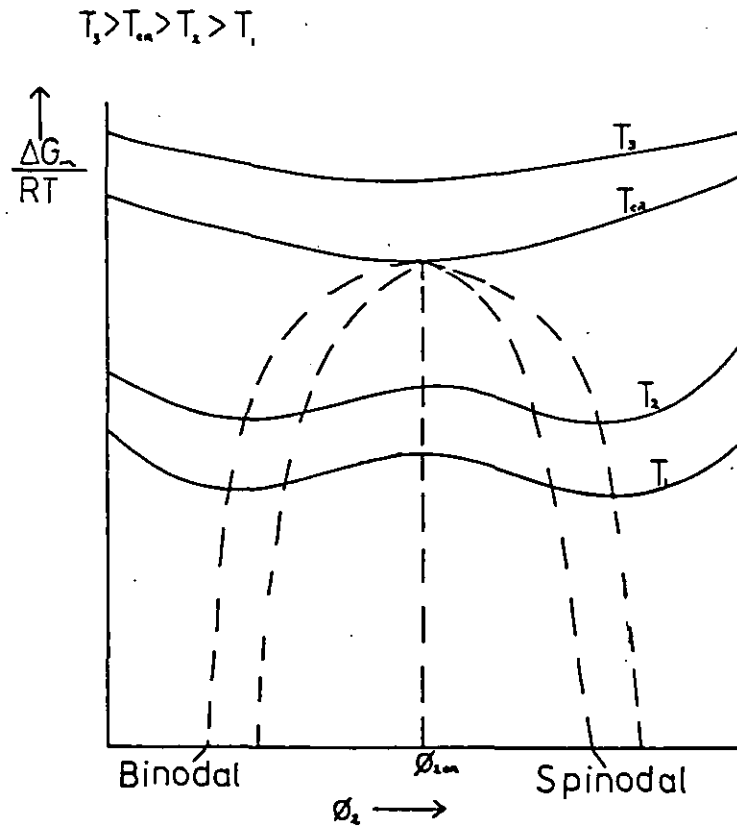
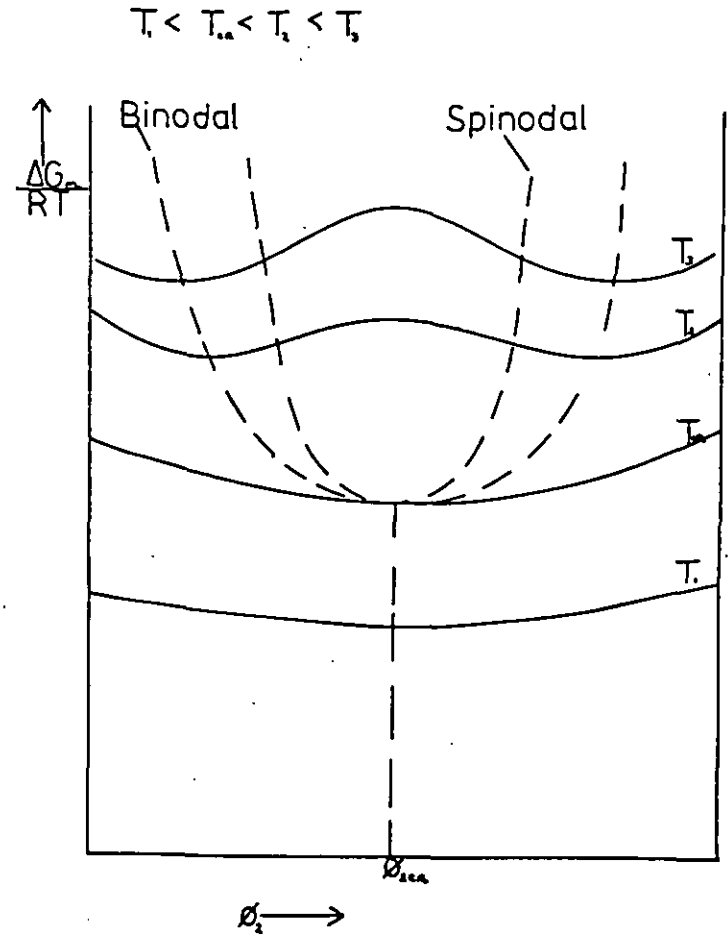


Figure (2.4)

Temperature Dependence of  $\Delta G_m$  in a Blend Showing L.C.S.T. Behaviour



The critical point is defined mathematically as

$$\left( \frac{\delta^3 \Delta G_m}{\delta \phi_2^3} \right)_{P,T} = 0 \quad (2.39)$$

Applying these conditions to eqn. (2.27) one obtains the critical conditions for  $x$ ,  $\phi_2$  and  $\phi_1$ .

$$(x)_{CR} = (1 - x_1/x_2)/2x_1(1 - 2(\phi_2)_{CR}) \quad (2.40)$$

$$(\phi_2)_{CR} = (x_1)^{1/2}/(x_1^{1/2} + x_2^{1/2}) \quad (2.41)$$

$$(\phi_1)_{CR} = (x_2)^{1/2}/(x_1^{1/2} + x_2^{1/2}) \quad (2.42)$$

Substitution of equation (2.41) into equation (2.40) gives for  $(x)_{CR}$

$$(x)_{CR} = \frac{1}{2}[(1/x_1)^{1/2} + (1/x_2)^{1/2}] \quad (2.43)$$

Figure-(2.3) demonstrates the behaviour of a system which becomes more miscible as the temperature is raised. This is termed upper critical miscibility and  $T_{CR}$  is called the upper critical solution temperature. Conversely Figure (2.4) exemplifies the behaviour of a system which becomes less miscible at higher temperatures. This is described as lower critical miscibility and  $T_{CR}$  is called the lower critical solution temperature. McMaster<sup>(25)</sup> was the first to state that in a blend of two high polymers lower critical miscibility is to be expected rather than U.C.M., which is the normal mode of phase separation behaviour observed in small molecule mixtures and polymer/solvent systems.

The examples given in Figures (2.3) and (2.4) represent the simplest conceivable situation. It is quite possible that the shape of the  $\Delta G_m(\phi_2)$  curve would be more complicated and would thus give rise to more elaborate phase behaviour. This has been observed indirectly with the measurement of bimodal cloud-point curves in short-chain<sup>(45,46)</sup> and long-chain<sup>(47,48)</sup> polymer mixtures.

### 2.1.8 Multicomponent Polymer Mixtures

Polymer blends can rarely be regarded as binary due to the polydispersity of the species, particularly in the case of synthetic polymers. Tompa<sup>(36)</sup> showed that in a polymer/solvent system the critical point shifts away from the peak in the cloud-point curve towards higher polymer concentration as polydispersity increases. Koningsveld<sup>(43)</sup> further pointed out the considerable shift of the critical point due to the value of  $\bar{M}_z$  where  $\bar{M}_w \approx \bar{M}_n < \bar{M}_z$ .

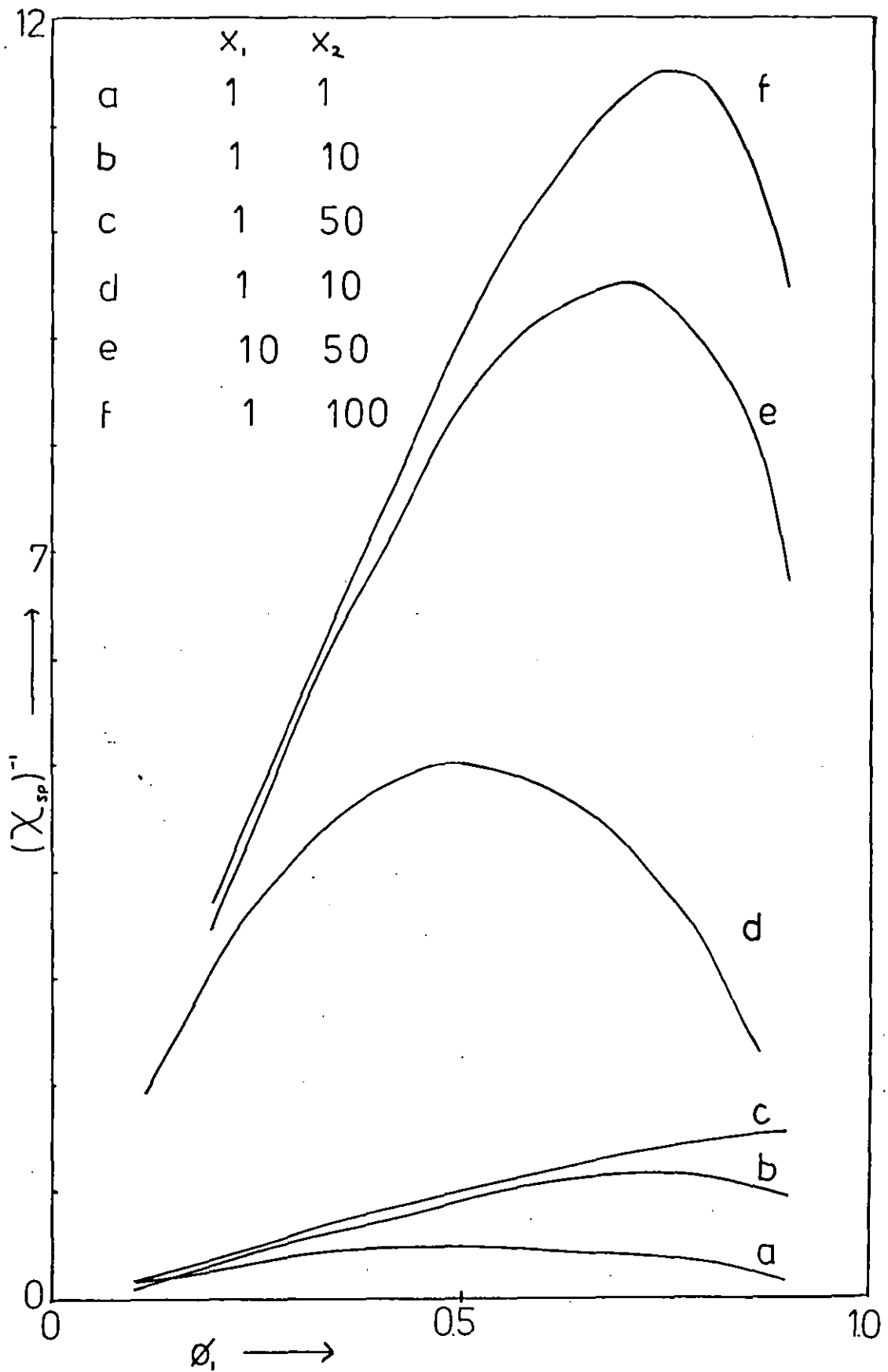
Koningsveld<sup>(43,44)</sup> and co-workers have investigated the influence of chain length, temperature and composition on miscibility curves calculated from the Flory-Huggins equation and compared them with experimental data. Figure (2.5) shows the effect on the calculated spinodal (equation (2.36)) shape of chain length. The boundary is symmetrical when  $x_1 = x_2$ , however it becomes increasingly asymmetric as the weight average chain lengths diverge. The critical point occurs at the spinodal maximum when  $a_1 = a_2$ , where  $a$  is the ratio of the  $z$  to weight average chain lengths

$$a_i = x_{z_i} / x_{w_i} \quad (2.44)$$

However, as the ratios diverge the critical point moves down the

Figure (2.5)

Spinodals Calculated Using Equation (2.36)



branch representing higher concentrations of the species with the higher value of  $a$ . Koningsveld<sup>(44)</sup> has also shown that calculated cloud-point curves are sensitive to polydispersity, resulting in reduced miscibility as it increases. The corresponding spinodals are however only dependent upon the weight average chain lengths of the two species.

The analysis was extended<sup>(44,49)</sup> to include the influence of temperature, composition and chain length using the interaction parameter functions given in equations (2.30) and (2.31). The utility and sensitivity of the treatment was tested by seeing whether experimentally determined cloud-point curves could be predicted after the fact. The treatment was applied to the data of Allen<sup>(50)</sup> *et al.* who found asymmetric cloud-point curves in poly(isobutylene)/poly(dimethylsiloxane). Another system of interest was provided by poly(isoprene)/poly(styrene) blends<sup>(49,51)</sup> where small increments in average chain length lead to distinct changes in the shape of the cloud-point curves.

Suitable choice of  $g$  function parameters allowed the description of the aforementioned systems. Bimodality was attributed to a quadratic dependence of  $g$  on  $\phi_2$ . The temperature dependence and that of polydispersity was accounted for by  $g_0$ , whilst chain length dependence was manifested in  $g_1$  and  $g_2$ .

The approach however remains empirical in the absence of satisfactory molecular theories. Nevertheless Koningsveld<sup>(52)</sup> has identified 4 parameters which seem relevant to the state of mixing of a polymer system:-

- (a) The interacting surface areas of the species, which was shown by Staverman<sup>(53)</sup> to influence  $\Delta H_m$  in a number of binary mixtures of small molecules.
- (b) The difference in chain flexibility between the two types of



segment and its dependence on temperature, composition and molecular weight. This notion was introduced by Huggins<sup>(54,55)</sup> as a correction term for the combinatorial entropy of mixing.

(c) Polydispersity.

(d) Non-combinatorial contributions to  $\Delta G_m$  as derived in equation of state theories.

It has been postulated<sup>(49)</sup> that parameters (a)-(c) are most relevant to systems exhibiting U.C.M. whilst for L.C.M. parameter (d) predominates. The majority of systems which show U.C.M. comprise of mixtures in which one or both components are either small molecules or oligomers<sup>(43,44,46,50-52,56,57)</sup>. In blends where both species are high polymers L.C.M. has been established as the normal mode of phase separation<sup>(25,58-62)</sup>. One blend in particular, poly(styrene)/poly(vinylmethyl ether), has been thoroughly investigated because of its elegant manifestation of this phenomenon<sup>(63-76)</sup>.

### 2.1.9 Lattice Theory and Lower Critical Miscibility

Assuming the validity of equation (2.24) to describe the free energy of mixing for a binary blend, let us see how this can be related to lower critical miscibility. The spinodal and critical conditions (equations (2.36), (2.43)) for  $\chi$  indicate that it can never be negative but will approach zero with increasing chain length. Consequently  $\Delta H_m$  as defined in equation (2.21) can also not assume negative values. It is therefore apparent that the basic Flory-Huggins approach cannot predict L.C.M. where the driving force is often a specific interaction between the two different segments, the entropic contribution to  $\Delta G_m$  being very small at high molecular weights.

The broader, semi-empirical  $g$  function of Koningsveld discussed earlier can, by the adjustment of certain terms, describe l.c.m. but

not of course in terms of a general predictive model.

It is now time to turn aside from simple lattice theory and briefly review a different approach to the theoretical description of the miscibility behaviour of high polymers.

## 2.2 EQUATION OF STATE THEORIES

An equation of state relates the pressure, volume and temperature of a system at equilibrium. The relationship can be derived empirically or calculated using statistical mechanics given a knowledge of the relevant intermolecular forces. The latter approach has been successfully applied to the treatment of non-ideal gases and crystals, however a definitive treatment of the liquid state is still being sought.

The two most important theories with regard to polymer solutions have been developed by Flory<sup>(21-24)</sup> and Sanchez<sup>(77-79)</sup> both of which are extensions of earlier treatments of simple liquids. The outline given below is restricted to the Flory treatment which has formed the basis of most discussions of lower critical miscibility in high polymer mixtures during the last decade.

Flory's theory is arrived at by considering the permutations in filling a lattice made up of cells of volume  $v$  with elements of volume  $v^*$ . The volume  $v^*$  is the hard core volume of a polymer segment and is less than  $v$  which represents the actual molecular volume of a segment. Consequently additional volume is available to the system because of this so-called free volume. This expanded configurational space is accounted for by the configurational integral of the system.

### 2.2.1 The Partition Function and Characteristic Parameters

One of the fundamental assumptions of the Flory theory is that the

degrees of freedom of a molecule in a liquid can be separated into internal and external contributions. This assumption was first made by Prigogine<sup>(80)</sup>. The external degrees of freedom depend in a polymer chain on intermolecular forces and relate to translational modes. The number of external degrees of freedom is usually represented as  $3c$  ( $c < 1$ ) per chain segment which is of course less than for a small molecule. The internal degrees of freedom depend on intramolecular forces and relate to rotations and vibrations. The partition function for a polymer consisting of  $n$  chains each of  $x$  segments is therefore given by

$$Z(T,V) = Z_{int}(T) \cdot Z_{ext} \quad (2.45)$$

$Z_{int}$  is assumed to be independent of density, and not influenced by neighbouring segments, consequently it makes no contribution to the equation of state. The partition function associated with the external degrees of freedom is calculated from the classical integral for a translational partition function, suitably modified to take into account chain length.

$$Z_{ext} = (2\pi m_{A_i} kT/h^2)^{3n_i x_i c_i / 2} Q \quad (2.46)$$

where  $m_{A_i}$  is the mass of one segment,  $h$  is Planck's constant and  $Q$  is the configurational integral

$$Q = Q(\text{comb}) [4\pi \gamma / 3 (v_i^{1/3} - v_i^{*1/3})]^{3n_i x_i c_i} \exp(-E_{0i}/kT) \quad (2.47)$$

$v$  is the actual volume of a segment,  $v^*$  is the hard-core volume of a segment,  $\gamma$  is a geometric factor and  $E_0$  is the lattice energy. The

lattice energy is assumed to be volume dependent of the form

$$E_0 \propto \frac{1}{v^a} \quad (2.48)$$

where  $a$  lies between 1.0 and 1.5<sup>(81)</sup>.

The pressure of the system is defined as

$$P = \frac{kT}{n_i r_i} \left( \frac{\delta \ln Z_i}{\delta v_i} \right)_{T, n_i} \quad (2.49)$$

and the equation of state for a pure component polymer is arrived at by differentiating equation (2.46). This results in

$$\frac{\tilde{P}_i \tilde{v}_i}{\tilde{T}_i} = \frac{\tilde{v}_i^{1/3}}{\tilde{v}_i^{1/3} - 1} - \frac{1}{\tilde{T} \tilde{v}_i^a} \quad (2.50)$$

where the reduced temperature, pressure and volume (marked with the tilde) are defined as

$$\tilde{P} = P/P^*; \quad \tilde{T} = T/T^*; \quad \tilde{v}_i = v_i/v_i^* \quad (2.51)$$

The starred symbols are the characteristic parameters of the equation of state. They can be obtained from measurements of the thermal expansion coefficient ( $\alpha$ ) and the thermal pressure coefficient ( $\gamma$ ).

$$\alpha = \frac{1}{v} \left( \frac{\delta v}{\delta T} \right)_{P, n_i} \quad (2.52)$$

$$\gamma = \left( \frac{\delta P}{\delta T} \right)_{v, n_i} \quad (2.53)$$

If these two quantities are extrapolated to zero pressure, the reduced parameters become

$$\tilde{v}_i = [(\alpha_i T / 3\alpha_i + 3) + 1]^3 \quad (2.54)$$

$$\tilde{T}_i = [(\tilde{v}_i^{1/3} - 1) / \tilde{v}_i^{(1/3 + a)}] \quad (2.55)$$

$$P_i^* = \tilde{v}_i \gamma_i T \quad (2.56)$$

These relationships for pure components are applied to binary or quasi-binary polymer systems through the use of a number of mixing rules which are discussed at length in the textbook of Olabisi *et al.*<sup>(10)</sup>.

Using this procedure one obtains equations for the characteristic temperature and pressure of a multicomponent mixture.

$$\frac{1}{T^*} = \frac{k}{P^* v^*} \left[ \begin{array}{ccc} n & n & j - 1 \\ \Sigma & \Sigma & \Sigma \\ c_i \psi_i & c_{ij} \psi_i \psi_j & \\ i = 1 & j = 2 & i = 1 \end{array} \right] \quad (2.57)$$

$$P^* = \begin{array}{ccc} n & n & j - 1 \\ \Sigma & \Sigma & \Sigma \\ \psi_i P_i^* & \psi_i \psi_j X_{ij} & \\ i = 1 & j = 2 & i = 1 \end{array} \quad (2.58)$$

The term in brackets in equation (2.57) gives the total number of external degrees of freedom per segment, the  $c_{ij}$  terms being correction parameters introduced by Lin<sup>(82)</sup> to account for deviations from additivity.

The  $\psi$  terms are segment fractions which are volume fractions based on

the hard-core volume  $v^*$ . The  $\chi_{ij}$  parameters of equation (2.58) arise from differences in interaction energy for unlike segments, whilst  $\theta_j$  represents the fraction of the total segmental surface area occupied by type  $j$  molecules.

### 2.2.2 The Free Energy of Mixing

The Helmholtz free energy of mixing for a multicomponent system can be determined using the standard relation of statistical thermodynamics

$$\Delta F^m = -kT \ln \left( \frac{Z}{\prod_{i=1}^n Z_i} \right) \quad (2.59)$$

Substitution into this expression from equations (2.46)-(2.48) yields the generalised form of  $\Delta F^m$ . The chemical potential of each component in a multicomponent system is given by

$$\Delta \mu_k = \left( \frac{\delta \Delta F^m}{\delta n_k} \right)_{T, U, n_j, j \neq k} + \left( \frac{\delta \Delta F^m}{\delta \tilde{U}} \right)_{T, n_k, n_j} \cdot \left( \frac{\delta \tilde{U}}{\delta n_k} \right)_{T, V, n_j} \quad (2.60)$$

Flory<sup>(22,24)</sup> did not include the second term of this equation as it makes a small contribution at low pressures; it was found necessary however by McMaster<sup>(25)</sup> for the true prediction of the effect of pressure.

Substitution of the full expression for  $\Delta F^m$  into equation (2.60) and differentiation of each term gives the chemical potential of any component  $k$  in the mixture. The original papers<sup>(21-24)</sup> can be consulted for the rather lengthy equations which result.

### 2.2.3 Phase Boundaries

The binodal curve for a binary polymer mixture can be determined as before by equating the chemical potential of each component in both phase. McMaster<sup>(25)</sup> presented this in the form

$$F_1 = (\Delta\mu_1 - \Delta\mu_1')/kT = 0 \quad (2.61)$$

$$F_2 = (\Delta\mu_2 - \Delta\mu_2')/kT = 0 \quad (2.62)$$

and solved these two non-linear equations using a non-linear optimizing operation by finding

$$\min_{\psi} \left\{ \frac{F_1^2 + F_2^2}{(\psi_1 - \psi_1')} \right\} \quad (2.63)$$

The spinodal and critical point for a binary mixture are found from the chemical potential relations using the conditions stated in equations (2.35) and (2.39). The spinodal equation yields either two or zero compositions with the same spinodal temperature except at the critical point which is single-valued. The treatment can be extended to quasi-binary systems using the formulation of Koningsveld *et al.*<sup>(83)</sup>. The interaction parameter is expressed in terms of the equation of state parameters and this relationship is then used to evaluate the spinodal and critical point equations for two polydisperse polymers.

### 2.2.4 Implications of Equation of State Theory for Polymer-Polymer Miscibility

McMaster<sup>(25)</sup> examined the implications of Flory's theory by calculating a series of binodal and spinodal curves for two hypothetical

binary polymeric mixtures. The first system was chosen so that the equation of state parameters for the pure components, poly(styrene) and poly(ethylene), were quite dissimilar. The second system used the poly(styrene) parameters only. In both cases sequential variations were made in these base parameters and the mixing parameters to study their influence on the shape and position of the phase boundaries.

The most important general conclusion reached was that polymer miscibility decreases with temperature in all cases when the interaction parameter is less than or equal to zero. Consequently in systems which are miscible by virtue of a specific interaction between the dissimilar species, lower critical miscibility is the expected mode of phase separation behaviour.

Miscibility was found to be very sensitive to the magnitude of the difference between the thermal expansion coefficients. Significant miscibility could only be attained if, at molecular weights of the two species of 50,000, this difference was less than 10%. At molecular weights of 200,000 the tolerance was reduced to less than 4% in the absence of specific interactions.

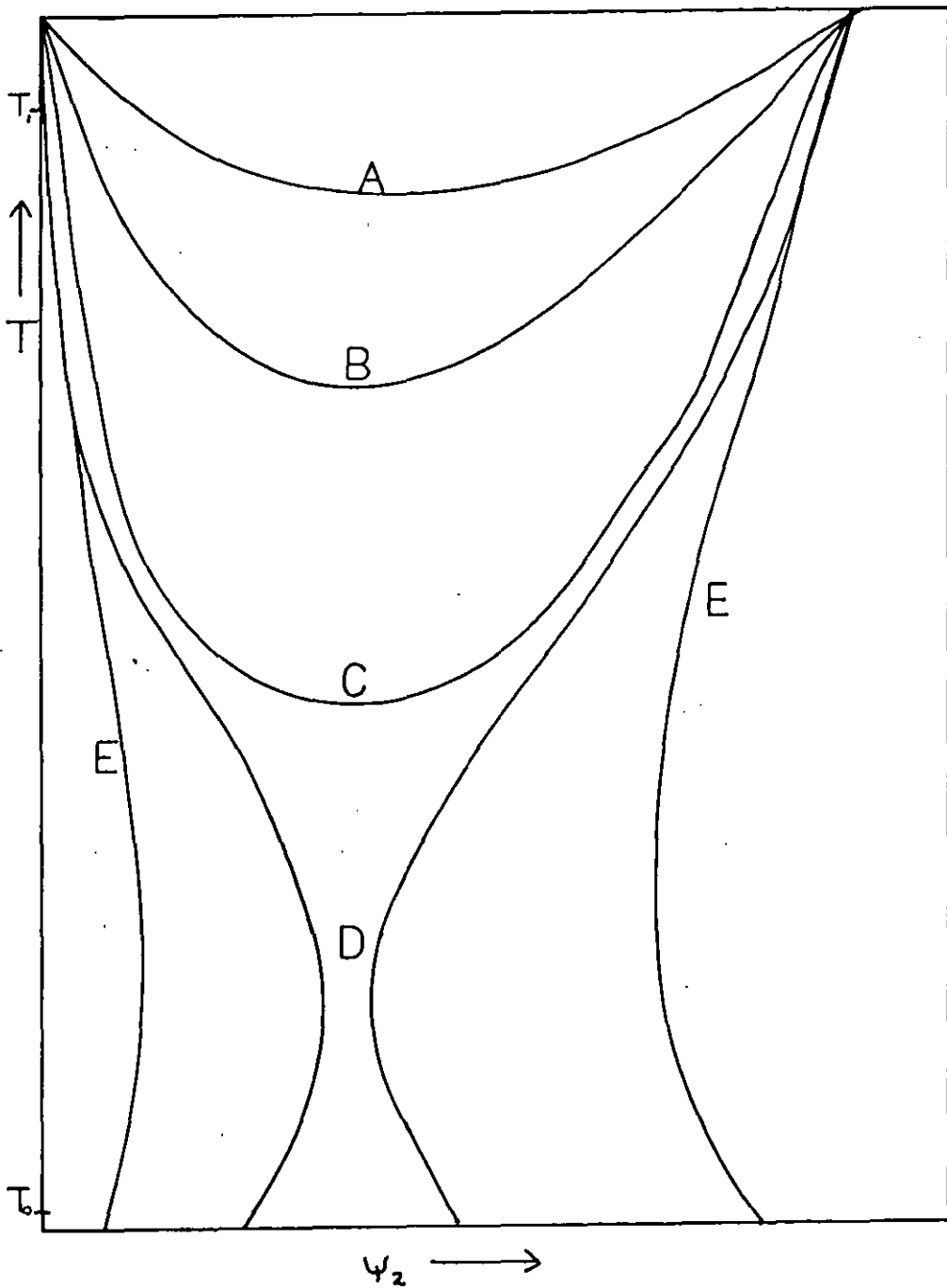
The influence of the interaction energy parameter on the shape and position in the temperature plane of the binodal is shown in Figure (2.6). When  $X_{12}$  is small and positive, simultaneous lcst and vcst behaviour is possible. As  $X_{12}$  becomes increasingly positive the two boundaries merge to yield hourglass shaped binodals (D). When  $X_{12}$  becomes increasingly negative the binodals tend to flatten and move to higher temperatures, indicating increased mutual solubility. McMaster found that for the poly(styrene)/poly(ethylene) system an increase of  $X_{12}$  from -0.05 to 0.1 caused the theoretical binodal to change from type A to type E, where  $(T_1 - T_0)$  was about 350°C. The poly(styrene) based system exhibited an even greater sensitivity as



Figure (2.6)

Dependence of Binodals on the Exchange Energy Parameter

$$\chi_{12}(A) < \chi_{12}(B) < \chi_{12}(C) < \chi_{12}(D) < \chi_{12}(E)$$



for example, a change of only 0.0015 in  $X_{12}$  resulted in a shift of the critical point of 80°C.

The difference in the thermal pressure coefficients was found to be less significant than that of the thermal expansion coefficients. Mutual solubility was found to increase with pressure except when there was a large difference between the thermal pressure coefficients of the pure components.

The effects of polydispersity and molecular weight were found to be similar to those found by Koningsveld, discussed in section (2.1.8). The empirical correction parameters  $c_{12}$  and  $a$  introduced in equations (2.57) and (2.48) and the parameter  $Q_{12}$ , introduced by Flory into the expression for  $\Delta F^m$  to account for the entropy of interaction between unlike segments, generally influenced the position but not the shape of phase boundaries. Negative values of  $Q_{12}$  and  $a$  decreased solubility whilst a negative  $c_{12}$  increased solubility and vice versa.

In conclusion, one can say that McMaster showed that Flory's equation of state theory was capable of providing a theoretical foundation to the observed phase separation behaviour of blends of high molecular weight polymers.

#### 2.2.5 Comparison of Calculated and Measured Phase Boundaries Using Flory's Equation of State Theory

Comparatively little work has been published which compares measured phase boundaries (generally cloud-point curves) with phase boundaries calculated using the equation of state parameters of the pure components for a quasi-binary polymer mixture. This is probably due to the lack of thermodynamic data available for all but a few polymers. However, this comparison is of paramount importance in evaluating the utility

and general applicability of the equation of state approach. In this section the pertinent features of the available data are discussed.

McMaster<sup>(25)</sup> made a qualitative comparison between the binodals calculated for the two aforementioned model systems and cloud-point curves measured for poly(styrene)/poly(vinyl methyl ether) and styrene-co-acrylonitrile/poly(caprolactone). He found that the measured curves were far less temperature sensitive than the computed curves and attributed this difference to three possible causes. The inaccuracies in the equation of state for the pure components, which Flory<sup>(84)</sup> had shown to cause too great a variation in  $\tilde{v}$  as a function of temperature; the polydispersity of the measured systems and the presence of specific interactions.

Olabisi<sup>(85)</sup> simulated spinodals for the system poly(vinyl chloride)/poly(caprolactone) using measured values of the pure component densities, thermal expansion coefficients, and thermal pressure coefficients. The exchange energy parameter for the mixture ( $\chi_{12}$ ) was estimated using inverse gas chromatography and was found to be negative, indicating the presence of specific interactions. The functional dependence of  $\chi_{12}$  was ignored and the other binary parameter of interest, the segmental surface area ratio ( $s_1/s_2$ ) was estimated using the group contribution approach of Bondi<sup>(86,87)</sup>. The spinodals were shown to become binodal in shape when  $\chi_{12}$  became more negative at constant  $s_1/s_2$  or when  $s_1/s_2$  decreased at constant  $\chi_{12}$ . Unfortunately, however, no phase boundaries were experimentally determined for the system.

Ten Brinke *et al.*<sup>(49,59)</sup> applied the equation of state theory to blends of isotactic poly(ethyl methacrylate)(PEMA)/poly(vinylidene fluoride)(PVDF). Isotactic PEMA was used as this was found to exhibit lower critical miscibility with PVDF<sup>(90,91)</sup> whilst the atactic form was completely miscible up to 250°C. The pure component values

of  $\alpha$  and  $\gamma$  were estimated in the region of the cloud-point curve to overcome the inaccuracies in the equation of state temperature dependencies. The binary parameter  $s_1/s_2$  was also estimated<sup>(86,87)</sup> and the calculated spinodal was fitted to the experimental cloud-point curve by adjustment of the number of external degrees of freedom of the mixture (as compared with the pure components)  $c_{12}$  and  $X_{12}$ . The best fit was found with a negative value of  $X_{12}$  (-3.7 cal/cm.<sup>3</sup>) and  $c_{12} \approx 0.02$ . It was found once again that the computed spinodal was far more temperature sensitive than the comparatively flat cloud-point curve.

The most constructive comparisons to date have been made by Walsh and Higgins and their colleagues. They have constructed equation of state spinodals for a number of measured cloud-point curves of the systems poly(methyl methacrylate)(PMMA)/chlorinated poly(ethylene<sup>(92)</sup>)(CPE), poly(butyl acrylate)(PBA)/chlorinated poly(ethylene<sup>(93)</sup>) and ethylene-co-vinyl acetate (EVA)/chlorinated poly(ethylene)<sup>(62)</sup>.

In all the systems the values of  $\alpha$ , where not available in the literature, were calculated from density measurements at two temperatures.  $\gamma$  was estimated using values available for similar materials and was found to have little influence on the calculated enthalpy of mixing or the position of the phase boundary.  $X_{12}$  was calculated from measurements of the enthalpy of mixing measured by calorimetry on low molecular weight analogues.  $\Delta H_m$  and  $X_{12}$  are related by (for a binary blend)

$$\Delta H_m = \bar{x}n\nu^* [\psi_1 P_1^* (\tilde{v}_1^{-1} - \tilde{v}^{-1}) + \psi_2 P_2^* (\tilde{v}_2^{-1} - \tilde{v}^{-1}) + \psi_2 X_{12} / \tilde{v}] \quad (2.64)$$

$s_1/s_2$  was estimated using Bondi's<sup>(86,87)</sup> technique. Using the measured

values of  $X_{12}$  the theoretical spinodals were adjusted to coincide with the measured cloud-point curves by alteration of the empirical correction parameter  $Q_{12}$ . The effect of  $Q_{12}$  and  $X_{12}$  is to considerably flatten the calculated spinodals and to greatly improve the correspondence between the predicted and calculated molecular weight dependence of the spinodal. This is because McMaster<sup>(25)</sup> used zero values of  $Q_{12}$  and  $X_{12}$  in his calculations of the influence of molecular weight which therefore gave prominence to the free volume term. Walsh *et al.* have shown that  $Q_{12}$  and  $X_{12}$  suppress this term, and are less molecular weight dependent themselves.

In the EVA/CPE and PBA/CPE mixtures the spinodal was much flatter than the measured C.P.C.'s using the value of  $X_{12}$  determined for the oligomeric analogues. It was found that the curves could only be fitted by using smaller values of  $X_{12}$  and  $Q_{12}$ , the difference in  $X_{12}$  being accounted for in terms of its temperature dependence and differences between the analogues and polymers.  $Q_{12}$  adjustments were rationalised in terms of correcting the overestimation of the calculated volume change on mixing to correspond more closely with measured values. The negative values of  $Q_{12}$  found appropriate to all three systems indicates that the presence of specific interactions in these mixtures has the effect of reducing the entropy.

This short survey has indicated that the equation of state theory is able to describe the phase separation behaviour of high molecular weight polymeric mixtures as long as suitable values of the binary parameters  $Q_{12}$  and  $X_{12}$  are used. Consequently the theory cannot be used as a delicate predictive tool in the absence of experiment.

The Flory equation of state theory in essence has three types of contribution taken into account in the expression for the free energy of mixing. The combinatorial entropy term, the free volume

change on mixing term, and the interaction energy term. In a mixture of two high molecular weight polymers the combinatorial entropy is negligible so the possibility of miscibility as expressed by a negative free energy of mixing depends upon the balance of the other two terms. The free volume term will always contribute unfavourably to  $\Delta F^m$ , but as discussed by Patterson and Robard<sup>(95)</sup>, the importance of this term depends upon the nature of the interaction energy. When specific interactions are present,  $X_{12}$  is negative and this tends to be the driving force for miscibility. However, a number of mixtures of high polymers have been found to be miscible in the absence of a specific interaction. In these systems miscibility seems to arise either as a result of a matching of the equation of state parameters of the two components<sup>(97)</sup> or because of the relation between the intermolecular and intramolecular forces. The latter hypothesis has recently been advanced by a number of authors and has arisen principally as an attempt to explain the observed behaviour of mixtures where one or both components are random copolymers.

### 2.3 THERMODYNAMIC THEORIES OF THE MISCIBILITY BEHAVIOUR OF RANDOM COPOLYMER MIXTURES

A mean field theory has been developed by three independent research groups which explains the observed miscibility in various random copolymer systems where a specific interaction has been shown not to exist. The theory was first advanced by Kambour *et al.*<sup>(98)</sup> to explain the phase behaviour of mixtures of poly(styrene) and poly(2,6-dimethyl-1,4-phenylene oxide) (PPO) which had been brominated to varying degrees to produce a series of copolymers. MacKnight *et al.*<sup>(99)</sup> extended the theory put forward by Kambour for homopolymer/copolymer systems to mixtures containing two copolymers. They discussed the theory with

reference to PPO mixtures with various halogen substituted styrene copolymers. Paul and Barlow<sup>(100)</sup> have used similar reasoning and have extended the application to the homopolymers of a homologous series such as the polyesters, which they treated as copolymers of  $(CH_2)_x$  and  $(COO)$ .

### 2.3.1 Copolymer/Homopolymer Systems

In a binary mixture of a random copolymer made up of repeat units 1 and 2 and a homopolymer of repeat unit 3, the simple Flory-Huggins expression for  $\Delta G_m$  takes the form

$$\Delta G_m = (\phi_A/x_A)\ln\phi_A + (\phi_B/x_B)\ln\phi_B + \phi_A\phi_B[\phi_1\chi_{13} + (1 - \phi_1)\chi_{23} - \phi_1(1 - \phi_1)\chi_{12}] \quad (2.65)$$

The volume fractions  $\phi_A$  and  $\phi_B$  represent the proportions of copolymer and homopolymer in the mixture respectively, and  $\phi_1$  denotes the copolymer composition. Comparison of equation (2.65) with the expression for a mixture of two homopolymers (equation (2.24)) shows they are identical if the effective interaction parameter of the mixture is defined as

$$\chi_{eff} = \phi_1\chi_{13} + (1 - \phi_1)\chi_{23} - \phi_1(1 - \phi_1)\chi_{12} \quad (2.66)$$

The first two terms on the right hand side of this equation define the interaction between a homopolymer segment and the copolymer segments whilst the third term expresses the intramolecular forces of the copolymer segments 1 and 2.

The miscibility of the system depends upon the sign of  $\chi_{eff}$  and

its temperature dependence. MacKnight *et al.*<sup>(99)</sup> discussed the effect on  $\chi_{\text{eff}}$  and the implications for miscibility of varying the magnitude and sign of the various  $\chi_{ij}(i \neq j)$  terms. Their findings are summarised below.

(a)  $\chi_{13}$ ,  $\chi_{23}$  and  $\chi_{12}$  All Positive

In this case there is no segmental specific interaction but miscibility can be achieved ( $\chi_{\text{eff}}$  negative) if the repulsion between the unlike copolymer segments is large enough, that is<sup>(100)</sup>

$$\chi_{12} > (\chi_{13}^{\frac{1}{2}} + \chi_{23}^{\frac{1}{2}})^2 \quad (2.67)$$

In this instance  $\chi_{\text{eff}}$  will be negative between certain copolymer compositions.

(b)  $\chi_{13}$ ,  $\chi_{23}$  and  $\chi_{12}$  All Negative

In this scenario there are specific interactions between the three segment pairs and the system will be miscible ( $\chi_{\text{eff}}$  negative) unless the magnitude of  $\chi_{12}$  exceeds the geometrical mean of the other two parameters, in which case  $\chi_{\text{eff}}$  will be positive between certain copolymer compositions.

(c)  $\chi_{23}$ , Negative,  $\chi_{13}$  and  $\chi_{12}$  Positive

This situation arises when there is a specific interaction between the homopolymer and one type of copolymer segment.  $\chi_{\text{eff}}$  will be negative at high copolymer compositions of segment 2 ( $\phi_2$ ).

Type (a) systems such as styrene-co-acrylonitrile mixed with poly(methyl methacrylate)<sup>(101)</sup> or poly(ethyl methacrylate)<sup>(102)</sup> are



well documented. The corresponding homopolymer blends are immiscible, but what MacKnight and co-workers have termed a 'window of miscibility' exists for certain copolymer compositions. This is shown quantitatively in Figure (2.7), the upper boundary to miscibility being the locus of the cloud-point curve minima. Type (b) systems have not been discovered as yet, but as shown in Figure (2.8) they would exhibit a 'window of immiscibility'. Type (c) systems have been discovered by MacKnight *et al.* (103,104) in their work on mixtures of PPO with styrene-co-  $\sigma$  or  $p$  halogenated styrenes. Poly(styrene) and PPO exhibit complete miscibility and the interaction parameter  $\chi_{PPO/St}$  has been shown by various techniques to be negative at 200°C, whilst the interaction parameters between PPO and the  $\sigma$  and  $p$  halogenated styrenes and between the comonomers have been shown to be positive. These blends exhibit a so-called 'door of miscibility' as shown in Figure (2.9).

### 2.3.2 Phase-Separation

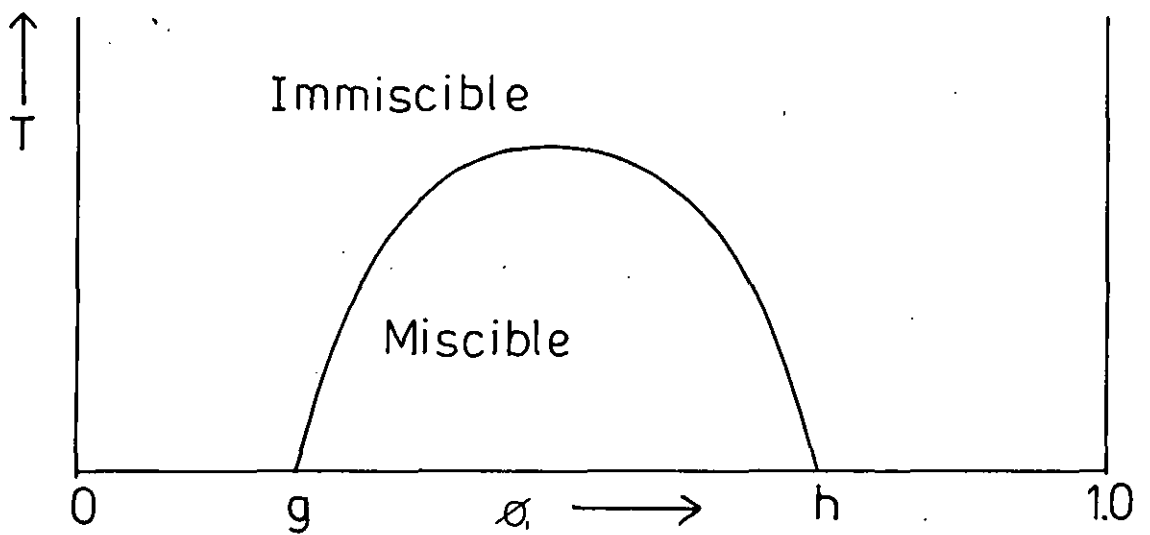
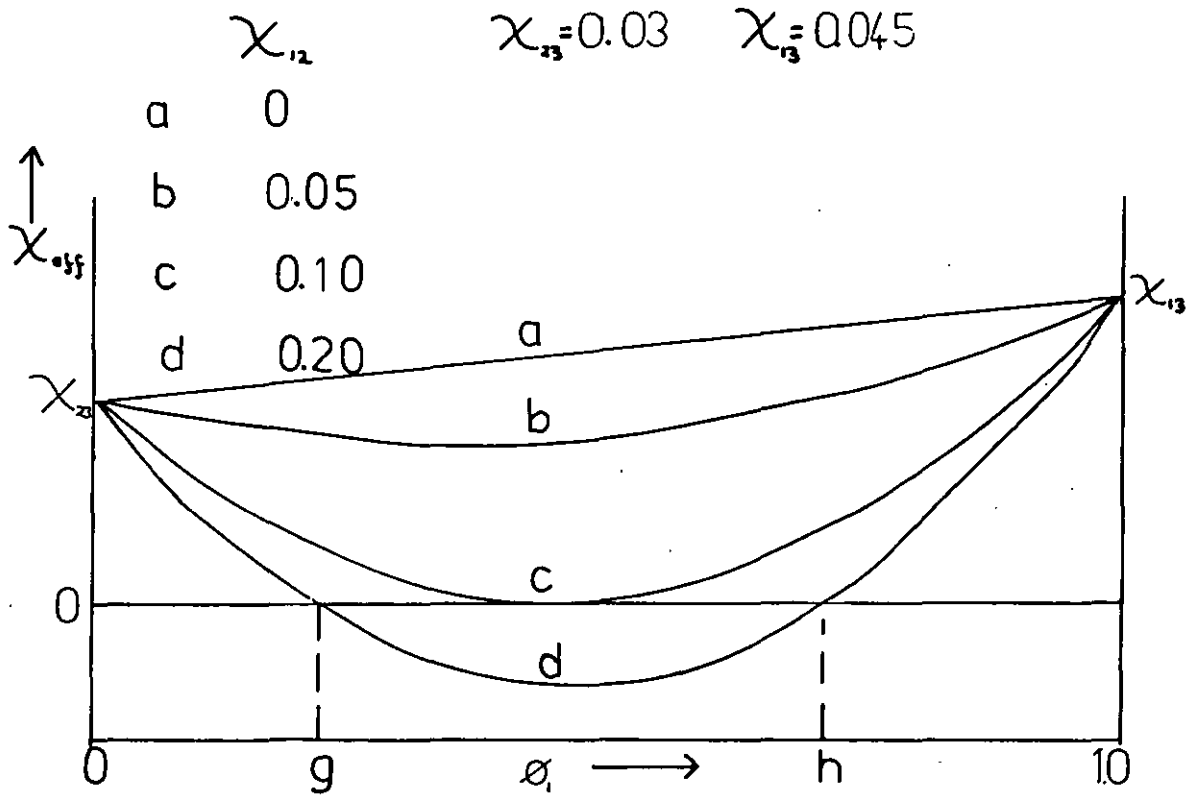
Restricting consideration to blends of type (a) which are miscible at moderate temperatures, how can one account for the observed lower critical miscibility? It has already been shown in the discussion of the Flory equation of state that for high molecular weight components miscibility is determined by the balance of the free-volume and interaction energy terms. The free-volume increases with temperature and so will the interaction energy if  $\chi_{eff} < 0$ . Consequently phase separation will occur at the temperature ( $T_1$ ) at which,

$$\chi_{eff}(T_1) + Y(T_1) = 0 \quad (2.68)$$

where  $Y$  represents the free volume terms. Consequently the implication

Figure (2.7)

Type (a) Systems



Figure(2.8)

Type (b) Systems

	$\chi_{12}$	$\chi_{23} = -0.03$	$\chi_{13} = -0.045$
a	0		
b	-0.05		
c	-0.10		
d	-0.20		

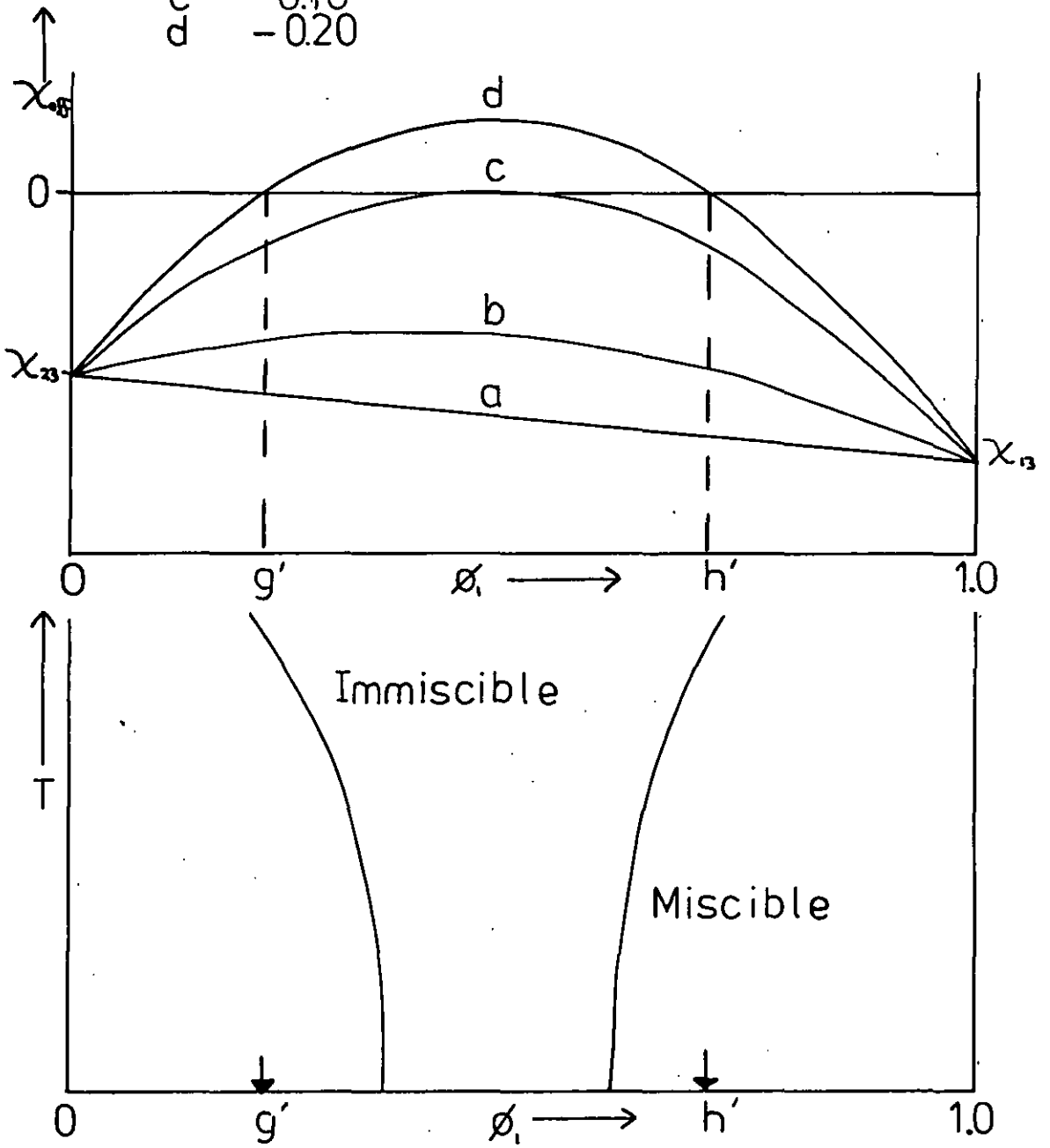
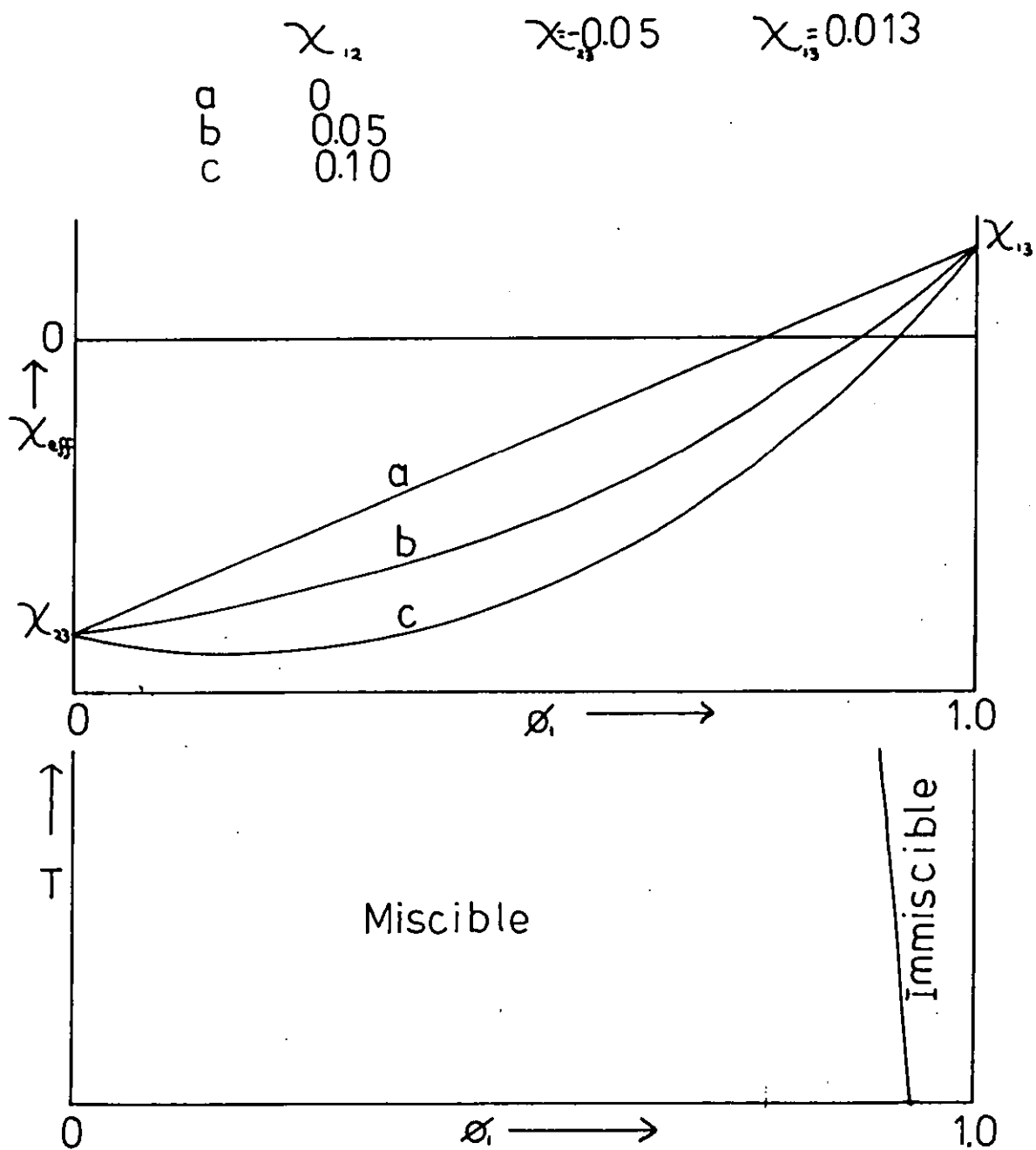


Figure (2.9)  
Type (c) Systems



of the Flory-Huggins approach that the effective interaction parameter need only be less than  $(\chi)_{CR}$  for miscibility is an oversimplification. At temperatures above  $T_1$  the free volume term will far outweigh  $\chi_{eff}$  and the mixture will lie well within the two phase region.

Macknight *et al.*<sup>(99)</sup> have shown that the copolymer composition corresponding to the maximum in the miscibility window  $(\phi_1)_m$  can be found by differentiating equation (2.68), realising that  $\chi_{eff}$  is at a minimum at this point. Thus

$$(\phi_1)_m = \frac{1}{2} + \frac{\chi_{23}(T_1) - \chi_{13}(T_1)}{2\chi_{12}(T_1)} \quad (2.69)$$

where  $T_1$  is the temperature of the maximum. Equation (2.69) implies that  $(\phi_1)_m$  will lie in the region of 0.5 for a type (a) system as  $\chi_{23}(T_1) - \chi_{13}(T_1) \ll 2\chi_{12}(T_1)$ . Macknight *et al.*<sup>(99)</sup> demonstrated the applicability of this equation by calculating  $(\phi_1)_m$  for the system PPO/ $\sigma$  chlorostyrene-co-p chlorostyrene to be  $\approx 0.55$ . It should be noted that  $(\phi_1)_m$  will only correspond to the critical point at that copolymer composition if the system is not polydisperse. Furthermore measured  $\chi$  parameters will be made up of a contribution from the exchange interaction and the free-volume, so the temperature at which measurements are made is of great importance.

The model has also been applied to mixtures of copolymers varying only in composition and to mixtures of chemically different copolymers<sup>(99,100)</sup>.

#### 2.4 MISCIBILITY PREDICTION USING SOLUBILITY PARAMETERS

The modified Flory-Huggins theory and the Flory equation of state approach have been shown to be capable of describing the miscibility behaviour of a quasi-binary polymeric mixture on an after the fact

basis. The overwhelming need is for an approach which can predict the mixing behaviour of a given polymer pair on the basis of tabulated pure component properties. It has been shown that the magnitude and sign of the binary interaction parameter plays a crucial role in determining miscibility, however no data base exists for this quantity and its measurement is not straightforward, especially for high molecular weight systems. One particular approach that has been used to estimate the value of the interaction parameter and hence infer the likely mixing behaviour of a polymer pair is that of solubility parameters.

Hildebrand<sup>(105)</sup> was the first to propose that the solubility of a solute in a range of solvents depended upon the internal pressures of the solvents. He later adopted Scatchard's<sup>(106)</sup> concept of the 'cohesive energy density' (CED) and proposed that the square root of the CED which he termed the solubility parameter ( $\delta$ ) could be used to characterise solvent properties. The approach was soon applied to polymer/solvent systems and was extended to polymer/polymer mixtures by Bohn<sup>(107)</sup>.

The solubility parameter of a species is determined by its chemical structure. Polymer/solvent or polymer/polymer compatibility is favoured if the solubility parameters of the two components are closely matched. Consequently structural similarity favours mutual solubility.

The cohesive energy of a species ( $E_{COH}$ ) is defined as the increase in internal energy per mole if all the intermolecular forces are discounted. The cohesive energy density is defined as

$$C.E.D. \equiv \frac{E_{COH}}{V} = \frac{\Delta U}{V} \quad J/cm^3 \quad (2.70)$$

The solubility parameter ( $\delta$ ) is defined as

$$\delta = \left( \frac{E_{\text{COH}}}{\tilde{V}} \right)^{\frac{1}{2}} \quad \text{J}^{\frac{1}{2}}/\text{cm.}^{\frac{3}{2}} \quad (2.71)$$

Both the C.E.D. and  $\delta$  are defined at 298K.

For volatile substances the determination of  $E_{\text{COH}}$  can be made by measuring the heat of evaporation as

$$E_{\text{COH}} = \Delta U_{\text{vap}} = \Delta H_{\text{vap}} - P\Delta\tilde{V} \quad (2.72)$$

Obviously this approach is not suited to polymers and indirect methods such as the comparative behaviour in various solvents of known C.E.D. have been used. Prediction of the C.E.D. using group additivity methods has been applied to polymers by a number of authors<sup>(108-110)</sup> and the tables they have produced have been gathered together in the text of Van Krevelen<sup>(111)</sup>. Similarly Small<sup>(112)</sup> tabulated group contributions to the molar attraction constant (F) which is defined as

$$F = (E_{\text{COH}} \tilde{V})_{T=298\text{K}}^{\frac{1}{2}} \quad (2.73)$$

Small's tables have been updated by Hoy<sup>(113)</sup> and van Krevelen<sup>(111)</sup>.

The group contribution technique of calculating  $E_{\text{COH}}$  or F and thus  $\delta$  only takes into account the chemical structure of the polymer repeat unit and the volume of a mole of repeat units.

According to Hildebrand<sup>(105)</sup> the enthalpy of mixing between two species 1 and 2 can be calculated from solubility parameters via

$$\frac{\Delta H_m}{V} = \phi_1 \phi_2 (\delta_1 - \delta_2)^2 \quad (2.74)$$

where  $V$  is the total volume of the mixture. Substitution for  $\Delta H_m$  from equation (2.21) yields the following equation where  $B$  is termed the binary interaction energy density

$$\frac{RT_X}{V_R} = B = (\delta_1 - \delta_2)^2 \quad (2.75)$$

It is obvious from equation (2.75) that using solubility parameters the enthalpy of mixing is always predicted to be greater than or equal to 0. The Hildebrand approach only takes dispersion forces into account and does not allow for specific interactions between the like or unlike components. The treatment has been extended to include the dependence of  $E_{COH}$  on the interactions of polar forces and hydrogen bonding thus

$$E_{COH} = E_d + E_p + E_h \quad (2.76)$$

where the subscripts refer to the contributions of dispersion forces, polar forces and hydrogen bonding respectively. Equation (2.74) thus becomes

$$\frac{\Delta H_m}{V} = \phi_1 \phi_2 [(\delta_{d1} - \delta_{d2})^2 + (\delta_{p1} - \delta_{p2})^2 + (\delta_{h1} - \delta_{h2})^2] \quad (2.77)$$

however as before  $\Delta H_m \geq 0$ . Furthermore, comprehensive tables for  $E_p$  and  $E_h$  are not available.

For a quasi-binary mixture miscibility can only be predicted on the basis of a matching of dispersion forces which severely limits the applicability of the approach. Nevertheless, Krause<sup>(114)</sup> has



set out a technique for predicting miscibility in dispersion dominated systems which can prove useful in certain cases. This involves calculation of  $\chi$  from equation (2.75) and its comparison with the critical value  $(\chi)_{CR}$  calculated from equation (2.43). If  $\chi > (\chi)_{CR}$ , immiscibility is predicted and vice versa.

Let us now examine another type of system also dominated by dispersion forces, namely random copolymer/homopolymer mixtures.

The analogous expression to equation (2.75) is

$$B = (\delta_{cop} - \delta_3)^2 \quad (2.78)$$

where 
$$\delta_{cop} = \delta_1 \phi_1 + \delta_2 \phi_2 \quad (2.79)$$

Once again  $B \geq 0$  and the Krause<sup>(114)</sup> technique can be used to gauge the range of copolymer compositions over which miscibility can be expected for various average chain lengths. Paul<sup>(100)</sup> however has recently shown that slight relaxation of the C.E.D. definition can result in exothermic mixing predictions ( $B < 0$ ).

## 2.5 THE GLASS TRANSITION TEMPERATURE

### 2.5.1 Definition of the Glass Transition Temperature

When an amorphous high molecular weight polymer is cooled through the glass transition region, its properties change from those of a soft, flexible rubber to those of a hard, brittle glass. Consequently within this region many thermodynamic and physical properties undergo a marked change.

At constant pressure the temperature dependence of quantities such as the volume, enthalpy, entropy, thermal expansion coefficient and specific heat undergo a discontinuity in the glass transition

region<sup>(115,116)</sup>. The glass transition temperature ( $T_g$ ) can be defined as the temperature at the point of intersection of the extrapolated curves for the melt and the glass when any of the above quantities are measured against temperature. A typical volume temperature relationship is given in Figure (2.10) for an amorphous polymer. The figure shows that more than one glass type can be formed from the same melt if different cooling rates are used. It is immediately apparent that  $T_g$  is in part dependent upon thermal history.

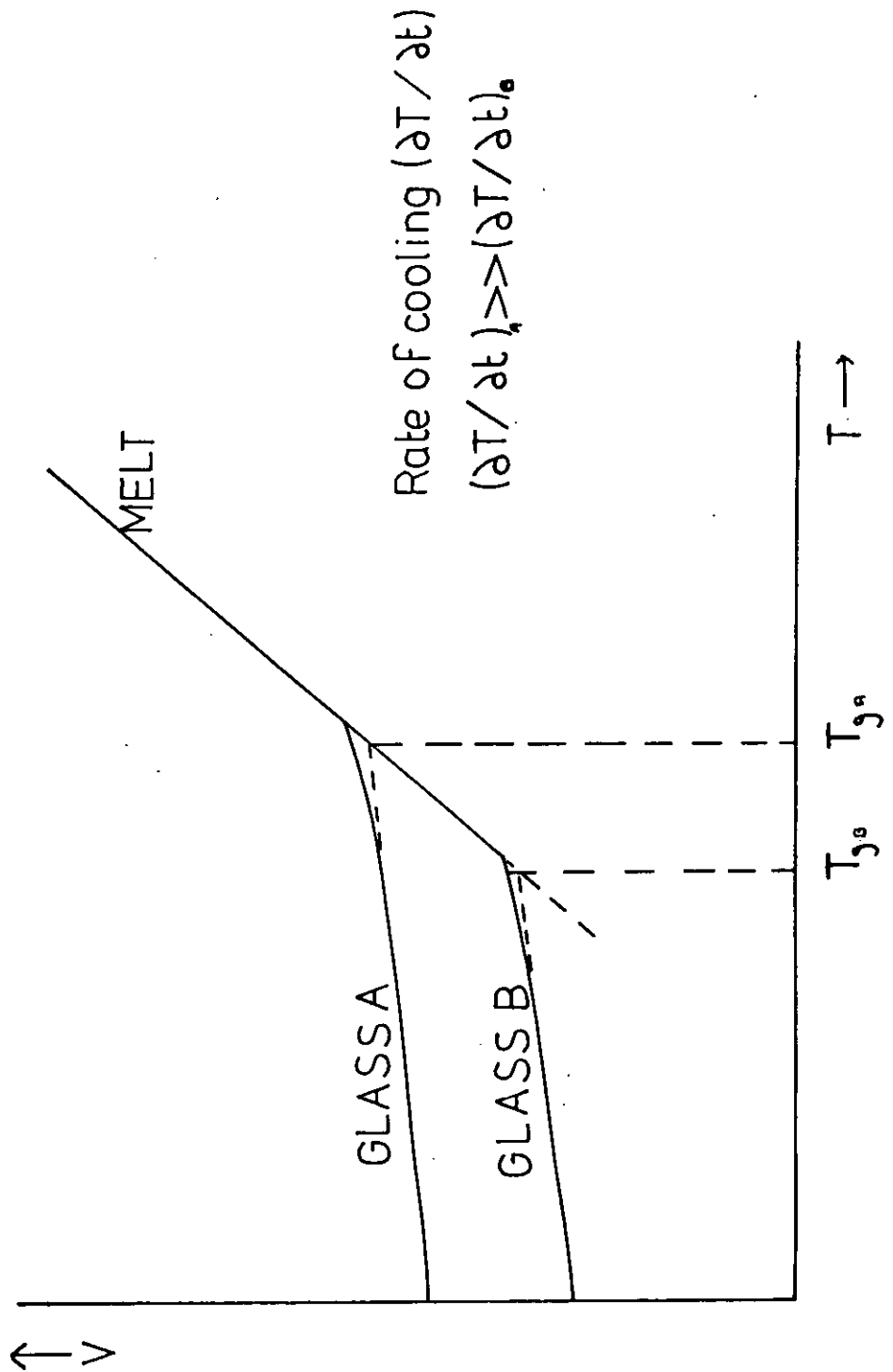
Rehage and Borchard<sup>(115)</sup> investigated the question of how appropriate it was to regard the glass transition as a true thermodynamic transition. They found that the temperature dependence of  $V$ ,  $H$ ,  $S$ ,  $\alpha$ ,  $C_p$  and  $\beta$  most closely resembled second-order transitions, but did exhibit significant differences especially with regard to rate effects. Furthermore unlike in a true second order transition the glass transition is not a divide between equilibrium thermodynamic states.

In terms of molecular behaviour  $T_g$  is widely interpreted as the temperature above which the polymer has acquired sufficient thermal energy for conformational changes, due to rotation about most of the bonds in the backbone of the molecule, to occur. Although segmental motion does occur within the glassy state, as evidenced by sub- $T_g$  transitions measured for many polymers, it tends to be subject to severe restrictions and occurs on a much more limited scale than above  $T_g$ .

The glass transition temperature does not lend itself to a single theoretical treatment enjoying widespread concord. The most popular treatments tend to lie within two opposing camps which can be broadly viewed as giving either a kinetic or a thermodynamic explanation of the phenomenon. Neither explanation has proved wholly successful

Figure (2.10)

Volume -Temperature Relationship for a Typical Amorphous Polymer



and it seems likely that the true interpretation lies somewhere in between.

### 2.5.2 Kinetic Theories

The rapid increase in conformational changes which occurs on heating an amorphous polymer through the glass transition region cannot be explained as being due to the surmounting of a single potential energy barrier. The kinetics of volume or viscosity changes with temperature do not follow an Arrhenius type relationship characterised by a single activation energy except at temperatures well above  $T_g$ . It has been shown repeatedly<sup>(117,118)</sup> that a wide spectrum of relaxation times, corresponding to a similarly wide range of energy barriers, is necessary to describe the behaviour of a polymer in the glass transition zone. Numerous attempts have been made to model relaxation behaviour using combinations of Maxwell and Voigt elements<sup>(118)</sup>. A Maxwell element consists of a spring and dashpot arranged in series whilst a Voigt element has the components in parallel. Each element in a particular model has a characteristic relaxation time corresponding to a molecular process. However, this approach does not generally yield a quantitative analysis of the glass transition. A much more widely used approach, because of its success in quantifying much of the observed behaviour in the transition region, is the kinetic free volume theory.

The kinetic theory of Flory<sup>(119,120)</sup> and Fox offers the following definition of free volume which has been defined differently by other authors. A material in the condensed state is regarded as having two contributions to its volume. The volume is partly occupied by molecules and part consists of vacancies, the sum of the latter being the free volume. Changes in conformation are regarded as movements

into the unoccupied volume and the amount of free volume present therefore defines the molecular mobility possible. Consequently the glass transition temperature is regarded as the point below which insufficient free volume exists for extensive conformational changes, resulting in an essentially "frozen" structure.

Below  $T_g$  the free volume is regarded as being constant; volume changes in the glass with temperature being due to molecular expansion or contraction. Consequently the total volume at  $T_g$  ( $V_g$ ) is given by

$$V_g = V_o + V_f + \left( \frac{dV}{dT} \right)_g T_g \quad (2.80)$$

where  $V_o$  is the occupied volume of the glass at absolute zero,  $V_f$  represents the free volume within the glassy region and  $(dV/dT)_g$  is the expansivity of the occupied volume in the glass. At  $T > T_g$  the total volume ( $V_R$ ) is given by

$$V_R = V_g + (dV/dT)_R (T - T_g) \quad (2.81)$$

$(dV/dT)_R$  represents the expansivity of the total volume above  $T_g$  and hence consists of both the molecular and free volume expansions.

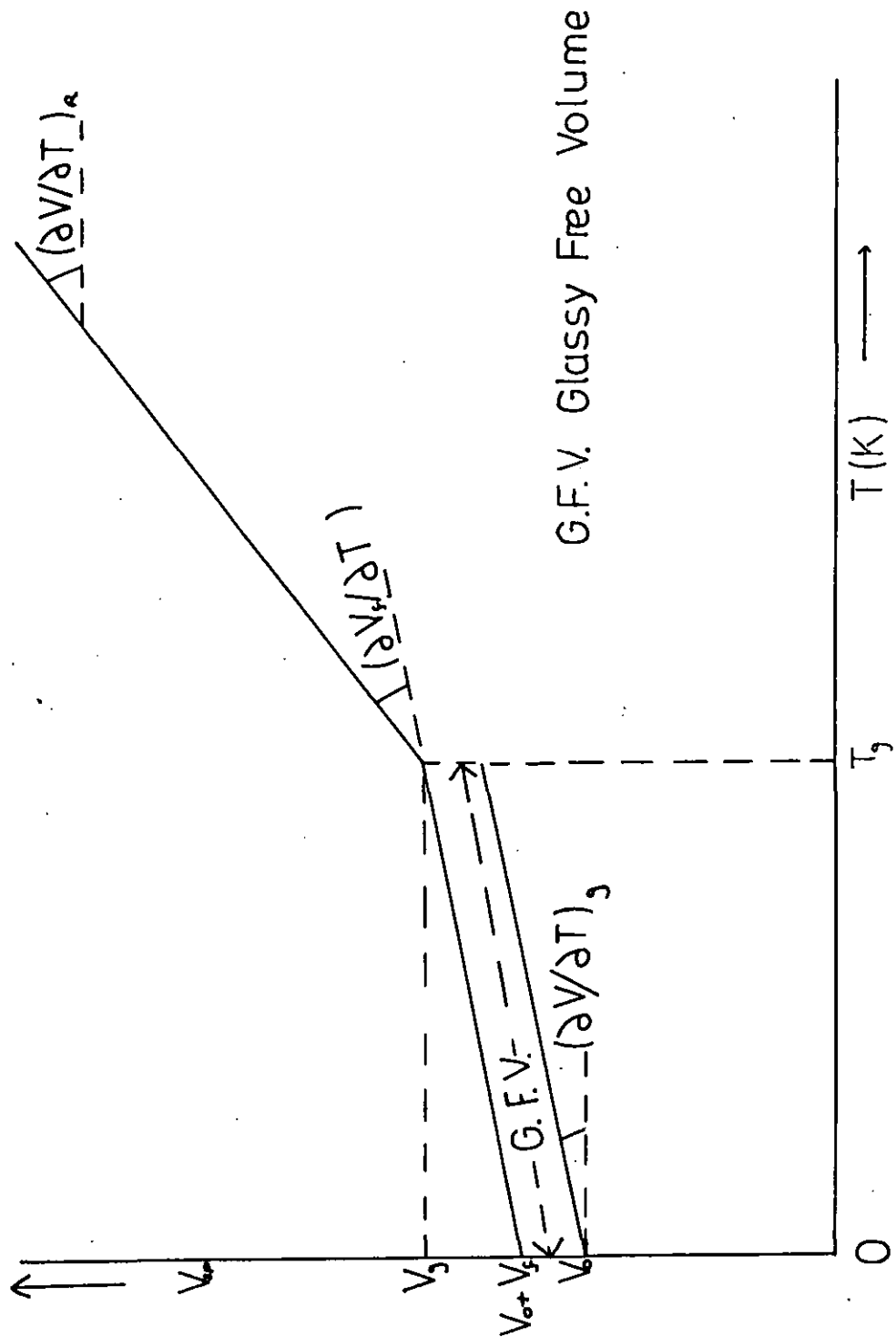
$$\left( \frac{dV_f}{dT} \right) = \left( \frac{dV}{dT} \right)_R - \left( \frac{dV}{dT} \right)_g \quad (2.82)$$

The above definitions are shown schematically in Figure (2.11) where specific volume is plotted against absolute temperature.

If the thermal expansion coefficients immediately above and below  $T_g$  are given by

Figure(2.11)

Variation of Specific Volume with Temperature



$$\alpha_R = \frac{1}{V_g} \left( \frac{dV}{dT} \right)_R \quad \text{and} \quad \alpha_g = \frac{1}{V_g} \left( \frac{dV}{dT} \right)_g \quad (2.83)$$

then the volume expansion of free volume in the region of  $T_g$  is given

by  $\alpha_R - \alpha_g = \Delta\alpha$ .

Doolittle<sup>(121,122)</sup> invoked the concept of free-volume in his empirical relationship between viscosity and volume which proved successful in treating small molecule liquids. In this equation A and B are constants and  $\eta$  is the viscosity of the liquid

$$\ln \eta = \ln A + B[(V - V_f)/V_f] \quad (2.84)$$

Defining the fractional free volume  $f$  as  $V_f/V$ , this equation can be rewritten as

$$\ln \eta = \ln A + B(1/f - 1) \quad (2.85)$$

If  $T_g$  is used as a reference point, the viscosity of a liquid at a temperature  $T$  ( $T > T_g$ ) is given by

$$\ln \left( \frac{\eta}{\eta_g} \right) = B \left( \frac{1}{f} - \frac{1}{f_g} \right) \quad (2.86)$$

where  $\eta_g$  and  $f_g$  represent the viscosity and fractional free volume at  $T_g$ . The value of  $f$  is taken to increase in a linear fashion above  $T_g$  and can therefore be rewritten as

$$f = f_g + \Delta\alpha(T - T_g) \quad (2.87)$$

Substitution of equation (2.87) into equation (2.86) yields

$$\ln \left( \frac{\eta}{\eta_g} \right) = \frac{B}{f_g} \left( \frac{T - T_g}{f_g/\Delta\alpha + (T - T_g)} \right) \quad (2.88)$$

Equation (2.88) is of the same form as the empirical relationship developed by Williams, Landel and Ferry<sup>(123)</sup> (WLF) found to be suitable for describing mechanical and electrical relaxation times in the region from  $T_g$  to  $(T_g + 100)$ . For many polymers the following expression has proved valid

$$\log a_T = \frac{-17.44(T - T_g)}{51.6 + (T - T_g)} \quad (2.89)$$

where  $a_T$  is the ratio of a relaxation time at  $T$  to the relaxation time at  $T_g$ . Rewriting the Doolittle equation in terms of logs and assuming that the value of  $B$  is unity as found for simple liquids, one obtains

$$\log a_T = \frac{-(T - T_g)}{2.303f_g(f_g/\Delta\alpha + (T - T_g))} \quad (2.90)$$

Comparison of equations (2.89) and (2.90) gives values of  $f_g$  (0.025) and  $\Delta\alpha$  ( $4.8 \times 10^{-4} \text{ K}^{-1}$ ) which were thought at one time to be universal constants. However, it has since been shown experimentally that  $\Delta\alpha$  does vary between polymers, yielding a range of values for the fractional free volume in the glassy state ( $\approx 0.015 - 0.036$ ).



### 2.5.3 Thermodynamic Theories

The glassy state has already been presented on a segmental level as a virtually unchanging picture of the liquid state at a single moment in time. Disorder is locked in and the degree of disorder is dependent upon the rate at which the glassy state is approached. Thermodynamic theories of  $T_g$  advance the notion that there is a true equilibrium glassy state underlying the rate dependent measured  $T_g$ s. It is proposed that this state could be attained theoretically by cooling from the melt at an infinitely slow rate.

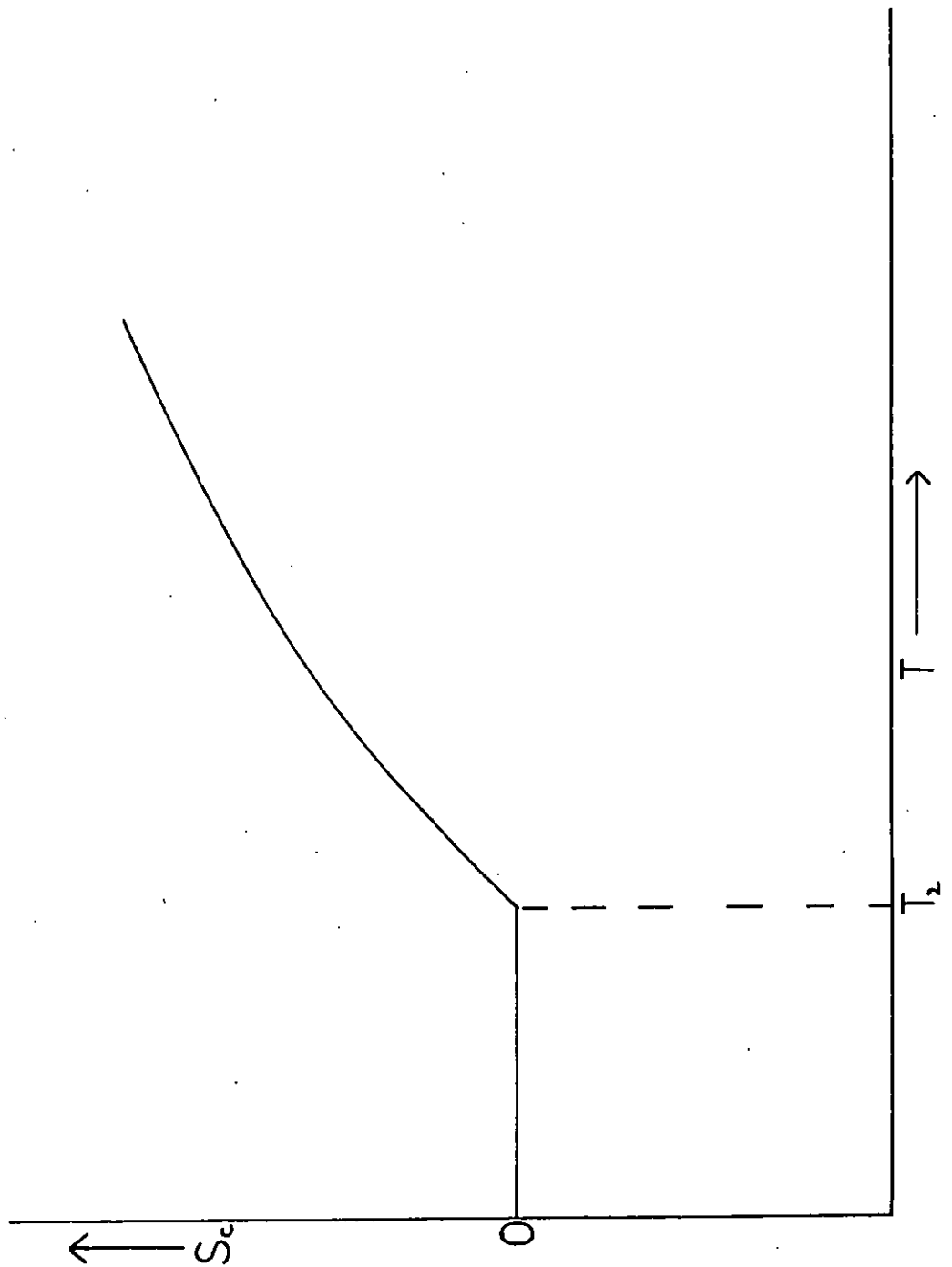
Kauzmann<sup>(124)</sup> analysed the available thermodynamic data for glass forming materials and demonstrated that the extrapolated entropy of the supercooled liquid at absolute zero was less than that of the crystalline state. The point of intersection of the entropy versus temperature plots for the supercooled liquid and the crystal may be regarded as the equilibrium glass transition temperature.

The most widely known thermodynamic theory of the glass transition was developed by Gibbs and DiMarzio<sup>(125-128)</sup>. They employed a lattice model akin to that used by Flory and Huggins. Each lattice site being defined such that it can accommodate a single chain segment and vacant sites allow for configurational changes.

Upon cooling a molecule is envisaged as having progressively fewer conformations available to it and thus appears to become more rigid and less mobile. A temperature  $T_2$  is defined as being a true second order transition temperature. At  $T_2$  it is assumed that there are no conformational changes available to the molecule which consequently has zero configurational entropy. This is depicted in Figure (2.12).

Figure (2.12)

Variation of Configurational Entropy with Temperature for a Glass Forming Liquid



Gibbs and DiMarzio have calculated a configurational partition function in terms of the hindered rotation about the main chain bonds in the molecule. The most significant term in determining  $T_2$  concerns the intramolecular rotational energy barriers. At temperatures just above  $T_2$  the energy barrier between one conformation and another is very high, consequently one would expect a slow response to the application of any external force. Some justification for the existence of  $T_2$  is the fact that dielectric and viscoelastic relaxation times have been shown to increase as temperatures fall in the direction of  $T_2$ . However acceptance of the concept of  $T_2$  is by no means universal.

The Gibbs-DiMarzio approach has been extended to include non-equilibrium conditions in the theory of Adam and Gibbs<sup>(129)</sup>. Their theory relates relaxational properties to  $T_2$ . The temperature dependence of the relaxation behaviour is explained in terms of the variation of the size of a 'co-operatively rearranging' region. This is defined as the smallest unit that can undergo a transition to a new configuration without simultaneous configurational change on or outside its boundary. At  $T_2$  the CRR must be the same size as the sample as there is only one available configuration. At temperatures well above  $T_2$  the large number of available configurations provides for individual mutations in a wealth of tiny co-operative regions.

Adam and Gibbs derived an expression similar in form to the W.L.F. equation

$$-\log a_T = \frac{a_1 (T - T_S)}{(a_2 + (T - T_S))} \quad (2.91)$$

where  $T_S$  is a reference temperature and  $a_1$  and  $a_2$  are defined as

$$a_1 = \frac{2.303C}{\Delta C_p T_s \ln(T_s/T_2)} \quad (2.92)$$

$$a_2 = \frac{T_s \ln(T_s/T_2)}{\ln(T_s/T_2) + [1 + T_s/(T - T_s)] \ln(T/T_s)} \quad (2.93)$$

In fact  $a_2$  is temperature dependent but only to a degree which marginally effects the calculations. If the appropriate value of  $T_s$  is used  $a_1$  and  $a_2$  closely approximate to the W.L.F. constants. The approach to a generally applicable expression is consequently shown to be possible without invoking the concept of free volume.

The Adam-Gibbs theory does contain elements of both thermodynamic and kinetic explanations of  $T_g$  in that the thermodynamic properties of the equilibrium melt are used to explain the kinetic properties of a glass-forming liquid.

#### 2.5.4 Factors Which Influence the Glass Transition Temperature

Both the free-volume and Gibbs-DiMarzio theories of the glass transition can rationalise the observed shifts in  $T_g$  in response to changes in one or more properties of the material. The principal factors which influence  $T_g$  are:- the chemical structure of the polymer; the degree of cross-linking; the molecular weight; the presence of diluents; and copolymerisation. These factors are discussed below.

##### (a) Chemical Structure

Intramolecular considerations tend to dominate the relation between chemical structure<sup>(130)</sup> and  $T_g$ . The most important factor is the degree of flexibility of the backbone polymeric chain. If one considers a vinyl type polymer  $(CH_2CHX)_n$  the size of the side

group X has a profound influence on  $T_g$ . Increasing X from hydrogen to a methyl group increases  $T_g$  by over a hundred degrees whilst if X is a benzene ring  $T_g$  is raised over two hundred degrees above that of poly(ethylene). However  $T_g$  depends also on the flexibility of the side group thus if X is an alkyl group going from methyl to ethyl for example lowers  $T_g$  by some fifteen degrees. In this case the expected elevation of  $T_g$  due to the increased size of the substituent is more than outweighed by its increased flexibility. The Gibbs-DiMarzio<sup>(126)</sup> theory explains the effect of substituent size in terms of the flex energy. This flex energy is the potential energy barrier between favoured conformational attitudes of the polymer chain segments. As the size of a side group increases so does the steric hindrance and hence the flex energy.

Symmetry in a repeat unit also influences  $T_g$ . Generally as symmetry increases,  $T_g$  is depressed. Taking poly(vinyl chloride) as an example ( $T_g = 87^\circ\text{C}$ ), the addition of a second chlorine group on an adjacent carbon (poly(vinylidene chloride)) decreases  $T_g$  by about  $100^\circ\text{C}$ . It appears that although the introduction of a second substituent has raised the flex energy and the absolute values of the potential energy minima, the energy difference between the stable conformations has been reduced.

The polarity or cohesive energy density of a substituent may also effect  $T_g$ . Poly(acrylonitrile) has a  $T_g$  over a hundred degrees above that of poly(propylene) due to increased, intermolecular forces. Bueche<sup>(117)</sup> has interpreted this observation in terms of the reduced expansion of a polymer with strong intermolecular attractions. Upon heating, the required fractional free volume for  $T_g$  to occur is achieved at an elevated temperature.

(b) Cross-linking

Nielson<sup>(131,132)</sup> has reviewed the effect of cross-linking upon  $T_g$  and has demonstrated that  $T_g$  increases with the degree of network formation. Free-volume is decreased by the process so the required fractional free volume necessary for the glass transition to occur is attained at higher temperatures. Thermodynamic treatments of  $T_g$  explain the process in terms of the decreased configurational entropy in the cross-linked state.

(c) Molecular Weight

For many polymers  $T_g$  has been shown to vary in an inverse fashion with molecular weight. This observation can be simply explained in terms of free volume<sup>(120)</sup>, the basis of the argument being that chain ends contribute more free volume than repeat units which are chemically bound at both ends. As the molecular weight of a polymer decreases the number of chain ends per unit volume rises giving a concurrent increase in fractional free volume. Consequently the temperature at which the fractional free volume reaches the glass-forming proportion is depressed. The considerations can be used to derive the following equation as shown by Bueche<sup>(117)</sup>

$$T_g = T_{g\infty} - K/M \quad (2.94)$$

where  $T_{g\infty}$  is the glass temperature of a polymer of infinite molecular weight,  $K$  is a constant and  $M$  is the molecular weight.

(d) The Effect of Diluents

The addition of compatible low molecular weight substances to polymers results in a reduction of  $T_g$ . The process is known as

plasticization and has been used in industry since the earliest days of polymer production. An example being the use of camphor to plasticize cellulose nitrate.

In terms of free-volume the effect can be viewed as resulting from an increase in the free volume of the system due to the addition of the diluent. The diluent contains more free volume than the pure polymer and assuming additivity, the plasticized polymer must be cooled to a lower temperature before the fractional free volume reaches the level at which the glassy state is entered.

If a second polymer is added instead of the plasticizer the  $T_g$  of the system depends upon the miscibility of the two components and the respective homopolymer  $T_g$ 's. When the two components are completely miscible the system exhibits a single  $T_g$  which lies between the component  $T_g$ 's; the position depending upon the composition of the mixture. A partially miscible system exhibits a  $T_g$  for each mixed phase whose positions vary according to the respective phase compositions. Immiscible blends demonstrate the transitions characteristic of the pure components.

A number of equations have been advanced to relate the  $T_g$  of a miscible polymer mixture to the  $T_g$ 's of the pure components. The equations were first developed to treat random copolymers and are consequently described in the next section. It should be noted that these relationships can also be applied to low molecular weight plasticizers, which have glass transitions in the range from  $-50^\circ\text{C}$  to  $-150^\circ\text{C}$ <sup>(130)</sup>.

#### (e) Copolymerisation and Blending

When two chemically different monomers are polymerised together to form a random, amorphous copolymer the glass transition of the

copolymer lies somewhere between the respective glass transitions of the homopolymers derived from the comonomers. Wood<sup>(133)</sup> has shown that the relationship between the copolymer glass transition ( $T_g$ ) and the homopolymer glass transitions derived from comonomers A and B ( $T_{gA}, T_{gB}$ ) is of the general form

$$T_g = A_A T_{gA} c_A + A_B T_{gB} c_B \quad (2.95)$$

where  $c_i$  is the concentration of repeat unit  $i$  in the copolymer and  $A_i$  is a constant relating to a property of homopolymer  $i$ .

Gordon and Taylor<sup>(134)</sup> derived an expression of this form by making the following suppositions. They assumed that in an ideal copolymer the partial specific volumes of the components are constant and equivalent to the specific volumes of the two homopolymers. It was also assumed that the thermal expansion coefficients in the rubbery and glassy states are the same in the copolymer as in the homopolymers. The copolymer  $T_g$  is found by equating the specific volumes in the glassy and rubbery states, resulting in the expression

$$T_g = \frac{T_{gA} + (KT_{gB} - T_{gA})w_B}{1 - (1 - K)w_B} \quad (2.96)$$

where 
$$K = \frac{A_B}{A_A} = \frac{[(\alpha_B/\rho_B)_r - (\alpha_B/\rho_B)_g]}{[(\alpha_A/\rho_A)_r - (\alpha_A/\rho_A)_g]} \quad (2.97)$$

The term  $\alpha_i/\rho_i$  is the specific thermal expansivity of component  $i$  and  $w_B$  is the weight fraction of repeat unit B in the copolymer. Mandelkern *et al.*<sup>(135)</sup> derived a similar expression using the Flory-Fox free volume theory.



The widely used Fox<sup>(136)</sup> relationship

$$\frac{1}{T_g} = w_A \frac{1}{T_{gA}} + w_B \frac{1}{T_{gB}} \quad (2.98)$$

can be seen as a special case of the Gordon-Taylor equation, when  $K$  is equal to the ratio of the equivalent homopolymer glass transition temperatures ( $T_{gA}/T_{gB}$ ). The Kelley-Bueche<sup>(137)</sup> equation which relates the composition dependence of  $T_g$  in polymer-diluent systems also has a similar form to the G-T equation,

$$T_g = \frac{\Delta\alpha_A \phi_A T_{gA} + \Delta\alpha_B \phi_B T_{gB}}{\Delta\alpha_A \phi_A + \Delta\alpha_B \phi_B} \quad (2.99)$$

the concentrations being expressed in volume fractions.

Gibbs and DiMarzio<sup>(138)</sup> have given a thermodynamic interpretation of the glass transition in random copolymers. As the configurational entropy is zero at  $T_{2i}$  for the two homopolymers

$$S\left(\frac{\epsilon_A}{kT_{2A}}\right) = S\left(\frac{\epsilon_B}{kT_{2B}}\right) = 0 \quad (2.100)$$

where  $\epsilon_i$  is the stiffness energy of the rotatable chemical bonds of homopolymer  $i$ .  $T_g$  is assumed to be independent of molecular weight so that entropy is only a function of  $(\epsilon/kT)$ . If  $\epsilon_A$  and  $\epsilon_B$  are similar then an average stiffness energy can be calculated for the copolymer

$$\epsilon = B_A \epsilon_A + B_B \epsilon_B \quad (2.101)$$

where  $B_i$  is the fraction of rotatable bonds of type  $i$ . Consequently for the copolymer it follows that

$$S \left( \frac{B_A \epsilon_A + B_B \epsilon_B}{kT_2} \right) = 0 \quad (2.102)$$

Equating this expression with equation (2.100) and substituting weight fractions for bond fractions one obtains

$$w_A \left( \frac{x_A}{M_A} \right) (T_2 - T_{2A}) + w_B \left( \frac{x_B}{M_B} \right) (T_2 - T_{2B}) = 0 \quad (2.103)$$

where  $x_i$  is the number of flexible bonds of repeat unit  $i$  with molecular weight  $M_i$ . The above equation relates the second order transition temperatures and not the observed glass temperatures. However application of the equation to  $T_g$  can be made within acceptable error limits.

The Gibbs-DiMarzio treatment does not consider the effect of A-B linkages in the copolymer. The stiffness energy of these linkages bears no unique correspondence to  $\epsilon_A$  and  $\epsilon_B$  and consequently the validity of equation (2.103) is dependent upon the number of A-B bonds. Applying the same consideration to the free volume treatments shows the other copolymer equations to have a similar deficiency. Furthermore a large number of measured copolymer systems show substantial deviations from the predicted values of  $T_g$ . This has led to efforts<sup>(139,140)</sup> to produce a copolymer equation which properly accounts for the observed results. The most practical approach is that of Johnston<sup>(141,142)</sup> which considers the sequence distribution of the copolymer. Homopolymer  $T_g$ 's hold for AA and BB dyads, whilst

AB dyads and other sequences are assigned their own  $T_g$  values. The probabilities of like ( $P_{AA}$ ) and unlike linkages ( $P_{AB}$ ) can be calculated using the expressions given in section (2.9.2). The resulting equation, accounting for the various dyads is

$$\frac{1}{T_g} = \frac{w_A P_{AA}}{T_{gAA}} + \frac{w_A P_{AB} + w_B P_{BA}}{T_{gAB}} + \frac{w_B P_{BB}}{T_{gBB}} \quad (2.104)$$

which can also be extended to deal with triads where necessary. Johnston<sup>(142)</sup> has described a number of methods for the determination of  $T_{gAB}$ , all of which use the experimentally determined  $T_g$ 's of a series of copolymers.

Miscible polymer blends have been reported<sup>(9)</sup> which exhibit a composition dependent  $T_g$  which can be approximated by one of the aforementioned expressions. However, many studies have presented data which does not conform to a simple relationship between the component homopolymer  $T_g$ 's. This is not surprising as although miscible blends do not contain covalent A-B bonds, in many systems the driving force for miscibility has been shown to be A ... B specific interactions giving rise to negative binary interaction parameters and thereby negative enthalpies of mixing. The interacting segments require a treatment similar to that of dyad sequences in copolymers but to date there has been no effort in this regard.

Couchman and Karasz<sup>(143,144)</sup> have presented a classical thermodynamic discussion of the composition dependence of  $T_g$  specifically applicable to miscible polymer mixtures. Two relations for blend  $T_g$ 's in terms of pure component properties were derived. One arising from the entropy continuity condition at  $T_g$ , the other from the volume continuity condition. In the derivations a quantitative argument was

used to justify disregarding the excess entropy ( $\Delta S_m$ ) and volume changes ( $\Delta V_m$ ) on mixing in terms of their influence on  $T_g$ . Thus  $\Delta S_m$  and  $\Delta V_m$  were assumed to be continuous at  $T_g$ , an assumption whose validity essentially depends on the nature and extent of specific interaction in a particular system. The entropy derived equation was of the following form for a quasi-binary mixture

$$\ln T_g = \frac{w_A \Delta C_{pA} \ln T_{gA} + w_B \Delta C_{pB} \ln T_{gB}}{w_A \Delta C_{pA} + w_B \Delta C_{pB}} \quad (2.105)$$

where the respective heat capacity differences ( $\Delta C_{pi}$ ) between the glassy and rubbery states in the pure components are assumed to be temperature independent and are defined per unit mass. The volume derived equivalent of equation (2.105) was identical to the Kelley-Bueche equation (2.99). The original quantitative analysis<sup>(144)</sup> and later experimental work which has recently been reviewed<sup>(145)</sup> indicate that the entropy derived expression is the more generally applicable.

Recently Goldstein<sup>(152)</sup> has shown that the Couchman-Karasch expressions cannot be justified from a purely thermodynamic standpoint. This is because the entropy of mixing derived by the latter authors is inappropriate when either or both components are in the glassy state. Goldstein further indicated that a suitable redefinition of  $\Delta S_m$  did not lead to a prediction of the glass transition temperature of the blend. However an identical expression to (2.105) can be derived from the Gibbs-DiMarzio molecular theory of  $T_g$  and the success of this equation can therefore be viewed as a justification of the Gibbs-DiMarzio approach.

## 2.6 DIELECTRIC RELAXATION

A dielectric material is one in which the application of an electrical field causes a reversible change in the orientation of the various electric components of the material. The dielectric constant ( $\epsilon$ ) of such an insulating material is the ratio of the capacities of a parallel plate condenser measured with and without the sample between the plates ( $C_S/C_0$ ). The difference is due to the polarization of the dielectric which has three components.

### 2.6.1 Polarization

#### (a) Electronic Polarization

When subjected to an electric field the electrons of an atom are shifted slightly relative to the nucleus. This displacement is small because the applied field is usually overshadowed by the atomic field between nuclei and electrons. Electronic polarization ( $P_e$ ) can respond to very high frequencies and is responsible for the refraction of light. The dielectric constant at such frequencies ( $\epsilon_u$ ) be expressed in terms of the refractive index ( $n$ ) by Maxwell's relationship

$$\epsilon_u = n^2 \quad (2.106)$$

In materials that have no permanent dipole moment the electronic polarization is the main contributor to the molecular polarization. The comparatively small contribution that the electronic polarization makes to the dielectric constant means that  $\epsilon$  is low in such materials.

#### (b) Atomic Polarization

Atomic polarization ( $P_A$ ) is the result of movement of nuclei in

a molecule or lattice under the influence of an electric field. Due to the mass difference between nuclei and electrons the response of the former is much slower, consequently atomic polarization is not observed above infra-red frequencies. The modes of displacement that comprise atomic polarization are bending and stretching. The bending mode is generally less energetic and makes the major contribution to atomic polarization. Atomic polarization is usually of the order of a tenth of that of electronic polarization except in ionic materials.

(c) Orientation Polarization

In the case of molecules containing a permanent dipole moment, there is a tendency for these to be aligned by the applied force yielding a net polarization in that direction. The rate of dipolar orientation is highly dependent on intermolecular forces but usually makes a large contribution to the total polarization of a material in an electric field. The characteristic response of the molecular polarization and thus the dielectric constant to increasing measurement frequency is shown in Figure (2.13).

2.6.2 Dielectric Dispersion

When a polar material is placed in an alternating field it experiences an alternating polarization. If polarization is measured instantaneously so that dipole alignment is not given time to occur then the corresponding dielectric constant is given the symbol  $\epsilon_u$ , the subscript referring to the unrelaxed state. The dielectric constant measured after orientation has occurred is termed relaxed (static) and is symbolised by  $\epsilon_r$ .

If the applied field has alternating voltage  $V$  and frequency  $\omega$

Figure(2.13)  
 Variation of Molecular Polarisation  
 with Frequency

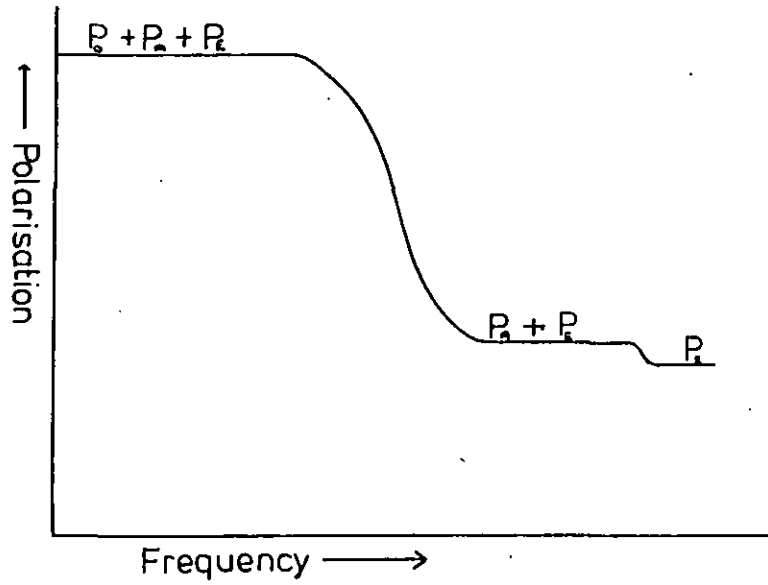
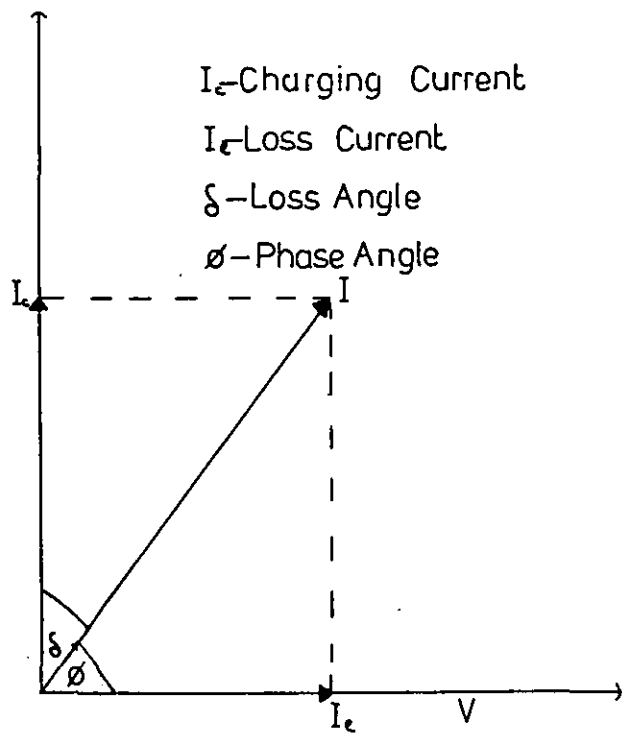


Figure (2.14)  
 Vector Diagram for a Capacitor with  
 Dielectric Exhibiting Relaxation



(in radians) a complex alternating current ( $I^*$ ) results which is made up of the loss current ( $I_1$ ) and the charging current  $I_C$  such that

$$I^* = I_1 + j I_C \quad (2.107)$$

where  $j$  is  $(-1)^{0.5}$ . This relationship is shown diagrammatically in Figure (2.14). The charging current charges the capacitor to the required instantaneous voltage and leads the voltage by  $90^\circ$ . The loss current is in phase with  $V$  and comes about if polarization cannot keep in phase with the applied voltage. Equation (2.107) can be rewritten as

$$I^* = j\omega\epsilon^* C_0 V \quad (2.108)$$

where  $\epsilon^*$  is the complex dielectric constant, defined as

$$\epsilon^* = \epsilon' - j\epsilon'' \quad (2.109)$$

The real part of  $\epsilon^*$  is termed the dielectric constant or relative permittivity whilst the imaginary term is called the loss factor.

The loss angle  $\delta$  shown in Figure (2.14) is related to  $\epsilon'$  and  $\epsilon''$  via the well known relationship

$$\tan \delta = \epsilon''/\epsilon' \quad (2.110)$$

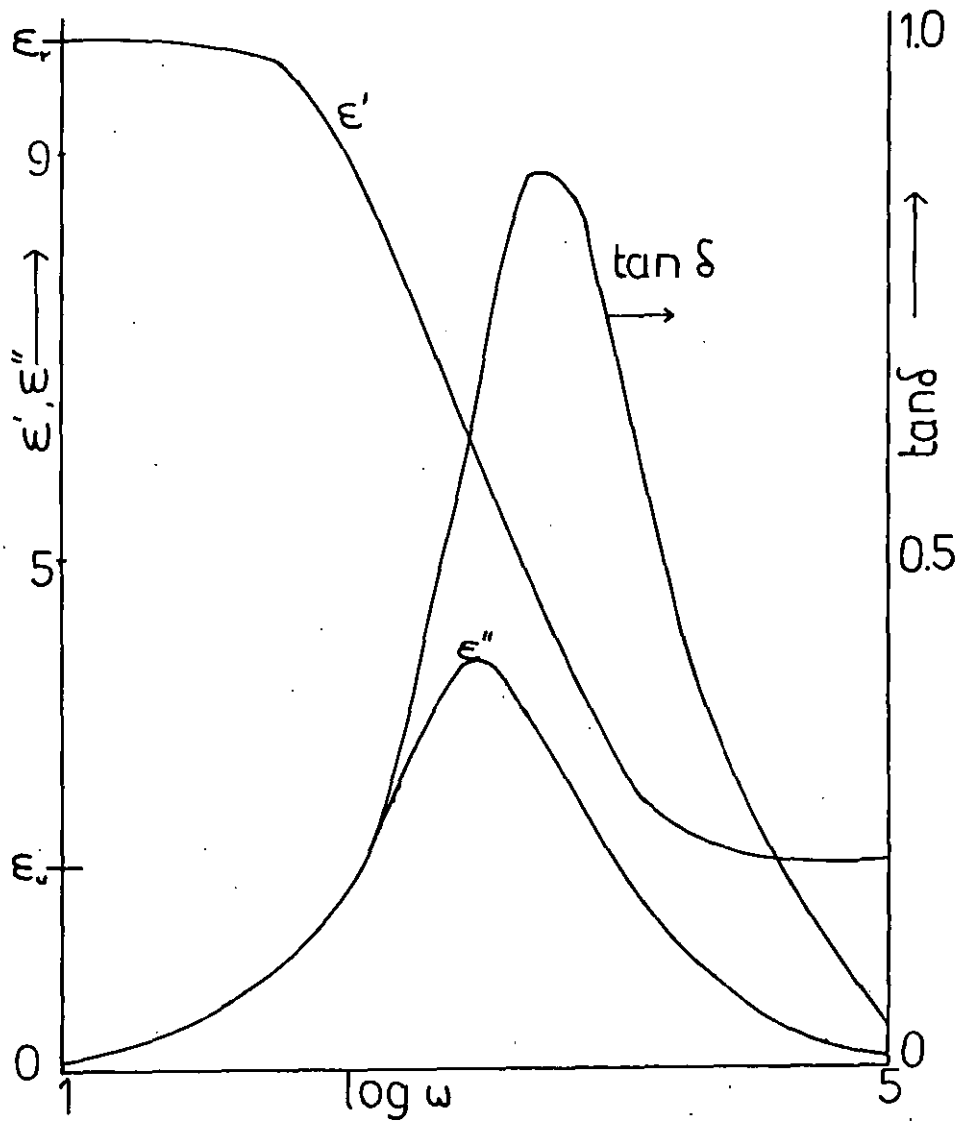
$\epsilon'$  is the energy stored per cycle whilst  $\epsilon''$  is the energy dissipated per cycle.

The typical variation of  $\epsilon'$ ,  $\epsilon''$  and  $\tan \delta$  with frequency is shown in Figure (2.15) for a simple liquid. The dependence of



Figure (2.15)

Variation of  $\epsilon'$ ,  $\epsilon''$  and  $\tan \delta$  with Frequency for a Dielectric with a Single Relaxation Time



$\epsilon'$  on frequency follows the pattern of the molecular polarization (Figure 2.13). In the region where the orientation polarization decreases the loss factor and loss tangent pass through maxima. At high frequencies the dipoles do not have time to orientate to the alternating electric field because the period of oscillation is much less than the relaxation time ( $\tau_R$ ) of the dipoles. At low frequencies the situation is reversed, the period of oscillation being large compared with  $\tau_R$ . Consequently at the extrema of frequency power loss is low. At intermediate frequencies the dipolar orientation is out of phase with the applied field and power losses occur. Power loss is maximised when

$$\omega_{\max} = \frac{1}{\tau_R} \quad (2.111)$$

Debye<sup>(146)</sup> has derived the following expressions for the frequency dependence of  $\epsilon'$  and  $\epsilon''$ , which are applicable to systems having a single relaxation time.

$$\epsilon^* (\omega) = \epsilon_U + \left( \frac{\epsilon_r - \epsilon_U}{1 + j\omega\tau_R} \right) \quad (2.112)$$

$$\epsilon' (\omega) = \epsilon_U + \left( \frac{\epsilon_r - \epsilon_U}{1 + \omega^2\tau_R^2} \right) \quad (2.113)$$

$$\epsilon'' (\omega) = \left( \frac{\epsilon_r - \epsilon_U}{1 + \omega^2\tau_R^2} \right) \omega\tau_R \quad (2.114)$$

Simple liquids have been shown to exhibit single relaxation times but this has never been observed in macromolecules<sup>(147)</sup>. This is on account of the complexity of the orientation process in polymers leading to a spectrum of relaxation times. The situation is illustrated in Figure (2.16) where  $(\epsilon'(\omega) - \epsilon_U)/(\epsilon_R - \epsilon_U)$  and  $\epsilon''(\omega)/(\epsilon_R - \epsilon_U)$  are plotted against  $\omega$  for a typical polymer and a Debye model material. Departure from the situation of a single relaxation time causes a broadening and a decrease in magnitude in each plot.

In the Debye model the relaxation time is an approximate measure of the reciprocal rate constant of dipole orientation. Consequently over a restricted temperature range the temperature dependence of  $\tau_R$  can be represented by an Arrhenius type equation

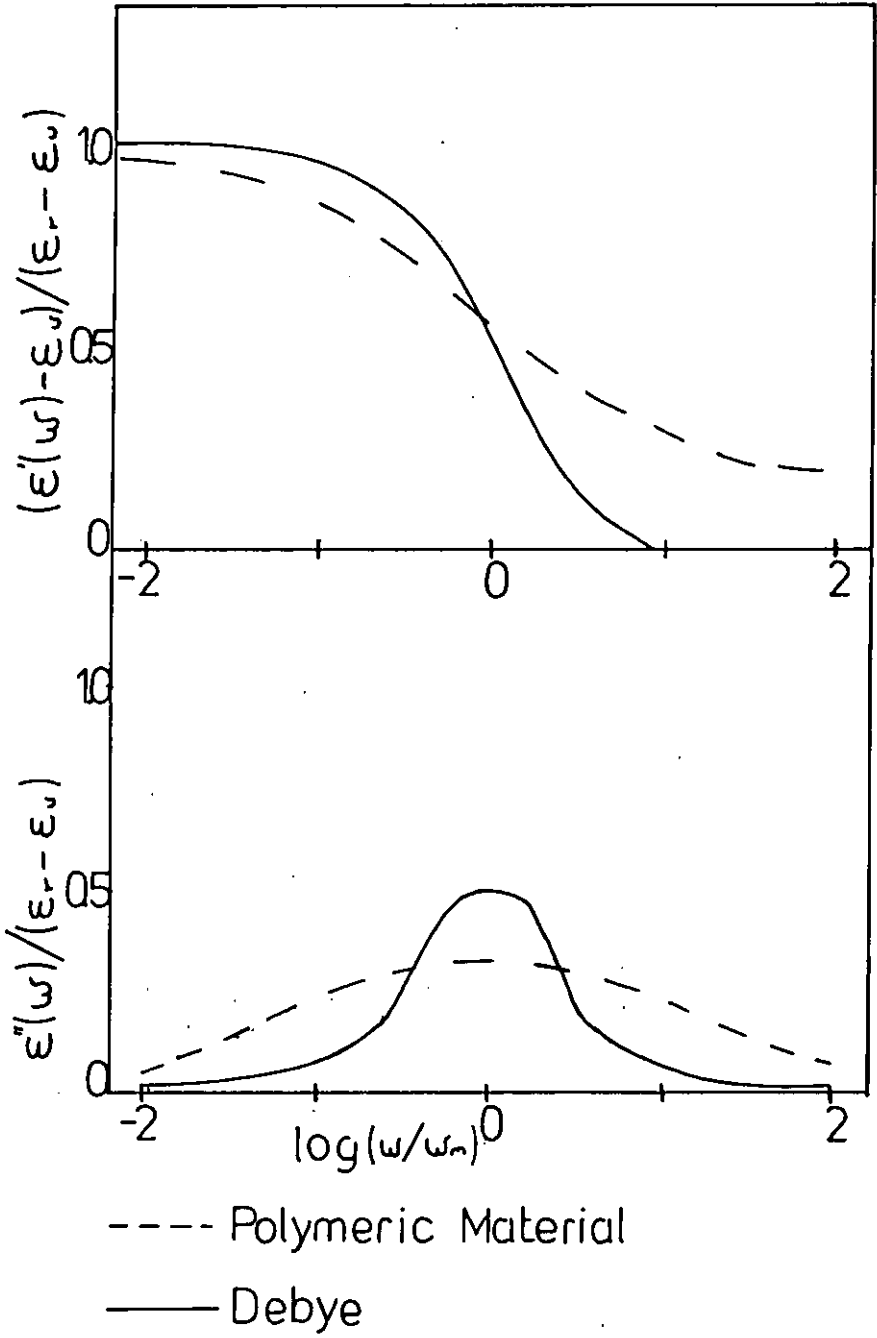
$$\tau_R = \tau_0 \exp(\Delta E/RT) \quad (2.115)$$

where  $\Delta E$  is the activation energy of dipolar orientation. Inspection of equation (2.115) reveals that a distribution of relaxation times can result from a distribution of  $\tau_0$ ,  $\Delta E$  or indeed both. A number of empirical distributions have been developed to describe experimental relaxation curves for polymeric materials. The most widely used are:- the Cole-Cole distribution<sup>(148)</sup>; the Fuoss-Kirkwood<sup>(149)</sup> distribution; and the Davidson-Cole<sup>(150,151)</sup> distribution.

### 2.6.3 Influence of Temperature on Dielectric Relaxation

The empirical distributions mentioned above describe the variation of the electrical properties with frequency. Temperature also has a large influence. As shown previously the temperature dependence of the retardation time can follow an Arrhenius plot (equation (2.115)). If the distribution of relaxation times is not itself temperature

Figure(2.16)  
Dielectric Relaxation Behaviour



dependent then it is possible to superimpose the experimental  $\epsilon''(\omega)/\epsilon''_{\max}$  vs.  $\omega$  and  $(\epsilon'(\omega) - \epsilon_U)/(\epsilon_r - \epsilon_U)$  vs.  $\omega$  curves, measured at different temperatures to form master curves. The 'Time-Temperature Superimposition Principle' is described by the semi-empirical W.L.F.<sup>(123)</sup> equation discussed previously (equation 2.89). The shift in  $\ln a_\tau$  can be written in terms of the Arrhenius equation thus,

$$\ln a_\tau = \frac{\Delta E}{R} \left( \frac{1}{T} - \frac{1}{T_g} \right) \quad (2.116)$$

The W.L.F. equation holds true in the region  $T_g \leq T \leq T_g + 100$ . It can however be used at temperatures below  $T_g$  if an effective temperature is included to account for the non-equilibrium condition of the glassy state<sup>(154)</sup>.

#### 2.6.4 Dielectric Relaxation Process

The nomenclature most generally used to label the various processes of relaxation is that proposed by Deutsch *et al.*<sup>(155)</sup>. In this system the processes are assigned the symbols  $\alpha, \beta, \gamma$  and so on in order of decreasing temperature at constant frequency.

In an amorphous polymer there are generally three possible transitions,  $\alpha_a, \beta_a$  and  $\gamma_a$ . The subscript refers to the nature of the transition phase, a-amorphous, c-crystalline.  $\alpha_a$  is associated with the glass transition whilst  $\beta_a$  generally arises due to side group or limited segmental motion in the glassy state. The latter category has been explained as occurring either due to crankshaft motion<sup>(156)</sup> or local mode motions<sup>(157)</sup>.  $\gamma_a$  has been observed in certain substituted polymers and it has been proposed that the independent motion of side groups<sup>(158)</sup> is responsible.

### 2.6.5 Maxwell-Wagner-Sillars (MWS) Interfacial Polarization

If a loss free dielectric material is mixed with a second material of higher conductivity to form an immiscible mixture MWS Interfacial Polarization<sup>(159-161)</sup> will result. Migration of charge through the conducting phase to the interface leads to an increase in the apparent dielectric constant. The dielectric loss is also affected at particular frequencies due to ohmic conduction occurring as current flows in the conducting phase producing changes in polarization at the interface.

The magnitude and frequency of this effect depends on the size and geometry of the conducting phase, the dielectric constants of the two phases and the volume fraction of each.

### 2.6.6 Dielectric Relaxation in Polymer Mixtures

Dielectric techniques have not been widely used in the examination of polymer blends. This is particularly noticeable in comparison with thermal analysis techniques such as D.S.C. (differential scanning calorimetry) and dynamic mechanical methods. Dielectric relaxation does however offer the opportunity to study the state of homogeneity of a system at a finer level than thermal analysis techniques allow in cases where one or both components are polar.

A miscible blend can be characterised by a single  $\alpha$  relaxation, as seen for example in a plot of  $\tan \delta(\epsilon''/\epsilon')$  vs. temperature, the position of the peak in the temperature plane being composition and frequency dependent. A qualitative measure of the range of local environments at sub- $T_g$  levels in a miscible blend is provided by comparison of the width of the normalised dielectric loss curves for the blend and the pure components. The normalised loss curves are plots of  $\epsilon''(\omega)/\epsilon''_{\max}$  vs.  $\log(f/f_{\max})$  where  $\epsilon''_{\max}$  and  $f_{\max}$  are the co-ordinates of the loss peak maximum in the frequency plane.

The normalised loss curves provide an indication of the range of relaxation processes occurring within a material.

Bank *et al.*<sup>(64)</sup> used the dielectric technique in their study of the effect of casting solvent on miscibility in poly(styrene)-poly(vinyl methyl ether) blends. In the miscible mixtures cast from toluene they found that the dielectric loss curves were broadened and decreased in height in comparison to PVME homopolymer. They attributed this broadening to heterogeneities on the molecular level which incidentally were not picked up by DSC. Similar trends are apparent in the dielectric data of:- Feldman *et al.*<sup>(162)</sup> in their study of poly(vinyl chloride)- ethylene-co-vinyl acetate (EVA) blends; Akiyama *et al.*<sup>(163)</sup> in their work on poly(vinyl nitrate)(PVN) - poly(vinyl acetate) and PVN-EVA mixtures; and Fujimoto *et al.*<sup>(164)</sup> in poly(butadiene)-(styrene-co-butadiene) blends.

The most elegant and detailed dielectric study on blends produced to date has been carried out by MacKnight and co-workers. They have investigated the dielectric behaviour of poly(2,6-dimethyl-1,4-phenylene oxide)(PPO) in miscible blends with PST<sup>(165)</sup> and poly(styrene-co-p-chlorostyrene)<sup>(166)</sup>, and poly( $\sigma$ -chlorostyrene)<sup>(167)</sup>- PST mixtures.

The blends of PST-PPO<sup>(165)</sup> exhibited a broadening in the normalised dielectric loss peaks which was rationalised in terms of the mixing process. The polymers were melt mixed at  $\approx 300^\circ\text{C}$  at which temperature PST is a much less viscous liquid than PPO ( $T_{g\text{PST}} \approx T_{g\text{PPO}} - 100^\circ\text{C}$ ). At compositions containing an excess of PST, it was hypothesised that PST would first form a continuous matrix with PPO dispersed in it. Mixing would then occur by interdiffusion but not completely so that on cooling there is a PPO rich phase dispersed in a PST rich matrix. The dimensions of the disperse phase are such that it does not display its own discrete  $T_g$ .

PPO-poly(styrene-co-p-chlorostyrene)<sup>(166)</sup> mixtures exhibited a 'door of miscibility' being a type (c) system as defined in section 2.3.1(c). Investigations were conducted on mixtures where the copolymer compositions bridged the boundary between miscibility and immiscibility. Miscible mixtures exhibited the usual broadening of loss peaks whilst immiscible mixtures exhibited a further shoulder to the broadened loss peaks at high frequencies. This behaviour was interpreted using the MWS theory which is applicable to any two-phase system of differing dielectric properties. The range of local concentration regimes necessary to cause the observed loss peak broadening in the miscible mixtures was calculated using the empirical Fuoss-Kirkwood<sup>(149)</sup> relation.

PST-Po-ClSt<sup>(167)</sup> mixtures exhibited miscibility which was highly sensitive to the molecular weight of the PST and temperature. Raising the PST weight average molecular weight from  $\approx 10^4$  to  $\approx 10^5$  caused the mixtures to change from being miscible up to degradation temperatures to exhibiting lower critical miscibility behaviour. Furthermore low molecular weight PST blends gave much narrower normalised loss spectra than miscible high molecular weight mixtures. One surprising observation was that as the measurement temperature crossed the cloud-point curve the corresponding loss spectra became narrower until they became as wide as those of the pure components. It appears then that after phase separation has occurred the resultant Po-ClSt rich and Po-ClSt poor phases are more homogeneous at a local level than the parent miscible mixture.

These examples serve to demonstrate the utility of dielectric relaxation in providing a deeper understanding of the complexities involved in making definitive categorisations of polymer mixtures. The varying sensitivities of different techniques to scales of hetero-



geneity must be borne in mind when analysing such mixtures.

## 2.7 MECHANICAL PROPERTIES OF POLYMERS

Perfectly elastic materials obey Hooke's law, which is to say the stress is directly proportional to the applied strain. Perfectly viscous liquids behave in accordance with Newton's law of viscosity which states that stress is directly proportional to the rate of strain. Polymeric materials have properties which lie between these two extreme states and have consequently been termed viscoelastic.

Application of a static load to a polymer will lead to a time dependent elongation (creep) in addition to the initial elongation characteristic of elastic materials. Stress relaxation occurs when a polymer is stretched to a constant length and the stress is measured as a function of time. Both of these techniques have been used to elucidate the mechanical properties of polymers, however they have to a large extent been superceded by dynamic mechanical techniques, especially in the field of polymer blends. In a dynamic mechanical test a sample is deformed by a stress which varies sinusoidally with time. The strain is neither in phase with the stress (as in perfect elastics) nor  $90^\circ$  out of phase (as in perfectly viscous liquids) but adopts an intermediate value. Discussion is limited in this section to dynamic mechanical measurement of polymers. However it should be noted that viscoelastic theory is capable of predicting creep and stress relaxation behaviour from dynamic mechanical data.

### 2.7.1 Dynamic Mechanical Analysis

Dynamic mechanical measurements can be made either at constant temperature as a function of frequency (frequency plane) or at constant frequency as a function of temperature (temperature plane). In both

instances the stress (strain) is measured resulting from the application of a sinusoidal strain (stress).

The strain ( $e$ ) and stress ( $\sigma$ ) variations with time can be written as

$$e = e_0 \sin \omega t \quad (2.117)$$

$$\sigma = \sigma_0 \sin(\omega t + \delta) \quad (2.118)$$

where  $e_0$  and  $\sigma_0$  are the respective strain and stress amplitudes and  $\delta$  is the phase lag. Expansion of equation (2.118) leads to

$$\sigma = \sigma_0 \sin \omega t \cos \delta + \sigma_0 \cos \omega t \sin \delta \quad (2.119)$$

Inspection of this equation reveals that the stress consists of two components one of which is in phase with the strain (magnitude  $\sigma_0 \cos \delta$ ) whilst the other is out of phase (magnitude  $\sigma_0 \sin \delta$ ). The stress-strain relationship can therefore be defined as

$$\sigma = e_0 G' \sin \omega t + e_0 G'' \cos \omega t \quad (2.120)$$

where  $G'$  is in phase with the strain and equal to  $(\sigma_0/e_0) \cdot \cos \delta$  and  $G''$  is out of phase and equal to  $(\sigma_0/e_0) \cdot \sin \delta$ . As the strain and stress can also be written in complex form, a complex modulus  $G^*$  can be derived such that

$$G^* = \frac{\sigma}{e} = \frac{\sigma_0}{e_0} e^{j\omega t} = (G' + jG'') \quad (2.121)$$

the quantity  $G'$  is termed the storage modulus as it defines the energy stored per cycle in a material due to the applied strain.  $G''$  is called the loss modulus and defines the energy dissipated per cycle. The complex compliance  $J^*$  is the inverse of  $G^*$  and can also be written in terms of a storage and loss component.

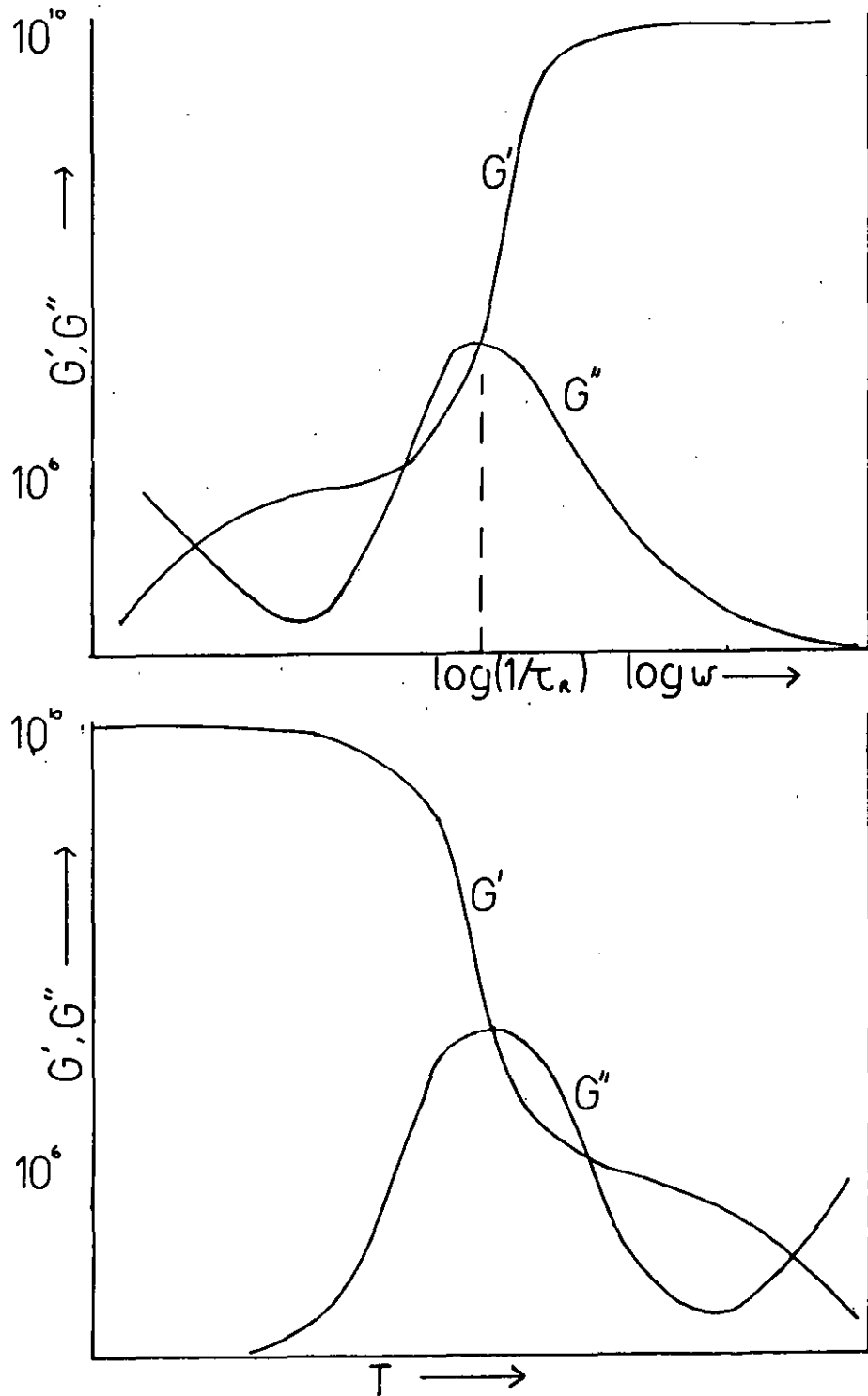
$$J^* = J' - jJ'' \quad (2.122)$$

Comparison of equations (2.121) with equation (2.109) illustrates the underlying theoretical similarities between dynamic mechanical and dielectric techniques. As before the loss tangent is defined as

$$\tan \delta = \frac{G''}{G'} = \frac{J''}{J'} \quad (2.123)$$

The variation of the storage and loss moduli in the frequency plane and temperature plane are shown in Figure (2.17) for a typical amorphous, linear homopolymer which does not have any transitions other than the  $\alpha$  process. In the frequency plane glassy state behaviour is found at high frequencies where  $G'$  is at its maximum value ( $G' = G_u$ ). As the frequency is reduced  $G'$  reduces rapidly near to the reciprocal relaxation time ( $\omega = \tau^{-1}$ ) whilst  $G''$  rises to a maximum at this frequency. At lower frequencies the polymer enters the rubbery or relaxed state ( $G' = G_r$ ) and as the frequency declines still further viscous flow will occur in linear polymers characterised by a decrease in  $G'$  and an increase in  $G''$ . In the temperature plane the storage modulus follows an inverse pattern with glassy behaviour being observed at low temperatures and  $G'$  decreasing as temperature rises.

Figure (2.17)  
Variation of  $G'$  and  $G''$  with Temperature  
and Frequency



This reciprocal relationship between frequency and temperature has been exploited to obtain full relaxation spectra from measurements over reasonable time scales conducted at various temperatures. This time-temperature superposition referred to in sections (2.5.2) and (2.6.3) can be applied to dynamic modulus - frequency curves<sup>(168)</sup> provided the polymer follows linear viscoelastic theory.

## 2.7.2 Factors Which Influence Dynamic Mechanical Behaviour

### (a) Molecular Weight and Crosslinking

Dynamic mechanical properties of polymers tend to be independent of molecular weight and crosslinking at low temperatures (high frequencies) where polymers are glasses. The influence of molecular weight and crosslinking on  $T_g$ , discussed in section (2.5.4), is reflected in a shift of the loss modulus and loss tangent maxima to higher temperatures (at constant frequency) as one or both of these measures increases towards terminal values. At very high levels of cross-linking however the storage modulus becomes virtually temperature independent and no relaxation peak is observed.

At temperatures beyond the  $\alpha$  relaxation region the breadth of the plateau in the storage modulus, reflecting rubber-like behaviour, is highly dependent on molecular weight and network formation. Highly cross-linked materials exhibit a plateau which extends to degradation temperatures, that is viscous flow does not occur. The breadth of the  $G'$  plateau increases directly with molecular weight in linear polymers due to chain entanglements acting as transitory cross-links. High molecular weight polymers have more entanglements than low molecular ones. In the viscous flow region  $G'$  decreases and  $G''$  increases.

(b) Copolymerisation

The effect of copolymerisation to form random copolymers upon dynamic mechanical properties can be predicted from glass transition behaviour. The copolymer  $T_g$  depends upon the glass transition temperatures of the constituent homopolymers and the copolymer composition as described in section (2.5.4). Similarly the positions of the maxima in the loss modulus and loss tangent for the copolymer can be calculated from a knowledge of the mechanical behaviour of the respective homopolymers and the copolymer composition.

The breadth of the copolymer  $\alpha$  relaxation peak, as indicated by Nielson<sup>(169)</sup>, depends upon the chemical homogeneity of the copolymer molecules. In many instances one comonomer is more reactive than the other, consequently at conversions above about ten per cent there is a drift in copolymer composition with time. This arises due to the reaction mixture becoming richer in the less reactive comonomer as the other component is depleted at a greater rate. Homogeneous copolymers exhibit a single  $\alpha$  relaxation peak whose breadth is similar to that of a homopolymer. As chemical heterogeneity increases so does the peak breadth in the majority of cases where the individual homopolymer equivalents are immiscible. When the homopolymers are miscible copolymer heterogeneity has a much smaller influence on the breadth of the relaxation peak.

(c) Plasticizers and Blending

The effect of plasticizers upon dynamic mechanical behaviour can, as with copolymers, be predicted from consideration of the glass transition. The relaxation peak position can often be found using a relation such as the Kelley-Bueche (equation (2.99)) equation. Plasticizers often broaden the loss peak in addition to shifting it

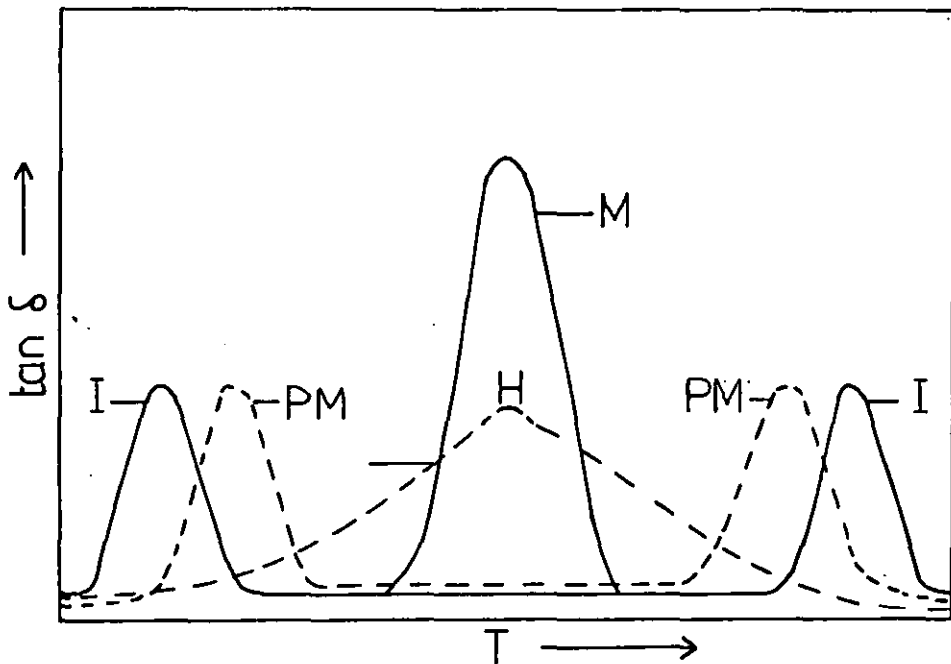
to lower temperatures. The degree of broadening depends on the nature of the plasticizer and its miscibility with the polymer<sup>(170)</sup>. If the plasticizer has a limited solubility in the polymer or a tendency to aggregate in the presence of the polymer then the loss peak broadens and decreases in height whilst the slope of the storage modulus also decreases.

The dynamic mechanical behaviour of two component polymer mixtures depends upon their miscibility. The typical variation of the loss tangent with temperature for the 4 general classes of miscibility is illustrated in Figure (2.18). A completely immiscible blend will exhibit the loss peaks characteristic of the two components. Although in such cases there is a very limited solubility of one component in the other usually this is too small to produce a noticeable property change, such as a shift in  $T_g$ , which would result in a shift of the loss peaks. Partially miscible blends have two distinct phases each being concentration rich in one component relative to the other. Each phase exhibits its own loss peak at a position reflecting the phase composition. Microheterogeneous blends can be regarded as a sub-category of the partially miscible class. The broad loss peak results from the presence of an infinite number of phases of differing composition. The loss tangent can be regarded in this instance as a reflection of the composition distribution. Most authorities regard miscible blends as having a single relaxation peak whose breadth is similar to that of its individual homopolymer constituents. However, as in the case of dielectric relaxation experiments, the dynamic mechanical testing technique is sensitive to the range of molecular relaxation processes occurring. In blends which appear miscible by techniques such as D.S.C. complete homogeneity at the molecular level can rarely be achieved in practice. Consequently a slight but

Figure(2.18)

$\tan \delta$  vs. Temperature for Representative Mixing Categories

		References
I	Immiscible	(171,172)
PM	Partially Miscible	(107,173)
M	Miscible	(64,97,174)
H	Microheterogeneous	(176)





distinct broadening in the loss peak is to be expected and should not alter our definition of miscibility. It should be noted that although there is a considerable similarity in the derivation and interpretation of mechanical and dielectric quantities, their correlation in a particular case will depend upon chemical structure.

There is considerable body of literature concerning the dynamic mechanical properties of polymer blends of all four miscibility categories. The reviews of Krause<sup>(114)</sup>, Olabisi *et al.*<sup>(10)</sup>, Manson and Sperling<sup>(176)</sup> and Robeson<sup>(49)</sup> can be consulted for fairly comprehensive lists of examples.

There is no definitive view of the effect of blending on secondary relaxations. In some miscible systems broadening or shifting of the  $\beta$  peaks has been observed<sup>(177)</sup>, whilst in others they have not been effected<sup>(178)</sup>. Interpretation is often complicated by the coincidence of secondary relaxations of the two components.

## 2.8 COPOLYMERISATION

### 2.8.1 Composition of Random Copolymers

The composition of a random copolymer is usually different to that of the initial monomer feed. This is due to the disparity in reactivities between the two species. The reactivity of a given monomer in copolymerisation depends upon both the comonomer and polymerisation conditions.

In a system consisting of monomers  $M_1$  and  $M_2$  there are two types of propagating species,  $M_1^*$  and  $M_2^*$  depending upon the monomer type at the growing end of the chain. Consequently four propagation reactions are possible<sup>(179-181)</sup>.





where  $k_{xy}$  is the rate constant for a growing chain with monomer  $x$  at the propagating end, adding monomer  $y$ . The rates of uptake of the two species into the copolymer derive directly from equations (2.124-2.127) such that

$$-\frac{d[M_1]}{dt} = k_{11}[M_1^*][M_1] + k_{21}[M_2^*][M_1] \quad (2.128)$$

$$-\frac{d[M_2]}{dt} = k_{12}[M_1^*][M_2] + k_{22}[M_2^*][M_2] \quad (2.129)$$

The copolymer composition is given by the division of equation (2.128) by equation (2.129). Assuming that a steady-state concentration exists for both  $M_1^*$  and  $M_2^*$  then

$$k_{21}[M_2^*][M_1] = k_{12}[M_1^*][M_2] \quad (2.130)$$

Rearrangement of this equation and substitution for  $[M_1^*]$  into the quotient of equations (2.128) and (2.129) yields the so called copolymerisation equation

$$\frac{d[M_1]}{d[M_2]} = \frac{[M_1](r_1[M_1] + [M_2])}{[M_2]([M_1] + r_2[M_2])} \quad (2.131)$$

where the parameters  $r_1$  and  $r_2$  are the reactivity ratios of the two species, defined as

$$r_1 = \frac{k_{11}}{k_{12}} \quad \text{and} \quad r_2 = \frac{k_{22}}{k_{21}} \quad (2.132)$$

In equation (2.131)  $d[M_1]/d[M_2]$  expresses the molar ratio of the two species in the copolymer whilst the concentrations on the right hand side relate to the monomer feed. Defining the molar ratios of  $M_1$  to  $M_2$  in the copolymer and feed as  $f$  and  $F$  respectively equation (2.131) can be rewritten as

$$f = (r_1 F + 1)/(1 + r_2/F) \quad (2.133)$$

Finemann and Ross<sup>(182)</sup> have shown that reactivity ratios can be determined graphically from a knowledge of  $f$  and  $F$  over a range of compositions. Equation (2.133) is rearranged in the form

$$\frac{F(f - 1)}{f} = r_1 \frac{F^2}{f} - r_2 \quad (2.134)$$

A plot of the left hand side of this expression against  $F^2/f$  should yield a straight line of slope  $r_1$  and intercept  $-r_2$ . However the copolymerisation equation is only valid at low degrees of conversion as there is a drift in the feed composition towards the less reactive monomer as the copolymerisation progresses. An exception to this general behaviour occurs in azeotropic copolymerisations where there is an equality of the copolymer and feed composition such that the comonomers are depleted at the same rate.

Kelen and Tudos<sup>(183,184)</sup> have improved upon this method of deter-

mining reactivity ratios, employing a procedure which gives a more even distribution of data points and more noticeably highlights deviations from the copolymerisation equation. These deviations can show up in a curvature of the data plot and be due either to shifts in the composition of the feed (conversions too high) or to the fact that the four propagating reactions considered in the derivation of the copolymerisation equation are not representative of the mechanisms for chain growth.

In the Kelen-Tudos method the  $x$  and  $y$  terms in equation (2.134) are divided by a constant before being plotted. This constant is given by  $(F^2/f + \alpha)$  where  $\alpha$  is calculated as the square root of the product of the maximum and minimum values of  $(F^2/f)$ . The terms  $\epsilon$  and  $\eta$  are defined as

$$\epsilon = \frac{F^2/f}{\alpha + F^2/f} \quad (2.135)$$

$$\eta = \frac{F(f - 1)/f}{\alpha + F^2/f} \quad (2.136)$$

The reactivity ratios can be found from the plot of  $\eta$  against  $\epsilon$ ;  $r_1$  is equal to the value of  $\eta$  at  $\epsilon=1$  and  $r_2$  is calculated by multiplying the intercept on the  $\eta$  axis by  $-\alpha$ .

### 2.8.2 Determination of Sequence Length Distribution in Random

#### Copolymers

The copolymerisation equation can be derived statistically without invoking steady-state assumptions and thereby provides an approach for analysing average sequence length distributions<sup>(185)</sup>.

The probability  $P_{11}$  of forming an  $M_1M_1$  diad is derived from reactions (2.124)-(2.125) such that

$$P_{11} = \frac{k_{11}[M_1^*][M_1]}{k_{11}[M_1^*][M_1] + k_{12}[M_1^*][M_2]} \quad (2.137)$$

simplification of this expression and substitution for  $r_1$  yields

$$P_{11} = \frac{r_1}{r_1 + [M_2]/[M_1]} \quad (2.138)$$

Similarly the probability of forming an  $M_2M_2$  diad is given by

$$P_{22} = \frac{r_2[M_2]}{r_2[M_2] + [M_1]} \quad (2.139)$$

As the sum of the probabilities of addition to both  $M_1^*$  and  $M_2^*$  are equal to one in each case then

$$P_{12} = 1 - P_{11} \quad (2.140)$$

$$P_{21} = 1 - P_{22} \quad (2.141)$$

The probability of forming a sequence of  $M_1$  units of length  $x$  is given by  $(N_1)_x$  where

$$(N_1)_x = (P_{11})^{(x-1)} \cdot P_{12} \quad (2.142)$$

assuming high molecular weights so that chain ends have a negligible influence. The number average sequence length of  $M_1$  is given by

$$\bar{n}_1 = \sum_{x=1}^{\infty} x(N_1)_x = (N_1)_1 + 2(N_1)_2 + 3(N_1)_3 + \dots \quad (2.143)$$

substitution for  $(N_1)_x$  and simplification of the resulting expansion series yields

$$\bar{n}_1 = \frac{1}{P_{12}} \quad (2.144)$$

Similarly the probability of forming sequences of  $M_2$  units of length  $x$  is given by

$$(N_2)_x = (P_{22})^{x-1} \cdot P_{21} \quad (2.145)$$

and the number average sequence length of  $M_2$  ( $\bar{n}_2$ ) is simply the reciprocal of  $P_{21}$ .

CHAPTER 3

EXPERIMENTAL DETAILS

### 3.1 PREPARATION OF HOMOPOLYMERS AND COPOLYMERS

#### 3.1.1 Solution Polymerisation

Solution polymerisations were conducted in a 100 ml. flanged flask fitted with mechanical stirrer, condenser, dropping funnel and nitrogen inlet as depicted in Figure (3.1). The flask was heated using an iso-mantle and all polymerisations were conducted under a nitrogen blanket. The experimental details for each reaction are presented in Table 3.1. It was found the glycidyl methacrylate and tetrahydrofurfuryl methacrylate tended to cross-link as evidenced by gel formation at low solvent to monomer molar ratios. Consequently ratios were used which led to the production of essentially linear polymers. Polymers were isolated from solution by precipitating dropwise into a ten-fold excess of an appropriate non-solvent. Solids were then filtered off, washed with non-solvent and dried under vacuum.

#### 3.1.2 Bulk Polymerisation

Bulk polymerisations were carried out in sealed ampoules. The appropriate monomer(s) and initiator were first weighed into a glass ampoule fitted with a vacuum joint. The ampoule was then attached to a standard vacuum line which could achieve a vacuum of 0.025 torr. The reaction mixture was degassed using a freeze-thaw technique. The mixture was first frozen in a vessel of liquid nitrogen and was then evacuated. On reaching the minimum pressure level (read off on a pirani gauge) the ampoule was isolated from the line and the mixture was thawed by surrounding it with a methanol bath. The procedure was repeated until no further gas was liberated on thawing. The ampoule was sealed using an oxygen/methane flame whilst the contents were frozen. Polymerisation was conducted in a thermostatted



Figure (3.1)  
Apparatus Used for Solution Polymerisation

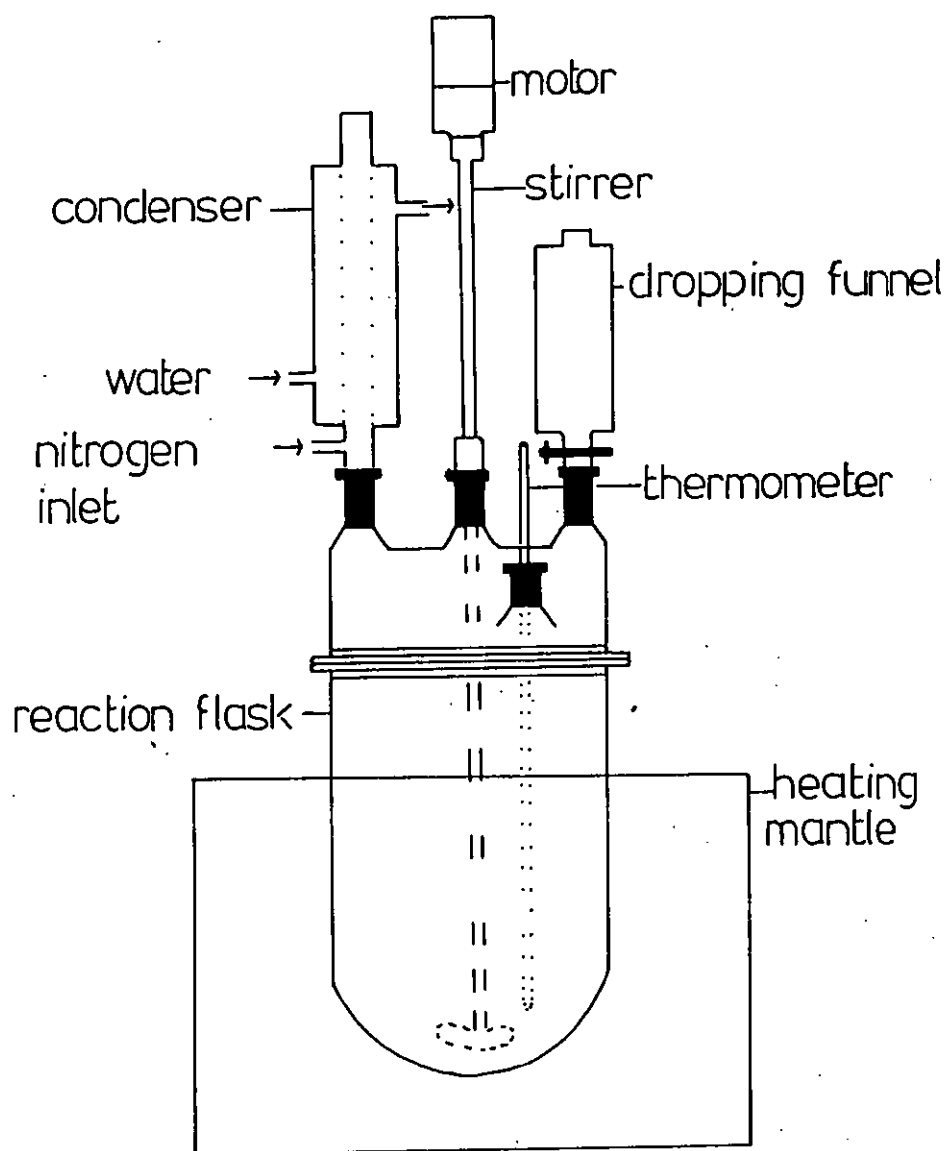


Table 3.1. Solution Polymerisations

Monomer (1) (m) (Source)	Monomer (2) (Source)	Solvent (S)	T(°C)	t(hours)	[S]/[M]	Benzoyl Peroxide Concentration	Yield Wt. %	Non-solvent for Isolation
Glycidyl methacrylate (Aldrich)	-	Methyl ethyl ketone	79°	4	7.9	1% of monomer weight	12	Methanol
Glycidyl methacrylate (Aldrich)	Methyl methacrylate (Aldrich)	Methyl ethyl ketone	79°	4	7.9	"	10	Methanol
Methyl methacrylate (Aldrich)	-	Isopropanol	83°	6½	2.0 14.0 23.3	1% of monomer weight	60 20 10	Methanol
Tetrahydrofurfuryl methacrylate (Ancomer)	-	Methyl ethyl ketone	79°	6½	15.8	"	10	Hexane
Ethoxy ethyl methacrylate (Ancomer)	-	Methyl ethyl ketone	79°	6½	7.9	"	15	Hexane

water bath. Details of the systems polymerised in this way are given in Table 3.2. Isolation of the product from the residual monomer(s) was again achieved by precipitation into non-solvent.

### 3.2 Purification of Homopolymers and Copolymers

All homopolymers and copolymers prepared using the above techniques were purified after isolation from their respective reaction mixtures. In the case of materials obtained as polymers similar purification was also carried out.

Purification involved dissolution in an appropriate solvent to form an approximately 5% (by weight) solution. This was filtered and dripped into a tenfold excess of non-solvent chosen so as to be miscible with the solvent. The precipitated polymer was then filtered off and washed with non-solvent before being dried under vacuum. The procedure was carried out three times in all. In most cases the solvent used was methylene chloride whilst the non-solvent was methanol. The chemical structure of all the polymers used is presented in Table (3.3).

#### 3.2.1 Fractionation of Poly(Glycidyl Methacrylate) (PGMA)

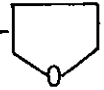
The reason for fractionating PGMA was the peculiar shape of the G.P.C. chromatogram measured for this particular polymer as discussed in Chapter (4). Fractionation was accomplished by firstly dissolving the polymer in methyl ethyl ketone (0.025 g/ml.) in a large (1 l.) conical flask. When dissolution was complete the flask was fitted with a condenser and suspended in a water bath thermostatted at  $40^{\circ}\text{C} \pm 0.1^{\circ}$ . Isopropanol, which is a non-solvent for PGMA, was then added dropwise from a burette through the condenser whilst the conical flask was gently agitated. Addition was stopped at the first

Table 3.2. Bulk Polymerisation

Monomer (1) (Source)	Monomer (2) (Source)	Temperature T(°C)	Time t(hours)	Yield (by Wt.)	Non-solvent for Isolation
Styrene (Fisons)	Methacrylonitrile (Aldrich)	60°	8	5-7%	Methanol
Methyl methacrylate (Aldrich)	Methacrylonitrile (Aldrich)	60°	8	5-8%	Methanol
Methacrylonitrile (Aldrich)		89°	5	10%	Methanol

Initiator Benzoyl peroxide (0.2% by weight)

Table 3.3. Repeat Unit Structures of Homopolymers Used

Polymer	Structure of Repeat Unit
PEPC	$\begin{array}{c} -\text{CH}-\text{CH}_2-\text{O}- \\   \\ \text{CH}_2\text{Cl} \end{array}$
PMMA	$\begin{array}{c} \text{CH}_3 \\   \\ -\text{CH}_2-\text{C}- \\   \\ \text{COOCH}_3 \end{array}$
PEEMA	$\begin{array}{c} \text{CH}_3 \\   \\ -\text{CH}_2-\text{C}- \\   \\ \text{COOCH}_2\text{CH}_2\text{OCH}_2\text{CH}_3 \end{array}$
PTHFMA	$\begin{array}{c} \text{CH}_3 \\   \\ -\text{CH}_2-\text{C}- \\   \\ \text{COOCH}_2-\end{array}$ 
PGMA	$\begin{array}{c} \text{CH}_3 \\   \\ -\text{CH}_2-\text{C}- \\   \\ \text{COOCH}_2\text{CH}(\text{O})\text{CH}_2 \end{array}$
PST	$\begin{array}{c} -\text{CH}-\text{CH}_2- \\   \\ \text{C}_6\text{H}_5 \end{array}$
PMAN	$\begin{array}{c} \text{CH}_3 \\   \\ -\text{CH}_2-\text{C}- \\   \\ \text{CN} \end{array}$

sign of permanent turbidity and the flask was transferred to an ice/water bath where the precipitate was allowed to sediment overnight. The precipitated fraction was isolated by pipetting off the clear supernatant solution, filtering the remaining solids and washing repeatedly with methanol before drying under vacuum at 55°C. The process was repeated a further four times using the supernatant solution to yield fractions of decreasing molecular weight.

### 3.3 CHARACTERISATION OF HOMOPOLYMERS AND COPOLYMERS

#### 3.3.1 Gel Permeation Chromatography (G.P.C.)

The G.P.C. technique separates species on the basis of size and does not distinguish structural differences between molecules. Molecules are eluted from the separating column in order of decreasing size. This arises as molecules which are larger than the gel pore size are excluded from the gel beads and pass rapidly through the column whilst smaller species diffuse into the gel and consequently have longer retention times.

Homopolymers and copolymers were characterised by this technique using a modified Waters 502 ALC/GPC with tetrahydrofuran (BDH, A.R. grade, stabilized with 0.1% quinol) as solvent. The column used was a 60 cm. mixed bed P.L. gel column (Polymer Laboratories) which was calibrated with poly(styrene) standards of molecular weights ranging from 200 to  $2 \times 10^6$ . Refractive index was used as the method of detection.

Samples were prepared by dissolution in THF (containing a small amount of toluene as marker) to form solutions containing 0.25-0.75 mg./ml. All solutions were filtered (Whatman glass microfibre filters) before injection. An injection volume of about 0.5 mls. was found to be sufficient.

G.P.C. yields values of the number and weight average molecular weights relative to the calibration standards used. A standard computer programme containing an internal calibration curve of the column was used to evaluate  $\bar{M}_n$  and  $\bar{M}_w$  relative to poly(styrene) from data of peak heights at various elution volumes.

### 3.3.2 Nuclear Magnetic Resonance (N.M.R.)

This technique was used to determine the composition of copolymers prepared from glycidyl methacrylate and methyl methacrylate. Proton N.M.R. reveals the range of magnetic environments of the hydrogen atoms in a molecule and has been widely used in the determination of the structural and stereochemical details of molecules.

Proton N.M.R. spectra were recorded using an EM-360 60 MHz spectrometer. Samples were prepared by dissolution of the copolymers in deuterated chloroform at a concentration of approximately 0.1 g./ml. The solvent contained a small amount of tetramethyl-siloxane as an internal standard.

In the copolymer there are  $m_1$  moles of glycidyl methacrylate repeat units and  $m_2$  moles of methyl methacrylate repeat units. Examination of the N.M.R. spectra of the equivalent homopolymers reveals that the quadruplet at 2.4-3.0  $\delta$  in poly(glycidyl methacrylate) occurs in a region where PMMA shows no magnetic resonance. The quadruplet arises from the resonance of the terminal methylene group in the ester side chain of PGMA. The integrated height corresponding to the area of this peak therefore corresponds to two GMA protons ( $I_{\text{GMA}}$ ) whilst the total integrated height of the copolymer spectrum represents the resonance of ten GMA protons plus eight MMA protons ( $I_{\text{T}}$ ). The relative amounts of  $m_1$  and  $m_2$  can be found by

$$\frac{m_1}{m_2} = \frac{I_{\text{GMA}}/2}{(I_T - 10I_{\text{GMA}})/8} = \frac{4I_{\text{GMA}}}{(I_T - 5I_{\text{GMA}})} \quad (3.1)$$

### 3.3.3 Elemental Analysis

Elemental analysis was found to be the most precise technique for determining the composition of copolymers containing methacrylonitrile. Quantitative infra-red measurements of chloroform solutions (0.02 g./ml.) using the CN absorption peak at  $2240 \text{ cm}^{-1}$  of the copolymers showed poor reproducibility. This is principally because the infra-red spectrometer (Perkin Elmer 457) records band intensities in per cent transmittance. Transmittance (T) is related logarithmically to absorbance (A) (Beer-Lambert Law) so slight inaccuracies in the measurement of T correspond to large discrepancies in A. N.M.R., as described in the previous section, can be used to determine copolymer composition but the precision of the method, as indicated by the standard deviation of a number of measurements on the same sample, is slightly inferior to that of elemental analysis. This probably arises from errors in the measurement of the integrated heights.

Elemental analysis was carried out by the Micro-Analytical Laboratory at Manchester University. The results gave the percentage content by weight of carbon, hydrogen, oxygen and nitrogen. As the nitrogen derives entirely from the methacrylonitrile sequences the molar ratio of the two species can be easily calculated.

### 3.4 PREPARATION OF POLYMER BLENDS

Blending was carried out using the mutual solvent method. The blend constituents were dissolved independently in a common solvent



at concentrations of 0.02 g. - 0.04 g./ml. and were then mixed in appropriate quantities to yield a solution of the required composition. After mixing the solution was stirred for about 30 minutes to ensure homogeneity. The solution was then poured into a crystallisation dish, covered with filter paper, and left to stand at room temperature. The time taken for the bulk of the solvent to evaporate varied with volatility. The removal of the last traces of solvent, most of which was trapped within the blend film, was undertaken in a vacuum oven heated to a temperature  $10^{\circ}\text{C}$  above the glass transition region of the component with the higher  $T_g$ . After the samples had attained constant weight they were then stored at this temperature until usage.

### 3.5 TECHNIQUES USED TO DETERMINE MISCIBILITY

#### 3.5.1 Optical Microscopy

Cast blend films were examined for signs of gross heterogeneity using a Leitz polarizing microscope (50x magnification) fitted with a Mettler FP5 hot-stage (ambient  $-300^{\circ}\text{C} \pm 0.1^{\circ}$ ). Samples were prepared by placing a few drops of the blend solution (as in 3.4) within a teflon 'O' ring (2 cm. diameter) sitting on a glass slide. The bulk of the solution tended to flow to the edges of the ring leaving a central circular area ( $\approx 1$  cm. diameter) of uniform thickness ( $t < 0.01$  mm.). Examination of film clarity and structure was restricted to this central area. To ensure complete solvent removal before observation films were slowly ( $3^{\circ}\text{C min}^{-1}$ ) heated to a temperature just above the glass transition temperature of the higher  $T_g$  constituent; annealed here for 30 mins.; and finally cooled to ambient at the same rate. Observations of blend appearance were made at this point and then as a function of temperature (heating

at  $3^{\circ}\text{C min}^{-1}$ ) until the film started to degrade.

### 3.5.2 Differential Thermal Analysis

The glass transition behaviour of homopolymers, copolymers and the various blends was measured using a Du Pont 900 Differential Thermal Analyser fitted with a Differential Scanning Calorimetry accessory. The essential features of the D.S.C. cell are depicted in Figure (3.2). A sample and reference (air) pan sit on nipples on the constantin disc and are heated at a constant rate by the silver heating block. In the calorimetric mode the temperature difference between the sample and reference is recorded against the temperature of the reference. The instrument was calibrated using mercury (m.pt. =  $-39^{\circ}\text{C}$ ) and indium (m.pt. =  $156.5^{\circ}\text{C}$ ). Figure (3.3) shows an idealized thermogram of a material passing through its glass transition. There is no widespread agreement about which parameters to use to determine  $T_g$  from such a thermogram. In this work the double tangent method was applied as shown in Figure (3.3).

Samples were prepared by accurately weighing a portion of the material into the aluminium pan, placing an aluminium lid on top and crimping the edges carefully. It was found to be essential that the bottom of the sample pan was flat to ensure good thermal contact with the constantin disc. Blend samples were either cut from the films whose preparation was described in section (3.4) or much smaller (1-2 ml.) casts onto teflon blocks were made. In the latter case heat treatment to ensure solvent removal was as described previously (3.4). In 50/50 (by weight) blends 15-20 mg. of sample proved sufficient however as the relative amounts of the components became more dissimilar it was tried wherever possible to increase the sample weight. This was of course limited by the size of the pan and the nature of the sample.

Figure (3.2)  
D.S.C. Cell

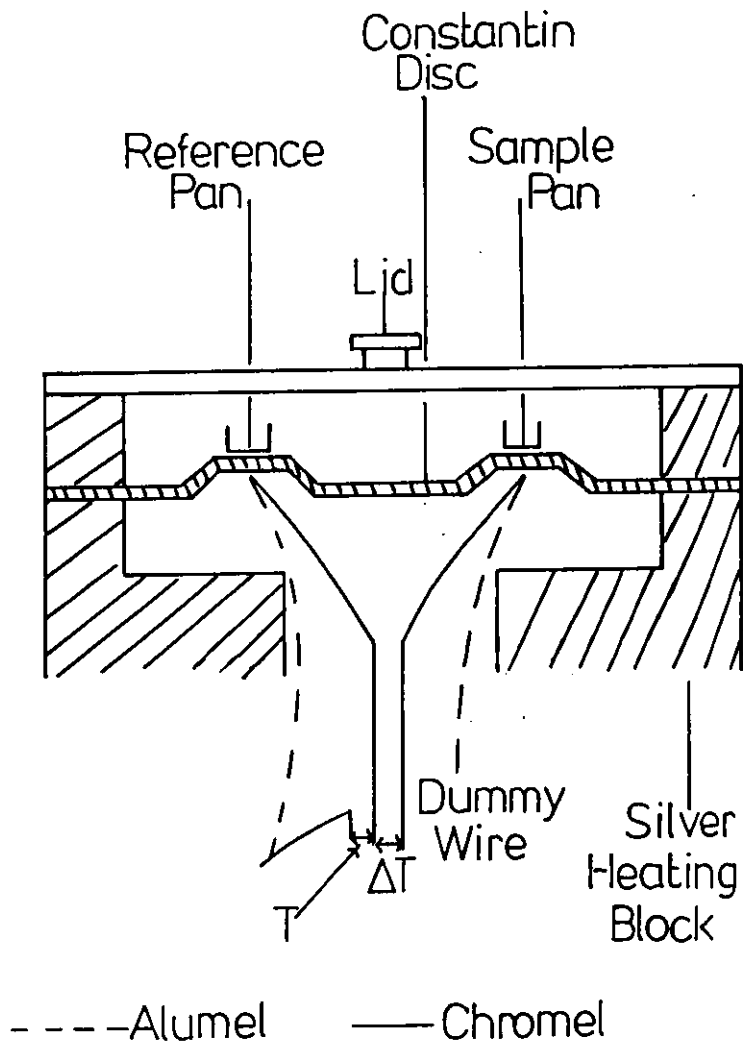
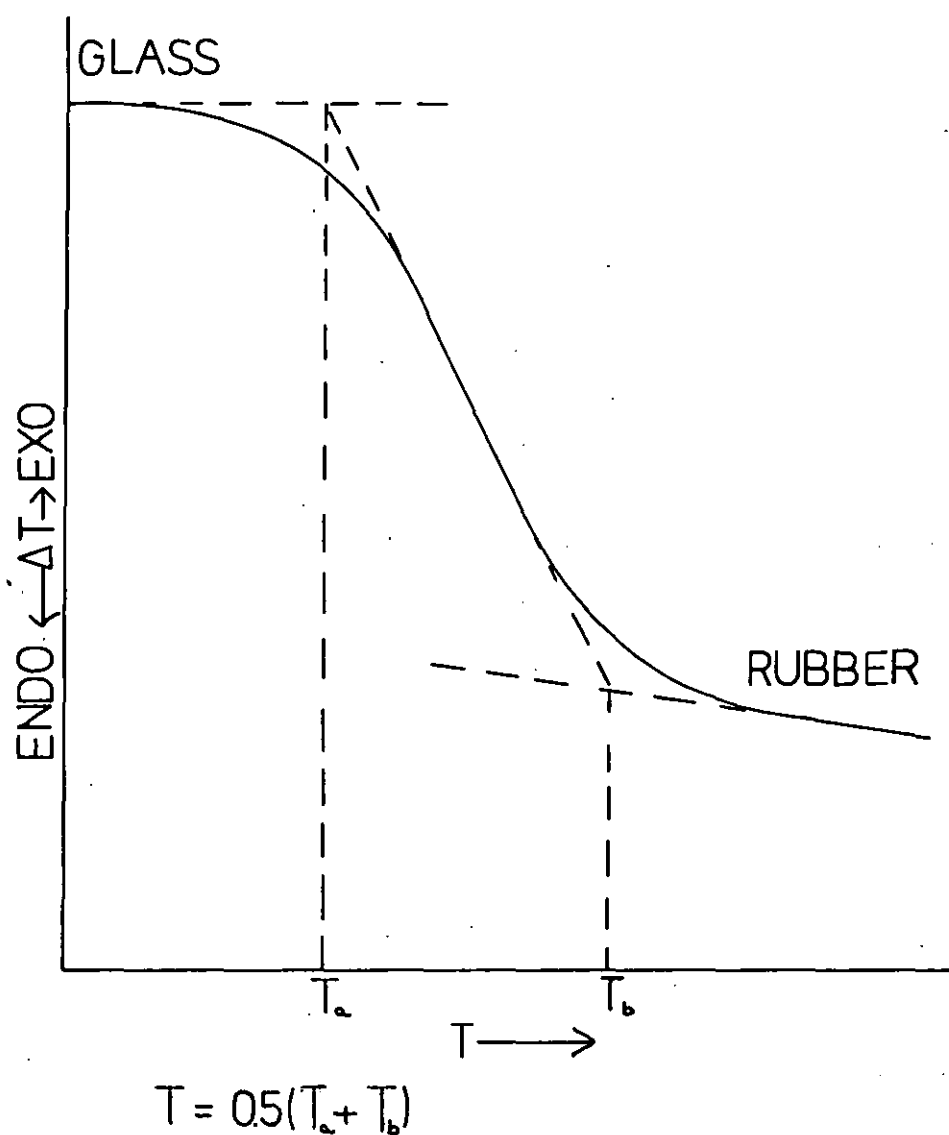


FIGURE (33)  
Schematic of Glass Transition Behaviour  
Observed by D.T.A.



Samples were loaded into the DTA cell at ambient temperatures and were then cooled to  $-100^{\circ}\text{C}$  using liquid nitrogen. They were heated from this temperature at  $20^{\circ}\text{C min}^{-1}$  to a point  $20^{\circ}\text{C}$  above the  $T_g$  of the glassier component. All samples were run at least twice as on the first scan one often observes anomalous effects due to settling within the pan.

### 3.5.3. Dynamic Mechanical Thermal Analysis

All mechanical measurements were made using a Dynamic Mechanical Thermal Analyser (Polymer Laboratories). The sample arrangement chosen requires a rectangular bar of material which is firmly clamped at both ends. A third, central clamp also holds the specimen and is attached to a drive shaft linked to a mechanical oscillator. The frequency and amplitude (strain) of oscillation are pre-set and the resistance to the applied deformation is recorded as a function of the magnitude and phase of the sample displacement. The associated solid state electronics convert these signals automatically to yield the dynamic storage (Young's) modulus and the loss tangent. The DMTA head and a block diagram of the electronics are shown in Figures (3.4) and (3.5) respectively.

Two methods of sample preparation were used. In the first case films, prepared as described in section (3.4), were shredded and then compression moulded to form rectangular bars. The press temperature was set at  $40\text{-}50^{\circ}\text{C}$  above the  $T_g$  of the glassier component. The mould containing sample was preheated on the lower platten for about 15 minutes and was then subjected to a pressure of  $1,000 \text{ lb./inch}^2$  for 45 seconds before being set aside to cool gradually to ambient temperature. The thickness and breadth of the pressed sample were accurately measured using a micrometer and vernier calipers respectively.

Figure (34)  
DMTA Measuring Head Assembly

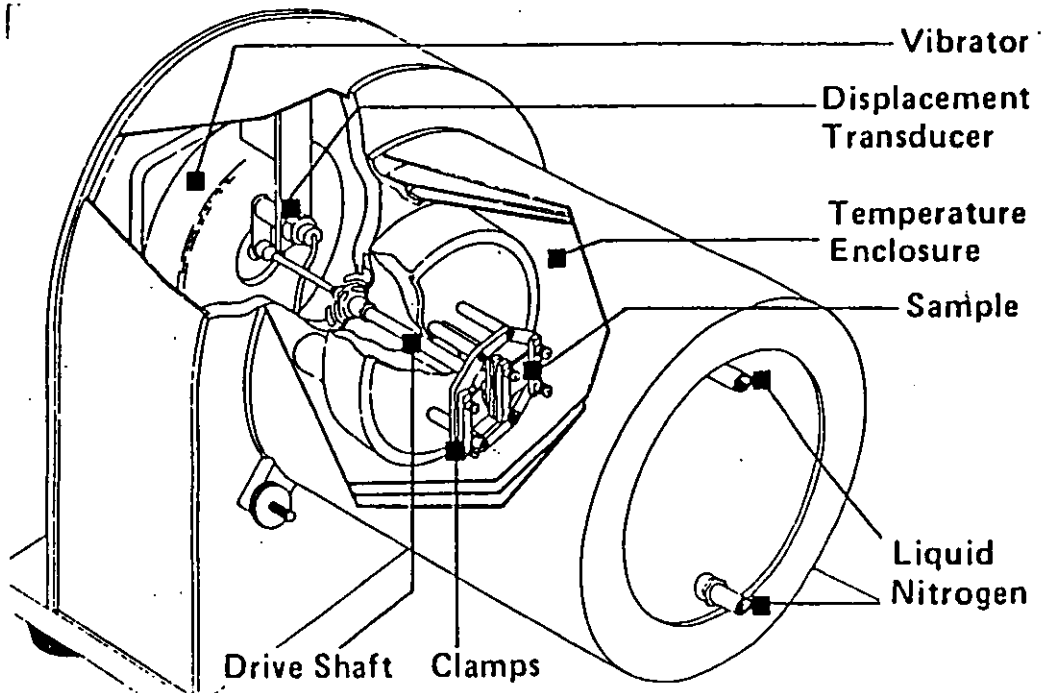
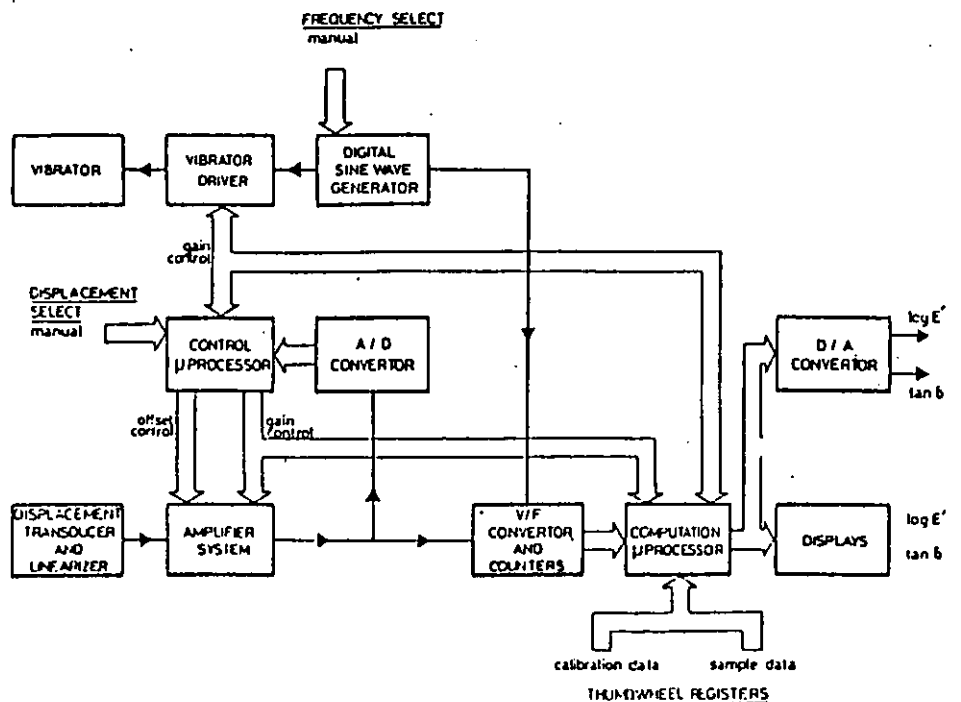


Figure (35)  
Block Diagram of DMTA Electronics



These figures were then used to determine a geometry constant ( $k$ ), the negative logarithm of which was dialled into the DMTA so as to obtain absolute values of the storage modulus.  $k$  was calculated from

$$k = 2b \left( \frac{t}{l} \right)^3 \quad (3.2)$$

where  $b$  and  $t$  are the breadth and thickness of the sample (in metres) and  $l$  corresponds to half the unclamped distance which can be selected from a range of available clamp frame sizes. The most suitable range of values for  $-\log k$  is 3.2-3.5 which was achieved in most cases using  $b = 0.8$  cm.;  $t = 0.3$  cm.;  $l = 1$  cm.

The second method of sample preparation involved casting thin films of material from solutions containing 0.02-0.04 g./ml. onto rectangular steel strips (thickness 0.2 mm.). The films were kept at ambient temperature for a few days to allow solvent evaporation after casting and were then annealed in the hot-stage, as described in section (3.5.1), to ensure complete solvent removal before running. Using such samples it is not possible to determine the storage modulus of the film as the recorded value is dominated by the steel and cannot be resolved. However the damping behaviour of the steel over the temperature range used produces a small constant value of  $\tan \delta$  which can be easily subtracted to yield a qualitative picture of the glass transition behaviour of the film.

Samples were clamped securely in the measurement head to prevent slippage and an outer cover containing a furnace and cooling coils was then fixed in place. The temperature range used in most cases matched that for DTA measurements. Samples were initially cooled

to the start temperature using liquid nitrogen and were then heated at  $4^{\circ}\text{C min}^{-1}$ . Most measurements were conducted at 1 Hz at a strain setting of  $\times 1$  corresponding to a displacement amplitude of 10 microns.

### 3.5.4 Dielectric Relaxation

Dielectric measurements were carried out using a Wayne-Kerr B221 Universal Bridge, a Wayne-Kerr A321 waveform analyser and an Advance Instruments low frequency oscillator. The Universal Bridge is a transformer ratio arm bridge designed for the measurement of high loss systems. The bridge treats the sample as a capacitance  $C$  in parallel with a resistance  $R$ . Cole and Cole<sup>(148)</sup> have shown that for such an arrangement

$$\epsilon' = \frac{C}{C_0} \quad (3.3)$$

$$\epsilon'' = \frac{1}{RC_0\omega} \quad (3.4)$$

$$\tan \delta = \frac{\epsilon''}{\epsilon'} = \frac{1}{RC\omega} \quad (3.5)$$

Values of the capacitance and reciprocal resistance (conductance) are read directly from the bridge, and  $\epsilon'$  and  $\epsilon''$  can be calculated from the following forms of equations (3.3) and (3.4) for a Wayne-Kerr set-up

$$\epsilon' = \frac{3.6Cd}{r^2} \quad (3.6)$$

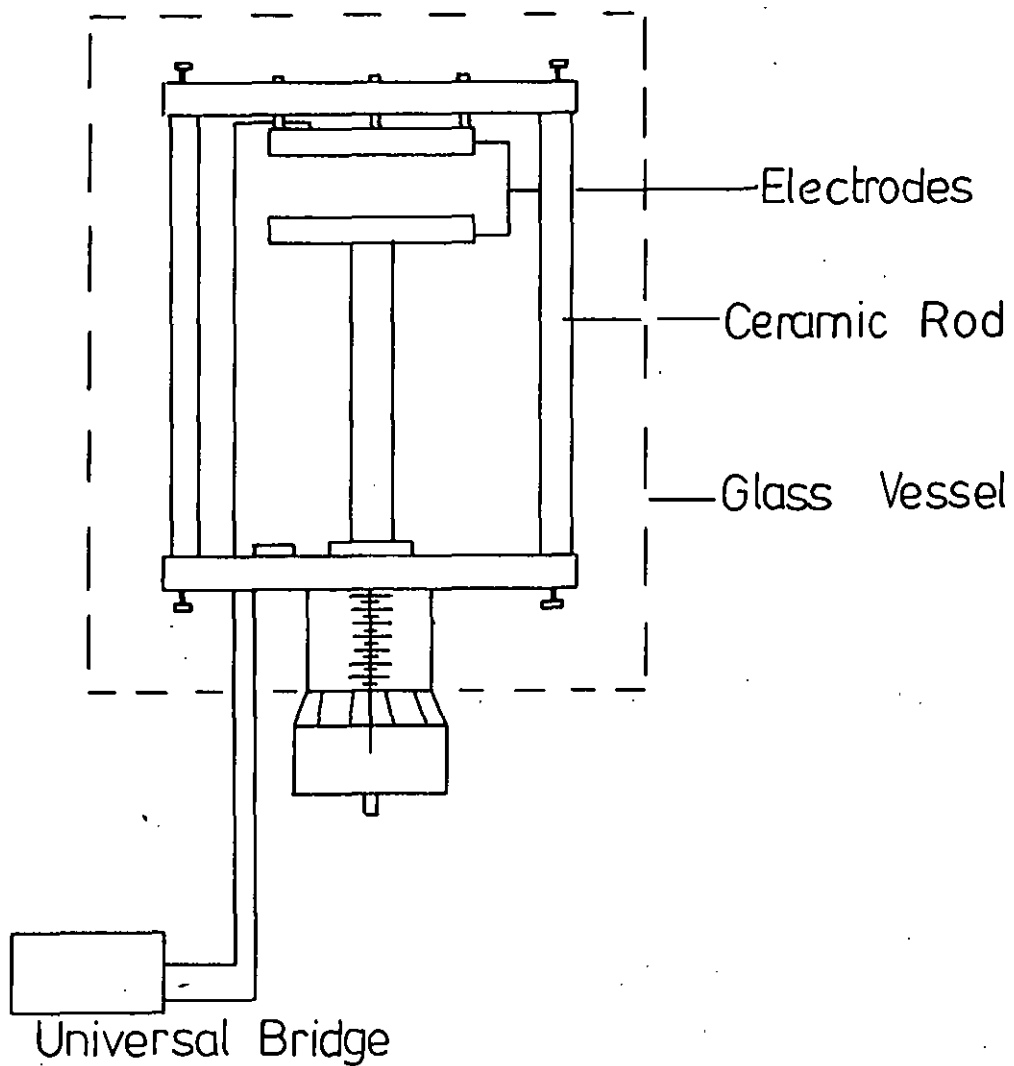


$$\epsilon'' = \frac{3.6 d}{2\pi fr^2 R} \quad (3.7)$$

where  $r$  is the electrode radius and  $d$  the sample thickness.

Samples were prepared by casting (section (3.4)) followed by compression moulding into the form of discs as described in section (3.5.3). The sample cell, built by Harrison<sup>(186)</sup>, consisted of two polished stainless steel electrodes, the lower one being fixed whilst the upper one was attached to a micrometer screw. This allowed direct reading of  $d$ . The electrodes were supported by a framework of two "macor" ceramic rods. The arrangement is shown in Figure (3.6). Temperature was measured via a copper-constantin thermocouple placed near to the electrodes. The cell was placed within a sealed glass vessel fitted with nitrogen inlet. Sub-ambient measurements were made by placing the cell assembly in a methanol bath which was then cooled gradually by the addition of solid carbon dioxide. This allowed temperature control to within  $\pm 0.5^\circ\text{C}$ . Measurements above ambient temperature were performed in an oil bath with a similar temperature control performance. Readings were taken at approximately  $10^\circ\text{C}$  intervals and to ensure thermal equilibrium the sample was held at each measurement temperature for 30 minutes prior to measurement. At each temperature the conductance and capacitance were recorded at a variety of frequencies in the range  $5 \times 10^2 - 2 \times 10^4$  Hz.

Figure (3.6 )  
Dielectric Cell



CHAPTER 4

RESULTS FOR HOMOPOLYMER/HOMOPOLYMER BLENDS

#### 4.1 POLY(METHYL METHACRYLATE)(PMMA)/(POLY(EPICHLOROHYDRIN)(PEPC)

##### 4.1.1 Characterisation of Polymers

The number and weight average molecular weights relative to poly(styrene) determined by G.P.C. are recorded in Table (4.1). The same sample of poly(epichlorohydrin) was used throughout this work.

##### 4.1.2 Optical Properties

Films cast from dichloromethane were opaque at weight fractions of PMMA greater than 0.1, at lower concentrations the films appeared transparent. The molecular weight of PMMA was found to have no influence on film appearance. Opacity was found to decrease gradually with temperature in the range 120-200°C.

##### 4.1.3 Thermal Analysis Data

The D.T.A. results are presented in Figure (4.1). Two transitions were observed at temperatures essentially independent of blend composition except at the extremes of concentration where single glass transitions were recorded. Comparison of the blend glass transitions with those of the pure components reveals a shift of some 10°C in each but little alteration of transition widths. Molecular weight had no influence on the glass transition behaviour of the blends.

##### 4.1.4 Dynamic Mechanical Data

Dynamic mechanical measurements were made on cast films which had previously been annealed at 120°C under vacuum. The variation of the loss tangent with temperature is plotted in Figure (4.2). Two transitions were evident except at the extremes of the composition range, although at 30 and 70 weight per cent PMMA the peak associated with the minor phase was not well defined. The glass transition

Table 4.1. G.P.C. Results for PEPC and PMMA

Polymer	Source	$\bar{M}_w$	$\bar{M}_n$	$\bar{M}_w/\bar{M}_n$
PEPC	Aldrich Chemical Co. Ltd.	397,731	74,449	5.34
PMMA #1	BDH Chemicals Ltd. - 'high molecular weight'	133,543	55,306	2.42
PMMA #2	Solution polymerisation, $[s]/[m]^* = 2.0$	57,032	34,215	1.67
PMMA #3	Solution polymerisation, $[s]/[m] = 14.0$	20,117	14,800	1.36
PMMA #4	Solution polymerisation, $[s]/[m] = 23.3$	17,108	13,497	1.28

[\* Molar ratio of solvent to monomer in feed]

Figure (4.1)  
D.T.A Data for PMMA/PEPC

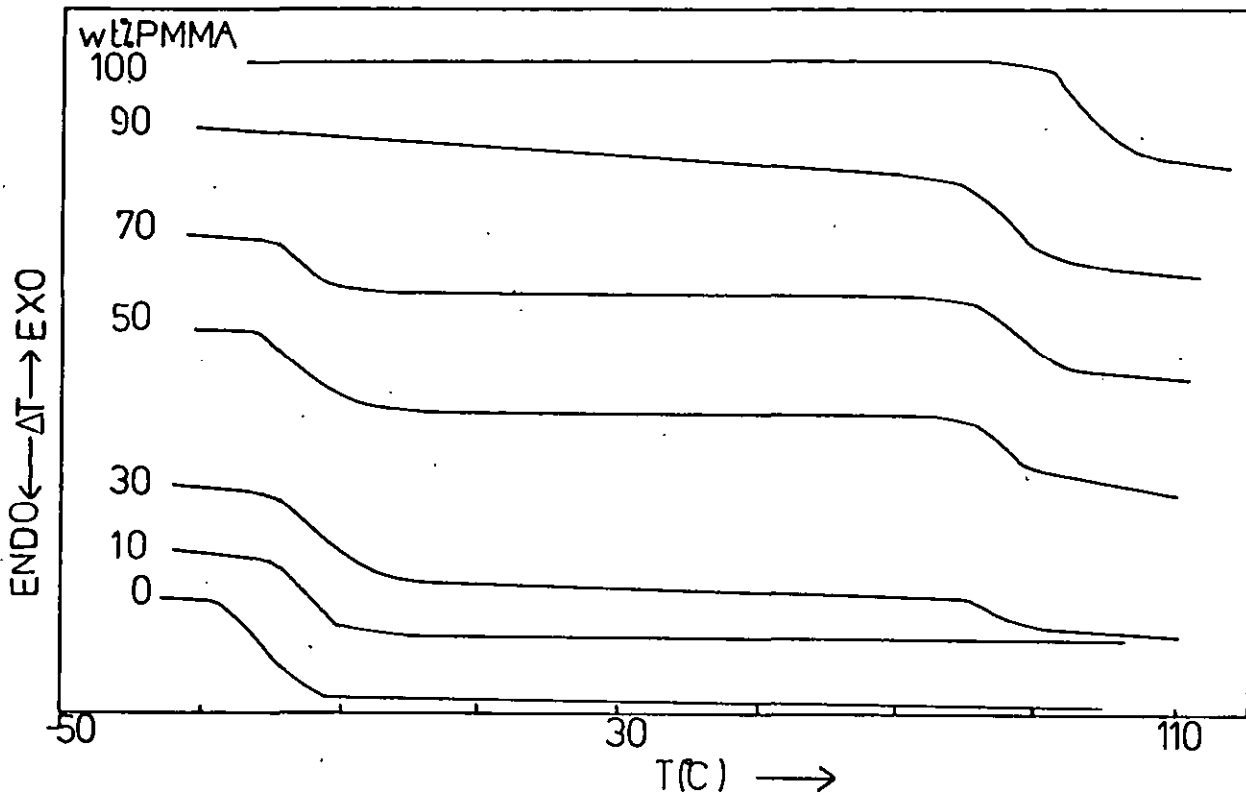
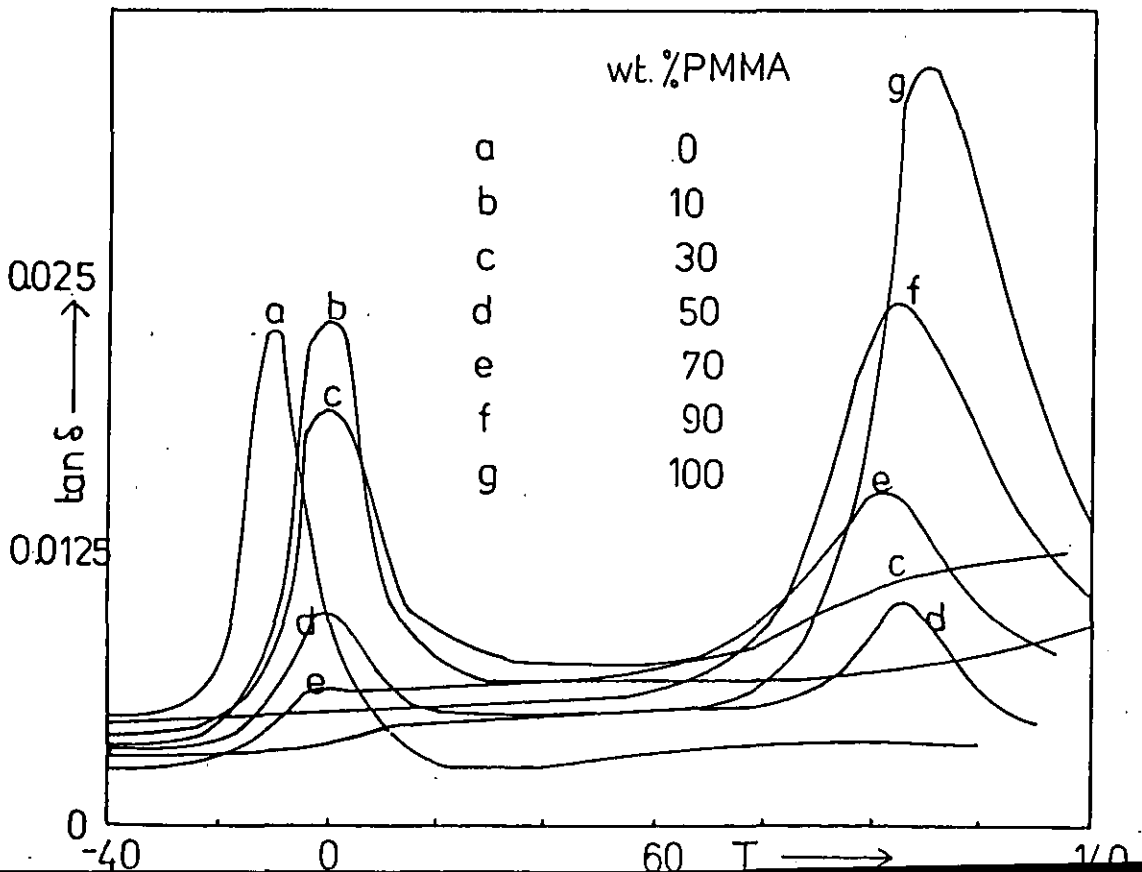


Figure (4.2)  
Loss Tangent vs. Temperature Curves  
for PMMA/PEPC



temperatures ( $\tan \delta$  maxima) were independent of blend composition as found by D.T.A.

## 4.2 POLY(ETHOXY ETHYL METHACRYLATE)(PEEMA)/POLY(EPOCHLOROHYDRIN)

### 4.2.1 Characterisation of PEEMA

PEEMA was prepared by free radical solution polymerisation under the conditions described in Table (3.1). The number and weight average molecular weights relative to poly(styrene), as determined by G.P.C. were

$\bar{M}_w$	$\bar{M}_n$	$\bar{M}_w/\bar{M}_n$
110,937	40,341	2.75

### 4.2.2 Optical Properties of PEEMA/PEPC

Transparent films were observed over the complete concentration range and remained so up to degradation temperatures in the region of 200°C.

### 4.2.3 Thermal Analysis

The blends exhibited a single glass transition, as shown in Figure (4.3) whose dependence on composition followed a Fox type relationship at high concentrations of PEEMA (Figure (4.4)). However below a weight fraction of PEEMA of 0.7 there was a negative deviation from the predicted glass transition values for a miscible blend, the value of which increased with PEPC content.

The breadth of the glass transition, measured by D.T.A., was defined as the difference between the temperatures at which deviation from the recorded base-line was observed. This is illustrated below where the breadth is taken as  $(T_2 - T_1)$ .

Figure (4.3)  
D.T.A. Data for PEEMA/PEPC

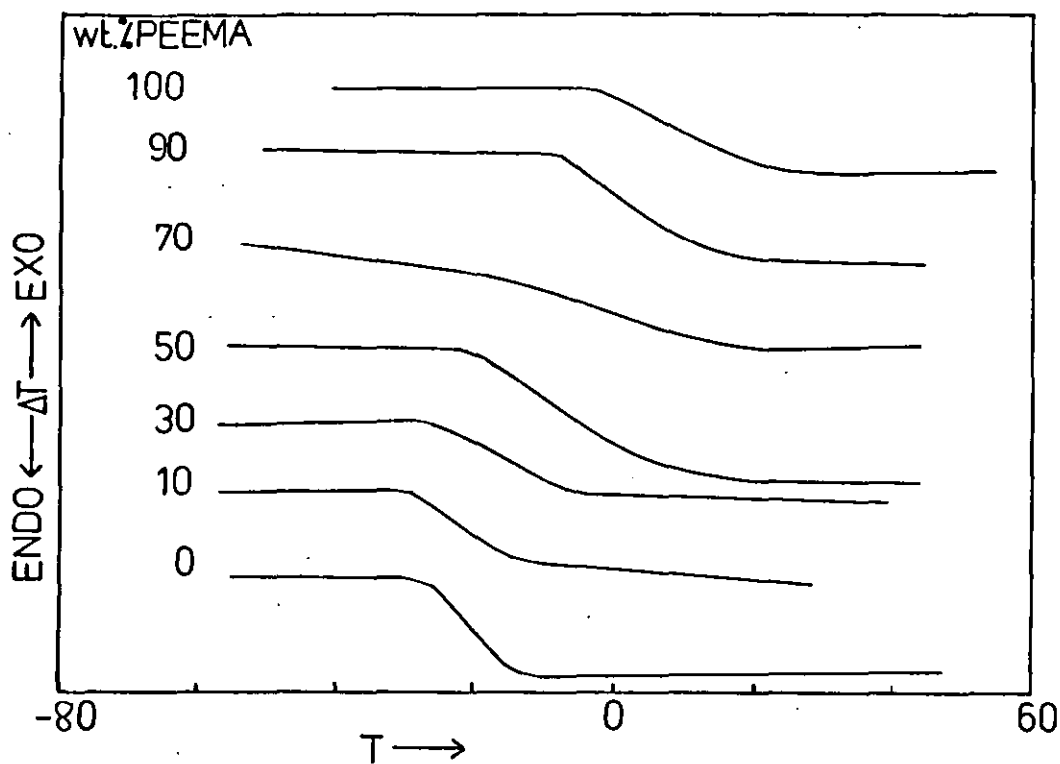
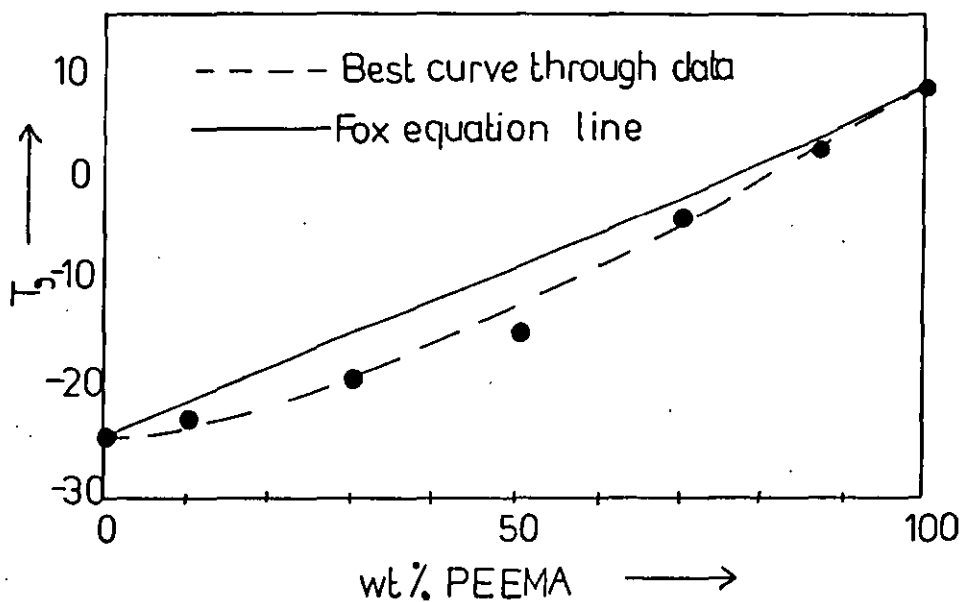
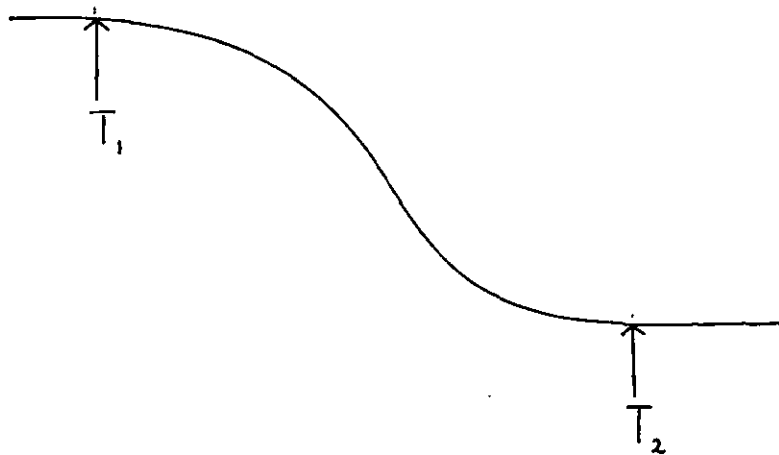


Figure (4.4)  
T<sub>g</sub> vs. Composition for PEEMA/PEPC  
Determined by D.T.A.







The transition widths for PEEMA/PEPC are recorded in Figure (4.5(a)) and were found to increase markedly in the range 0.5-0.7 PEEMA.

#### 4.2.4 Dynamic Mechanical Behaviour of PEEMA/PEPC

Samples were measured in the form of thin films, supported by steel, which had been annealed at 45°C under vacuum prior to use. The variation of the loss tangent with temperature at constant frequency (1 Hz) over the complete concentration range is reproduced in Figure (4.6). The peak maxima were found to be composition dependent in the manner of the glass transition temperatures measured by D.T.A. as shown in Figure (4.7). The transition breadth was quantified by measuring the peak width ( $w$ ) at half-height ( $l/2$ ) above the baseline extrapolated from the low temperature side. This is illustrated below.

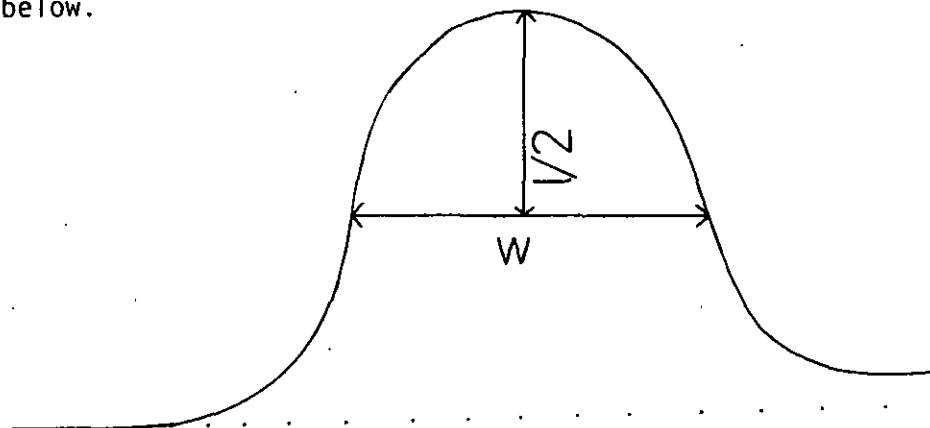


Figure (4.5)  
Transition Width (tw.) vs. Composition  
for PEEMA / PEPC

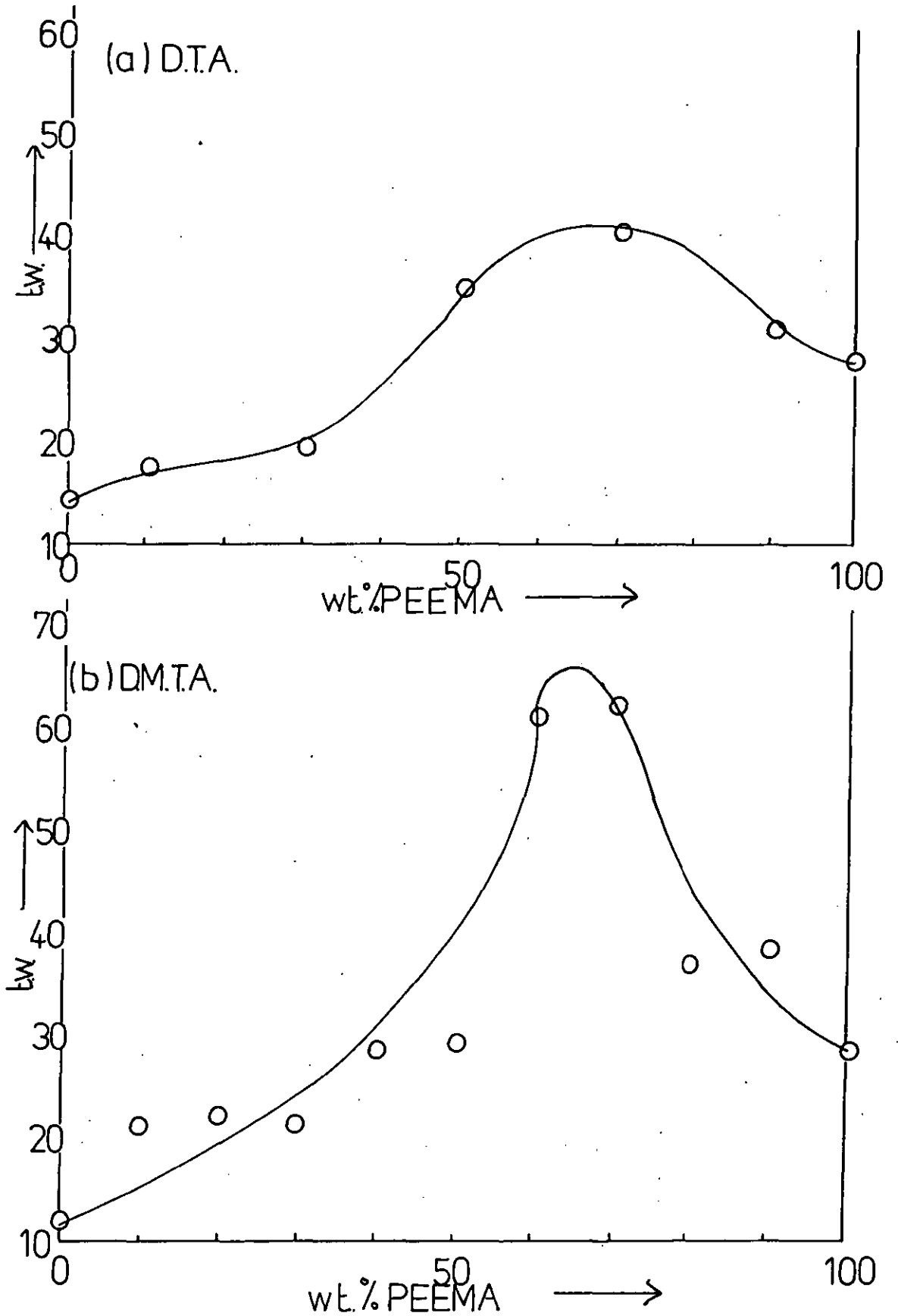


Figure (4.6)  
 Loss Tangent vs. Temperature Curves  
 for PEEMA / PEPC.

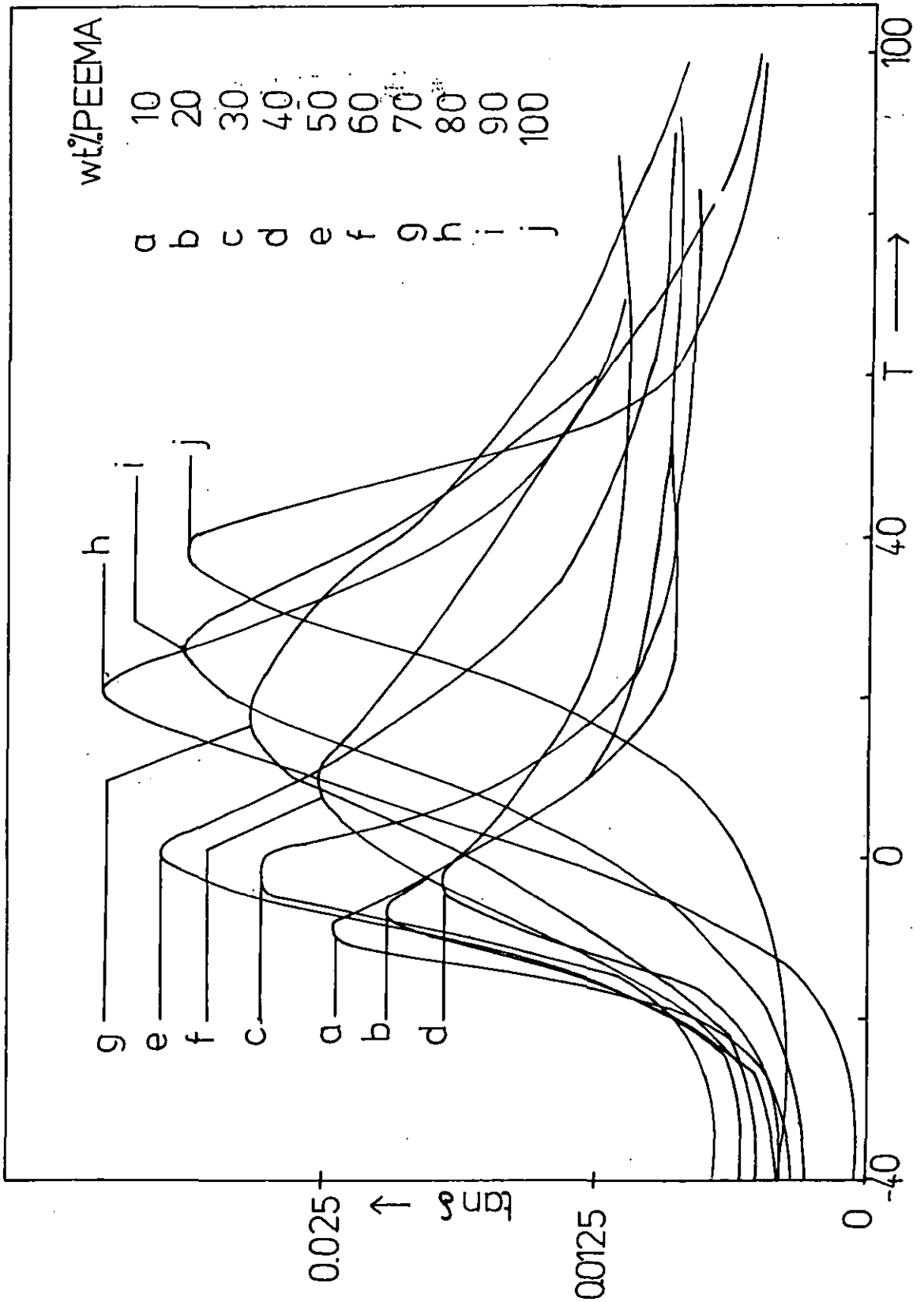


Figure (4.7)  
Composition Dependence of  $T_g$  for PEEMA /  
PEPC Measured by DMTA.

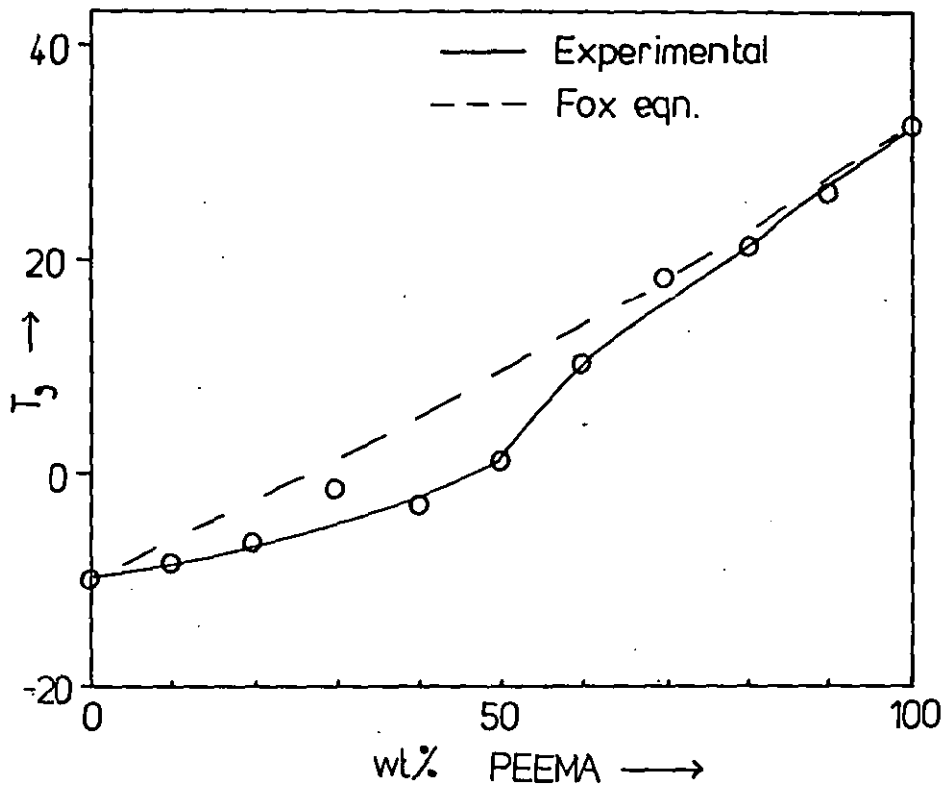
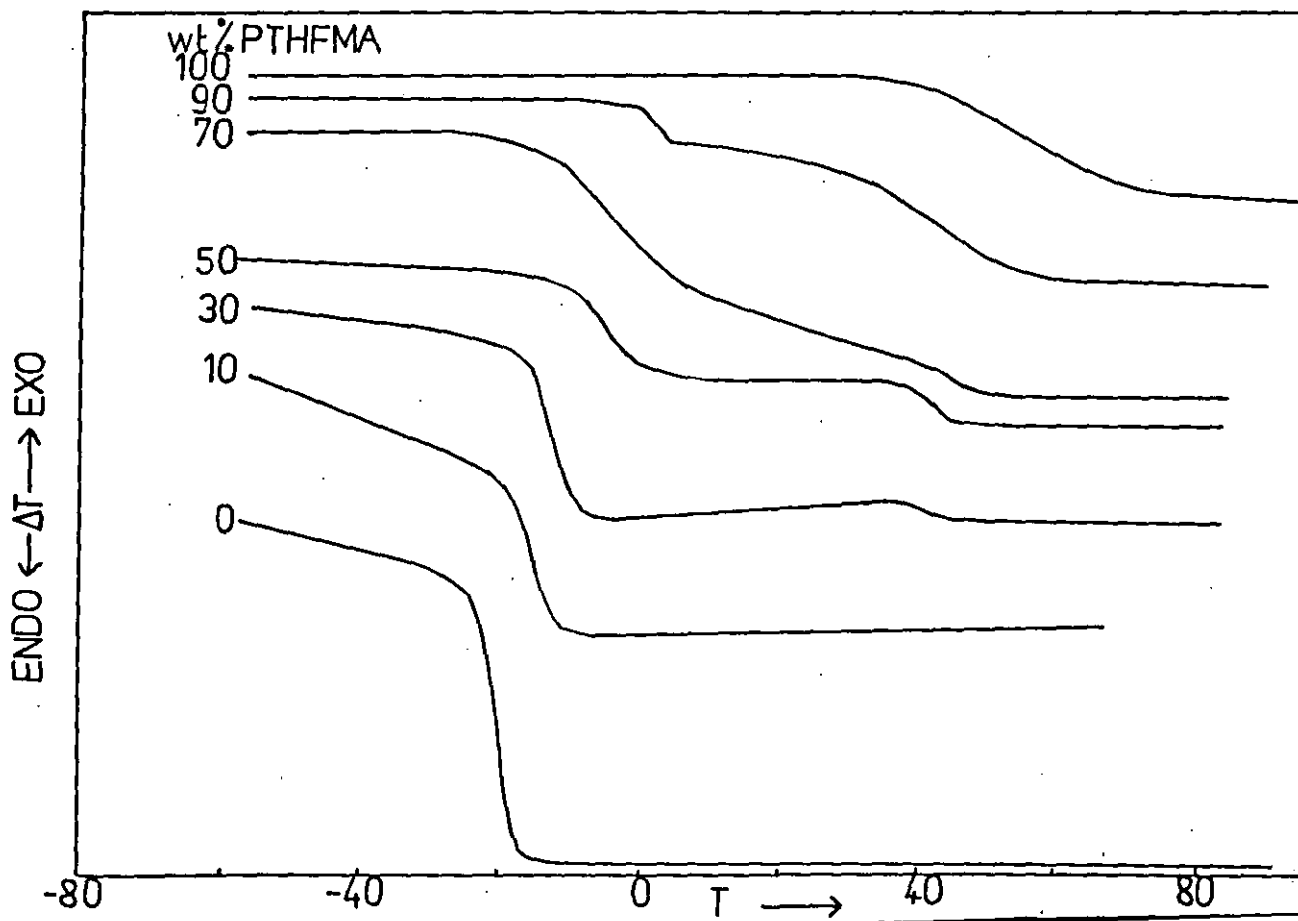


Figure (4.8)  
D.T.A. Data for PTHFMA / PEPC



The variation of  $w$  with composition is presented in Figure (4.5(b)) and was found to increase by a factor of 2 at weight fractions of PEEMA in the range 0.6-0.7. The trend in  $w$ , whilst resembling that measured by D.T.A., showed a much more pronounced maximum and higher overall values except for the pure components.

#### 4.3 POLY(TETRAHYDROFURFURYL METHACRYLATE)/POLY(EPICHLOROHYDRIN)

##### 4.3.1 Characterisation of PTHFMA

Free radical solution polymerised THFMA was found to have the following molecular weights relative to poly(styrene)

$\bar{M}_w$	$\bar{M}_n$	$\bar{M}_w/\bar{M}_n$
98,460	27,350	3.60

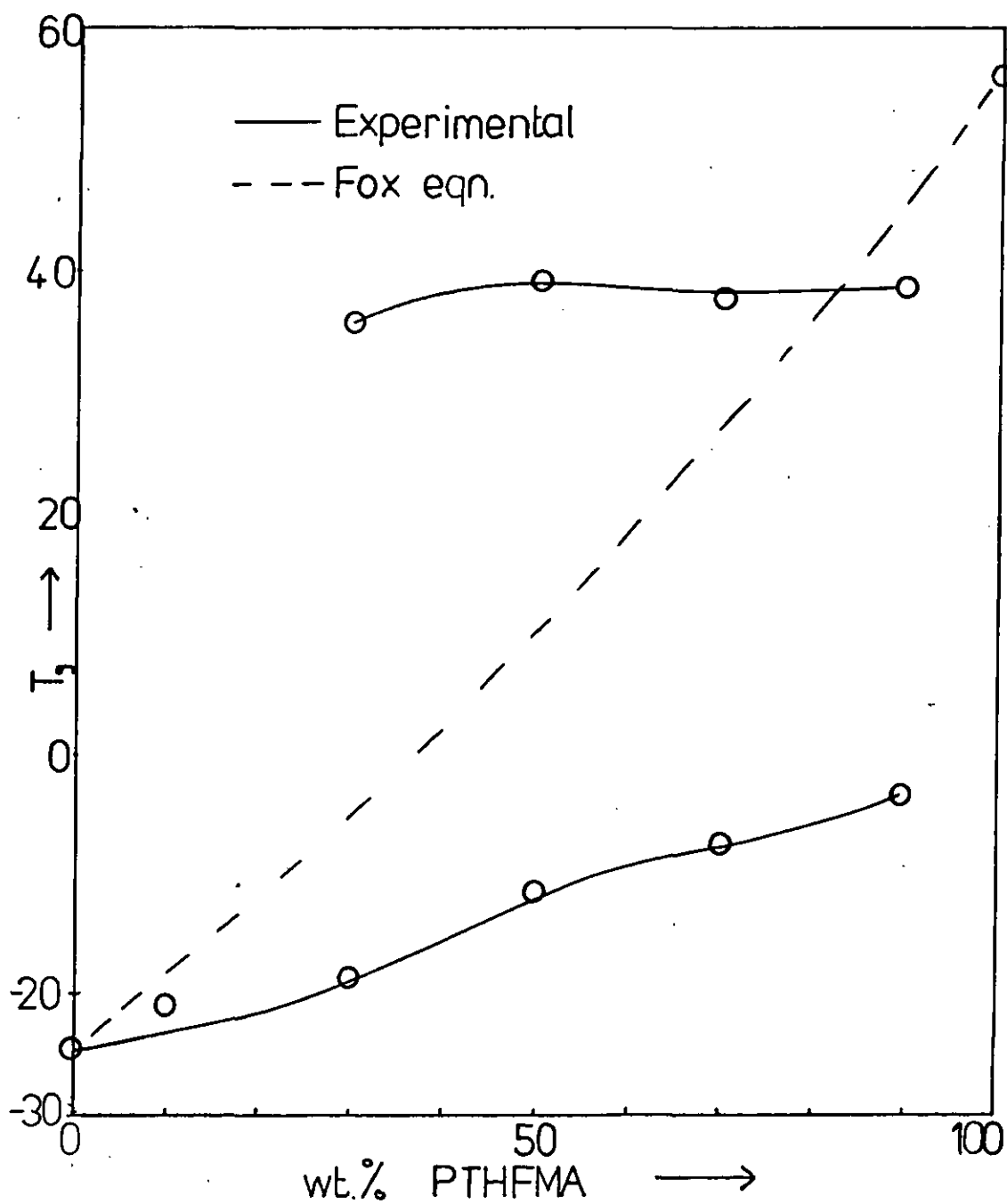
##### 4.3.2 Optical Properties of PTHFMA/PEPC

Transparent films were observed at weight fractions of PTHFMA up to 0.6, at higher concentrations the casts appeared slightly translucent when viewed in reflected light. Film appearance was found to be essentially independent of temperature up to 200°C at which point yellowing of the films, due to degradation, was observed.

##### 4.3.3 Thermal Analysis of Blends

The glass transition behaviour of PTHFMA/PEPC as determined by D.T.A. is presented in Figure (4.8). Two transitions were apparent for the blends except at high elastomer content. The composition dependence of the glass transition temperatures is plotted in Figure (4.9). It appears that whilst the lower temperature transition, relating to PEPC rich domains, showed a slight composition dependence, the  $T_g$ 's of the PTHFMA rich regions were independent of overall blend

Figure (4.9)  
Composition Dependence of  $T_g$  for PTHFMA/  
PEPC Measured by D.T.A.



composition. The breadth of the major transition at each composition is recorded in Figure (4.10(a)), and is seen to increase sharply at the intermediate composition.

#### 4.3.4 Dynamic Mechanical Behaviour of PTHFMA/PEPC

Dynamic mechanical measurements were made on films cast onto stainless steel strips. The samples were annealed at 100°C under vacuum prior to measurement. The variation of the loss tangent with temperature is shown in Figure (4.11). Examination of the variation of the maximum in the major relaxation peak ( $T_g$ ) with overall blend composition (Figure (4.12)) clearly indicates that the nature of the composition dependence varied according to which component was present in excess. Although there is clear evidence of the presence of more than one phase at weight fractions of PTHFMA in the range 0.5-0.8, the shape of the secondary relaxations does not allow for the assignment of a clear maximum value and hence a unique glass transition temperature. The variation of transition width with composition shown in Figure (4.10(b)) exhibited a similar pattern to that observed by D.T.A.

#### 4.4 POLY(GLYCIDYL METHACRYLATE)(PGMA)/POLY(EPICHLOROHYDRIN)

##### 4.4.1 Characterisation and Fractionation of PGMA

Solution polymerised glycidyl methacrylate was found to show quite a high degree of polydispersity (Table (4.2)) and exhibited a very distinct step at the high molecular weight side of the elution profile as shown in Figure (4.13). To investigate this feature the polymer was separated into five fractions whose molecular weights are recorded in Table (4.2). The elution profiles of the fractions are reproduced in Figure (4.14), however about 20 per cent of fraction

Figure (4.10)  
Plots of Major Transition Breadth ( $t_b$ ) vs.  
Composition for PTHFMA/PEPC

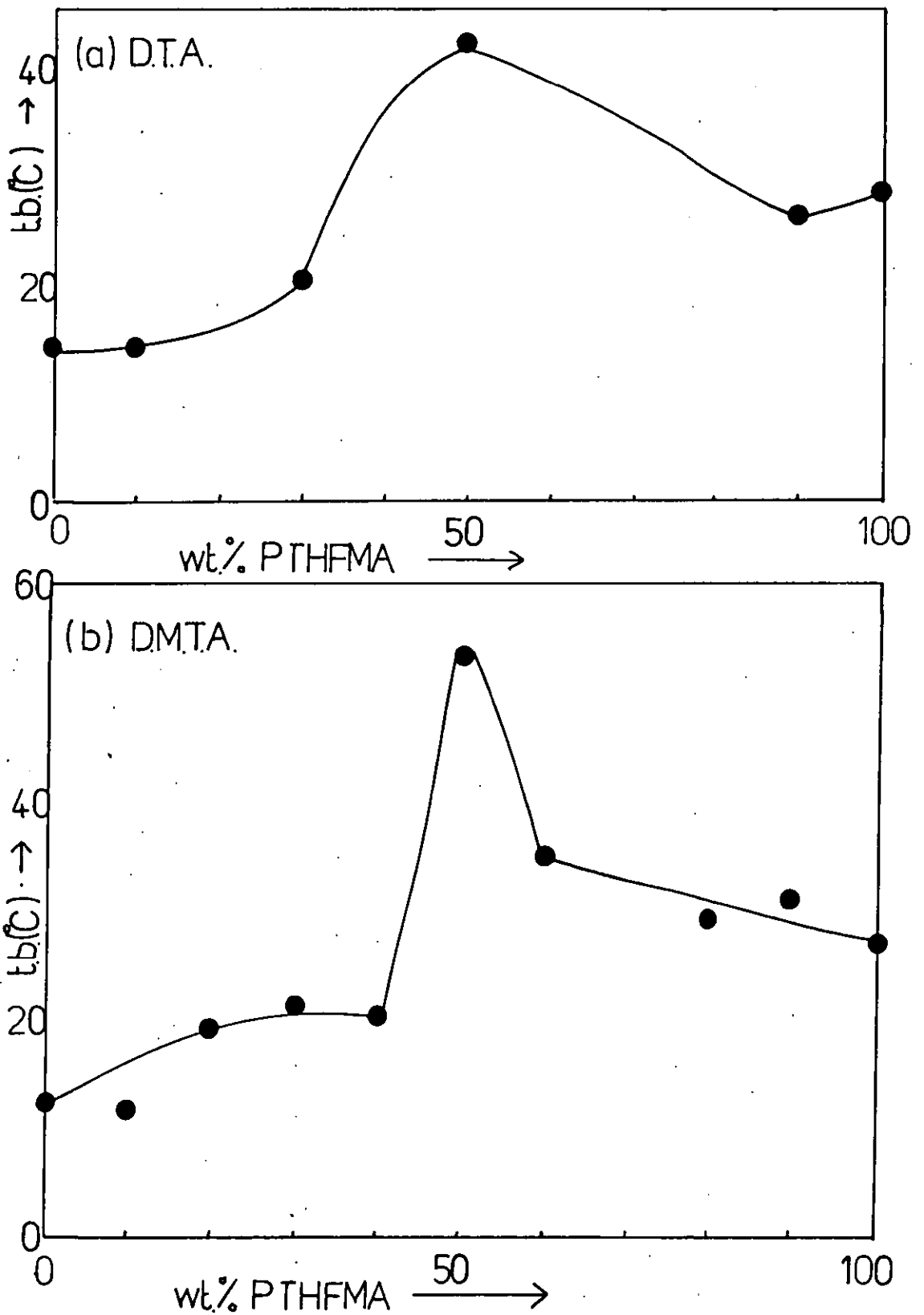




Figure (4.11)  
Loss Tangent vs. Temperature Curves  
for PTHFMA/PEPC

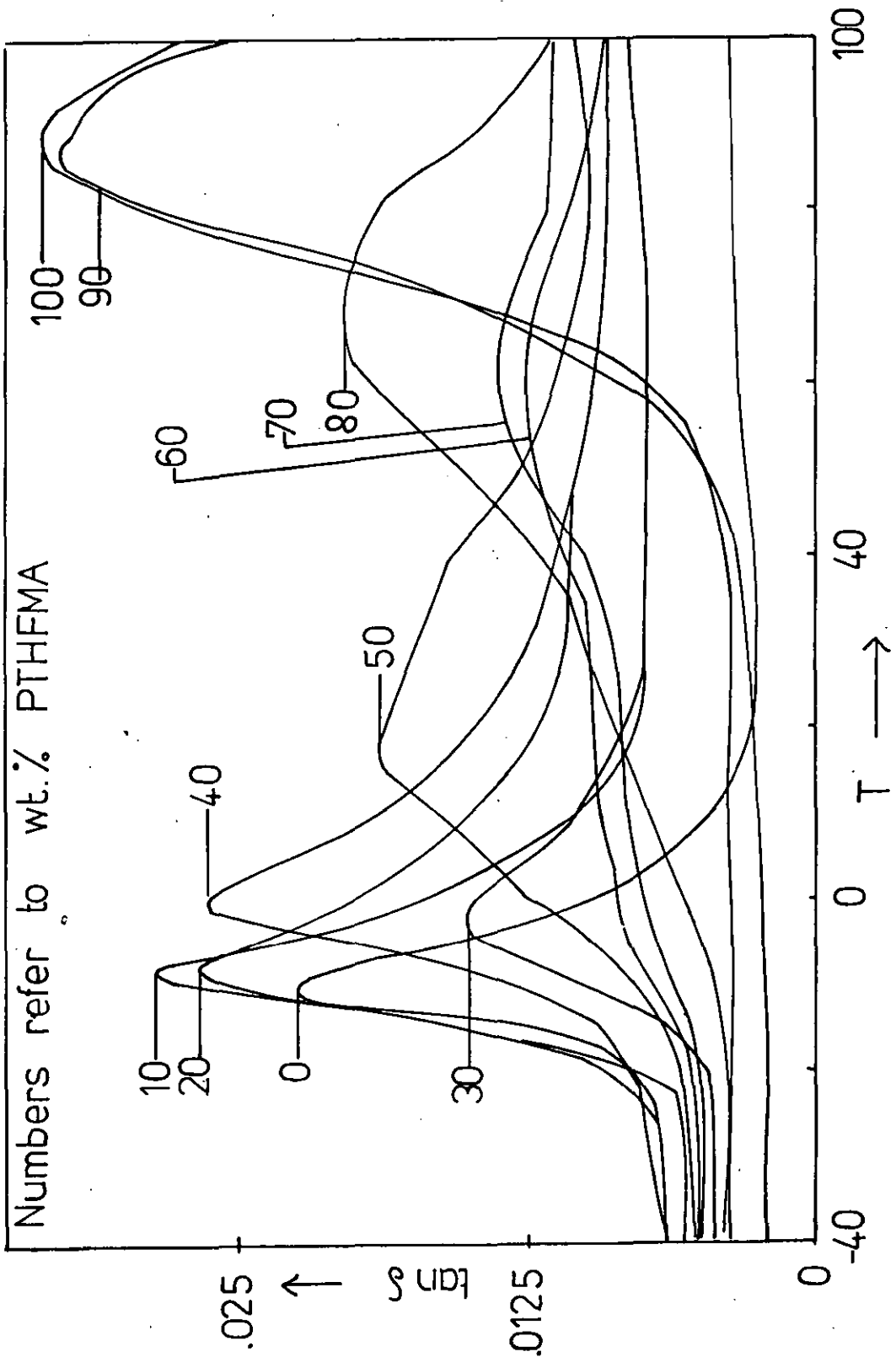


Figure (4.12 )  
Composition Dependence of  $T_g$  for PTHFMA  
/PEPC Measured by D.M.T.A.

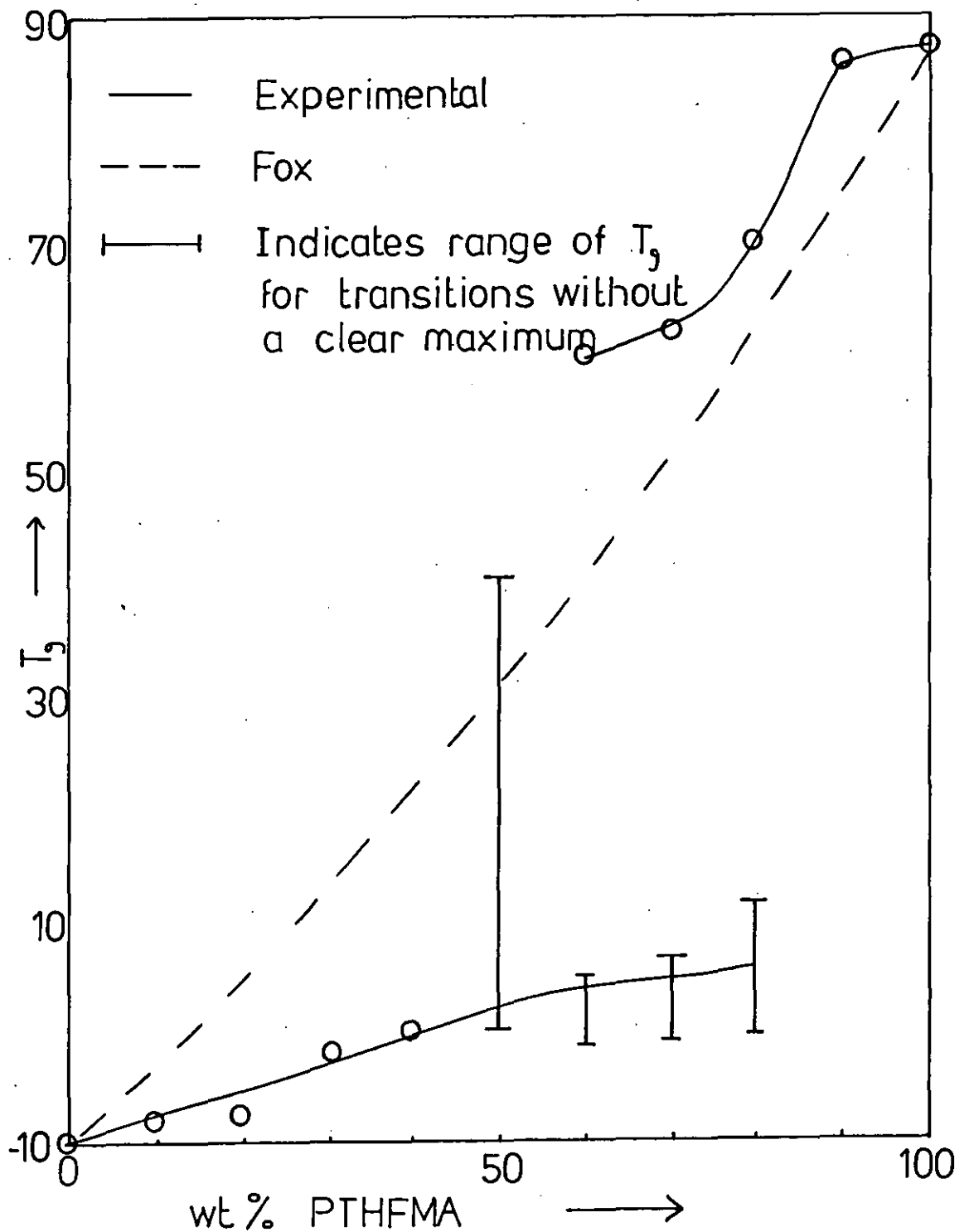


Table 4.2. G.P.C. Results for PGMA and its Fractions

	$\bar{M}_w$	$\bar{M}_n$	$\bar{M}_w/\bar{M}_n$
PGMA	183,178	33,049	5.54
Fraction #1	121,762	53,386	2.28
Fraction #2	71,369	42,246	1.69
Fraction #3	40,867	29,044	1.40
Fraction #4	23,223	17,283	1.34
Fraction #5	13,423	10,857	1.24

Figure (4.13)  
G.P.C. Chromatogram of PGMA

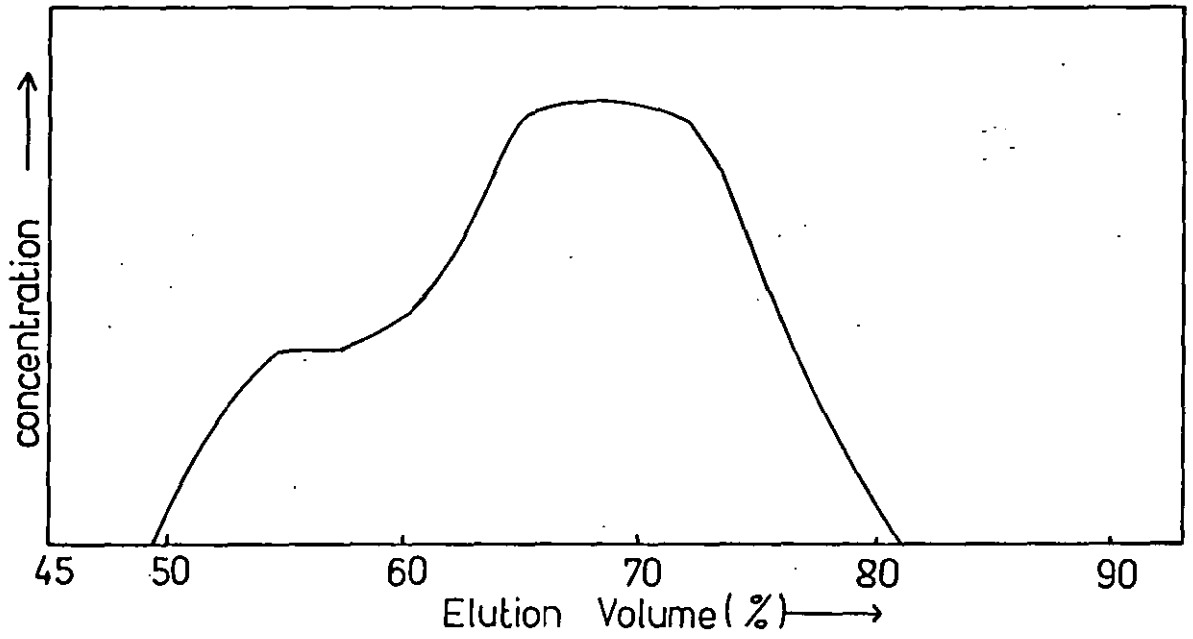
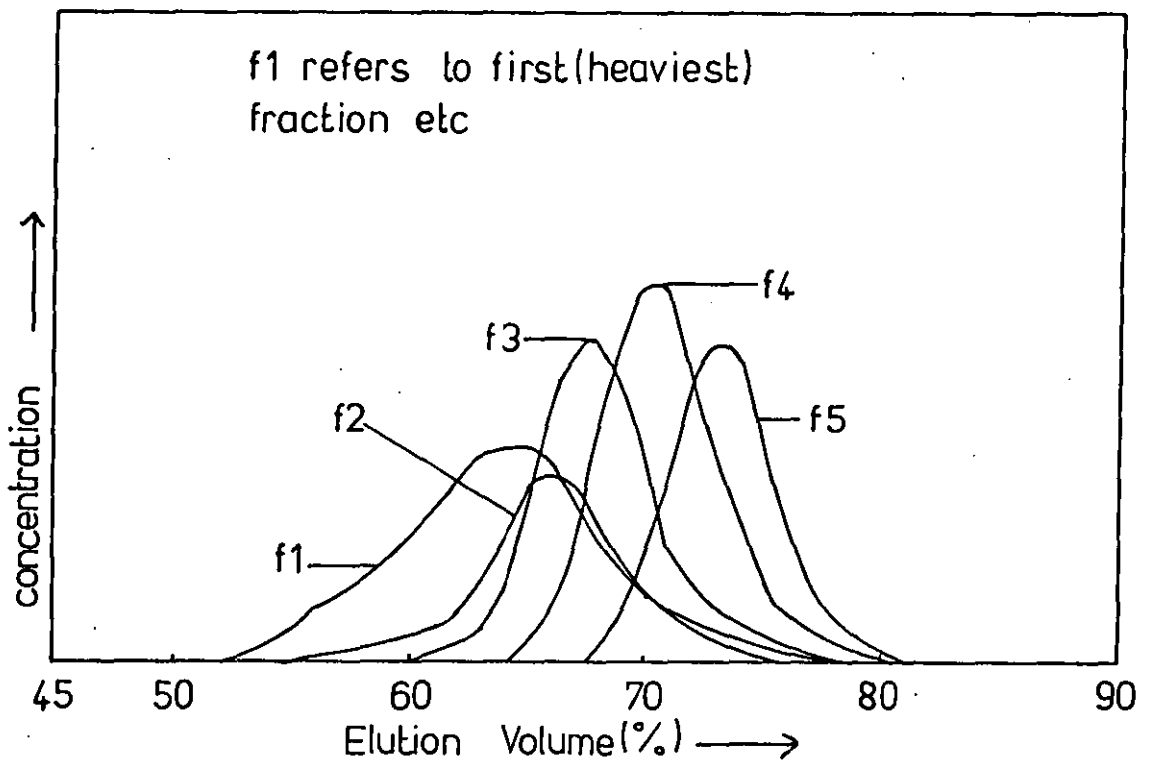


Figure (4.14)  
G.P.C. Chromatograms of PGMA Fractions



#1 was found to be insoluble and is therefore not represented in the diagram or in the blends of this fraction with PEPC.

#### 4.4.2 Optical Properties

All films were transparent, irrespective of the PGMA molecular weight, and remained so up to 200°C.

#### 4.4.3 Thermal Analysis Data

The following data relates to a blend of fraction #1 with PEPC. The thermal analysis results as shown in Figure (4.15) clearly displayed a single glass transition at all blend compositions. The breadth of the blend transitions lay between those of the pure components, that is in the range of 14-25°C. The variation of the glass transition temperature with blend composition, shown in Figure (4.16), approximately followed that predicted by the Fox equation at weight fractions of PGMA greater than 0.5. At lower concentrations of the glassy component the measured values lay 4-9°C below the predicted ones.

#### 4.4.4 Dynamic Mechanical Results

The loss tangent vs. temperature curves, plotted in Figure (4.17) over the complete composition range, complement the D.T.A. results in that a single, narrow glass transition was found at all concentrations. Prior to measurement, the samples, in the form of thin films supported on steel, were annealed at 95°C under vacuum. The variation of the glass transition temperature with blend composition (Figure (4.18)) showed a slight positive deviation from the Fox line at high PGMA concentrations and a distinct negative deviation at concentrations below 60 wt.%.

Figure (4.15)  
D.T.A. Data for PGMA/PEPC

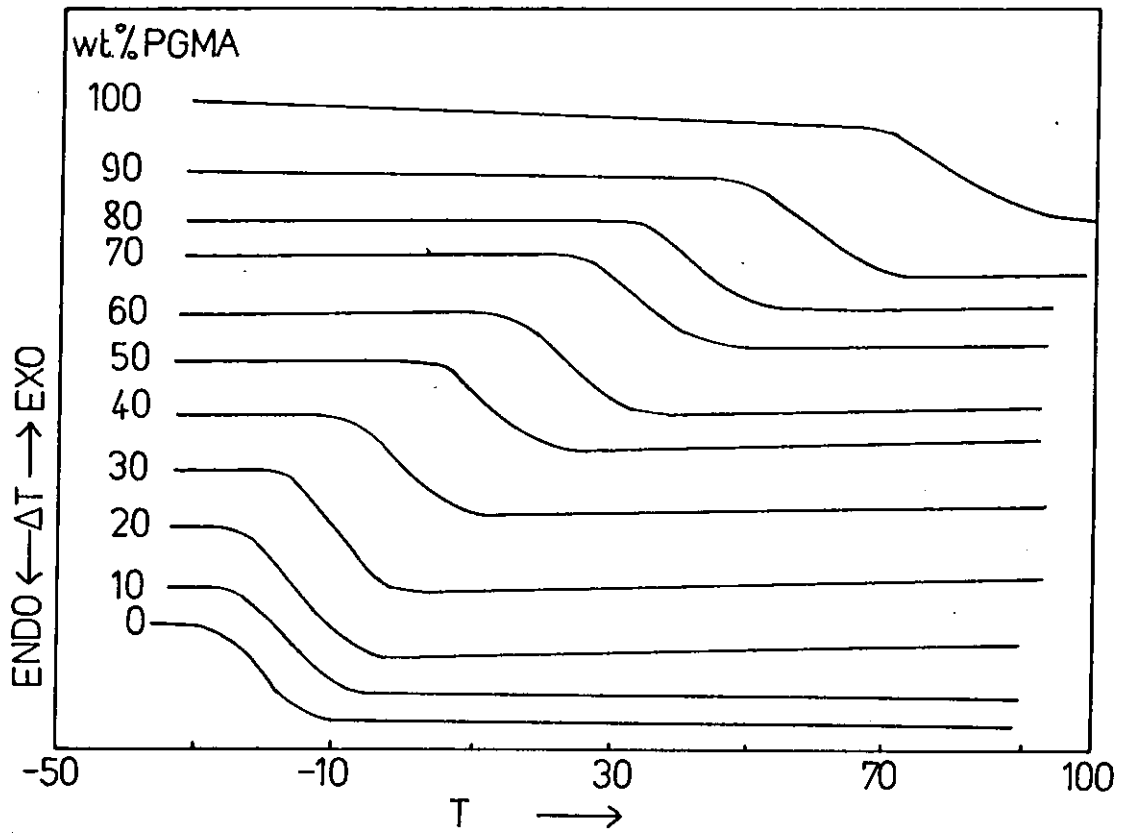


Figure (4.16)  
Composition Dependence of T<sub>g</sub> for PGMA /  
PEPC Measured by D.T.A.

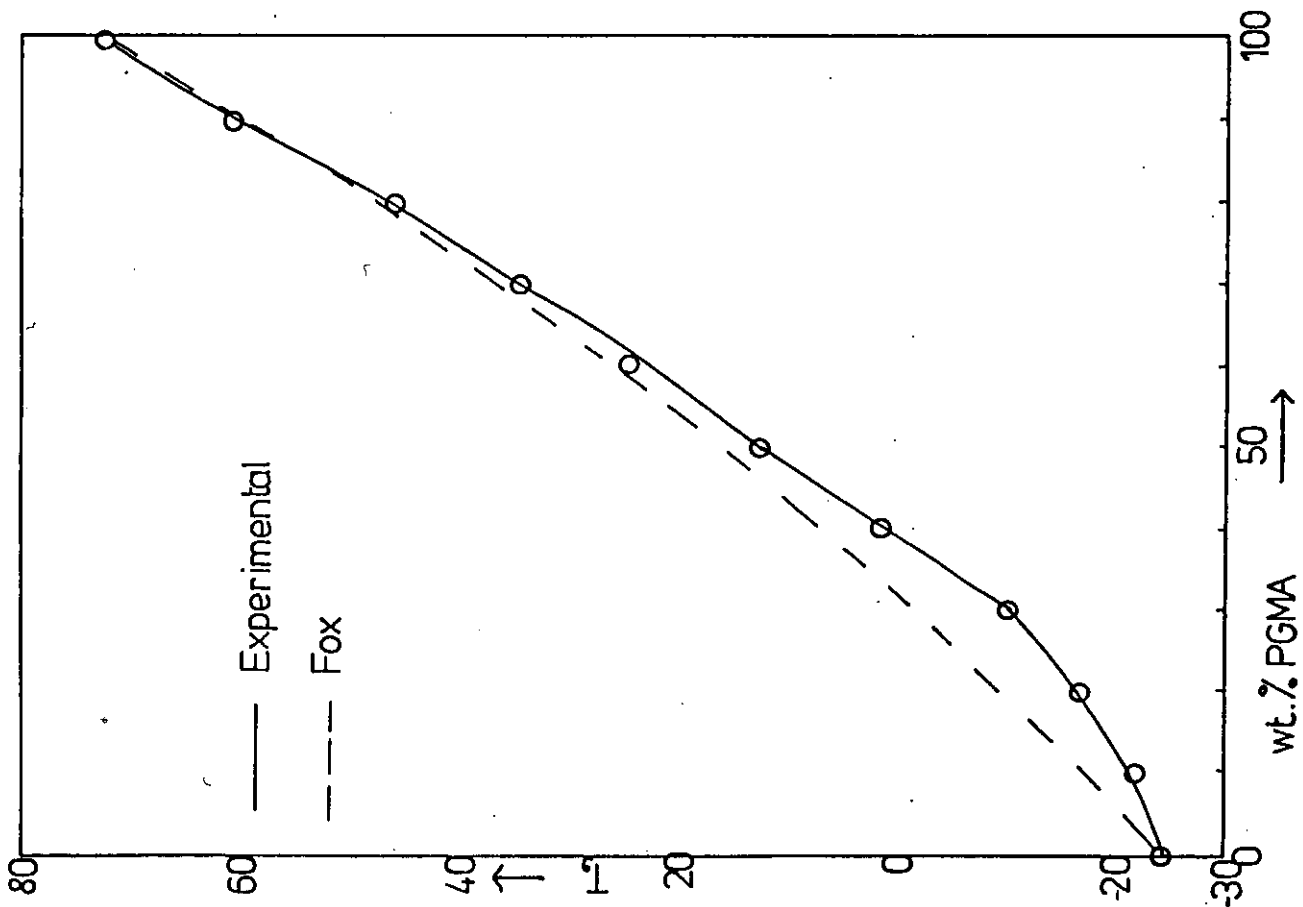


Figure (4.17)  
 Loss Tangent vs. Temperature Curves  
 for PGMA/PEPC

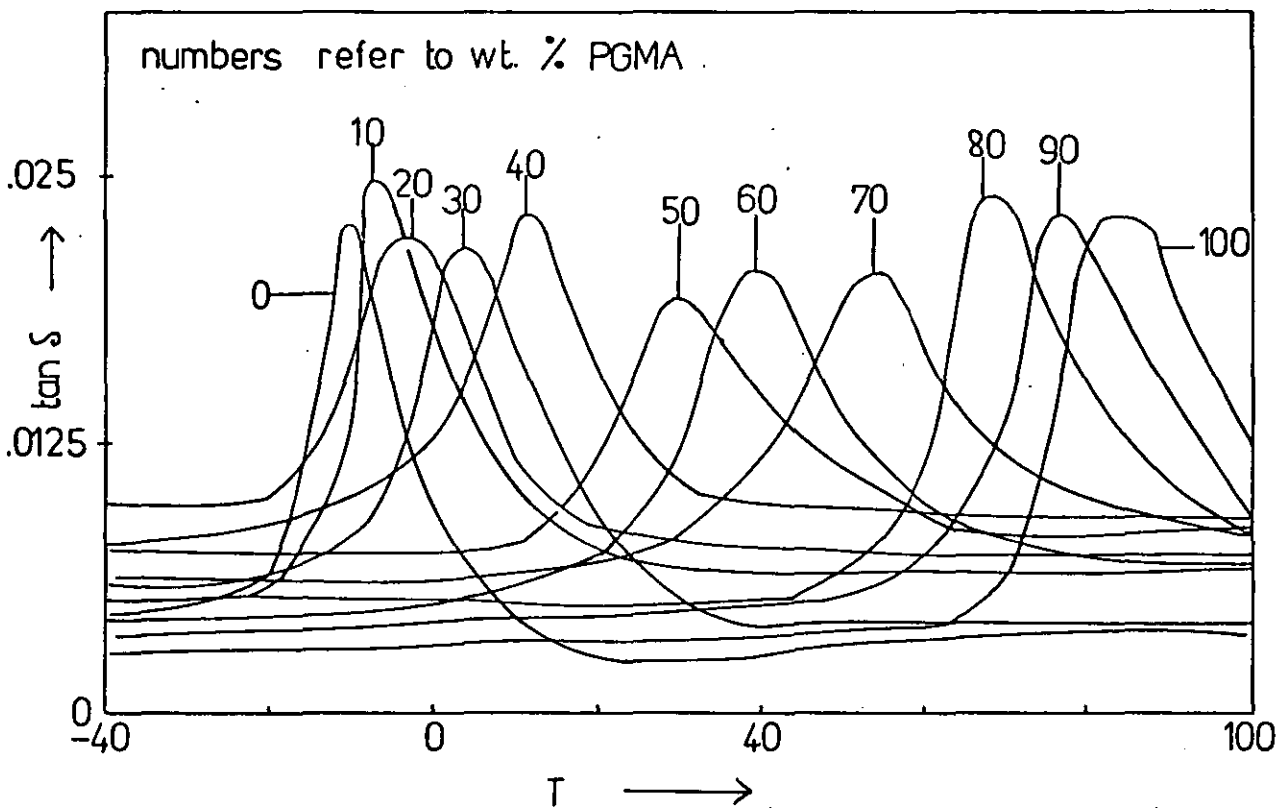
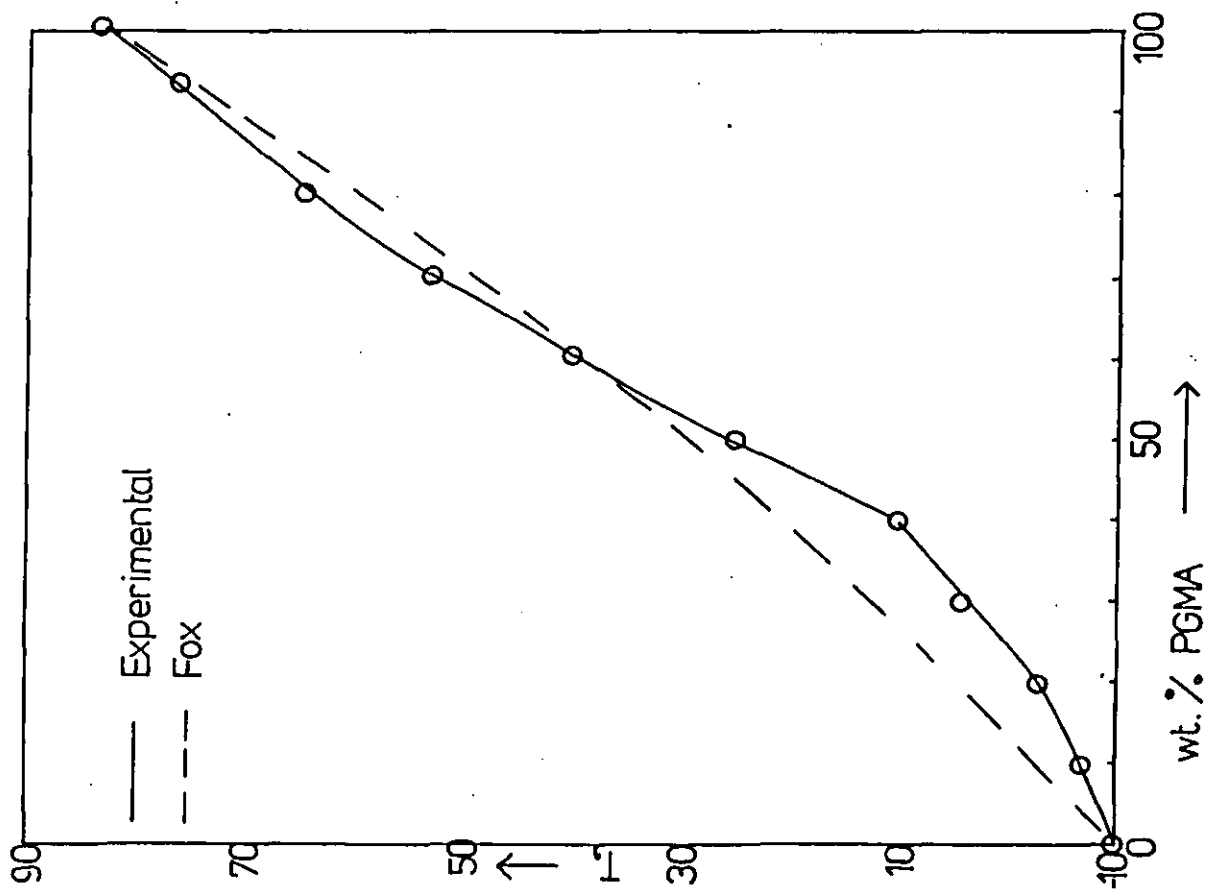


Figure (4.18)  
 Composition Dependence of  $T_g$  for PGMA /  
 PEPC Measured by DMTA.



The foregoing dynamic mechanical and thermal analysis results were measured on blends containing PGMA fraction #1. Similar results were obtained using the lower molecular weight fractions, however the unfractionated PGMA gave rise to broader transitions at compositions of 40-60 wt.% PGMA. In this composition range the transition breadths were increased by 40-50%, nevertheless the glass transition temperatures remained constant to within one degree.

The influence of temperature upon the dynamic mechanical properties of the blends was studied by annealing samples for thirty minutes at various temperatures in the range 100-200°C. Immediately prior to measurement samples were quenched from the anneal temperature in a bath of liquid nitrogen and rapidly clamped in the previously cooled measuring head of the D.M.T.A.

Blends of fraction f1 with PEPC exhibited distinct broadening and then splitting of the  $\tan \delta$  relaxation peak in the composition range 40-60 wt.% PGMA. This occurred when the quench temperature lay above 150°C and as the temperature was raised from 150-200°C the definition of the split peaks increased. Figure (4.19) compares the  $\tan \delta$  curves of blends quenched from 200°C with those treated as outlined earlier in this section. Outside this intermediate composition band some peak broadening was observed at higher temperatures but no new maxima were discernible. In Figure (4.20) the approximate temperatures at which peak broadening was first observed is plotted against blend composition.

The lower molecular weight fractions of PGMA behaved similarly, but as shown in Figure (4.20) the onset of the broadening process was shifted to higher temperatures as the PGMA molecular weight decreased.

The experiment was repeated at selected compositions and molecular weights, replacing the quench procedure by a linear cool ( $2^\circ\text{C min}^{-1}$ ).



Figure (4.19)  
 Representative Loss Tangent vs. Temperature  
 Curves for PGMA/PEPC Showing the  
 Influence of Anneal Temperature

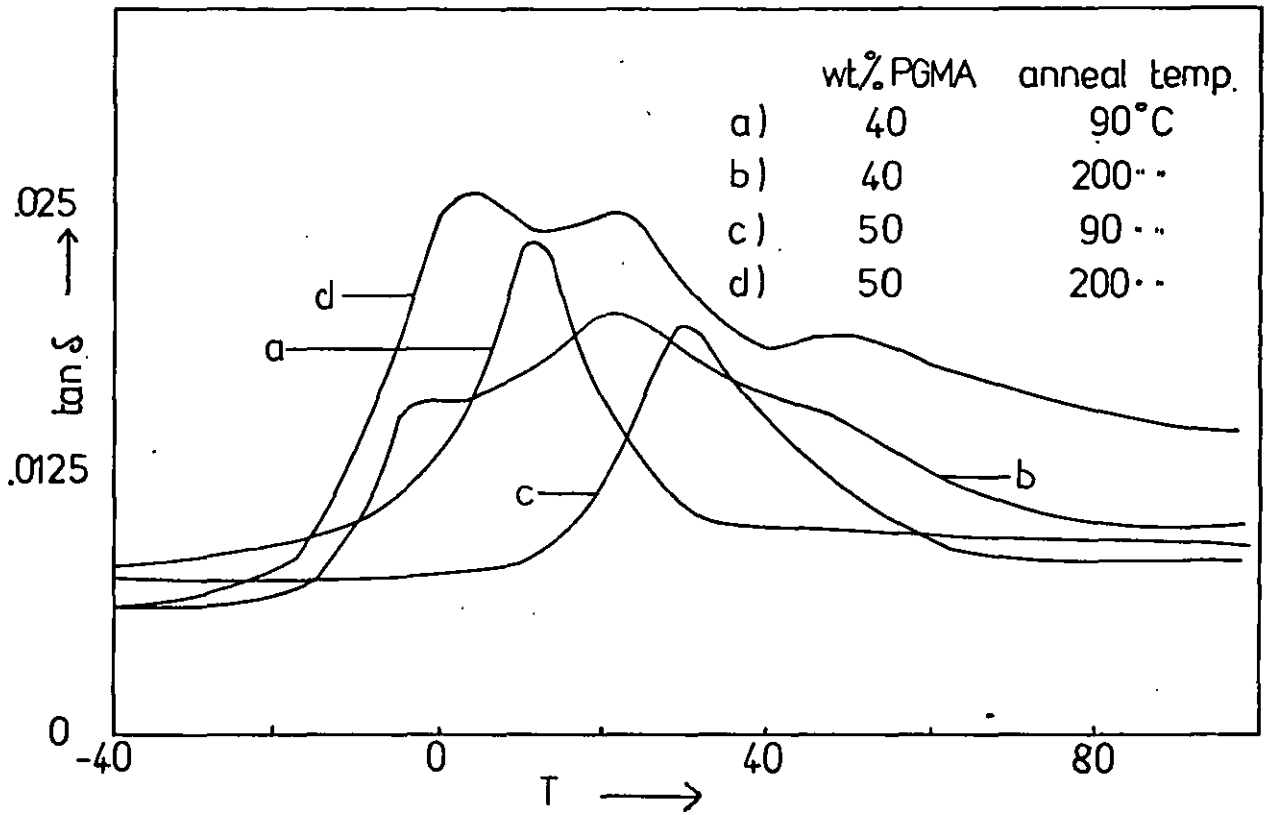
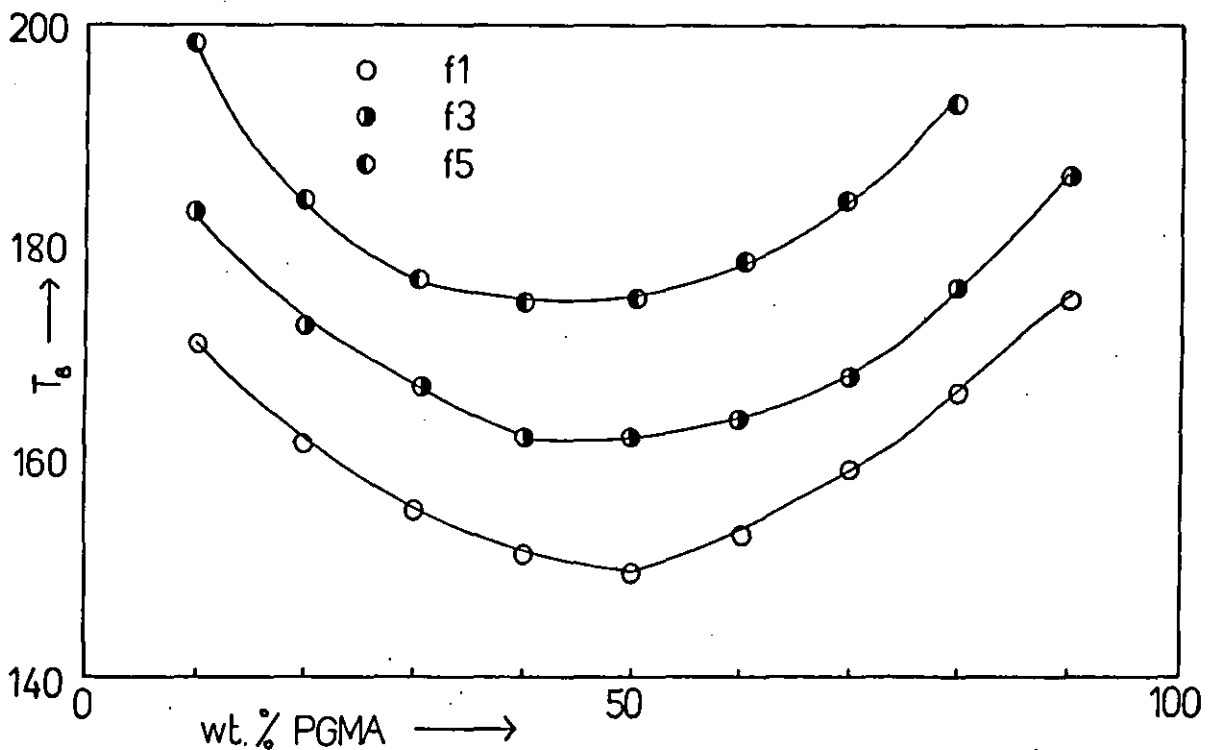


Figure (4.20)  
 Variation of Peak Broadening Temperature ( $T_b$ )  
 with Composition for Blends of PEPC with  
 Various PGMA Fractions



It was found that the loss tangent curves were of the same form whichever cooling method was employed.

As a corollary of these experiments the thermal stability of the blends was investigated by observing the dissolution behaviour of films, annealed as previously described, in dichloromethane. Blend samples were found to contain insoluble material when the anneal temperature lay above 120°C. The proportion of this material increased with PGMA content, anneal time and anneal temperature. On treating the homopolymers in a corresponding fashion, PGMA exhibited the same tendency to cross-link above 120°C, irrespective of the molecular weight of the sample.

CHAPTER 5

RESULTS FOR RANDOM COPOLYMER/HOMOPOLYMER BLENDS

## 5.1 GLYCIDYL METHACRYLATE-CO-METHYL METHACRYLATE/POLY(EPOCHLOROHYDRIN)

### BLENDS

#### 5.1.1 Characterisation of Copolymers

The molecular weights of the copolymers, determined by GPC, are listed in Table 5.1 together with details of the copolymer and monomer feed compositions. The copolymers were prepared by a free radical solution method, described in section 3.1.1. The reaction yields were restricted to approximately 10% by weight in an effort to prepare copolymers which were homogeneous with respect to composition. Copolymer composition was measured using N.M.R. as detailed in section 3.3.2.

The monomer reactivity ratios were initially determined using the Fineman-Ross method where  $F(f-1)/f$  is plotted against  $F^2/f$ .  $F$  is the molar ratio of the two monomers in the initial feed and  $f$  is the molar ratio of the different segments in the copolymer. The plot is shown in Figure (5.1) and indicates that all but one point, corresponding to the highest GMA content, lie on a straight line of correlation coefficient 0.991 as determined by least squares. The data was then replotted using the technique of Kelen and Tudos described in section 2.8.1 (Figure (5.2)). Using only those points related linearly the monomer reactivity ratios were measured from the two plots.

	$r_{GMA}$	$r_{MMA}$
Fineman-Ross	0.424	0.267
Kelen-Tudos	0.450	0.356
Average	0.44	0.31

Table 5.1. Details of Composition and Molecular Weight for GMA-co-MMA Random Copolymers

Copolymer	Feed Composition (Mole % GMA)	Copolymer Composition (Mole % GMA)	$\bar{M}_w$	$\bar{M}_n$	$\bar{M}_w/\bar{M}_n$
K	50.00	50.36	91,026	38,450	2.37
C	61.96	59.08	125,964	34,323	3.67
H	70.12	65.70	136,891	32,593	4.20
F	80.00	72.38	134,013	33,420	4.01
J	90.00	76.19	153,682	32,207	4.77

Figure (5.1)  
Fineman-Ross Plot for GMA-co-MMA  
Copolymers

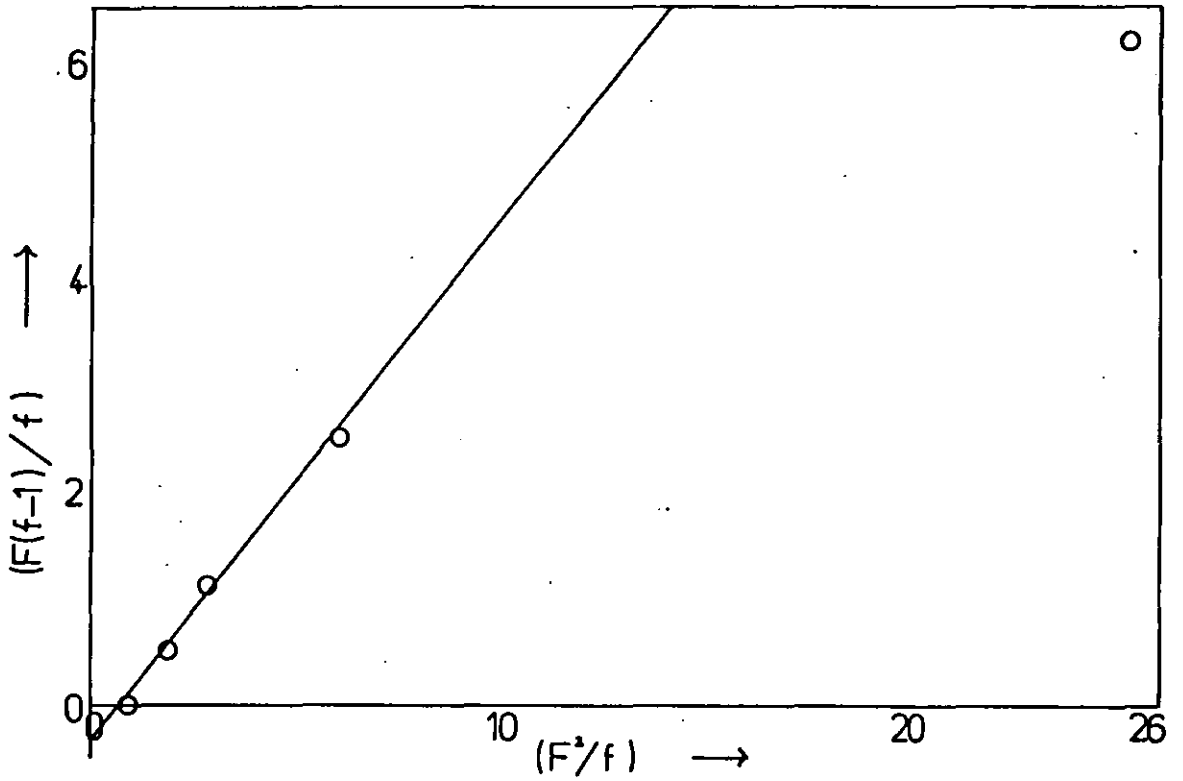
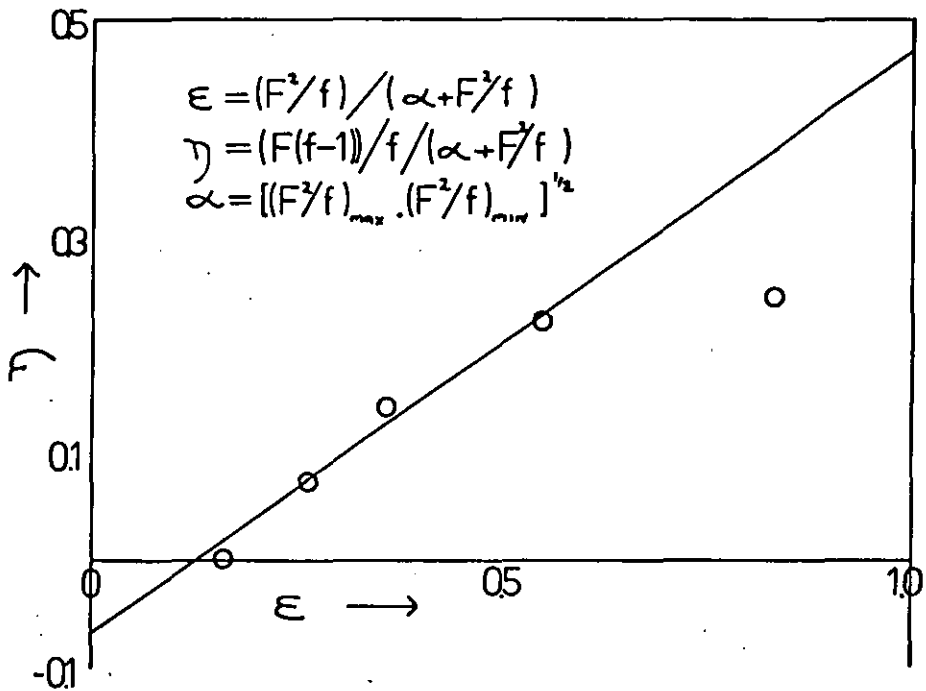


Figure (5.2)  
Kelen-Tudos Plot for GMA-co-MMA Copolymers



The sequence length distribution of each segment and the number average sequence length were calculated for the copolymers using the average values of the reactivity ratios in equations (2.184)-(2.191). The results are recorded in Table (5.2).

### 5.1.2 Optical Properties of GMA-co-MMA/PEPC Blends

The optical properties of thin films of the copolymers blended with poly(epichlorohydrin) are recorded as a function of blend composition in Figure (5.3). Two general trends were apparent. Firstly as the copolymer content increased in a blend so did the tendency to exhibit optical inhomogeneity. Secondly, with the exception of copolymer K which has the lowest GMA content, as the proportion of GMA in the copolymer increased so did the optical homogeneity of the films at high loadings of copolymer. Films of the pure copolymers were transparent in all cases.

### 5.1.3 Thermal Analysis of GMA-co-MMA/PEPC Blends

The variation of the pure copolymer glass transition temperatures with composition is shown in Figure (5.4). The composition dependence was akin to that predicted by the Fox equation and the copolymer  $T_g$ 's lay within 1°C of the predicted values.

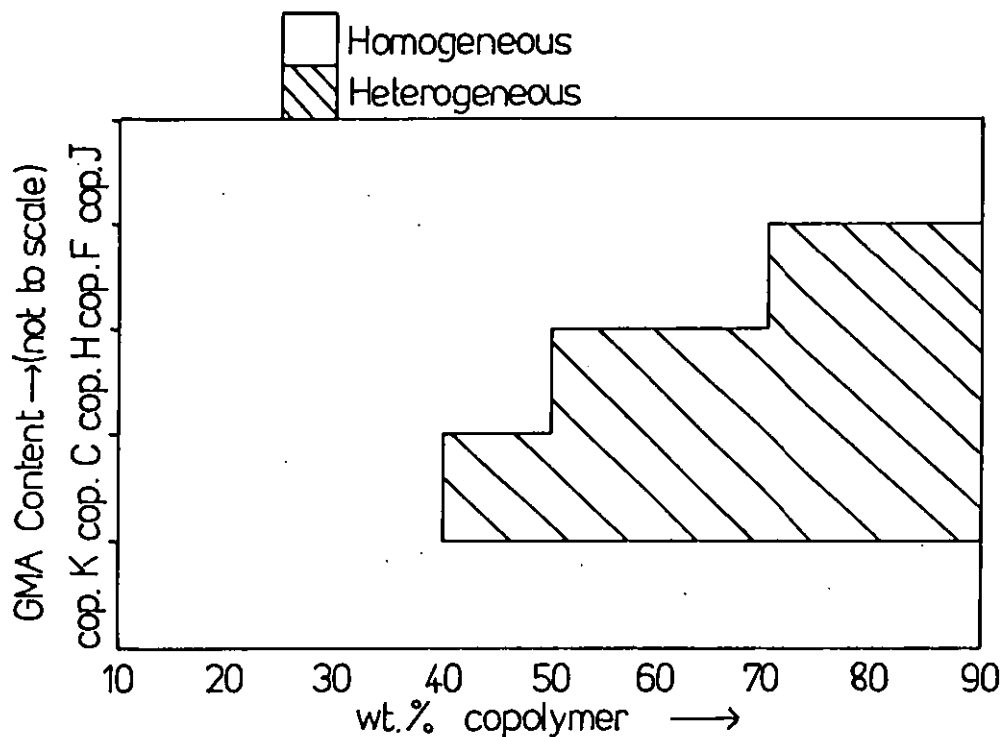
Representative thermograms of blends of the five copolymers with PEPC are reproduced in Figures (5.5)-(5.9). The thermal behaviour of the blends changed little with copolymer composition and did not clearly demonstrate those characteristics observed in either one-phase or two phase mixtures. At copolymer contents up to 50% by weight, a single low temperature transition was predominant whose breadth gradually increased with decreasing rubber content. At higher compositions the transitions extended over the range flanked

Table 5.2. Details of Sequence Length Distribution in GMA-co-MMA Copolymers

		Copolymer K		Copolymer C		Copolymer H		Copolymer F		Copolymer J	
		GMA	MMA	GMA	MMA	GMA	MMA	GMA	MMA	GMA	MMA
Number Average Sequence Length - $\bar{n}$		1.44	1.32	1.72	1.20	2.03	1.14	2.76	1.08	4.96	1.04
Mole Percentage of Particular Repeat Unit in Sequences X Units Long	X										
	1	69.4	75.8	58.2	83.6	49.2	88.0	36.2	92.6	20.1	96.6
	2	21.2	18.4	24.3	13.7	25.0	10.6	23.1	6.9	16.1	3.3
	3	6.5	4.5	10.2	2.3	12.7	1.3	14.7	0.5	12.8	0.1
	4	2.0	1.1	4.3	0.4	6.4	0.2	9.4	0.0	10.3	0.0
	5	0.6	0.3	1.8	0.0	3.3	0.0	6.0	0.0	8.2	0.0
	6	0.2	0.0	0.7	0.0	1.7	0.0	3.8	0.0	6.5	0.0



Figure(5.3)  
 Optical Properties of Blends of PEPC with  
 Various GMA-co-MMA Samples



Figure(5.4)  
 Variation of Copolymer  $T_g$  with Composition  
 Measured by D.T.A.

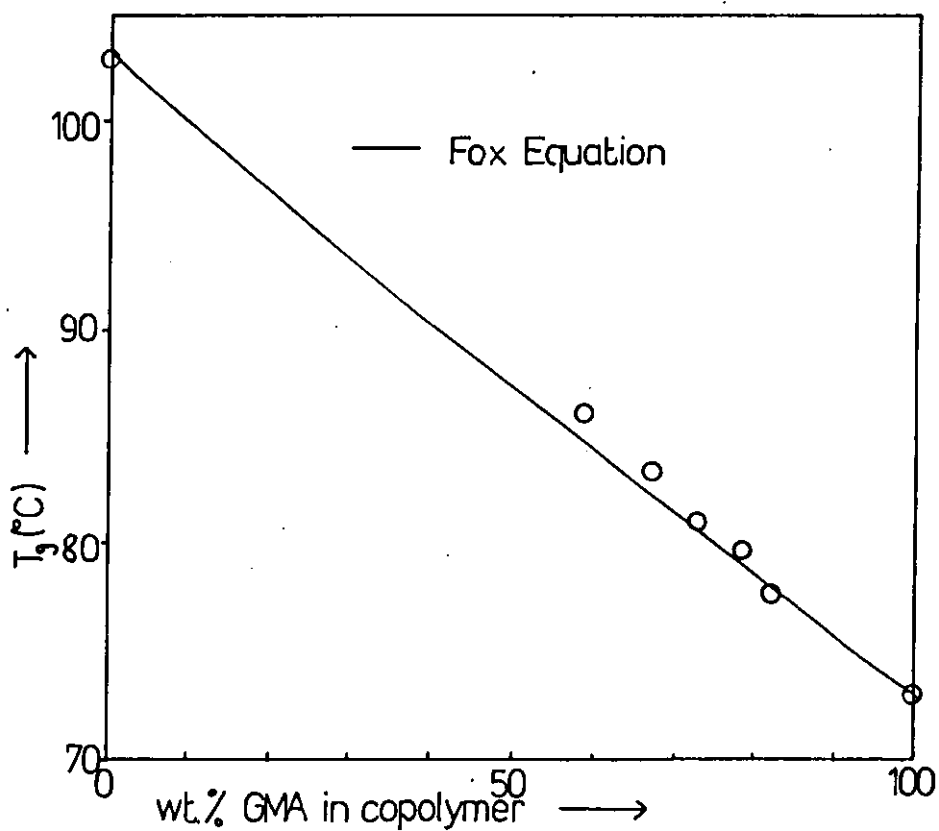


Figure (5.5)  
D.T.A. Results for Copolymer K/PEPC

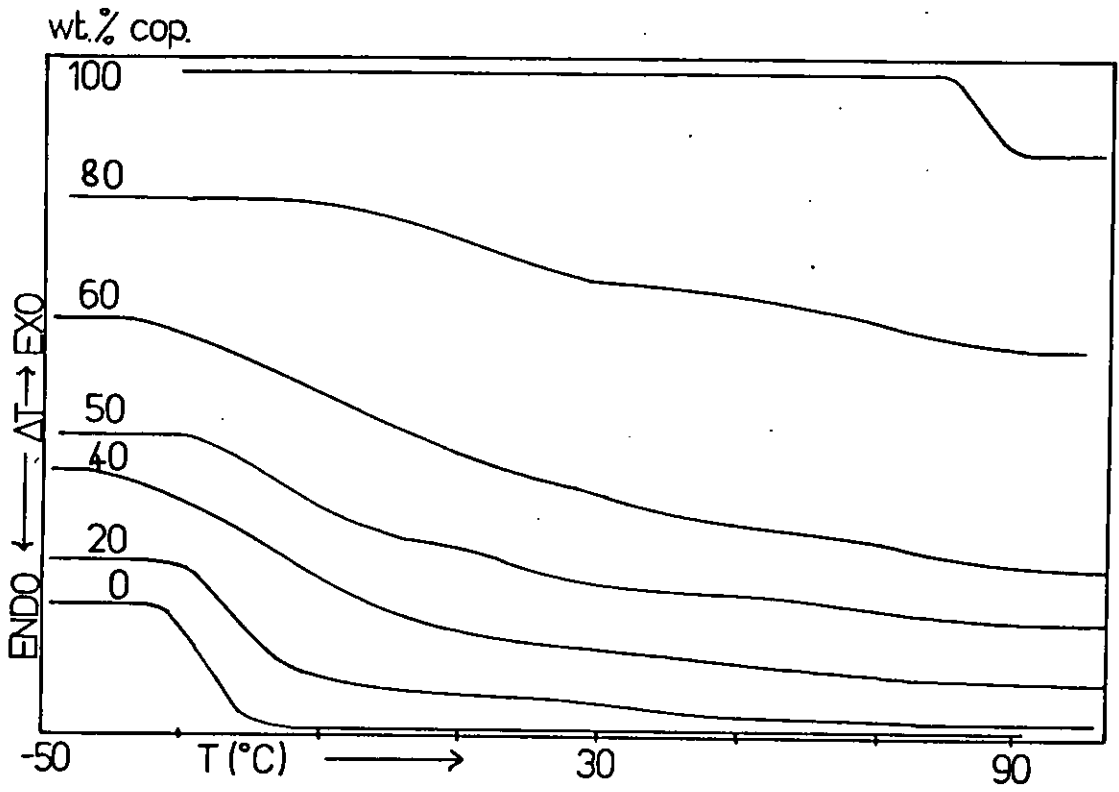


Figure (5.6)  
D.T.A. Results for Copolymer C/PEPC

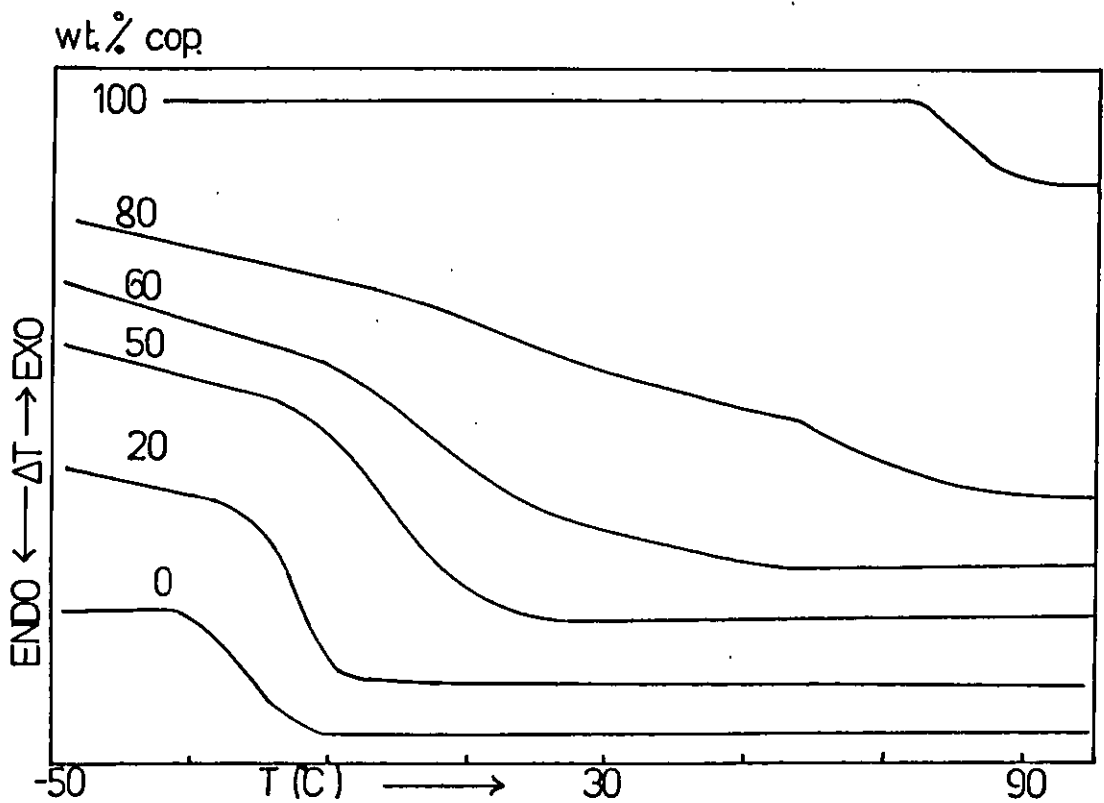


Figure (5.7)

D.T.A. Results for Copolymer H/PEPC

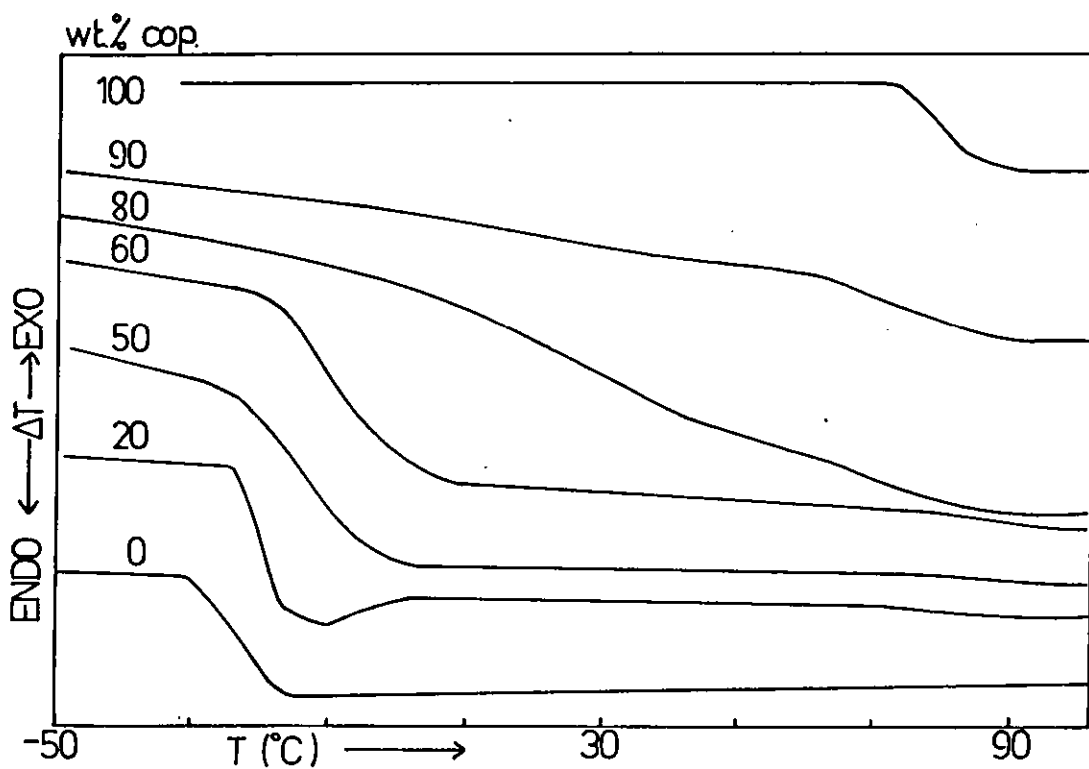


Figure (5.8)

D.T.A. Results for Copolymer F /PEPC

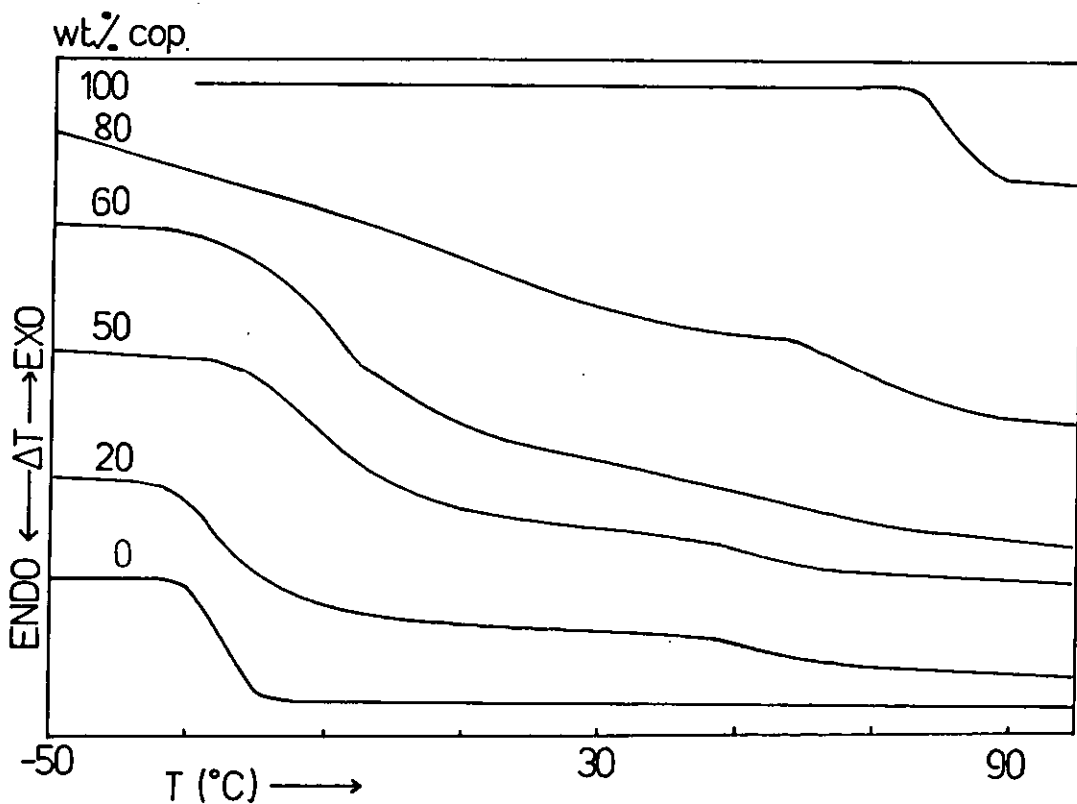


Figure (5.9)

DTA. Results for Copolymer J / PEPC

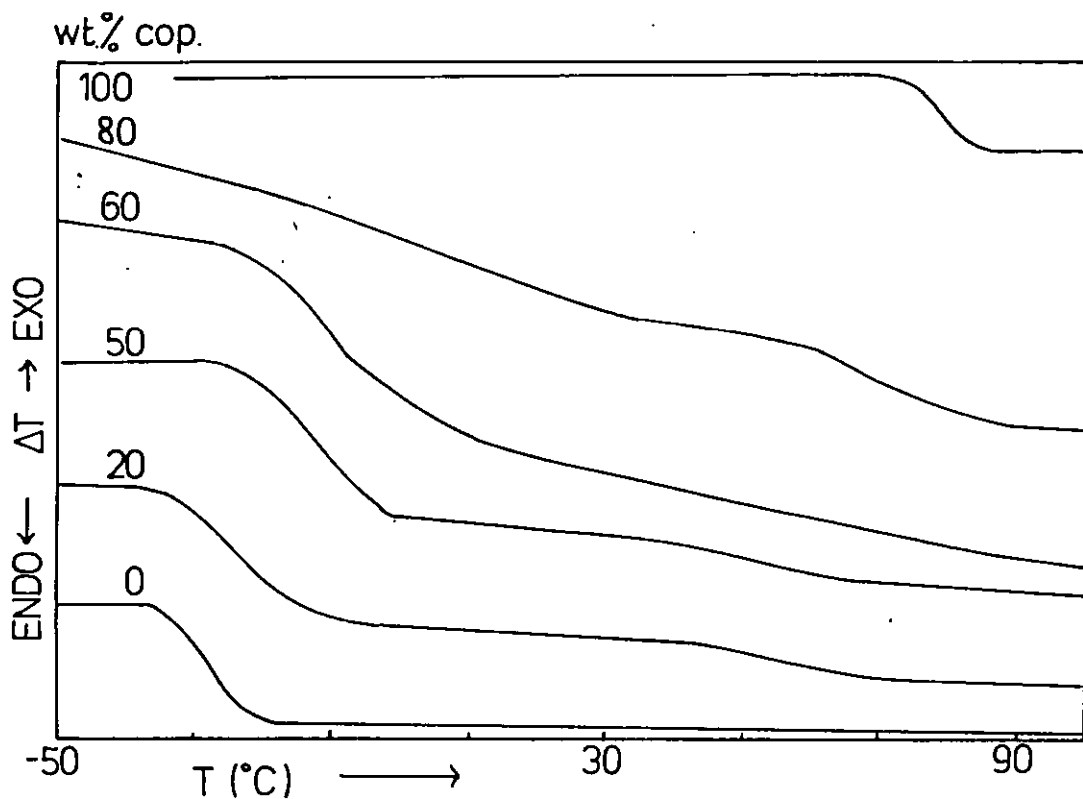
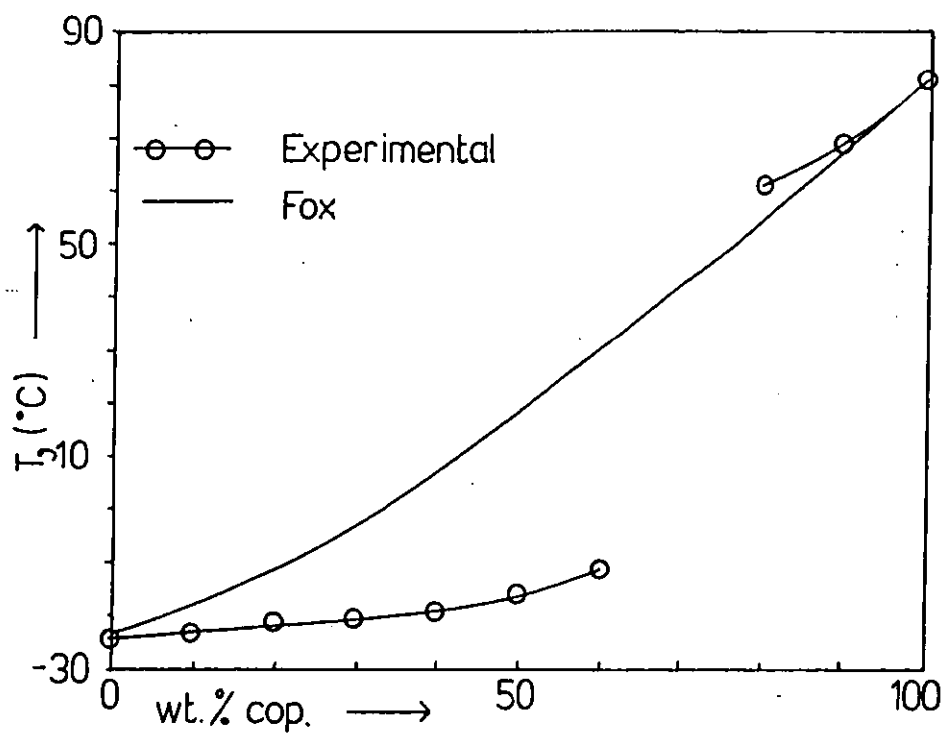


Figure (5.10)

Composition Dependence of  $T_g$  for Copolymer H / PEPC Measured by DTA.



by the pure component  $T_g$ 's but a transition in the region of 70°C became increasingly prominent.

The low temperature  $T_g$  exhibited a slight composition dependence, as illustrated in Figure (5.10) for blends of copolymer H. However the  $T_g$ 's of blends containing up to 60% copolymer by weight lay well below those predicted for a miscible blend and this disparity increased with increasing copolymer content.

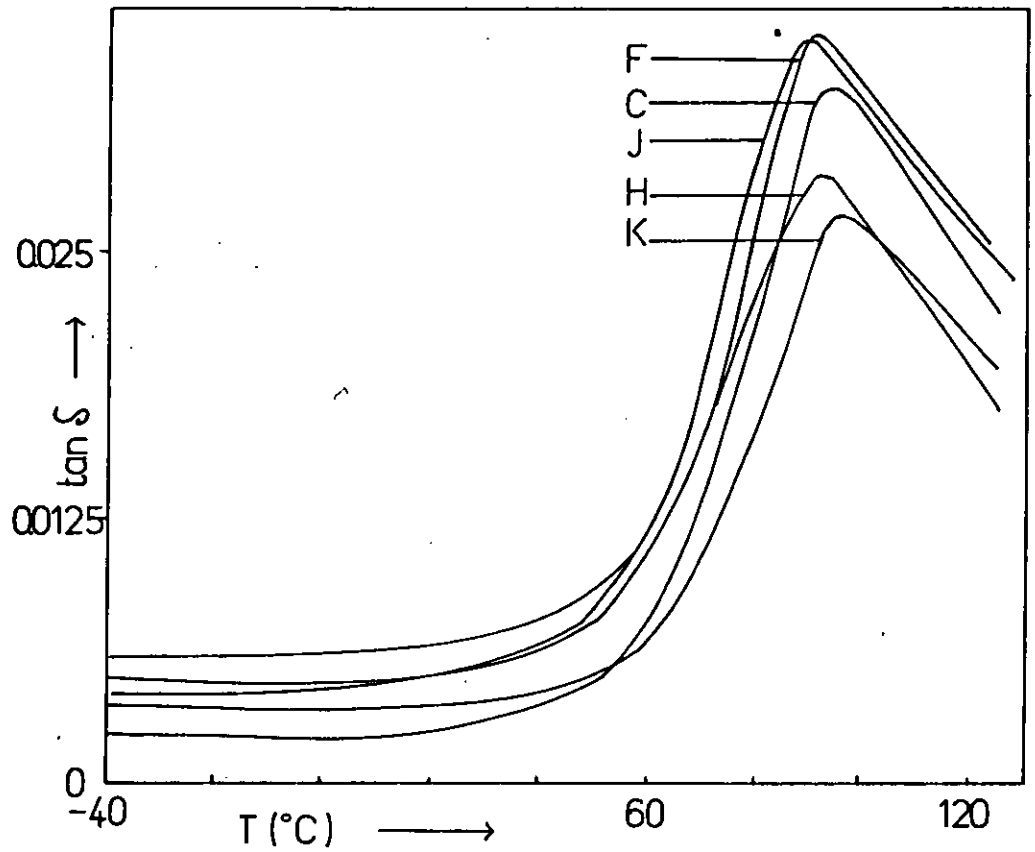
#### 5.1.4 Dynamic Mechanical Results

The loss tangent curves and corresponding glass transition temperatures for the pure copolymers are presented in Figures (5.11) and (5.12). The composition dependence of  $T_g$  mirrored that previously found by D.T.A. (Figure (5.4)).

The loss tangent curves for blends of the copolymers with PEPC and the glass transition data derived from them appear in Figures (5.13)-(5.22). The shape and position in the temperature plane of the  $\tan \delta$  relaxation peaks depended upon the composition of both the blend and the copolymer.

In blends of all five copolymers, mixtures containing 10-30 wt.% copolymer exhibited a single peak, which was composition dependent and became broader with increasing copolymer content. At a composition of 40 wt.% copolymer two distinct relaxations were observed for cop. K and there was a shoulder to the main peak for cop. C. Thereafter in copolymers containing greater proportions of GMA a single peak was observed. Blends containing an equal weight of both constituents yielded a single, very broad relaxation in all cases other than cop. K. At compositions containing 60-90 wt.% copolymer the principal relaxation peak showed some dependence on composition and became decreasingly broad. Copolymers C, H and F exhibited a

Figure (5.11)  
 Loss Tangent vs Temperature Curves for  
 GMA-co-MMA Copolymers



Figure(5.12)  
 Variation of Copolymer  $T_g$  with Composition  
 Measured by DMTA

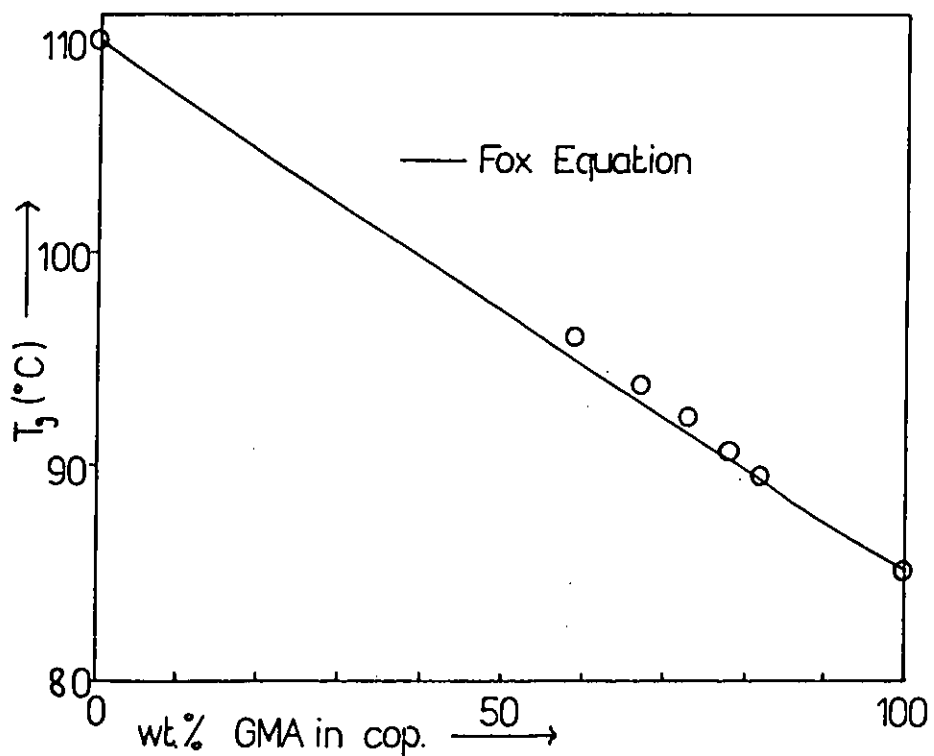


Figure (5.13)  
 Loss Tangent vs. Temperature Curves for  
 Copolymer K / PEPC Blends

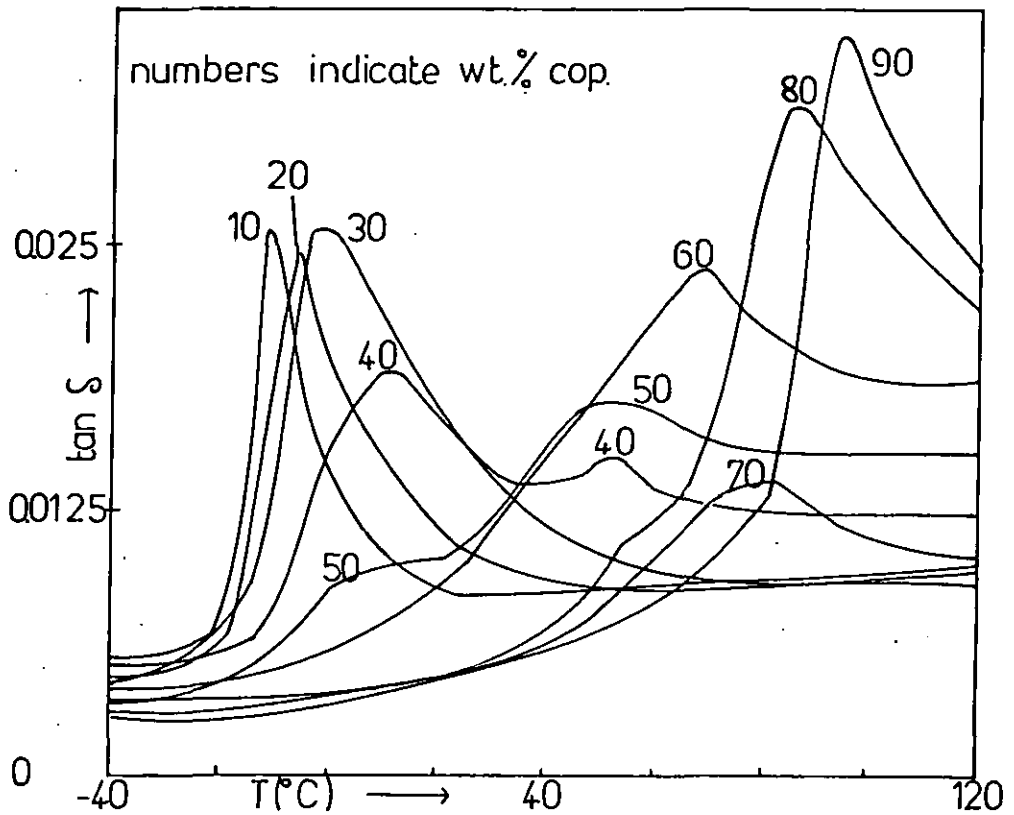


Figure (5.14)  
 Variation of Blend  $T_g$  with Composition  
 for Copolymer K / PEPC Measured by  
 DMTA.

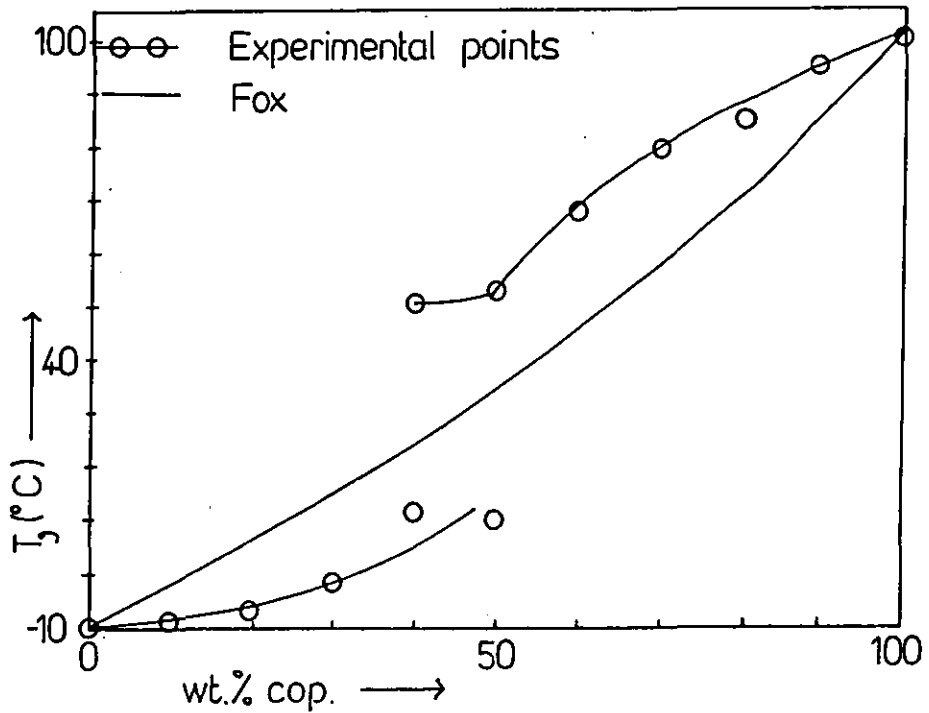
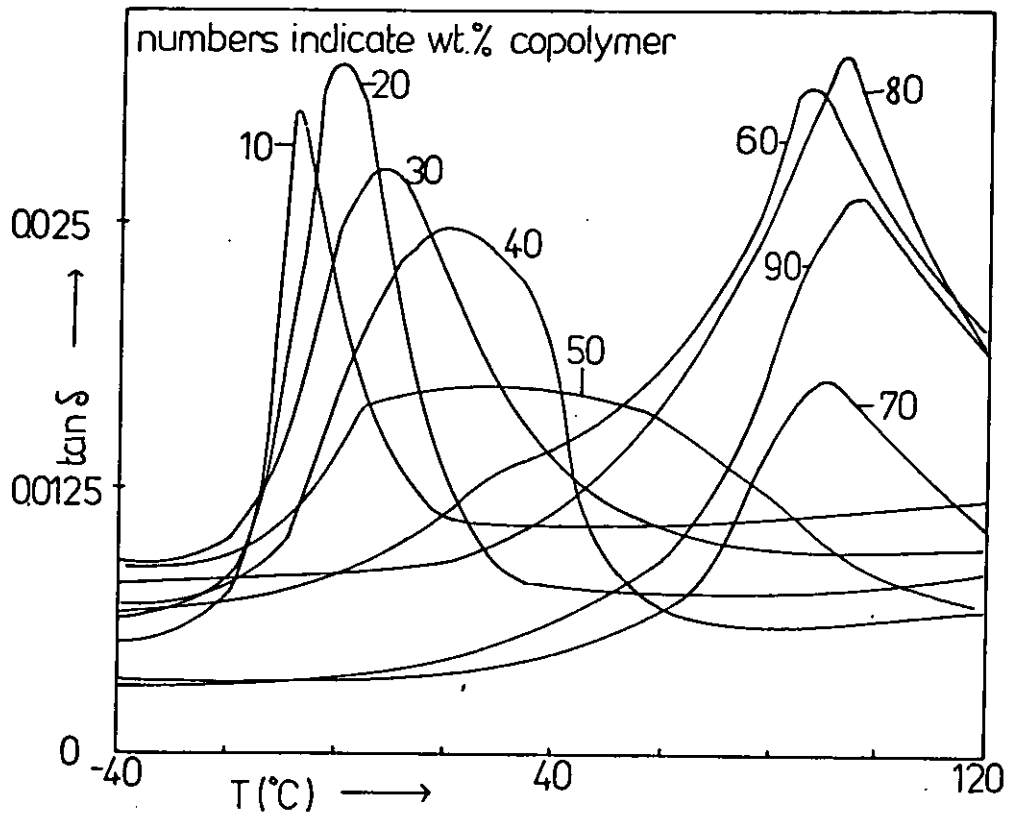


Figure (5.15)

Loss Tangent vs. Temperature Curves for Copolymer C / PEPC Blends



Figure(5.16)

Variation of Blend  $T_g$  with Composition for Copolymer C / PEPC Measured by DMTA.

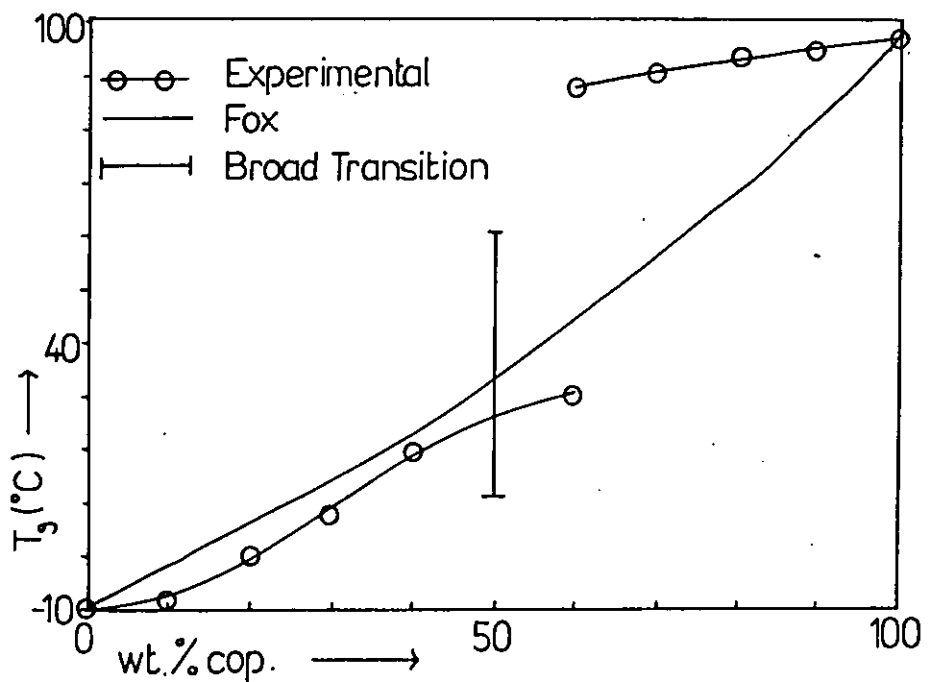




Figure (5.17)

Loss Tangent vs. Temperature Curves for Copolymer H /PEPC Blends

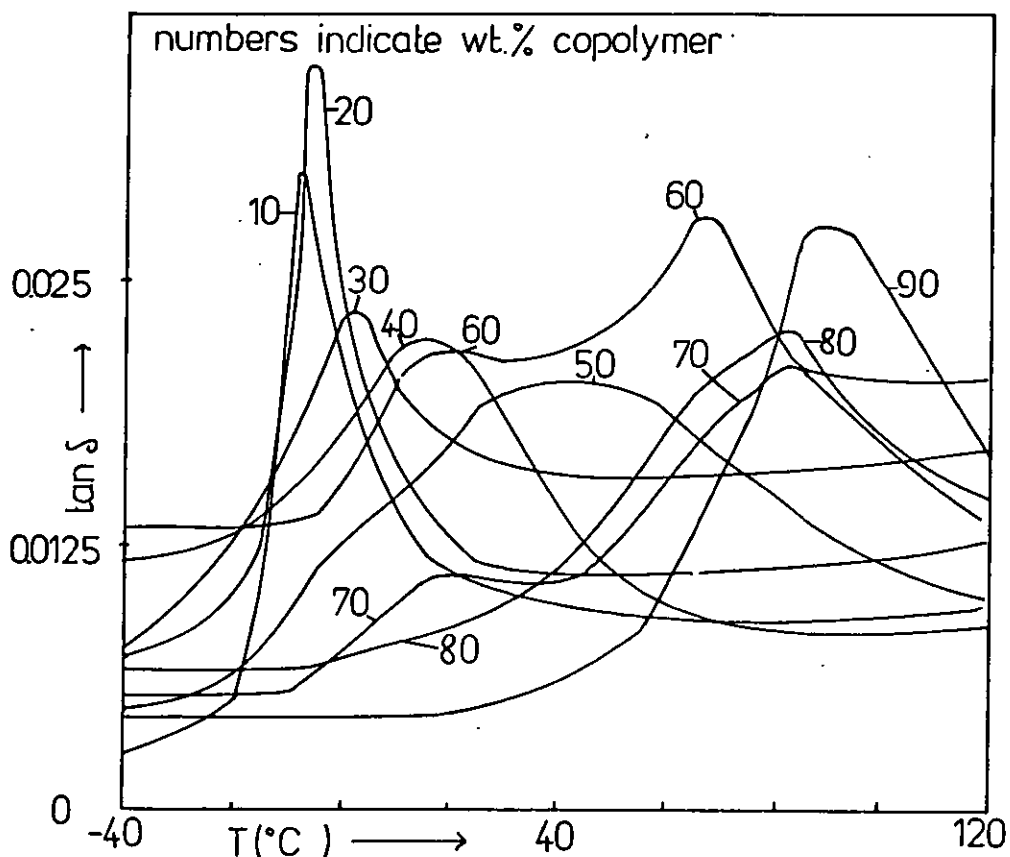


Figure (5.18)

Variation of Blend  $T_g$  with Composition for Copolymer H /PEPC Measured by DMTA.

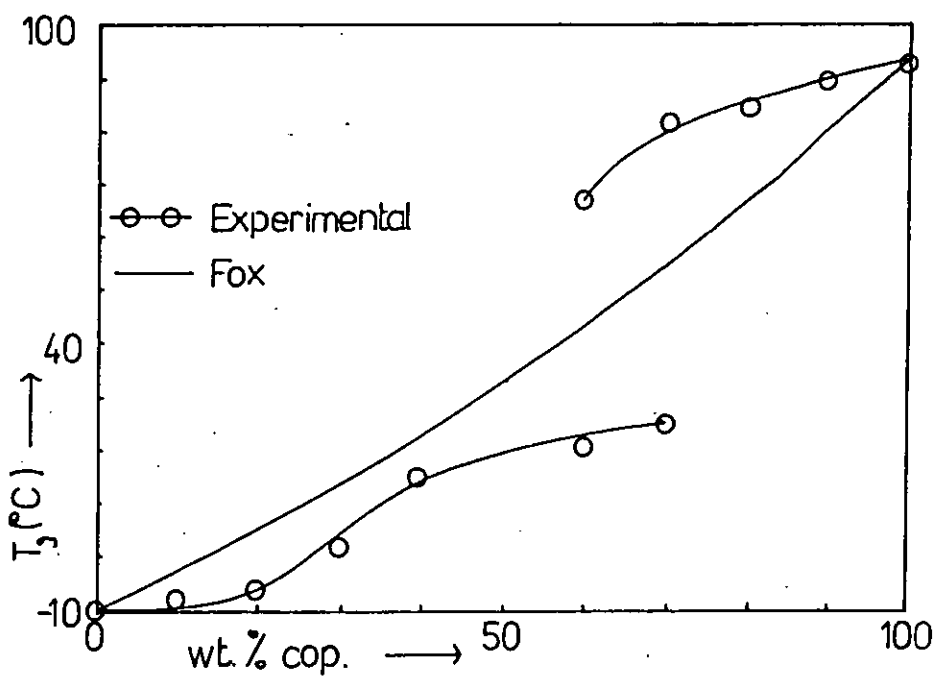


Figure (5.19)  
Loss Tangent vs. Temperature Curves for  
Copolymer F/PEPC Blends

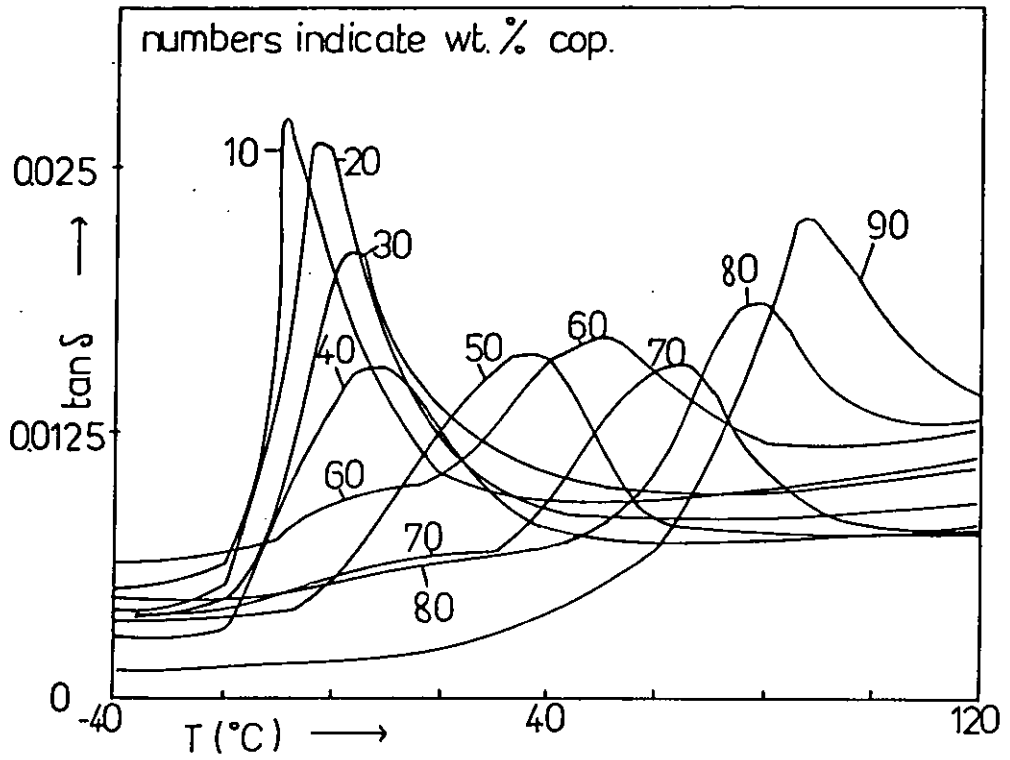


Figure (5.20)  
Variation of Blend  $T_g$  with Composition  
for Copolymer F/PEPC Measured by  
DMTA.

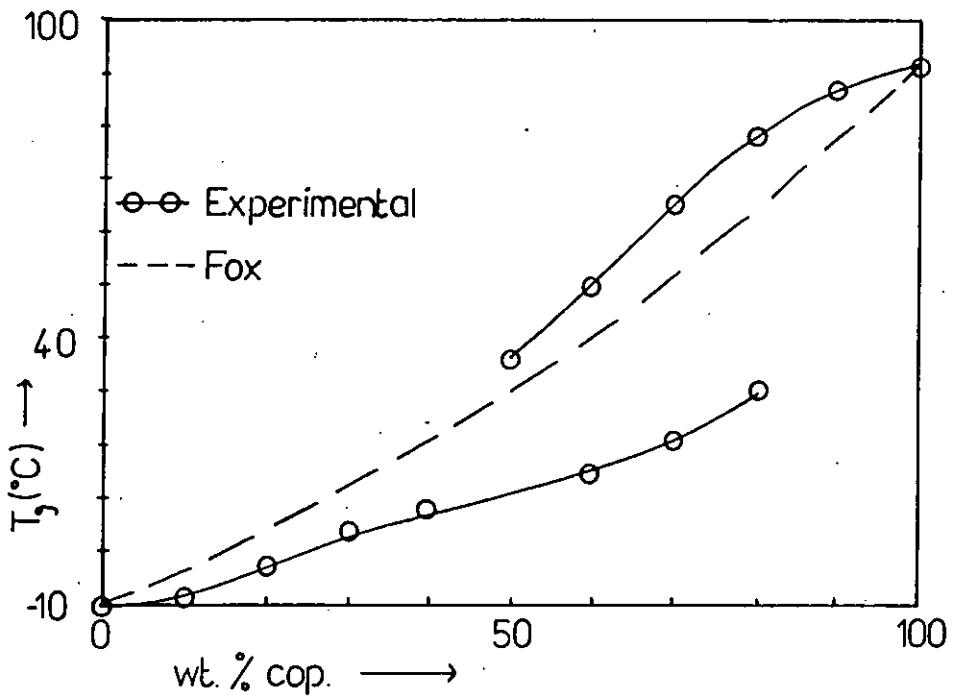


Figure (5.21)  
 Loss Tangent vs. Temperature Curves for  
 Copolymer J / PEPC Blends

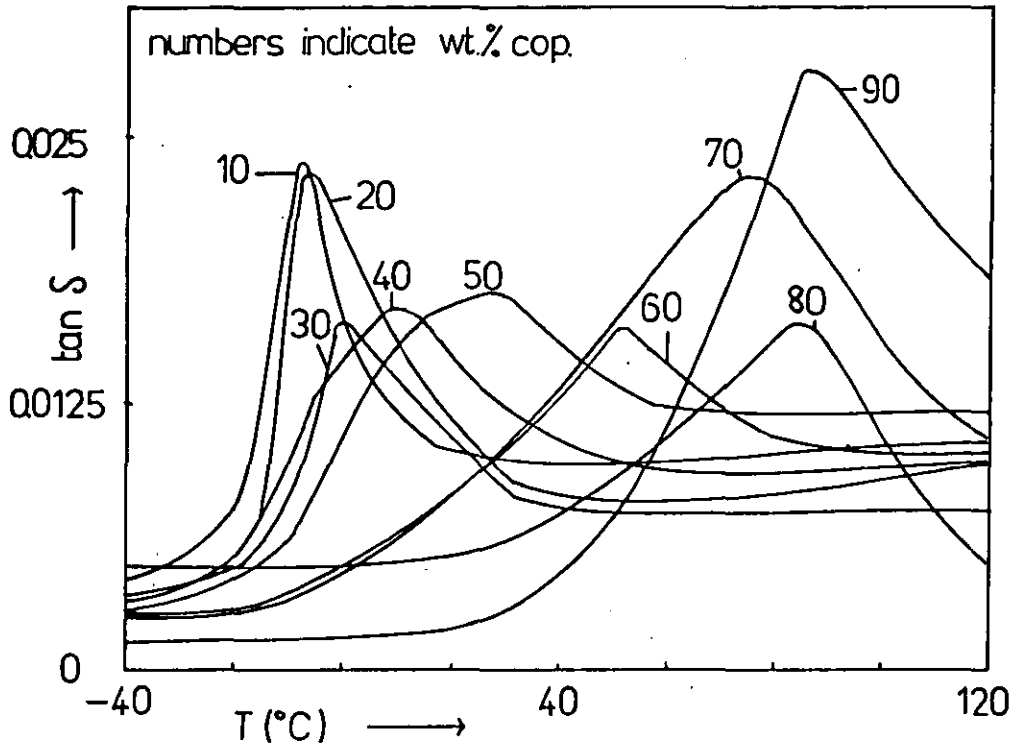
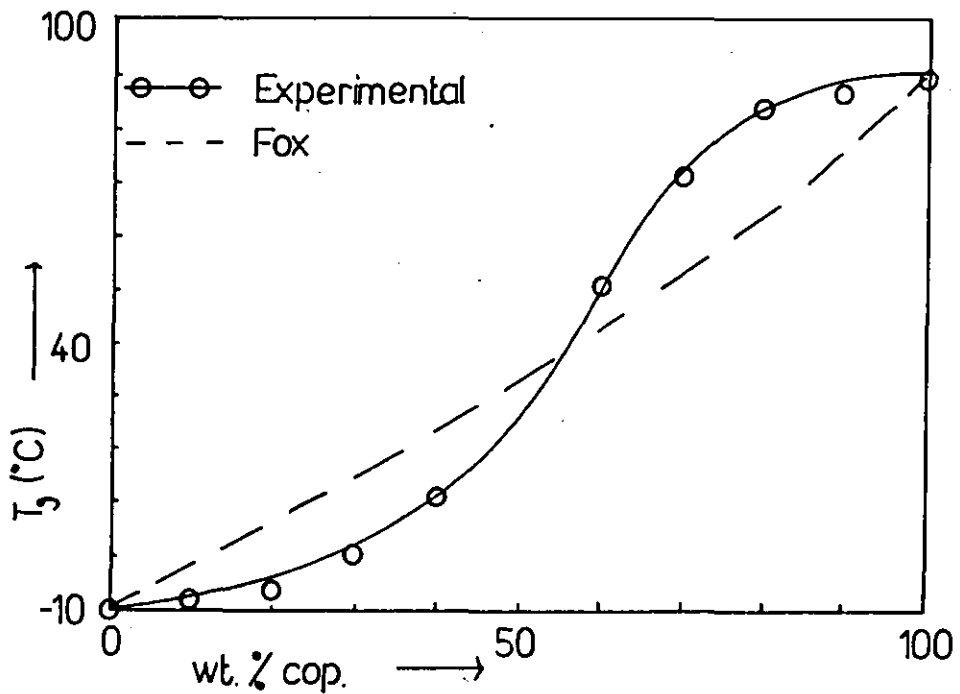


Figure (5.22)  
 Variation of Blend  $T_g$  with Composition  
 for Copolymer J / PEPC Measured by  
 D.M.T.A.



secondary low temperature peak or shoulder at compositions of 60%; 60-80% and 60-80% respectively. Copolymer J blends, containing the largest proportion of GMA, displayed a single relaxation peak at all compositions, however the breadth of the transitions at intermediate compositions proscribes description of the blend as one phase. These observations are presented in a simplified pictorial manner in Figure (5.23). The variation of the observed blend  $T_g$  with overall composition, taking only the major relaxations into consideration had a similar overall pattern for all copolymers. At loadings of 10-40% copolymer the  $T_g$ 's lay below those predicted by the Fox equation, whilst at 60-90% they lay above the predicted temperature. The range of values obtained at each composition over the five copolymers is depicted in Figure (5.24) and can be seen to increase greatly in the range 50-70 wt.% copolymer.

## 5.2 STYRENE-CO-METHACRYLONITRILE/POLY(EPOCHLOROHYDRIN) BLENDS

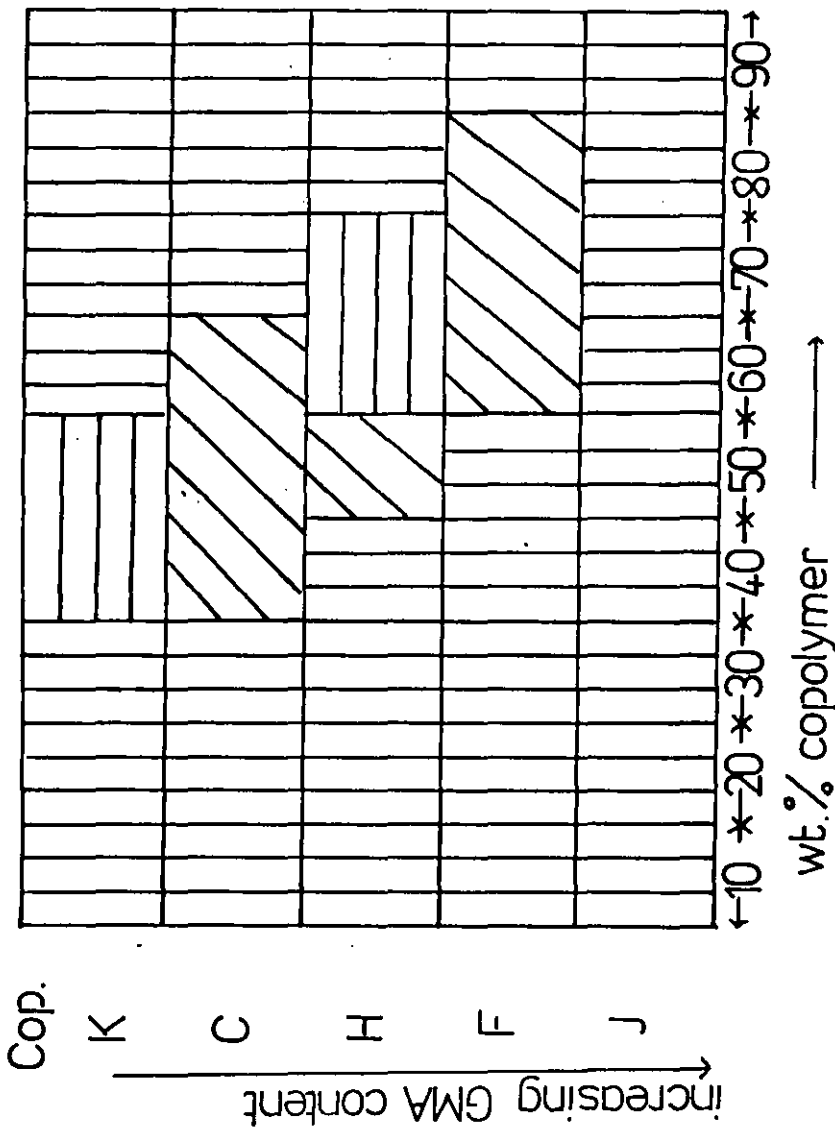
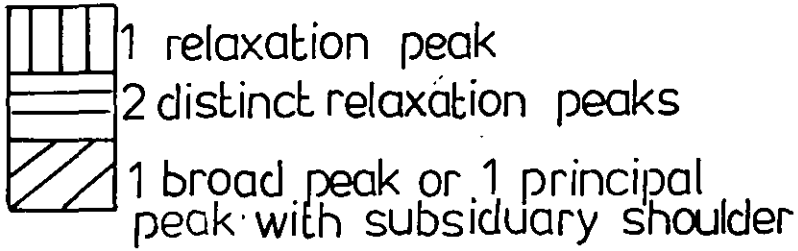
### 5.2.1 Characterisation of Copolymers

The molecular weights of the copolymers measured by GPC are listed in Table (5.3) together with the copolymer composition data determined by elemental analysis. The monomer reactivity ratios were calculated using the graphical techniques of Fineman and Ross and Kelen and Tudos. Both plots (Figures (5.25) and (5.26)) were linear over the whole composition range and yielded the following reactivity ratios

	$r_{MAN}$	$r_{ST}$
Fineman-Ross	0.24	0.39
Kelen-Tudos	0.23	0.38
Average	0.235	0.385

Figure (5.23)

Variation of Relaxation Behaviour with Copolymer Content and Blend Composition



Figure(5.24)  
Variation of Blend  $T_g$  with Composition  
Indicating Range of Values Measured  
for the Different Copolymers

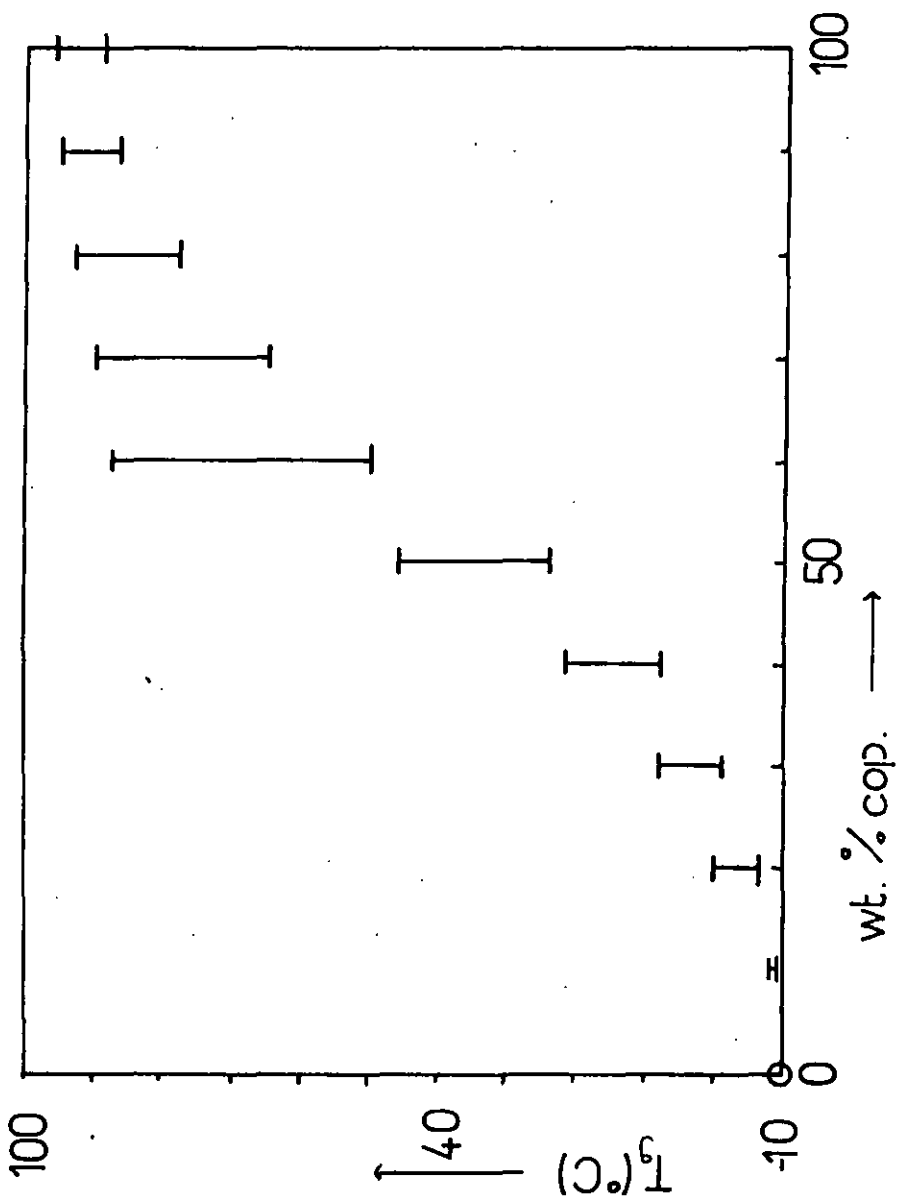
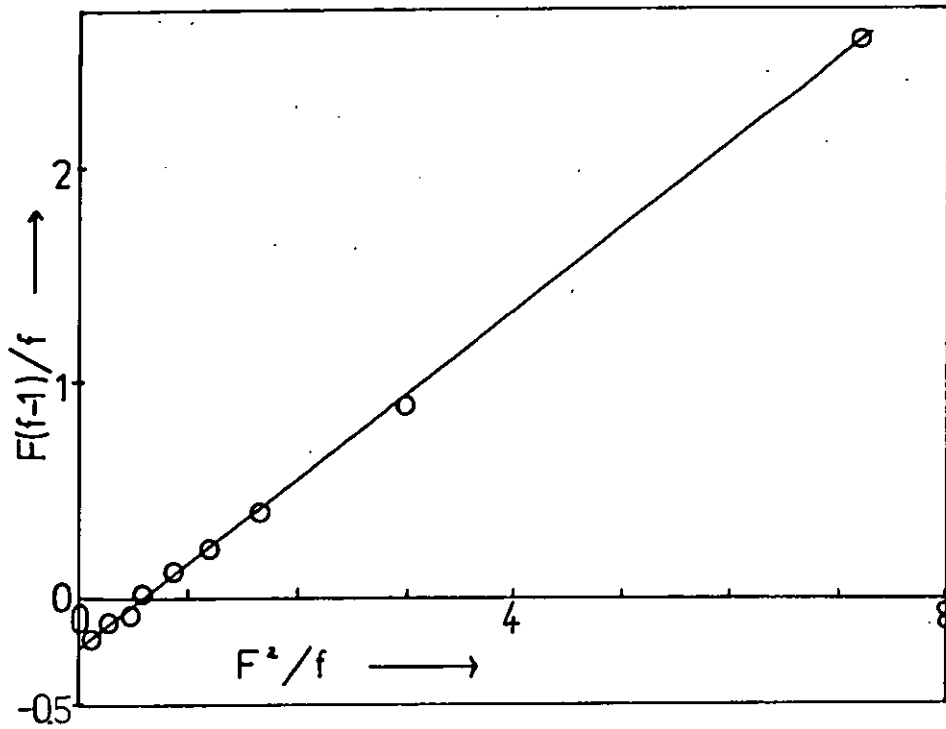


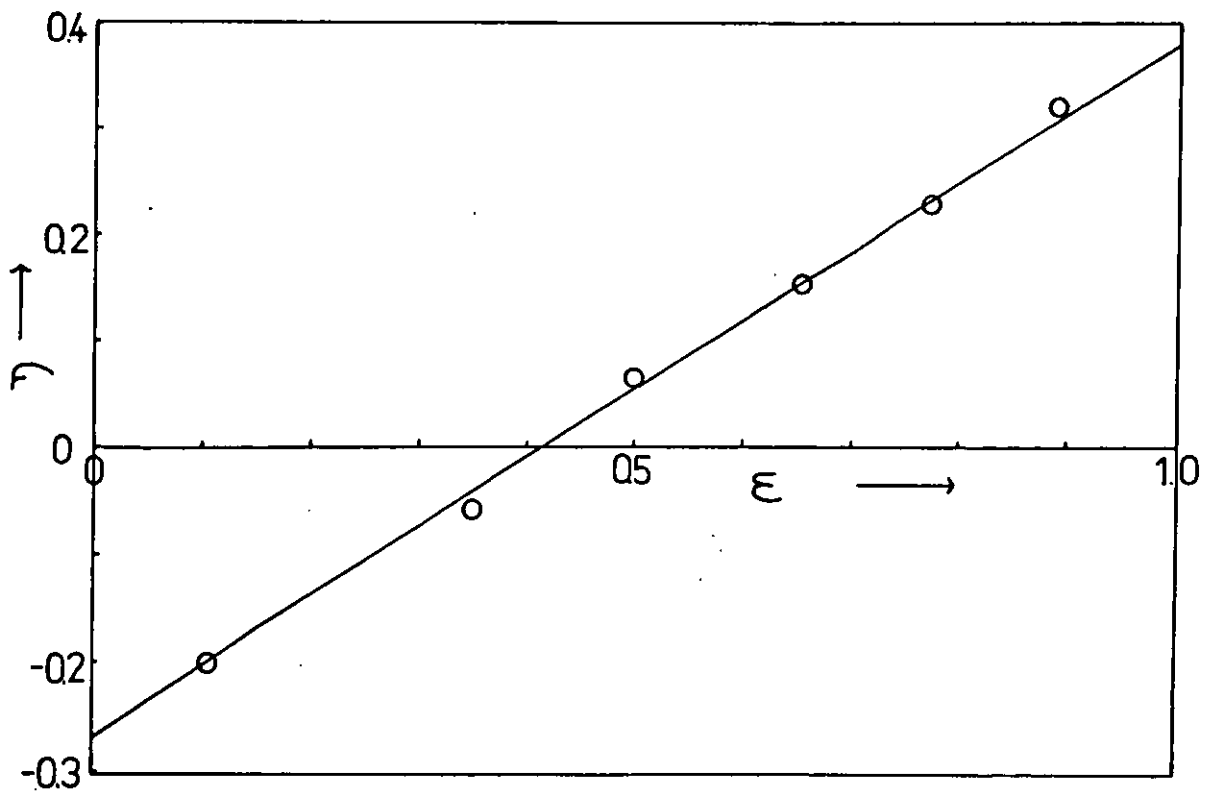
Table 5.3. Details of SM Copolymer Compositions and Molecular Weights

Copolymer	Feed Composition (Mole % MAN)	Copolymer Composition (Mole % MAN)	$\bar{M}_w$	$\bar{M}_n$	$\bar{M}_w/\bar{M}_n$
SM1	18.9	28.2	257,334	136,446	1.89
SM12	30.9	37.5	236,424	129,193	1.83
SM2	39.9	42.4	216,789	119,279	1.82
SM6	45.1	44.9	206,853	98,493	2.10
SM5	50.1	46.9	215,269	114,852	1.87
SM7	55.2	49.6	217,873	116,324	1.87
SM3	60.8	52.8	177,069	95,609	1.85
SM10	64.0	54.3	161,538	84,978	1.90
SM9	68.0	55.6	135,149	75,440	1.79
SM8	71.9	57.8	167,993	86,537	1.94
SM4	80.5	63.8	131,583	73,101	1.80

Figure(5.25)  
Fineman-Ross Plot for SM Copolymers



Figure(5.26)  
Kelen-Tudos Plot for SM Copolymers





Using the average values of  $r_{\text{MAN}}$  and  $r_{\text{ST}}$  the sequence length distributions and number average sequence lengths were calculated and are listed in Tables (5.4) and (5.5).

### 5.2.2 Optical Properties of Blends

Films cast from 1,4-dioxane appeared transparent except for those containing copolymers with either a low methacrylonitrile (SM1) or a high methacrylonitrile (SM4) content. In blends of these copolymers with PEPC translucent films were obtained over the complete concentration range. The intensity of translucence increased with copolymer content up to 50-60 wt.% copolymer and then declined. The appearance of the transparent films was found to be independent of temperature up to 220°, however the intensity of translucence was found to decline slightly in the region 150-200°C.

### 5.2.3 Thermal Analysis Data

The glass transition temperatures of the pure copolymers varied with composition in a manner approximated by the Fox equation. This is shown in Figure (5.27) where the copolymer composition has been converted to weight fractions of methacrylonitrile. Blends of the copolymers and corresponding homopolymers with poly(epichlorohydrin) exhibited three distinct categories of glass transition behaviour.

The first category (A) is comprised of blends which exhibited two distinct  $T_g$ 's that were essentially independent of the overall composition. This behaviour was found in the two homopolymer blends, PMAN/PEPC and PST/PEPC, and in blends of the two copolymers at the extremes of the range of composition investigated (SM1 and SM4), as shown in Figures (5.28) and (5.29). The second category (B) consisted

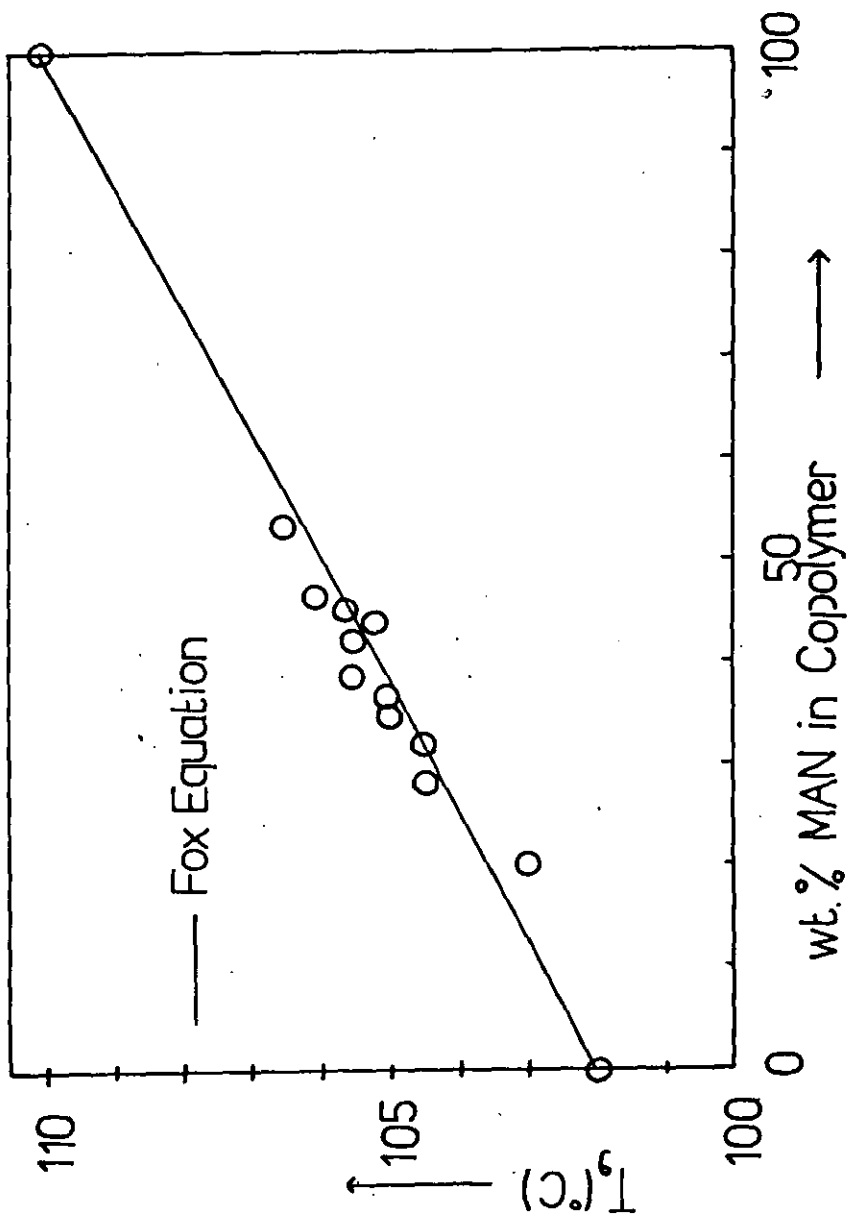
Table 5.4. Sequence Length Distributions of SM Copolymers

		SM1		SM12		SM2		SM6		SM5		SM7	
		MAN	ST	MAN	ST	MAN	ST	MAN	ST	MAN	ST	MAN	ST
Number Average Sequence Length - $\bar{n}$		1.05	2.60	1.10	1.83	1.15	1.56	1.18	1.45	1.22	1.37	1.27	1.30
Mole Percentage of Particular Repeat Unit in Sequences X Units Long	X												
	1	95.1	38.6	91.1	54.7	87.2	64.3	84.7	68.9	81.9	73.0	78.7	76.9
	2	4.6	23.7	8.2	24.8	11.1	23.0	13.0	21.4	14.8	19.7	16.8	17.8
	3	0.2	14.6	0.7	11.2	1.4	8.2	2.0	6.7	2.7	5.3	3.6	4.1
	4	0.0	8.9	0.0	5.1	0.2	2.9	0.3	2.1	0.5	1.4	0.8	1.0
	5	0.0	5.5	0.0	2.3	0.0	1.1	0.0	0.6	0.1	0.4	0.2	0.2
	6	0.0	3.4	0.0	1.0	0.0	0.4	0.0	0.2	0.0	0.1	0.0	0.0

Table 5.5. Sequence Length Distributions of SM Copolymers

		SM3		SM10		SM9		SM8		SM4	
		MAN	ST	MAN	ST	MAN	ST	MAN	ST	MAN	ST
Number Average Sequence Length - $\bar{n}$		1.34	1.24	1.39	1.21	1.47	1.17	1.56	1.15	1.91	1.09
Mole Percentage of Particular Repeat Unit in Sequences X Units Long	X										
	1	74.5	80.7	71.9	82.8	68.2	85.1	64.0	87.4	52.3	91.8
	2	19.0	15.5	20.2	14.3	21.7	12.6	23.0	11.1	24.9	7.5
	3	4.8	3.0	5.7	2.5	6.9	1.9	8.3	1.4	11.9	0.6
	4	1.2	0.6	1.6	0.4	2.2	0.3	3.0	0.2	5.7	0.1
	5	0.3	0.1	0.5	0.1	0.7	0.0	1.1	0.0	2.7	0.0
	6	0.1	0.0	0.1	0.0	0.2	0.0	0.4	0.0	1.3	0.0

Figure (5.27)  
Compositional Dependence of  $T_g$  in SM  
Copolymers Measured by D.T.A.



Figure(5.28)

DTA. Data for PST/PEPC Blends

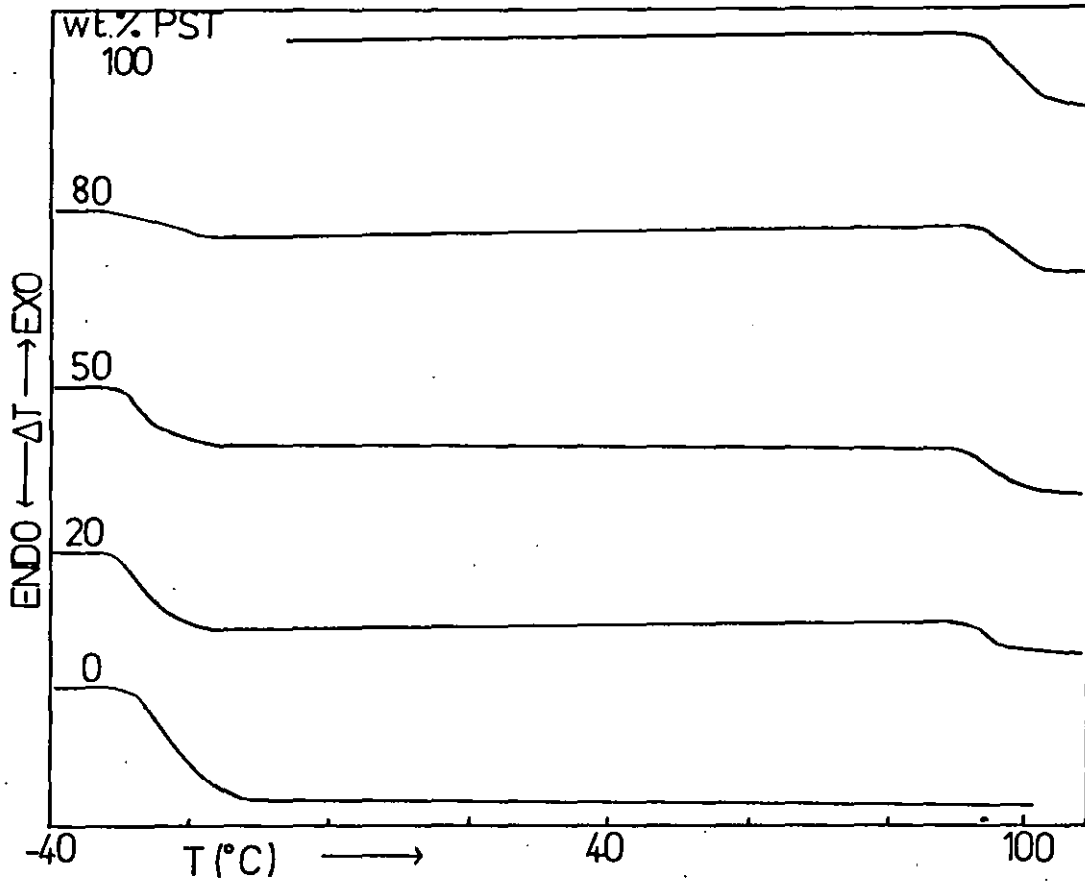
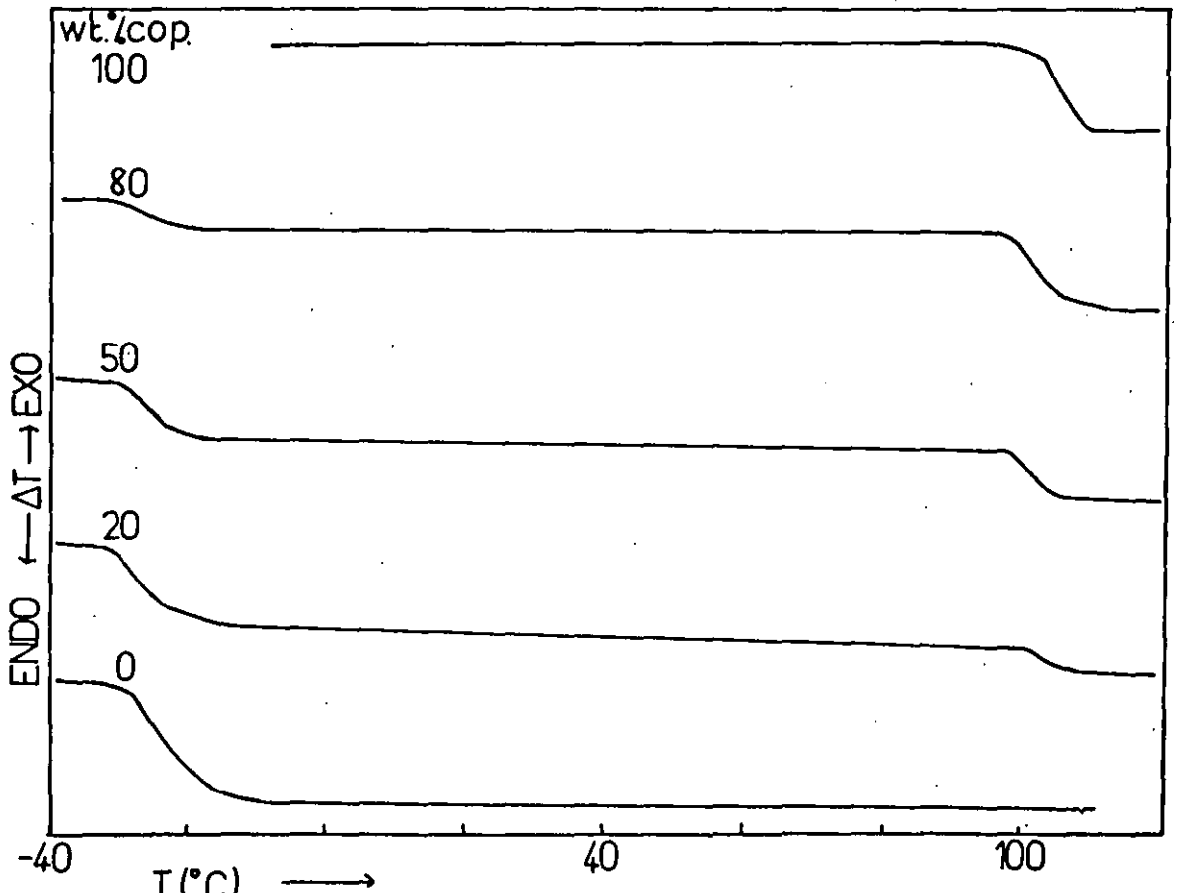


Figure (5.29)

DTA. Data for SM1/PEPC Blends



of blends which had a single, relatively narrow, composition dependent  $T_g$ . Blends of SM3 and SM7 behaved in this manner as shown in Figures (5.30) and (5.31). The variation of  $T_g$  with blend composition (Figure (5.32)) followed the Fox equation at intermediate compositions, but showed some deviation at the extremes. The final category (C) comprised mixtures which displayed a very broad step in the thermogram. The transition breadth could not be resolved and increased markedly at copolymer contents of 50 wt.% and above. This behaviour was observed in blends of copolymers SM12, SM6, SM5, SM10, SM9 and SM8 with PEPC and representative thermograms are presented in Figures (5.33)-(5.35).

#### 5.2.4 Dynamic Mechanical Results

Blends were studied as thin films cast onto steel from solutions of 1,4-dioxane. Prior to running all films were annealed at 120° under vacuum.

The glass transition temperatures of the pure copolymers followed those predicted by the Fox equation  $\pm 1.5^\circ$  (Figure (5.36)). Blends with PEPC fell into the same three categories described above. Category (A) behaviour was displayed by PMAN/PEPC and SM4/PEPC, shown in Figures (5.37) and (5.38), and similar results were obtained for PST/PEPC and SM1/PEPC. As found in the previous section SM3/PEPC and SM7/PEPC fell into category (B) with a single composition dependent glass transition (Figure (5.39)-(5.40)). Examples of category (C) blends are shown in Figures (5.41)-(5.43) and it is clear that the loss tangent curves had a superior resolution to the equivalent thermograms. Consequently low temperature minor transitions are apparent in the form of shoulders or secondary peaks in some cases at copolymer contents of 50-80 wt.%.

Figure (5.30)

D.T.A. Data for SM3/PEPC Blends

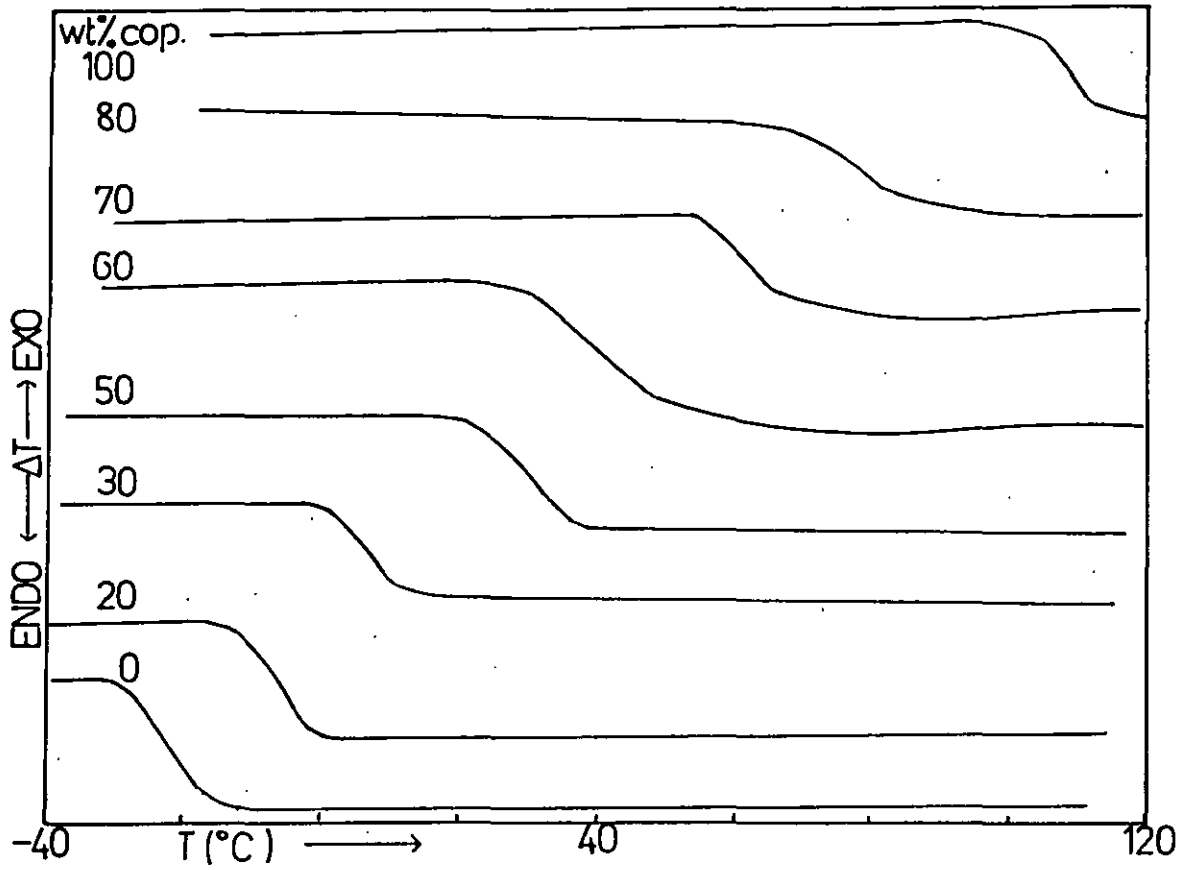


Figure (5.31)

D.T.A. Data for SM7/PEPC Blends

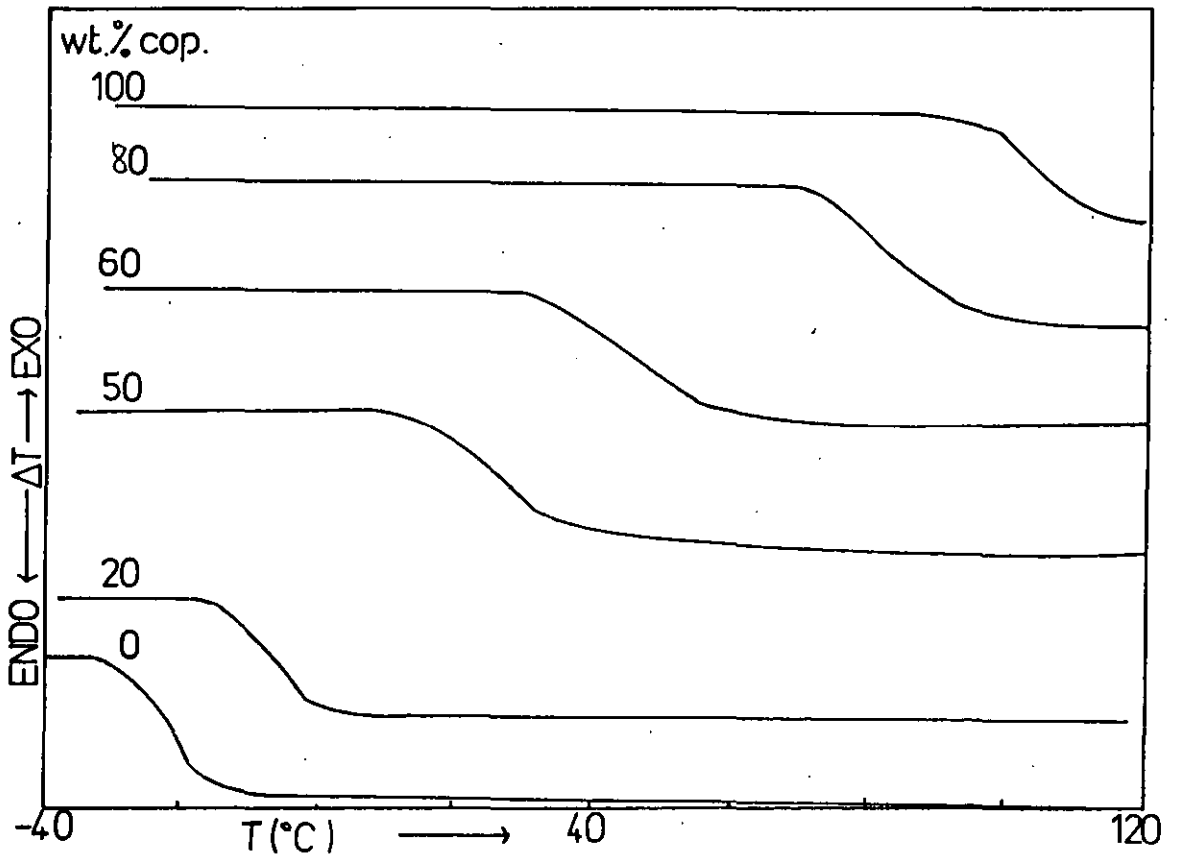
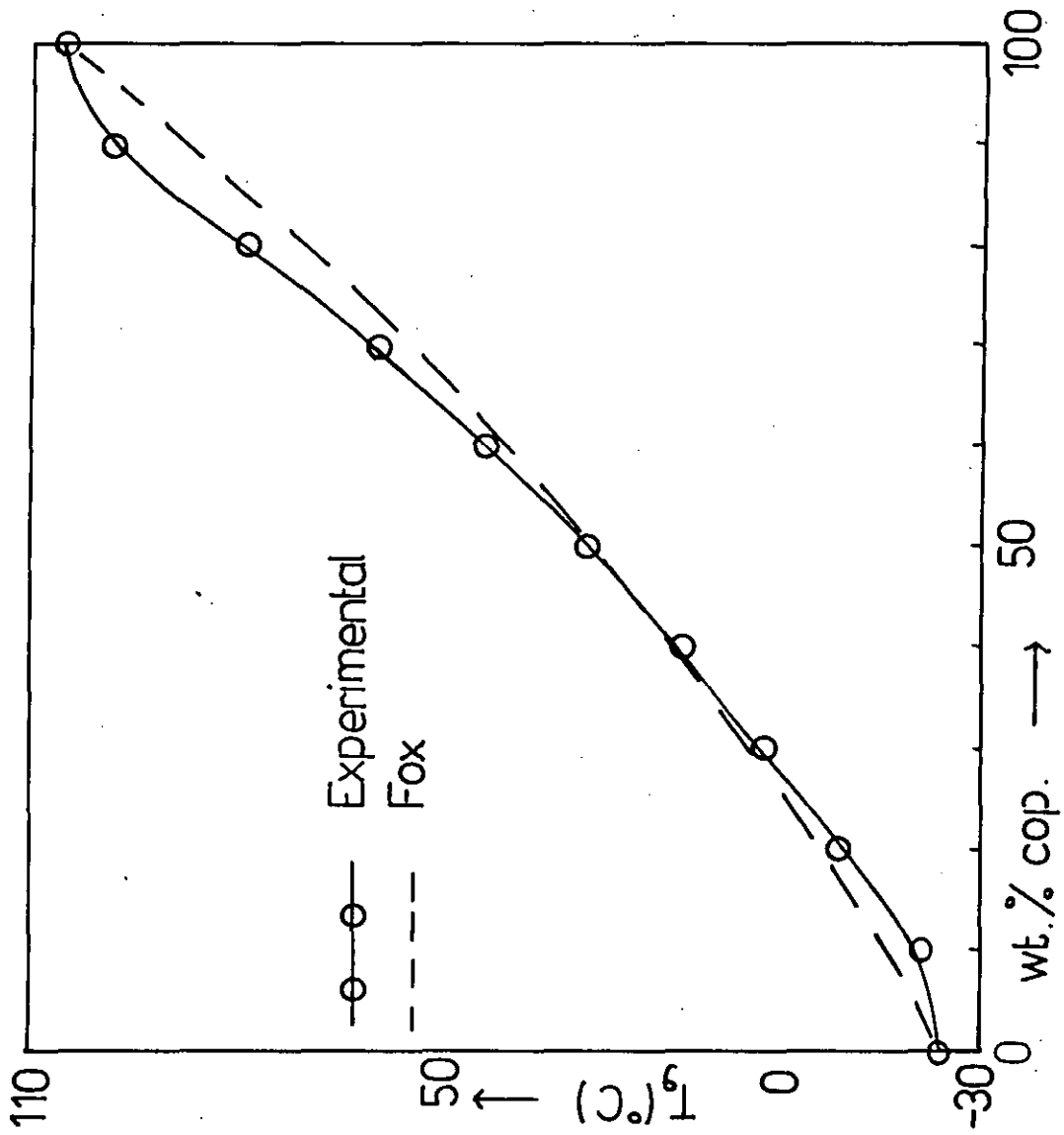


Figure (5.32)

Variation of  $T_g$  with Composition for SM3 / PEPC Blends Measured by D.T.A.





Figure(5.33)

DTA. Data for SM12 /PEPC Blends

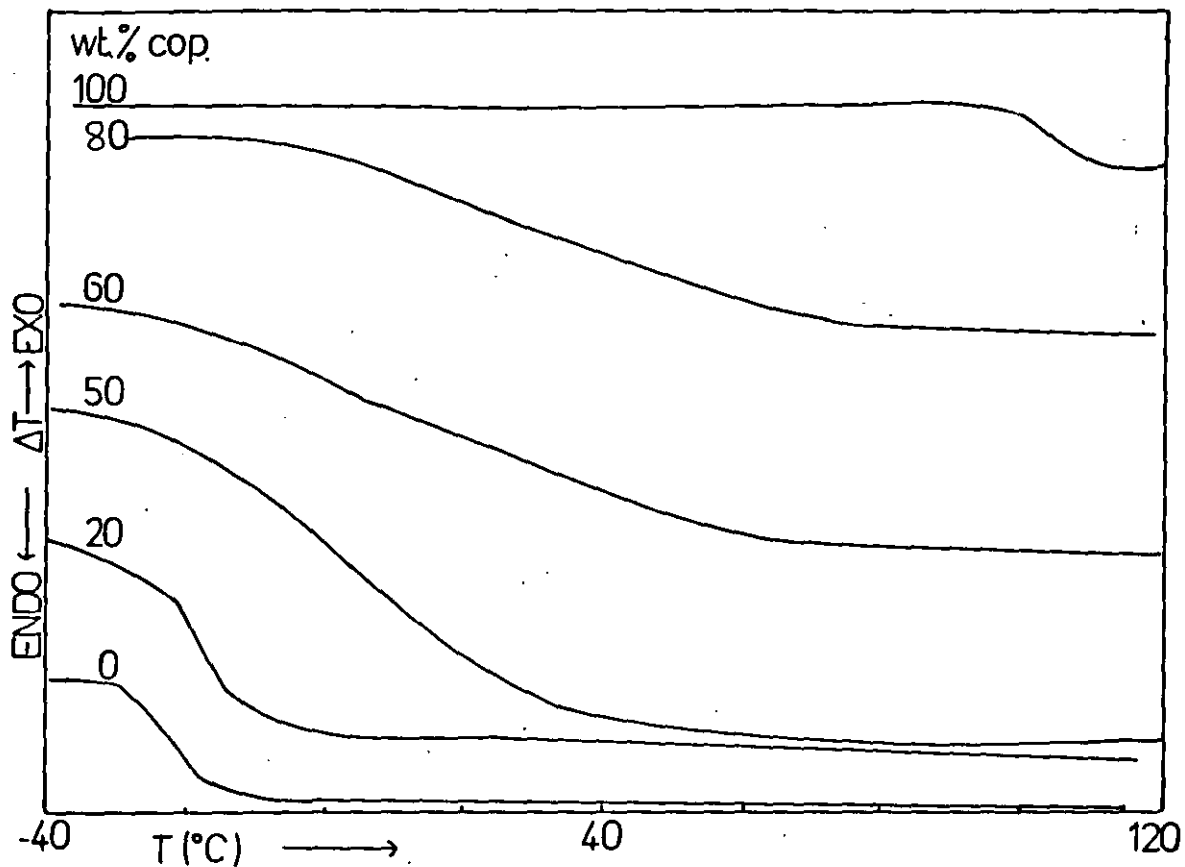


Figure (5.34)

DTA. Data for SM9/PEPC Blends

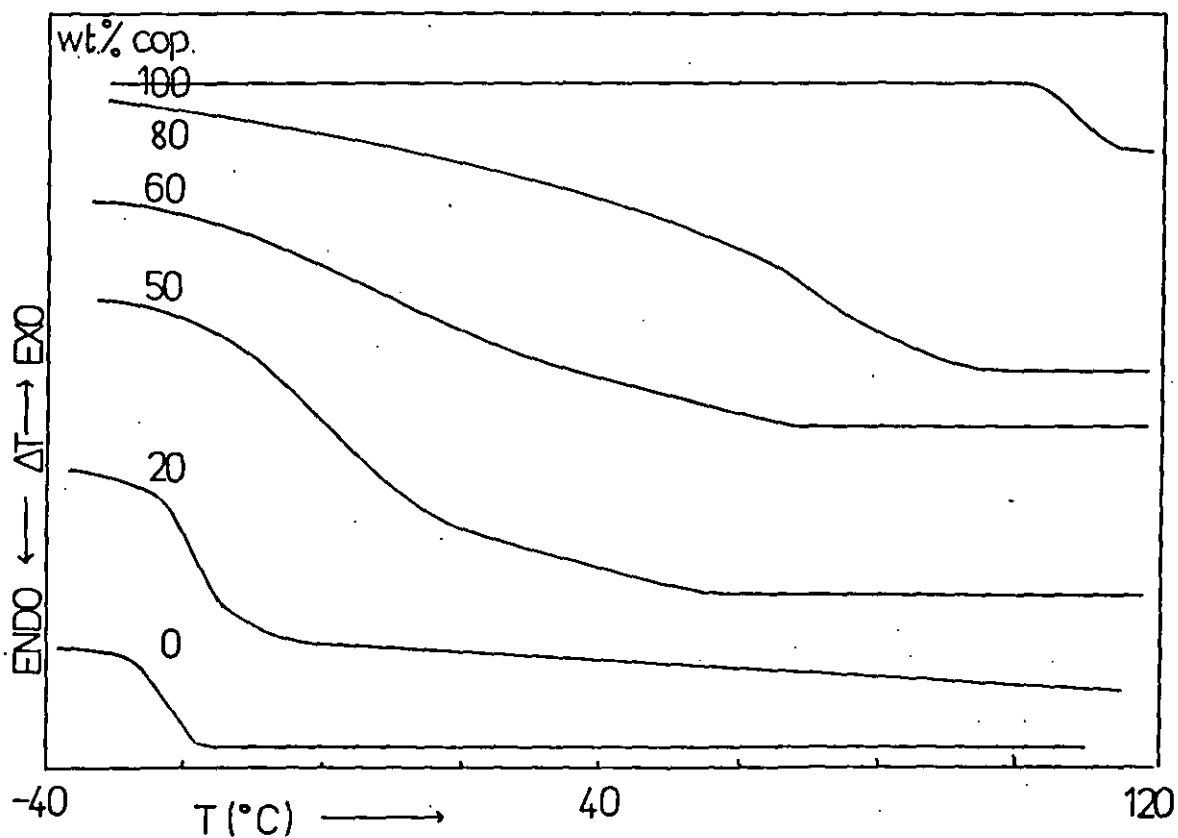


Figure (5.35)

DTA. Data for SM6/PEPC Blends

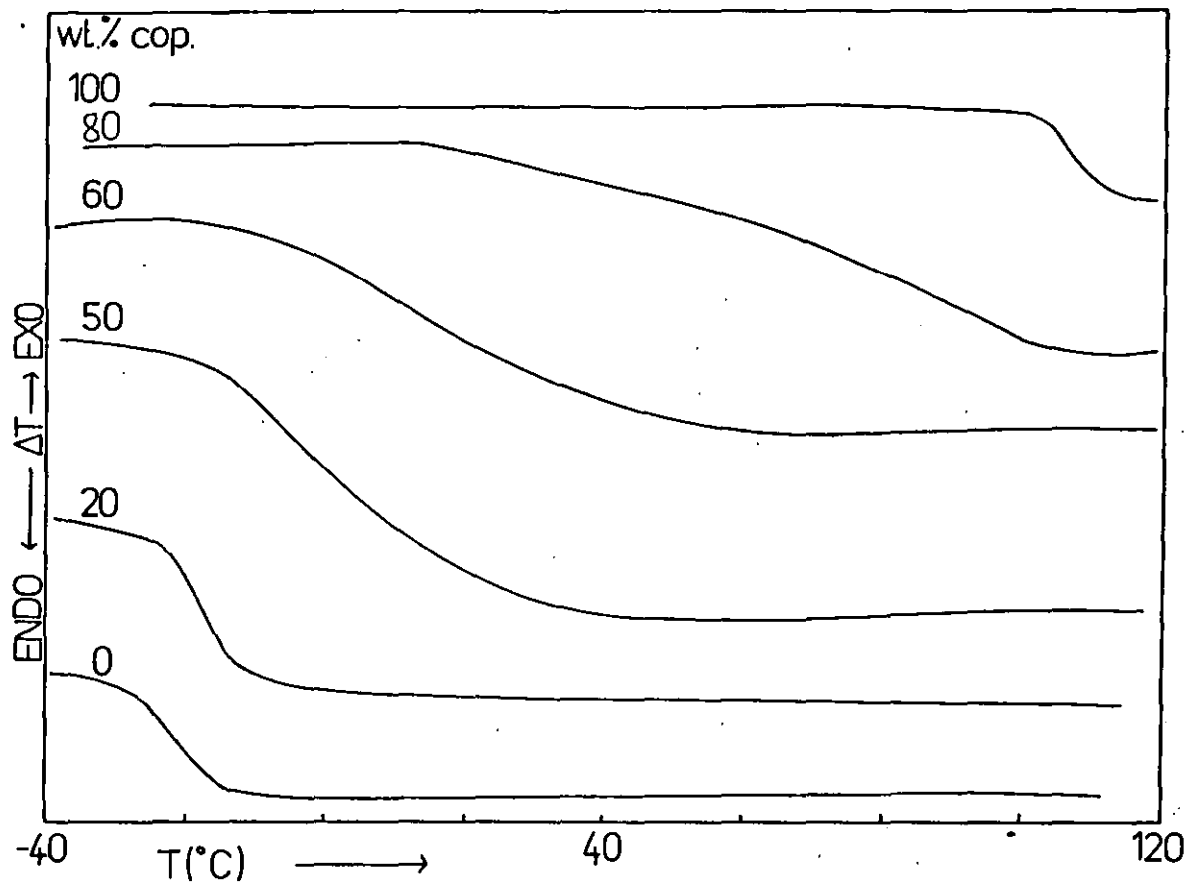
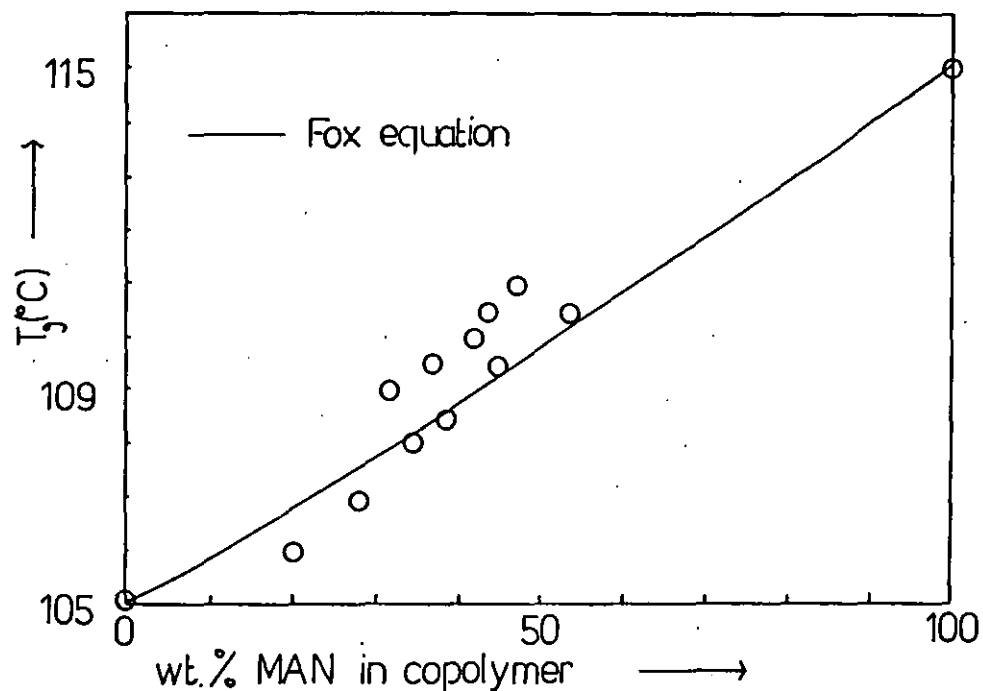


Figure (5.36)

Variation of SM Copolymer  $T_g$  with Composition Measured by DMTA.



Figure(5.37)

Loss Tangent vs. Temperature Curves  
for PMAN/PEPC Blends

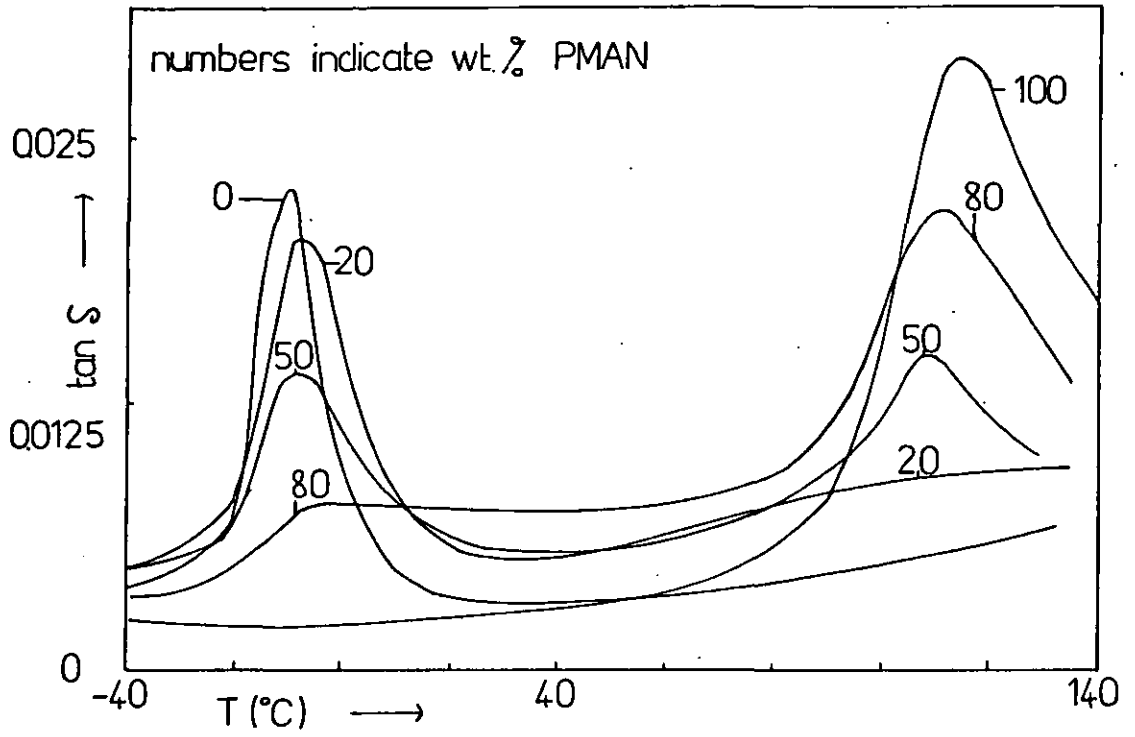


Figure (5.38)

Loss Tangent vs. Temperature Curves for  
SM4 /PEPC Blends

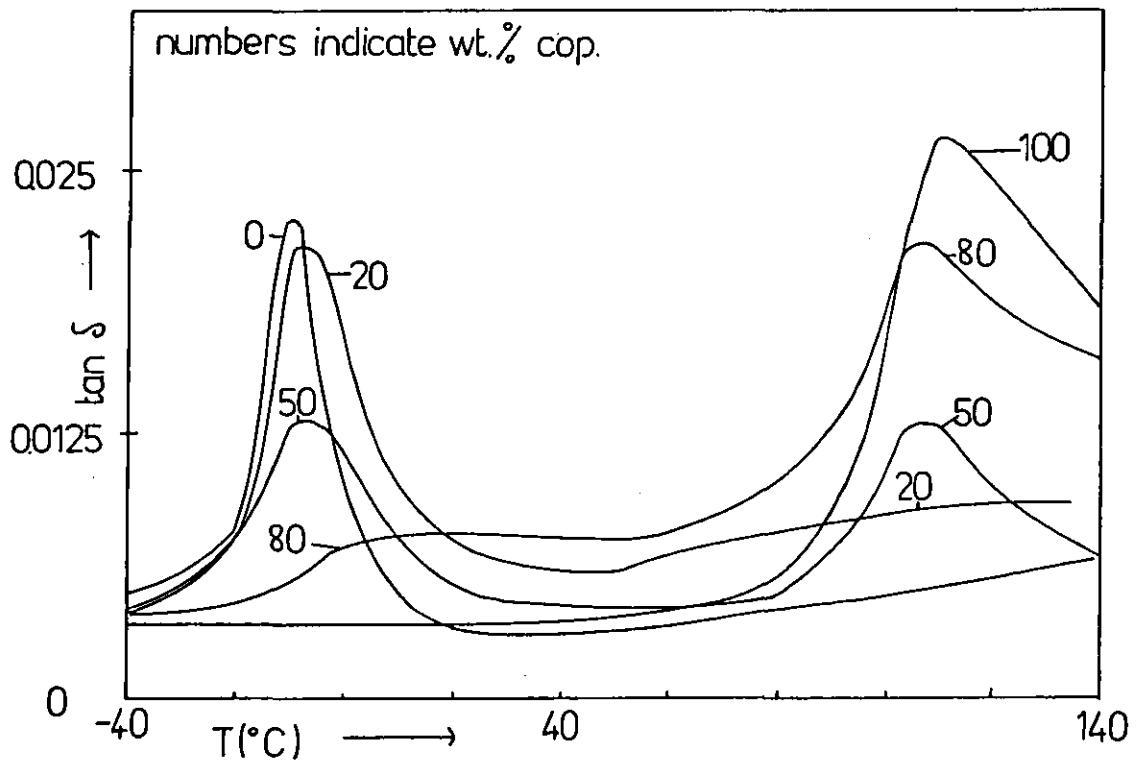


Figure (5.39)  
Loss Tangent vs Temperature Curves for  
SM3 /PEPC Blends

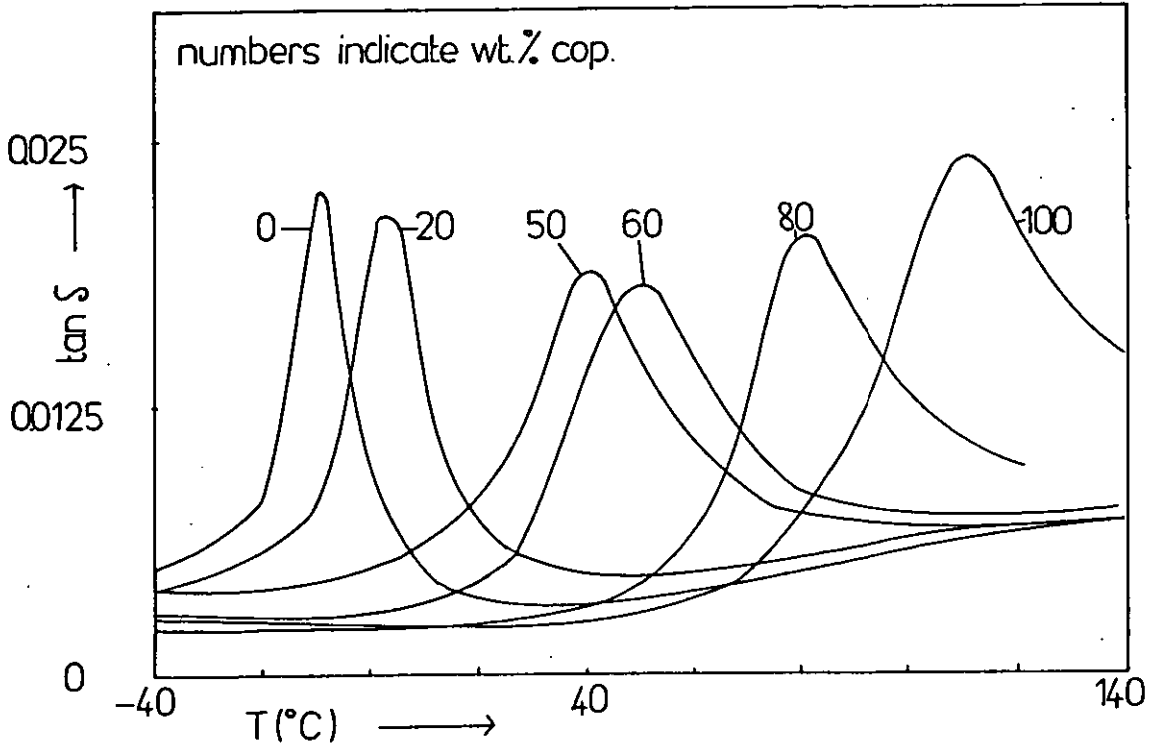


Figure (5.40)  
Variation of  $T_g$  with Composition for  
SM3/PEPC Blends Measured by DMTA.

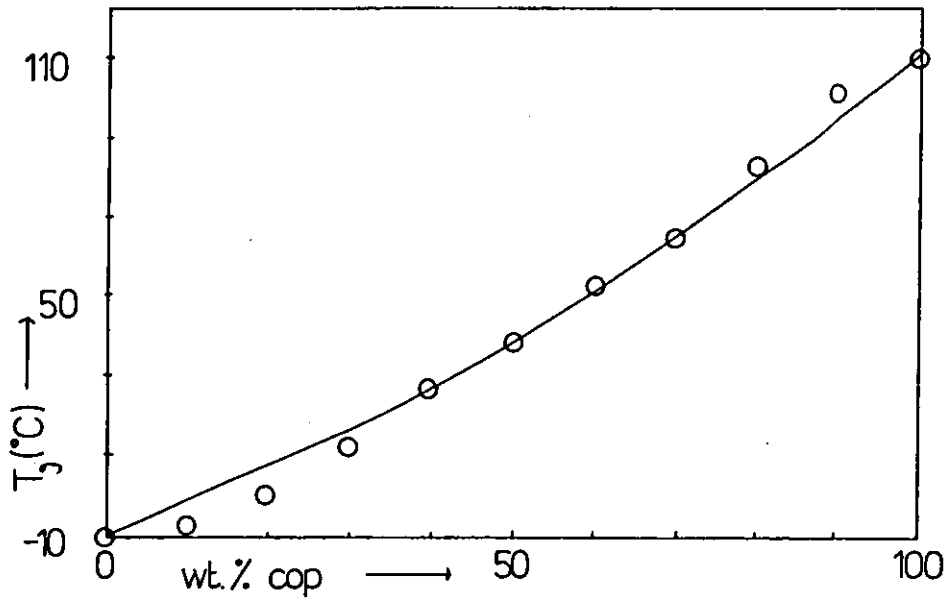


Figure (5.41)

Loss Tangent vs. Temperature Curves for  
SM12/PEPC Blends

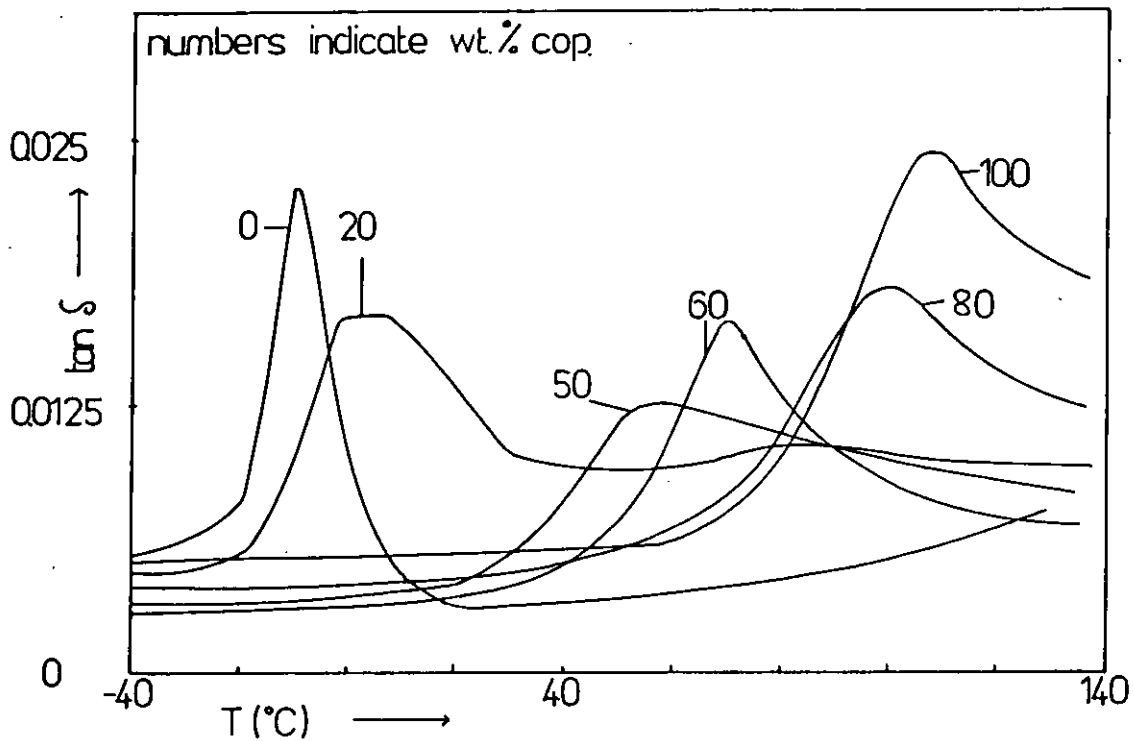


Figure (5.42)

Loss Tangent vs. Temperature Curves for  
SM6/PEPC Blends

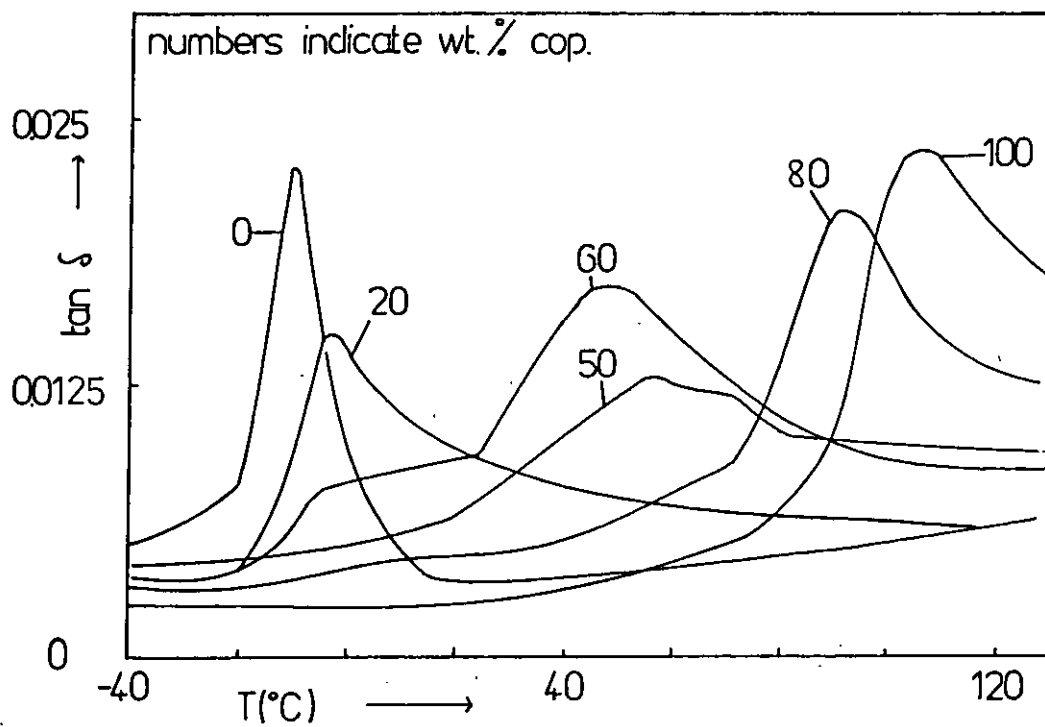
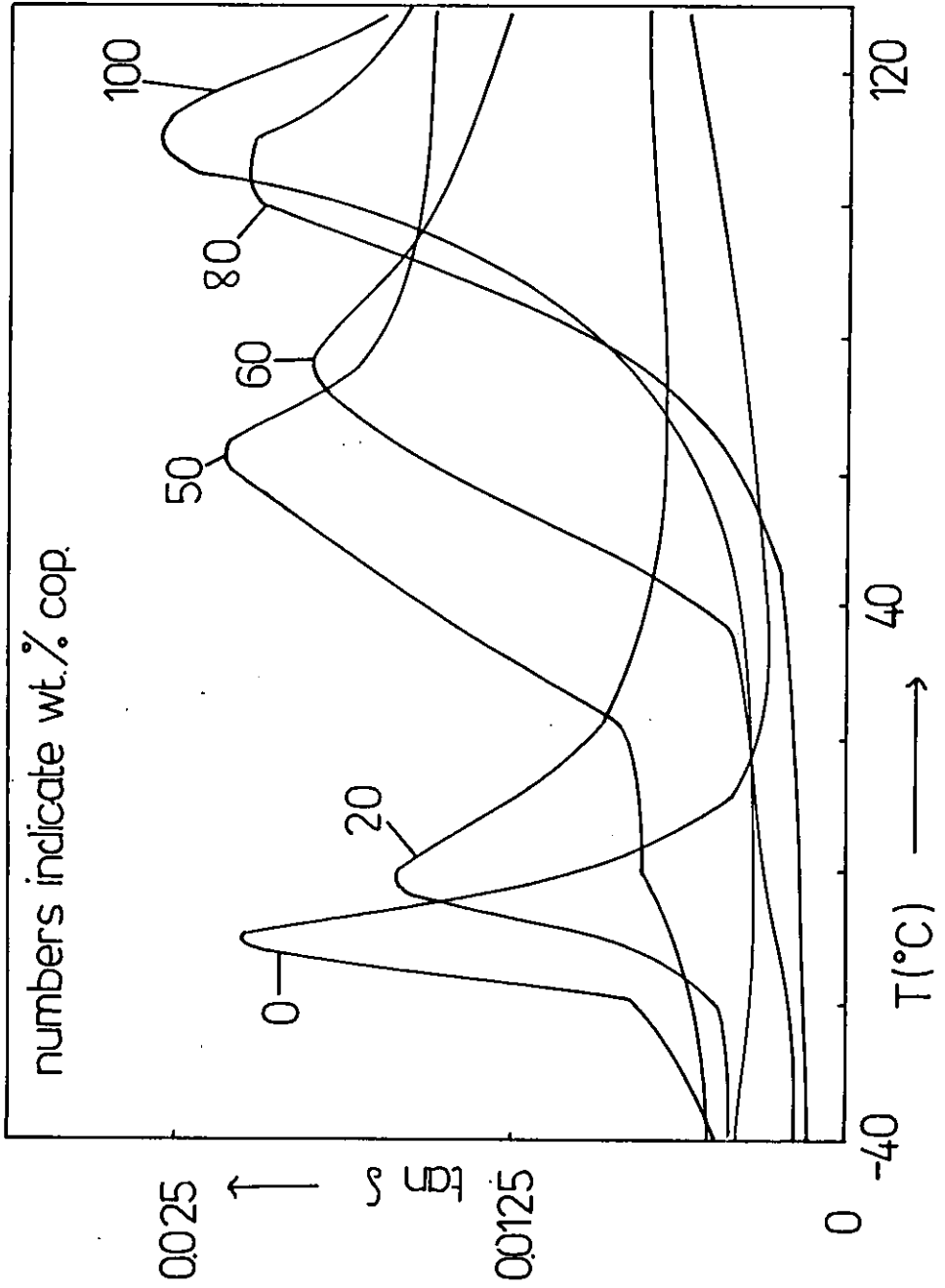


Figure (5.43)

Loss Tangent vs. Temperature Curves for  
SM9 /PEPC Blends



Dynamic mechanical testing was also conducted on compression moulded bars of the SM copolymers blended with 50 wt.% PEPC. The loss tangent curves are shown in Figures (5.44) and (5.45) for a number of representative samples. The copolymers formed the same three types of blends but using these much larger samples one obtained vastly superior resolution in comparison with the data for the steel supported films. This was particularly noticeable for type C blends where the maximum value of  $\tan \delta$  ( $T_g$ ) became very clearly defined. There was also some evidence of a small amount of almost pure PEPC in these blends indicated by the slight  $\tan \delta$  peak at  $-10$  to  $-5^\circ\text{C}$ . The corresponding plots of the temperature dependence of the logarithmic storage modulus are given in Figures (5.46) and (5.47). The variation in the type of glass transition behaviour observed by both DTA and DMTA with copolymer composition is presented schematically in Figure (5.48).

Dynamic mechanical measurements were also performed on films of SM3/PEPC quenched from various temperatures in the range  $130$ - $200^\circ\text{C}$ . The  $\tan \delta$  curves of these samples did not however show any significant differences from the result obtained following annealing at  $120^\circ\text{C}$ .

#### 5.2.5 Dielectric Measurements on Selected SM/PEPC Blends

Dielectric measurements were made on selected blends, containing equal weights of the two components, which represented the three categories of behaviour previously observed.

The pure rubber (Figures (5.49)-(5.50)) exhibited a peak at low temperatures in the dielectric loss plot, which shifted to higher frequencies as the temperature was raised. To facilitate comparison with the dynamic mechanical results the data was replotted in terms of  $\tan \delta$  ( $\epsilon''/\epsilon'$ ) against temperature. This plot is presented in Figure (5.51) at a few selected frequencies and displayed a peak in

Figure (5.44)  
 Loss Tangent vs. Temperature Curves for  
 Various 50/50 Blends with PEPC

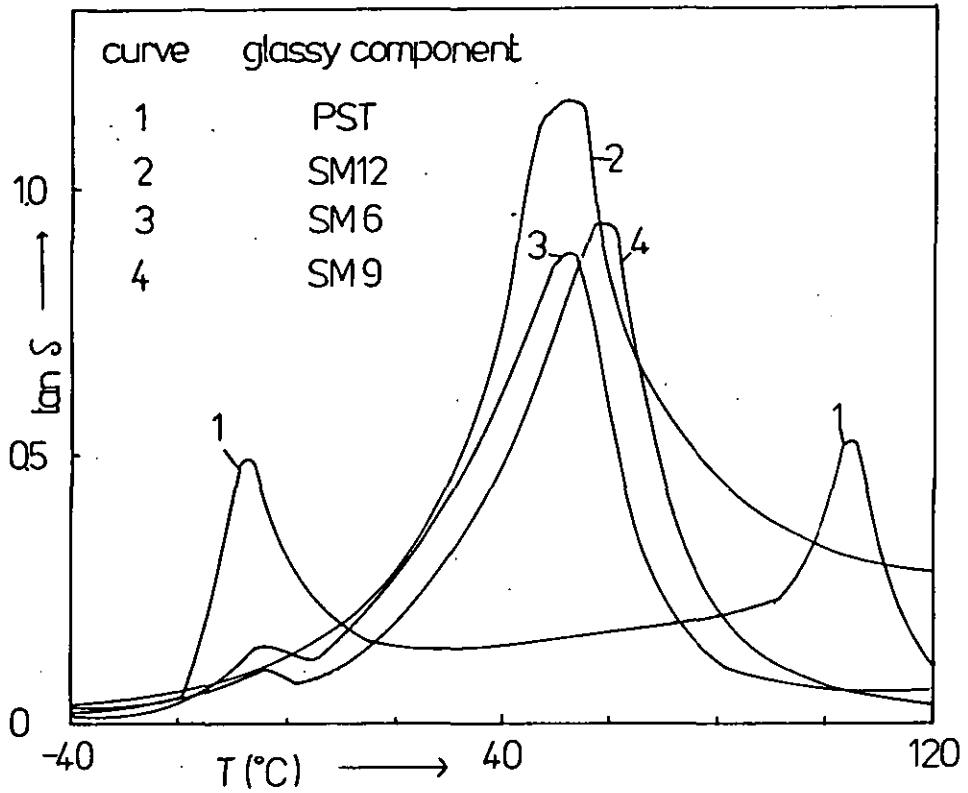
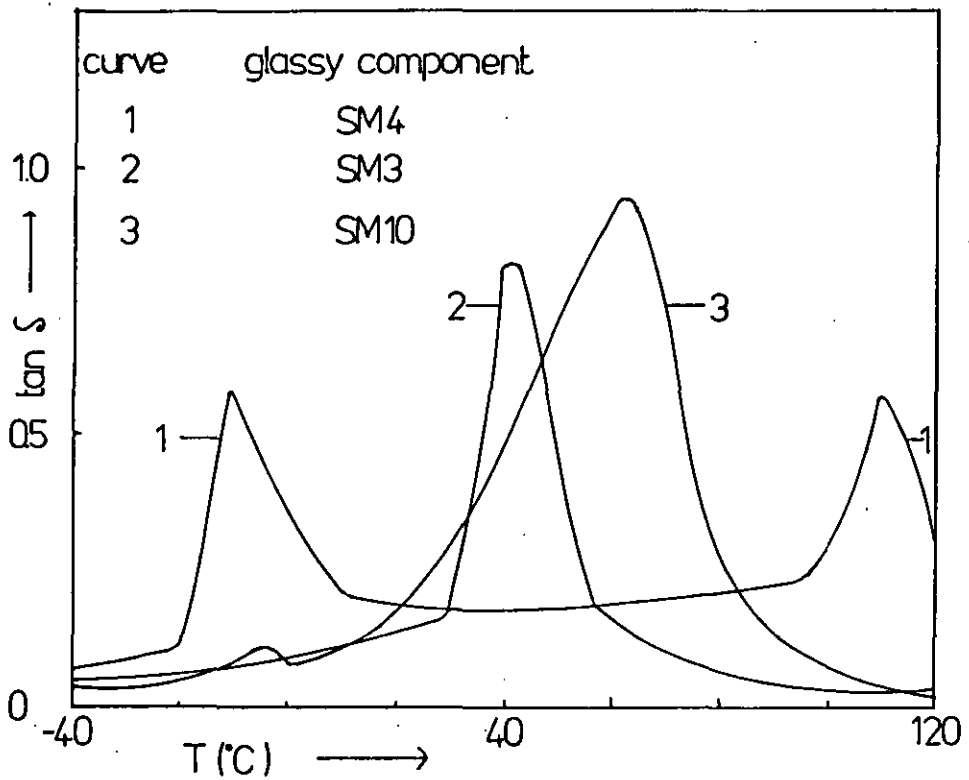


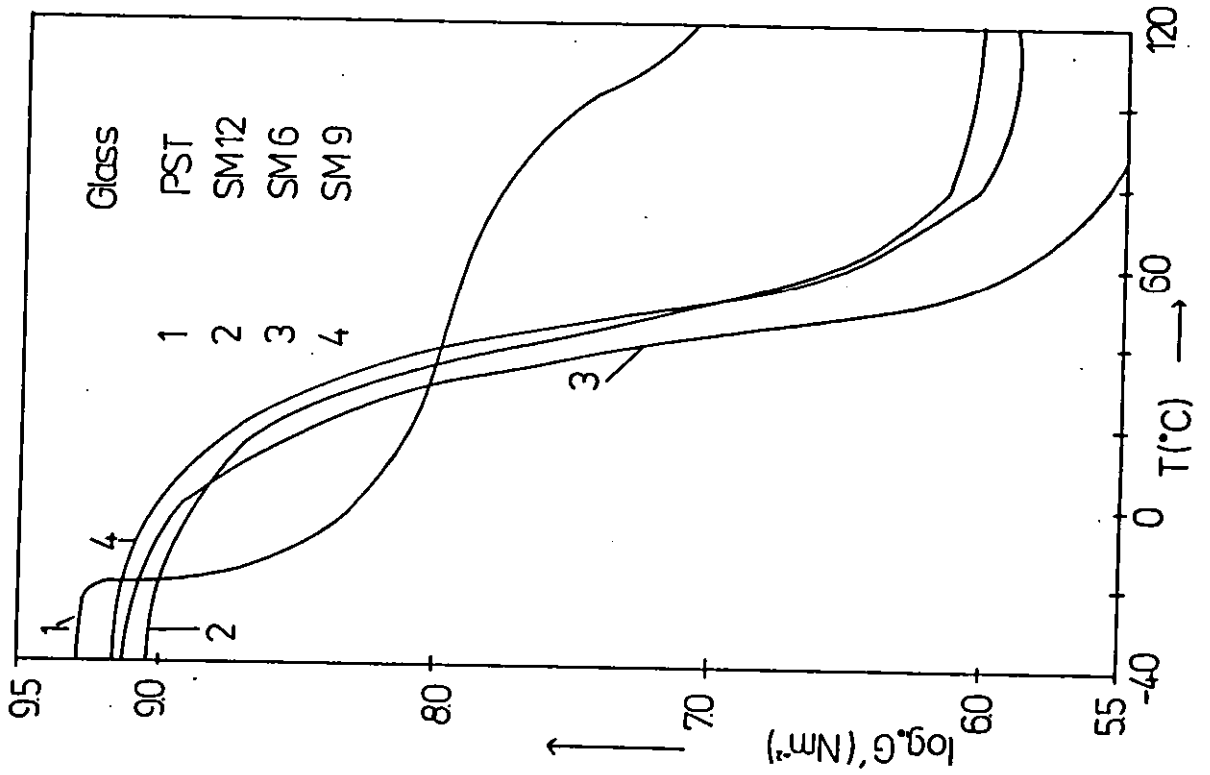
Figure (5.45)  
 Loss Tangent vs. Temperature Curves for  
 Various 50/50 Blends with PEPC





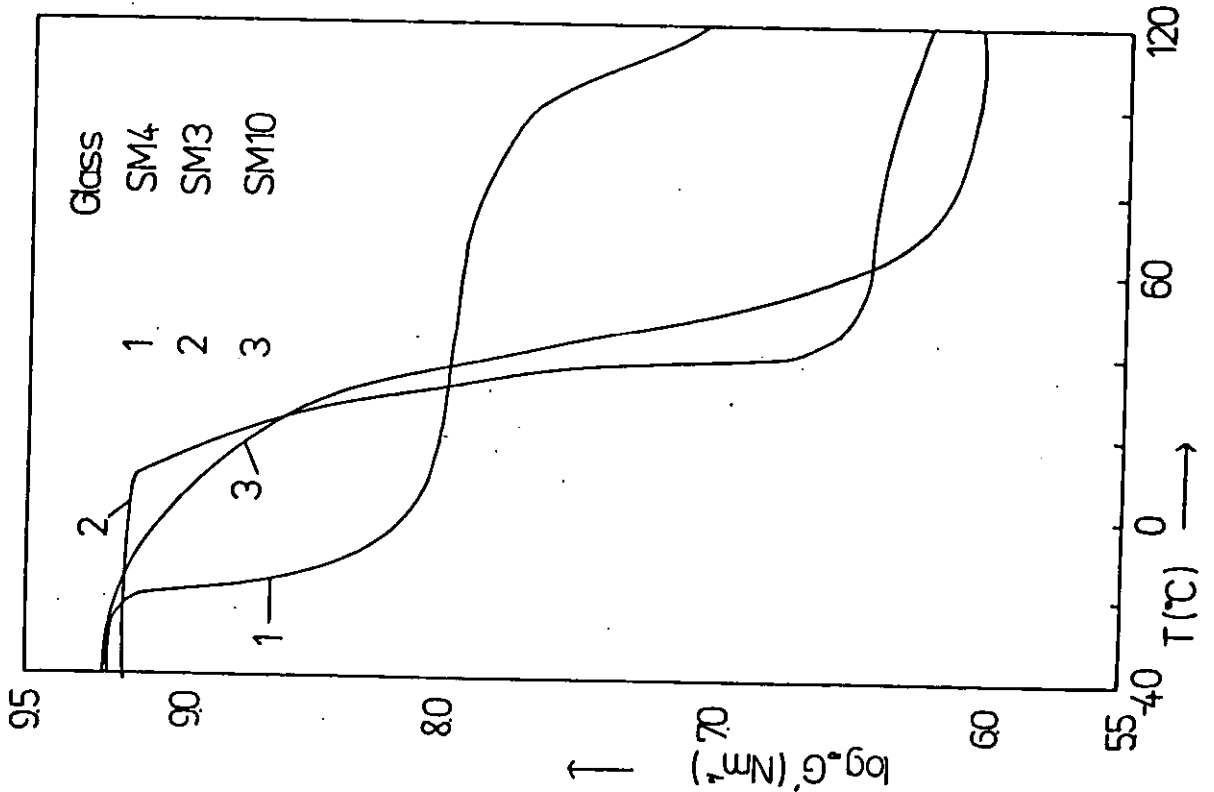
Figure(546)

Storage Modulus vs. Temperature Curves  
for Various 50/50 Blends with PEPC

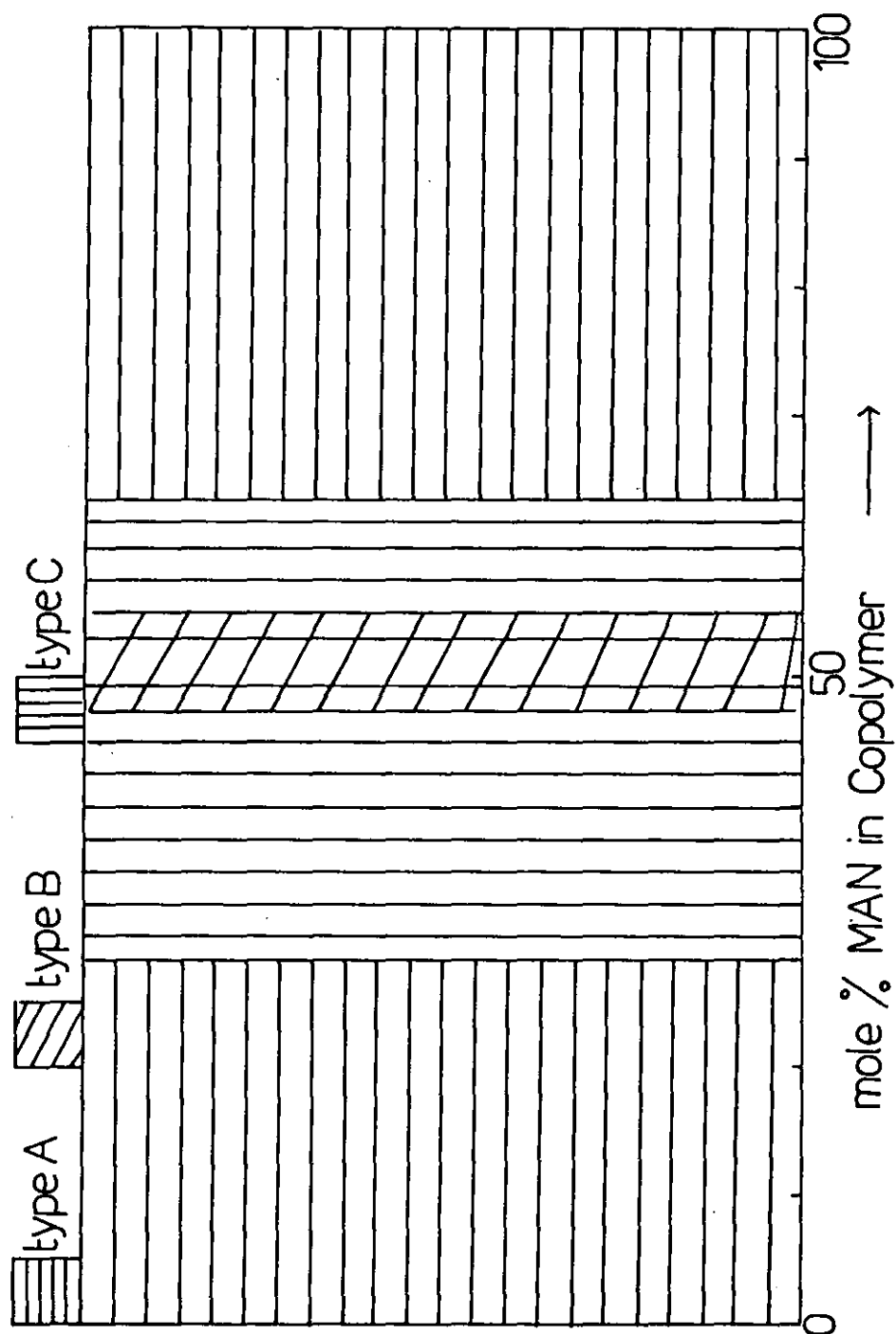


Figure(547)

Storage Modulus vs. Temperature Curves  
for other 50/50 Blends with PEPC

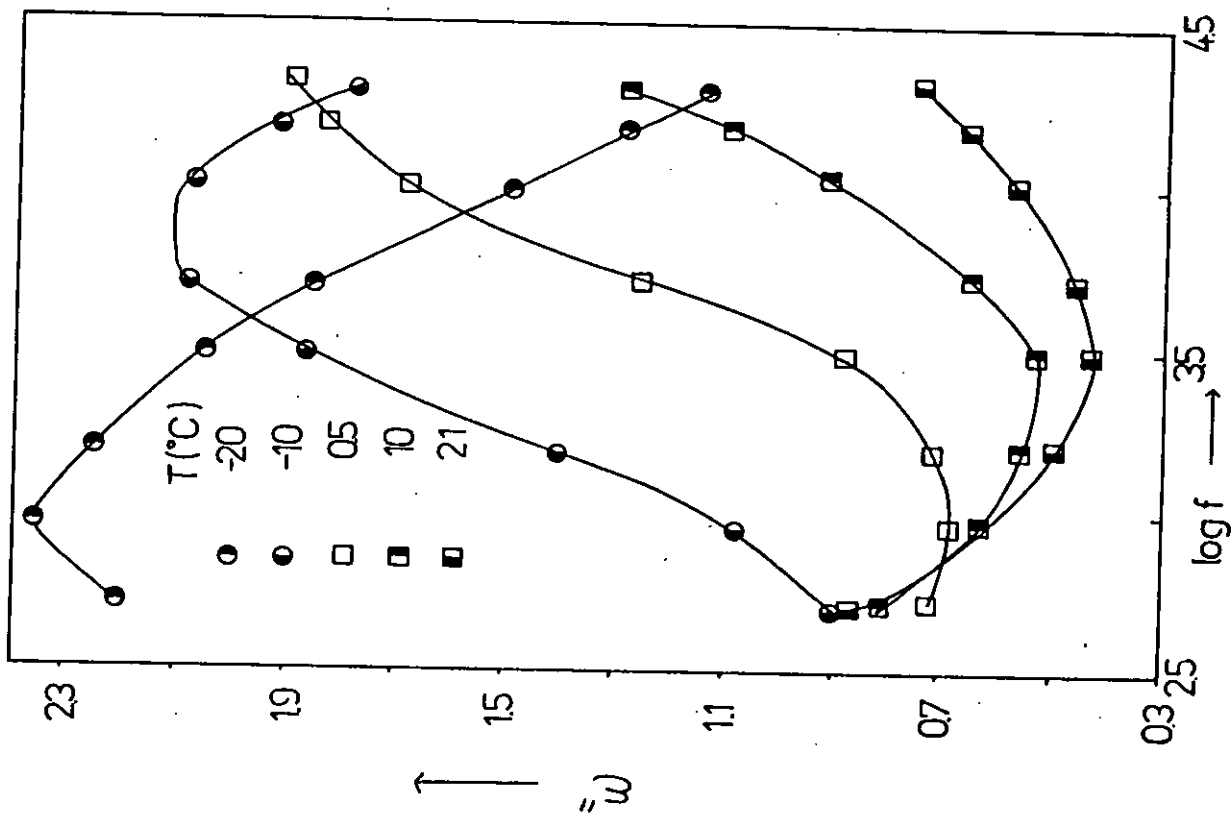


Figure(5.48)  
Schematic of the Influence of Copolymer  
Composition on Observed Blend Category  
for SM /PEPC



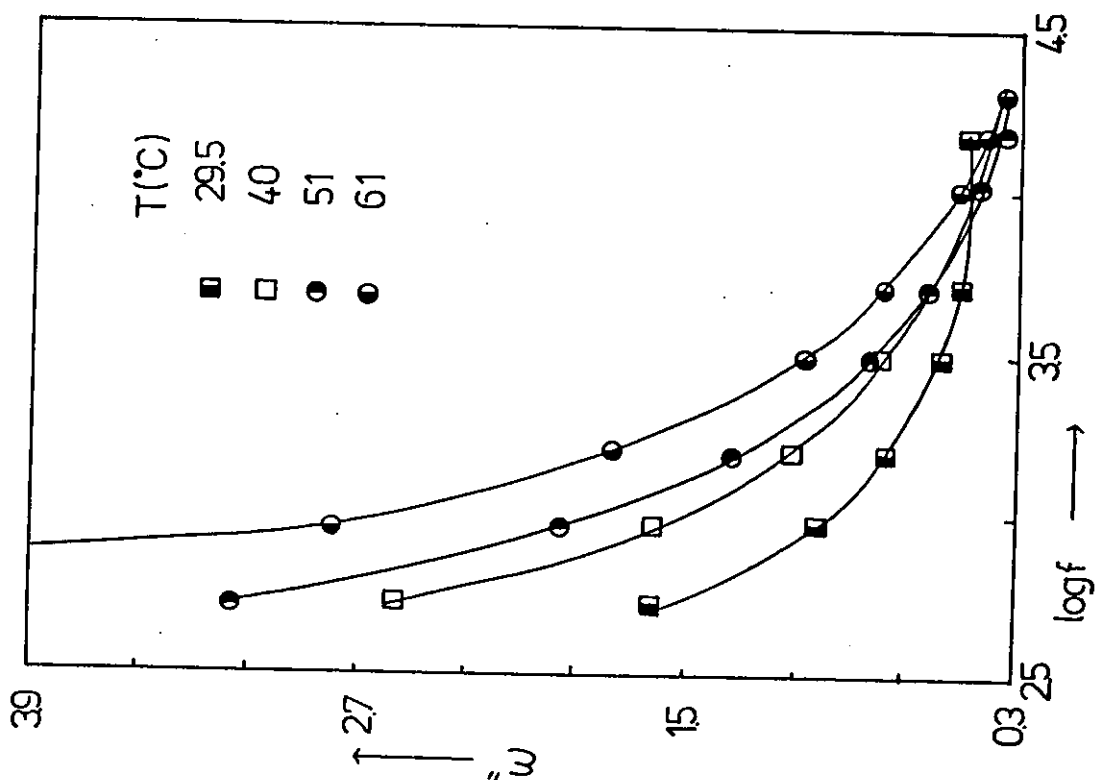
Figure(5.49)

Frequency Dependence of Dielectric Loss at Various Temperatures for PEPC

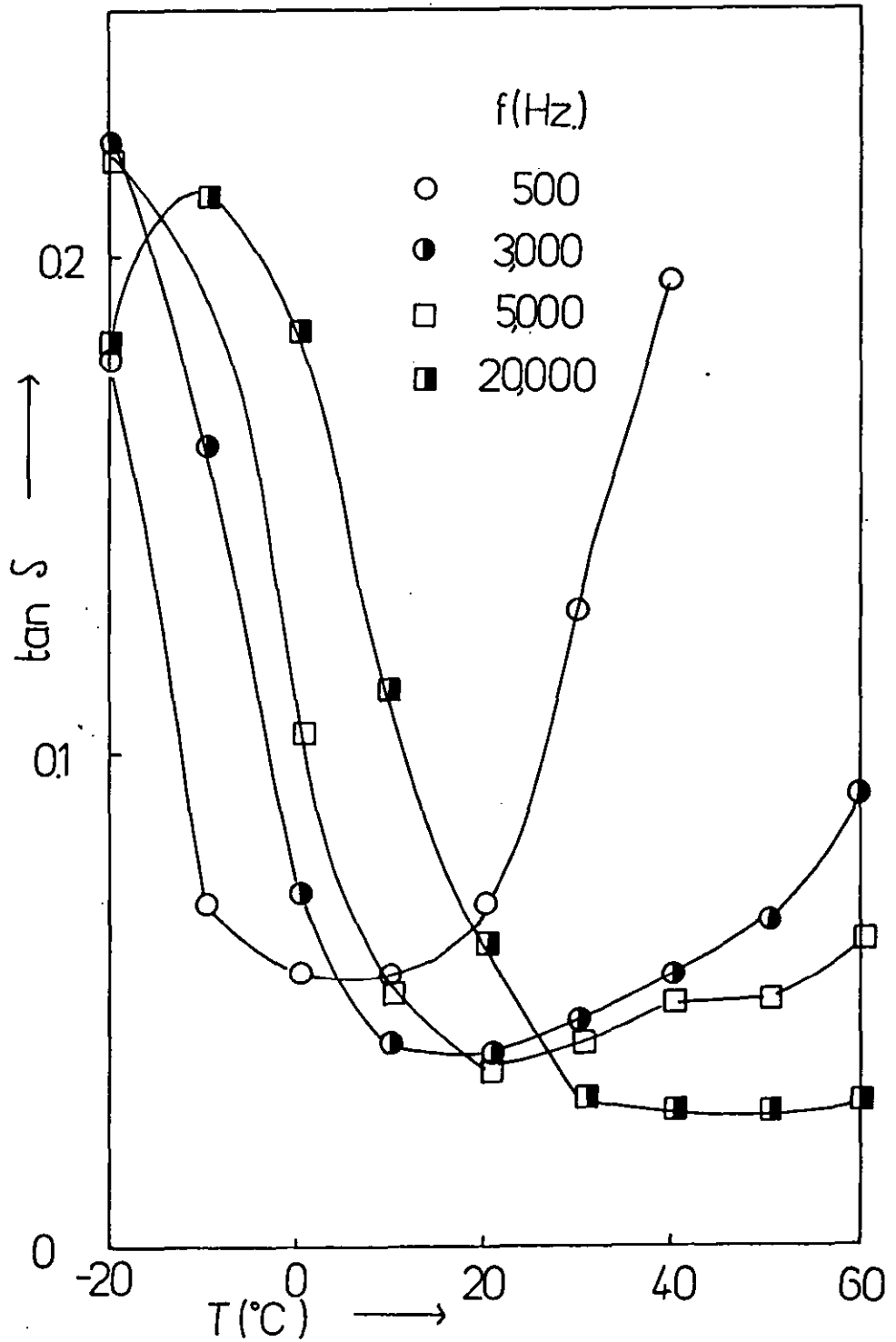


Figure(5.50)

Frequency Dependence of Dielectric Loss at Various Temperatures for PEPC



Figure(5.51)  
Temperature Dependence of Loss Tangent  
at Various Frequencies for PEPC



the region of  $-10^{\circ}\text{C}$  at 20 KHz which moved to lower temperatures as the frequency decreased.

Type (A) blends, represented by SM4/PEPC exhibited a similar family of dielectric loss curves (Figures (5.52)-(5.53)) to those of PEPC, except that the peaks were less pronounced and occurred at slightly lower frequencies for equivalent temperatures. Consequently the peaks observed in  $\tan \delta$  for this blend, shown in Figure (5.54), occurred at slightly higher temperatures than in PEPC and showed a considerable reduction in peak height.

SM3/PEPC, previously designated a type (B) blend, did not exhibit pronounced maxima in the frequency plane plots of  $\epsilon''$  (Figures (5.55)-(5.56)). However the loss tangent did display a distinct peak in the region of  $40-50^{\circ}\text{C}$ , preceded by a shallow shoulder (Figure (5.57)).

SM9/PEPC (type (C)), although having no maxima in  $\epsilon''$ , displayed a peak in  $\tan \delta$  (Figures (5.58)-(5.60)) at about  $10^{\circ}\text{C}$ , which broadened with increasing frequency.

### 5.3 METHYL METHACRYLATE-CO-METHACRYLONITRILE/POLY(EPICHLOROHYDRIN) BLENDS

#### 5.3.1 Characterisation of Copolymers

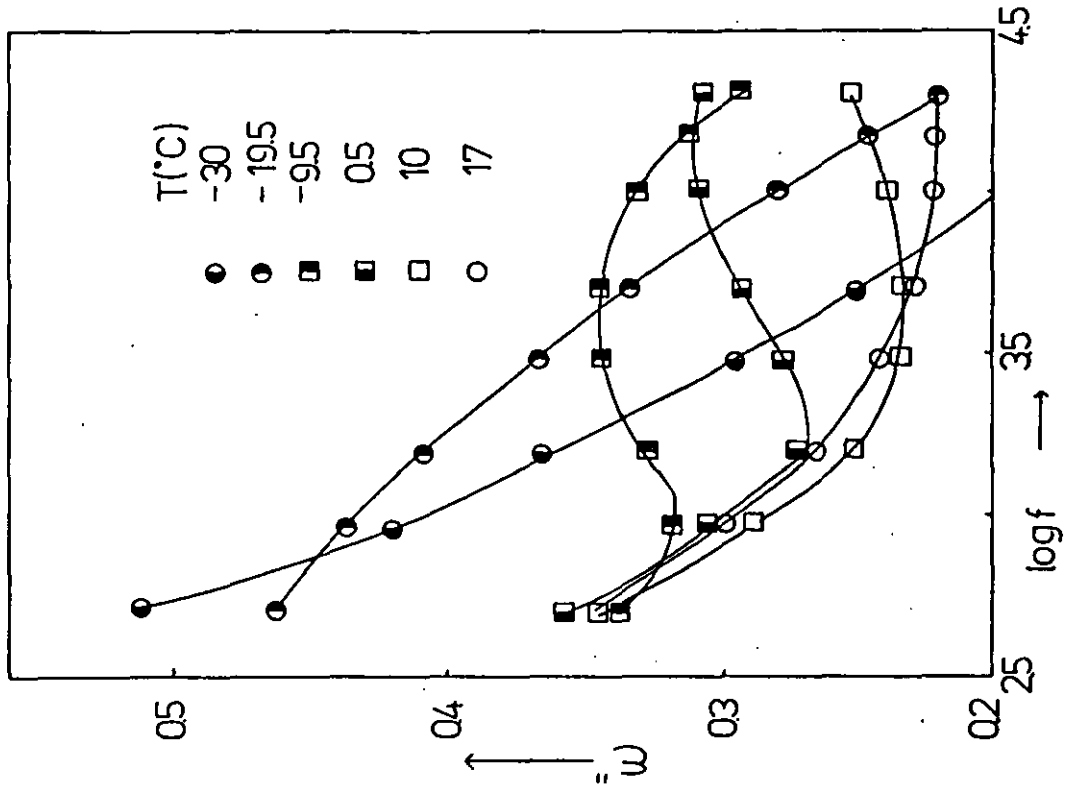
Details of the copolymer molecular weights and copolymer compositions, ascertained as for the styrene-co-methacrylonitrile copolymers, are listed in Table (5.6). Values of the weight and number average molecular weights decreased slightly with increasing methacrylonitrile content. The Kelen-Tudos and Finemann-Ross plots (Figures (5.61) and (5.62)) were both linear over the compositions studied and yielded the same value for the monomer reactivity ratios.

$$r_{\text{MAN}} = 0.68$$

$$r_{\text{MMA}} = 0.71$$

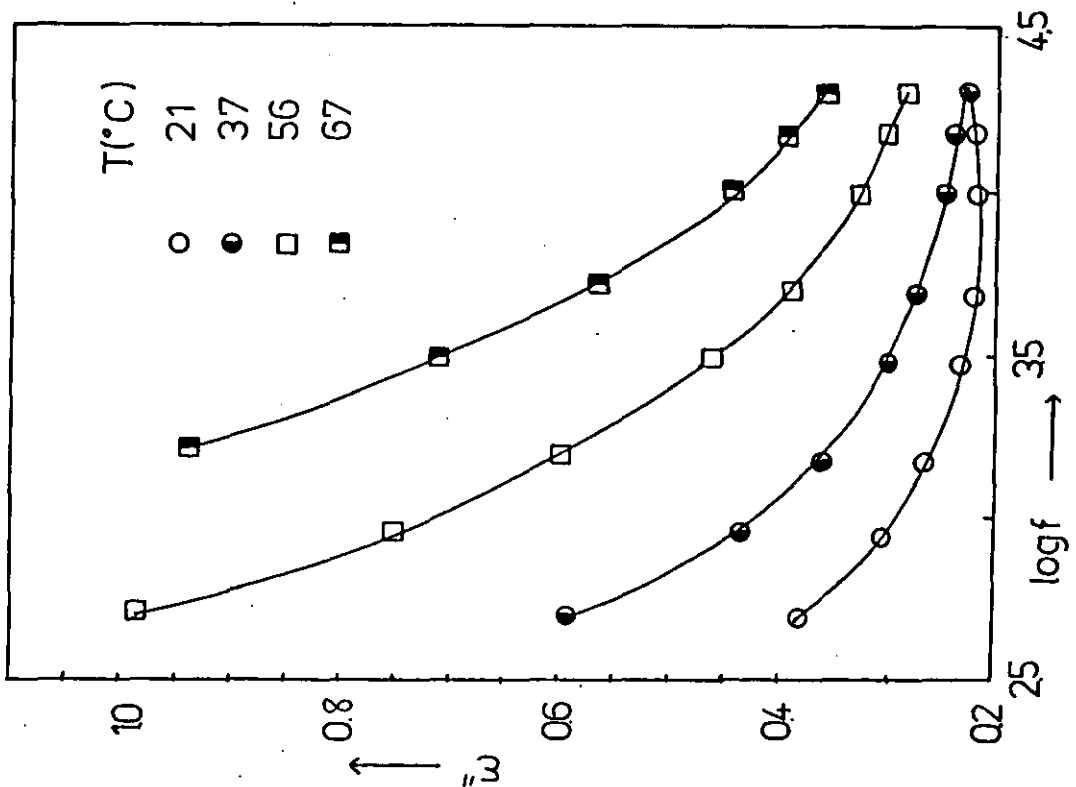
Figure(552)

Variation of Dielectric Loss with Frequency at Various Temperatures for SM4/PEPC



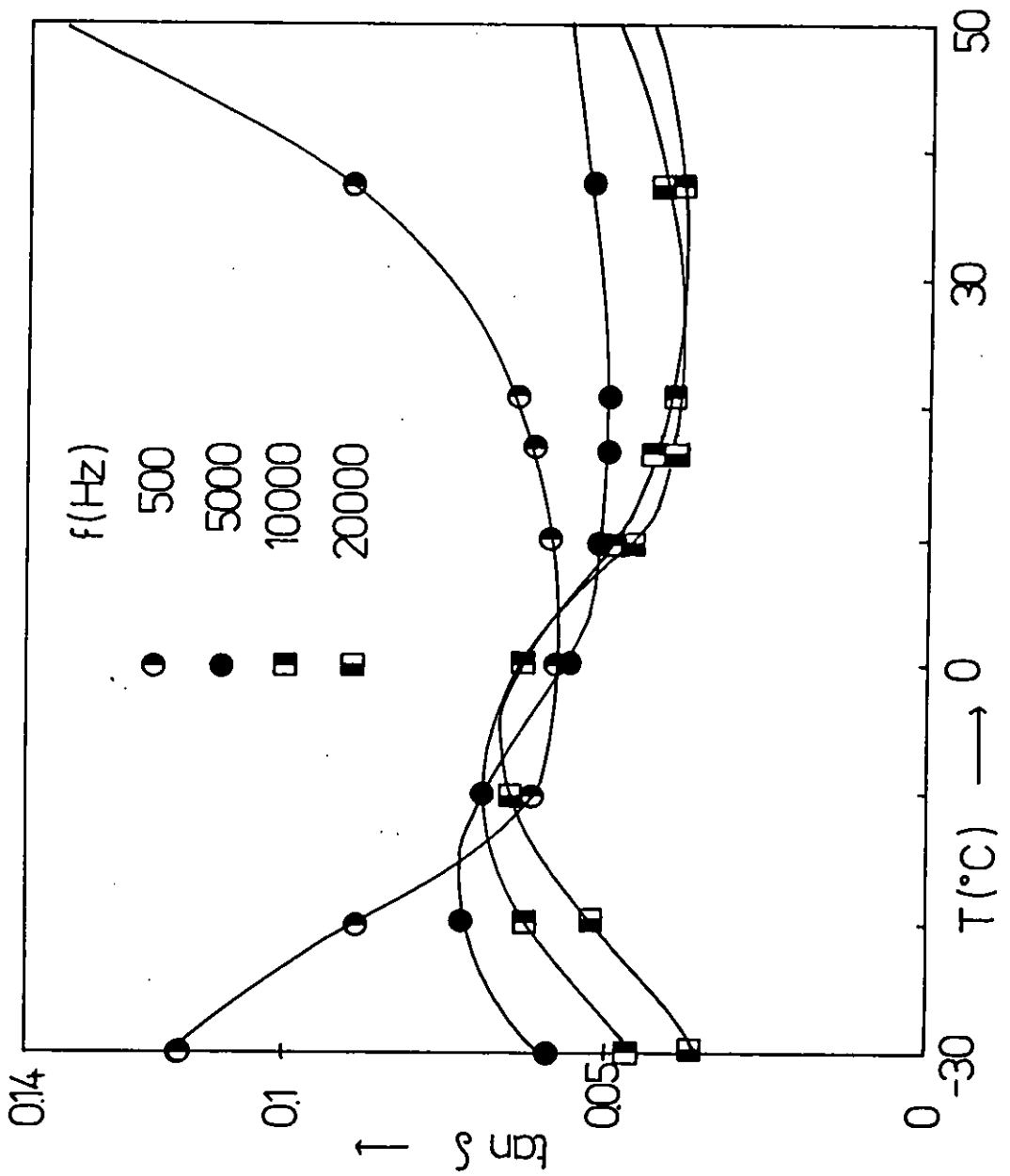
Figure(5.53)

Variation of Dielectric Loss with Frequency at Various Temperatures for SM4/PEPC



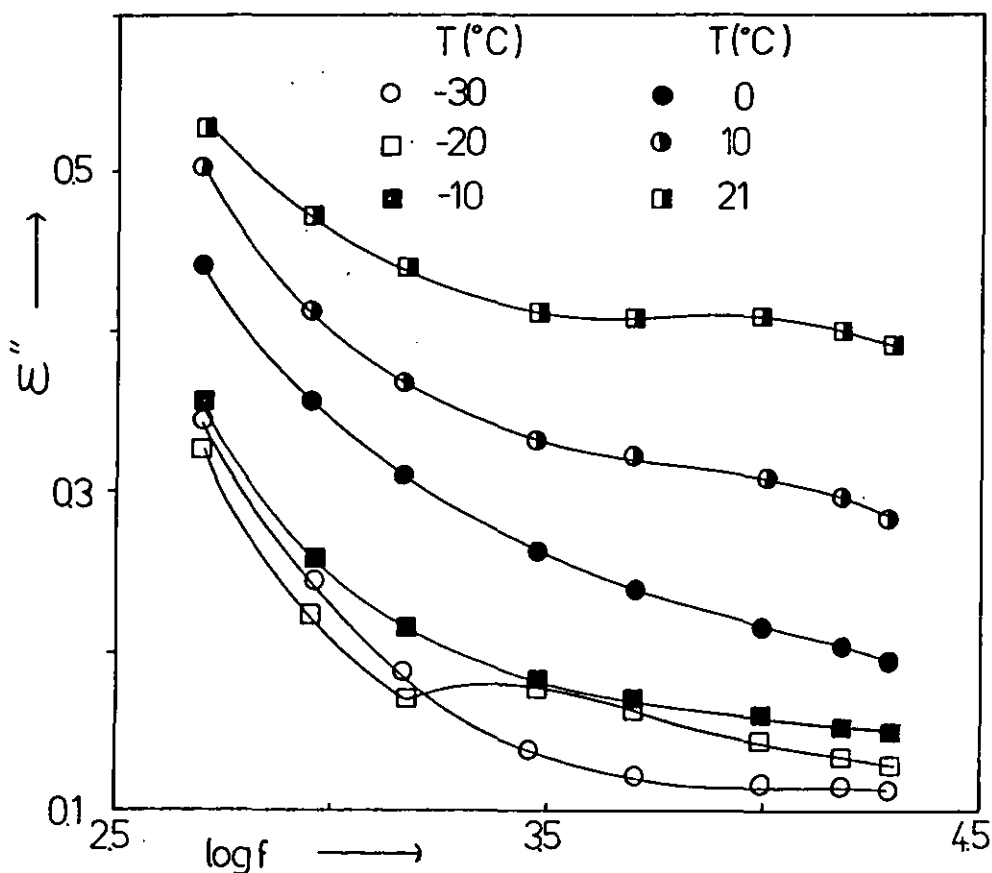
Figure(5.54)

Loss Tangent vs. Temperature Curves at Various Frequencies for SM4/PEPC



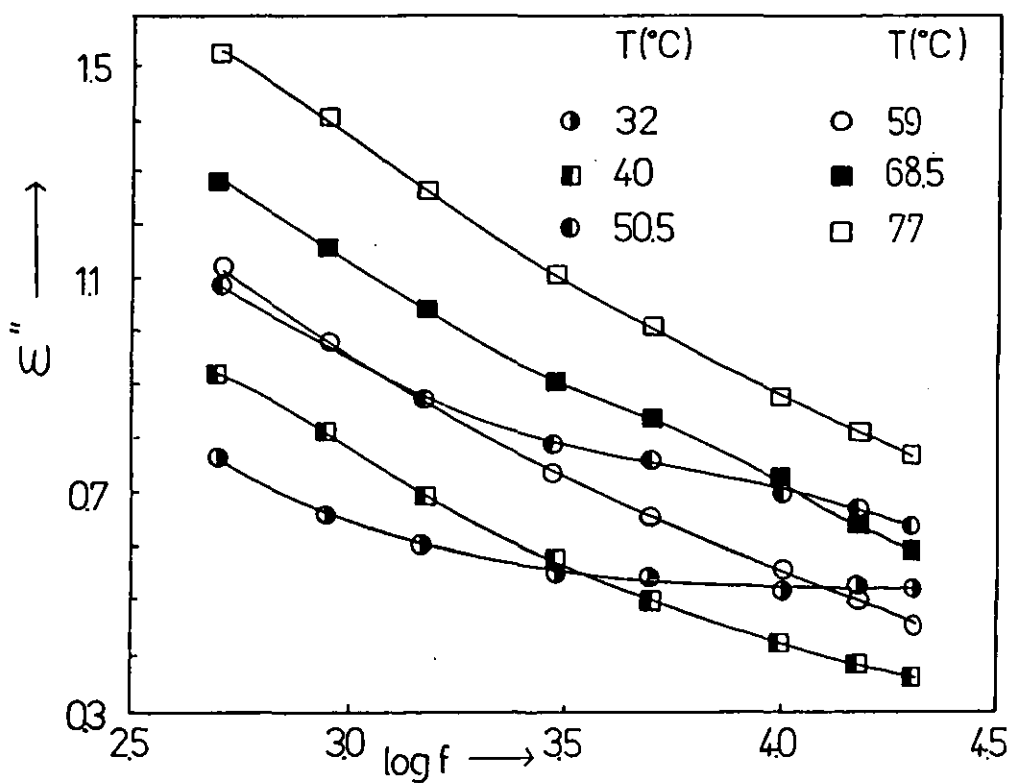
Figure(555)

Frequency Dependence of Dielectric Loss at Various Temperatures for SM3/PEPC



Figure(556)

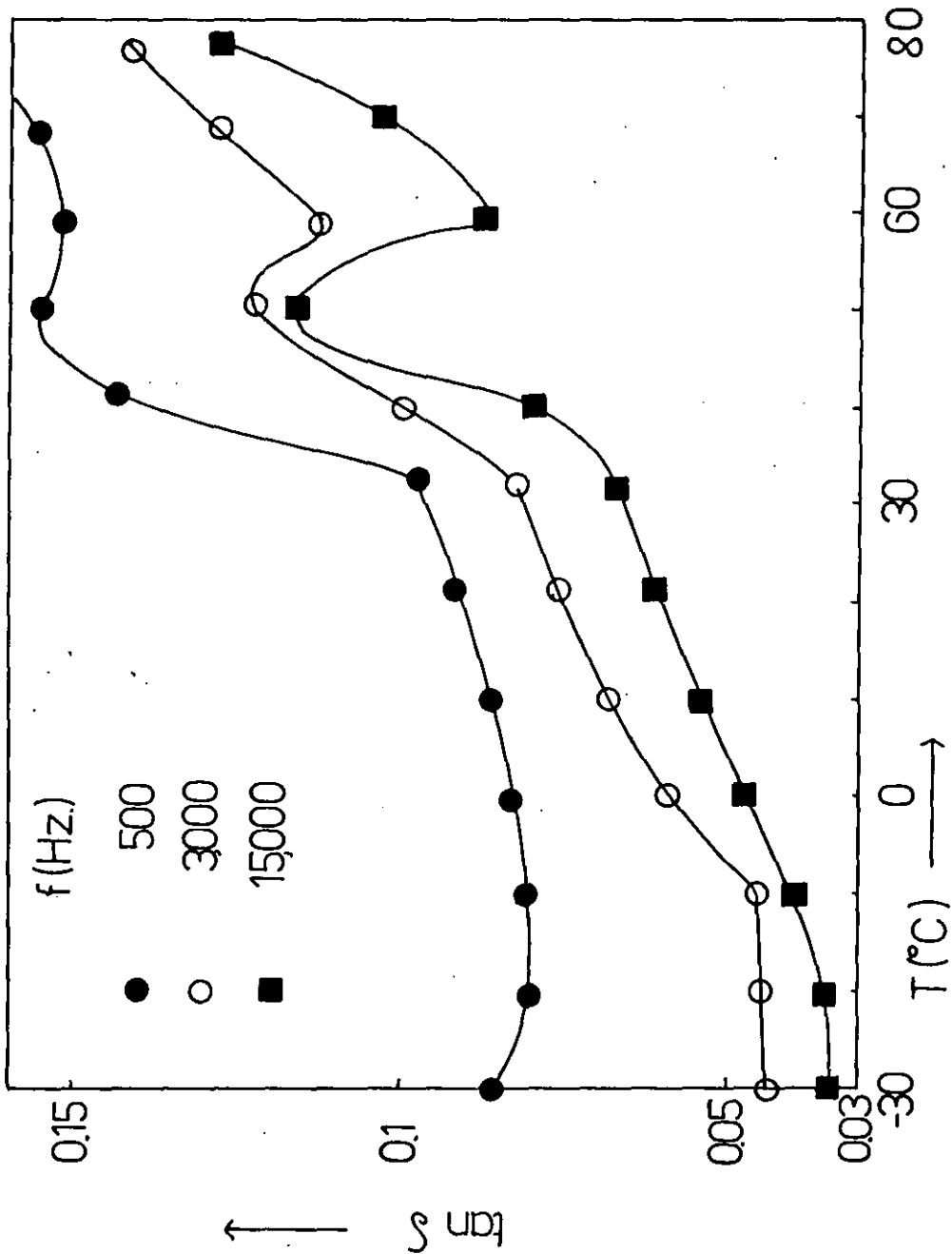
Frequency Dependence of Dielectric Loss at Various Temperatures for SM3/PEPC





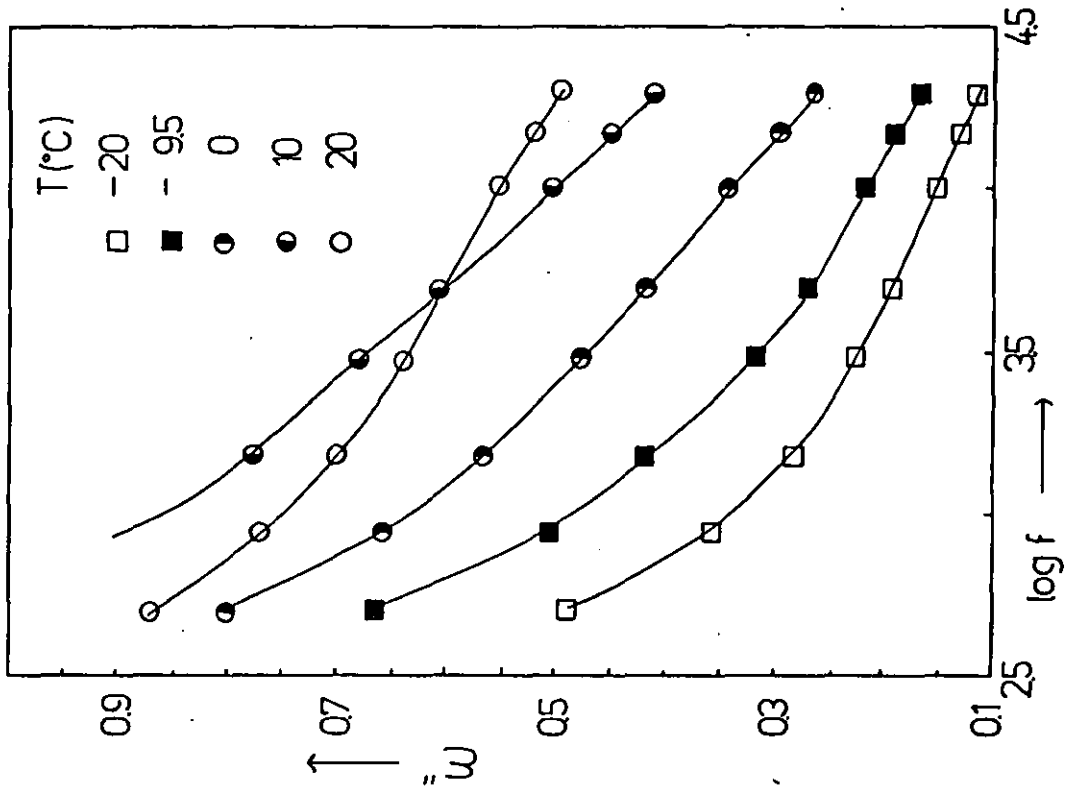
Figure(5.57)

Loss Tangent vs. Temperature Curves at Various Frequencies for SM3/PEPC



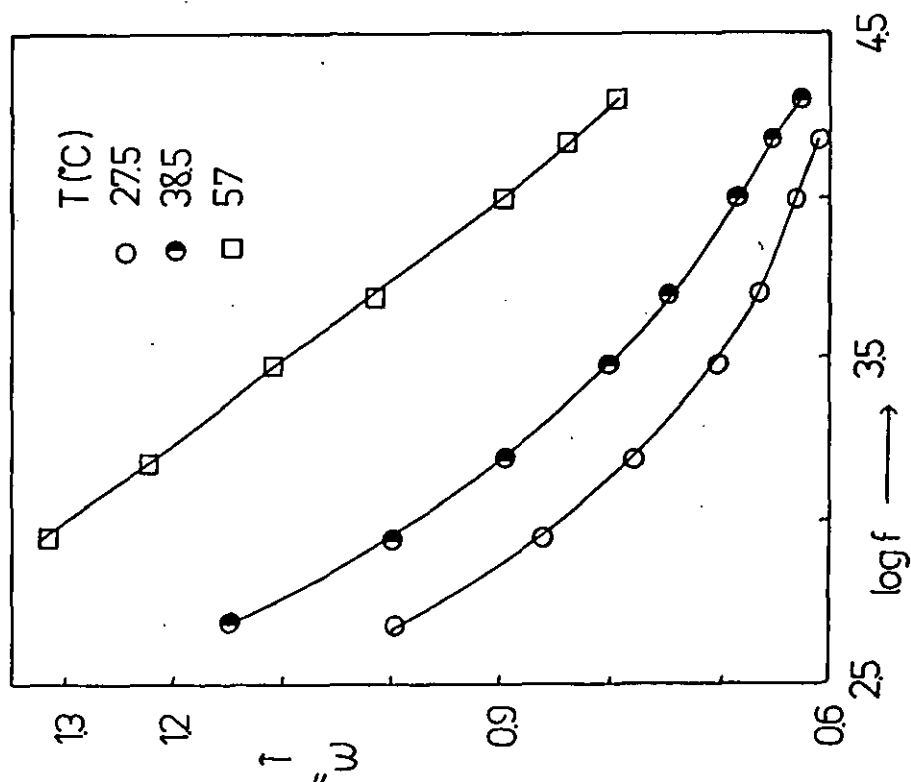
Figure(558)

Variation of Dielectric Loss at Various Temperatures with Frequency for SM9/PEPC



Figure(559)

Variation of Dielectric Loss with Frequency at Various Temperatures for SM9/PEPC



Figure(5.60)

Loss Tangent vs. Temperature Curves for SM9/PEPC at Selected Frequencies

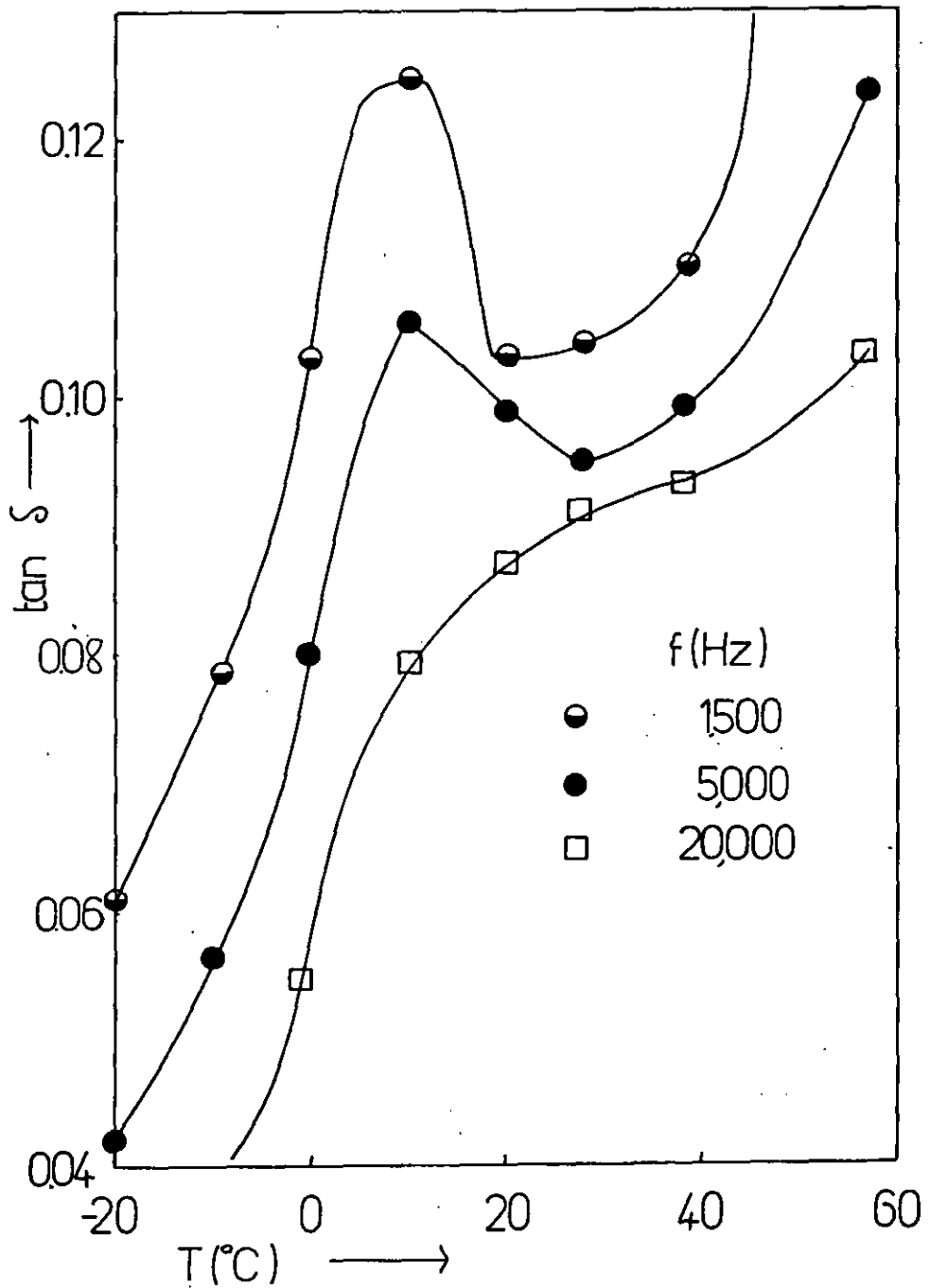
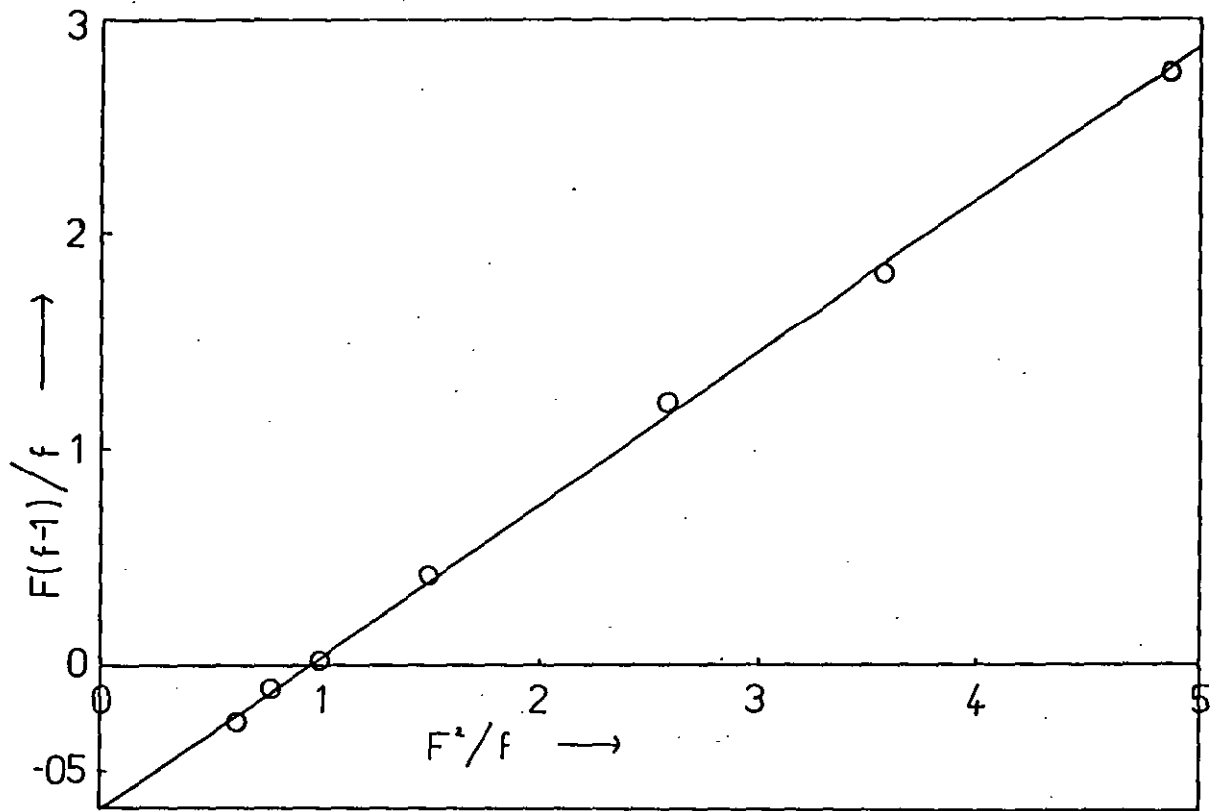


Table 5.6. Molecular Weights and Compositions of MA Copolymers

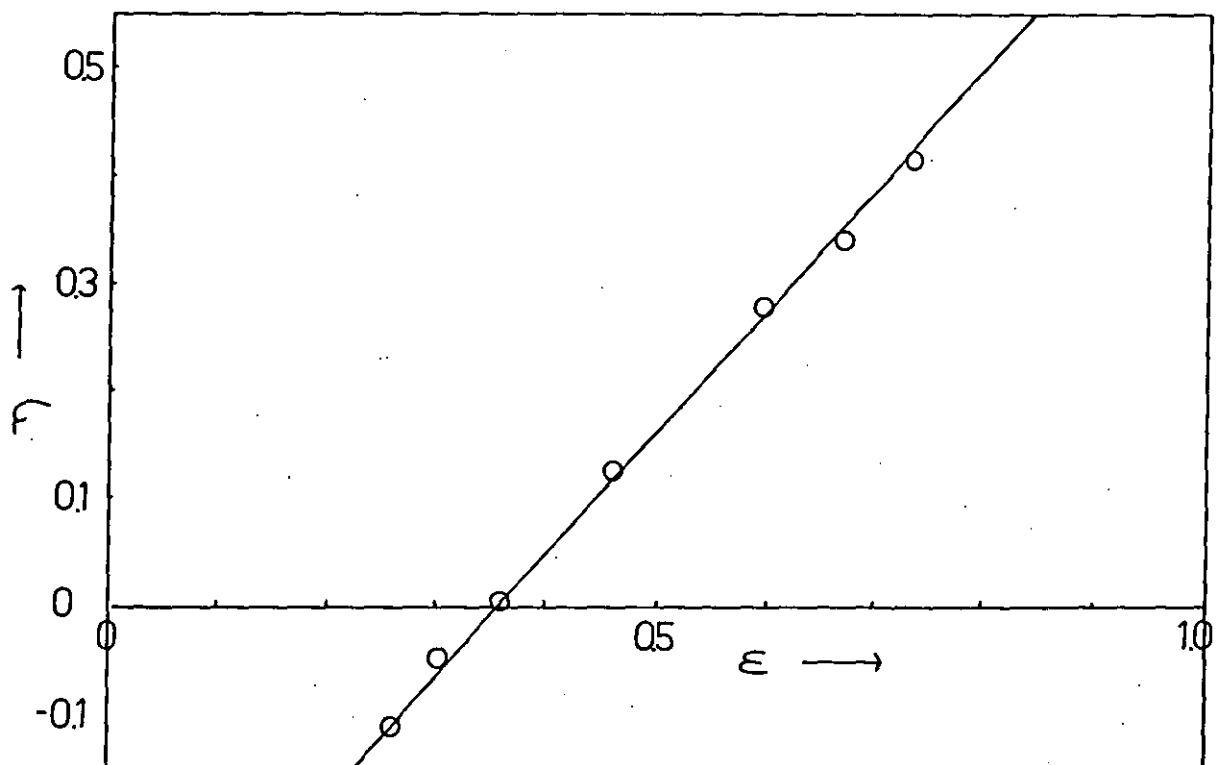
Copolymer	Feed Composition (Mole % MAN)	Copolymer Composition (Mole % MAN)	$\bar{M}_w$	$\bar{M}_n$	$\bar{M}_w/\bar{M}_n$
MA8	20.08	23.55	90,437	47,850	1.89
MA7	24.90	28.29	87,630	47,885	1.83
MA4	30.04	32.30	86,085	47,905	1.80
MA3	40.79	41.65	73,300	43,655	1.68
MA5	49.85	49.59	71,510	44,142	1.62
MA6	54.98	53.45	68,360	43,266	1.58
MA2	59.88	58.16	63,012	40,682	1.55

Figure(561)  
Fineman-Ross Analysis of MA Copolymers



Figure(562)

Kelen-Tudos Plot for MA Copolymers



The number average sequence lengths and sequence length distributions were calculated using these  $r$  values for each copolymer, and the results are listed in Table (5.7).

### 5.3.2 Optical Properties of Blends

The optical clarity of blends of the various copolymers with PEPC is summarised in Figure (5.63). All films were cast from solutions in 1,4-dioxane. The blends appeared transparent over the complete concentration range until the methacrylonitrile content reached  $\approx$  50 mole%. Optical clarity was found to be independent of temperature up to at least 200°C.

### 5.3.3 Thermal Analysis of MAN-co-MMA/PEPC Blends

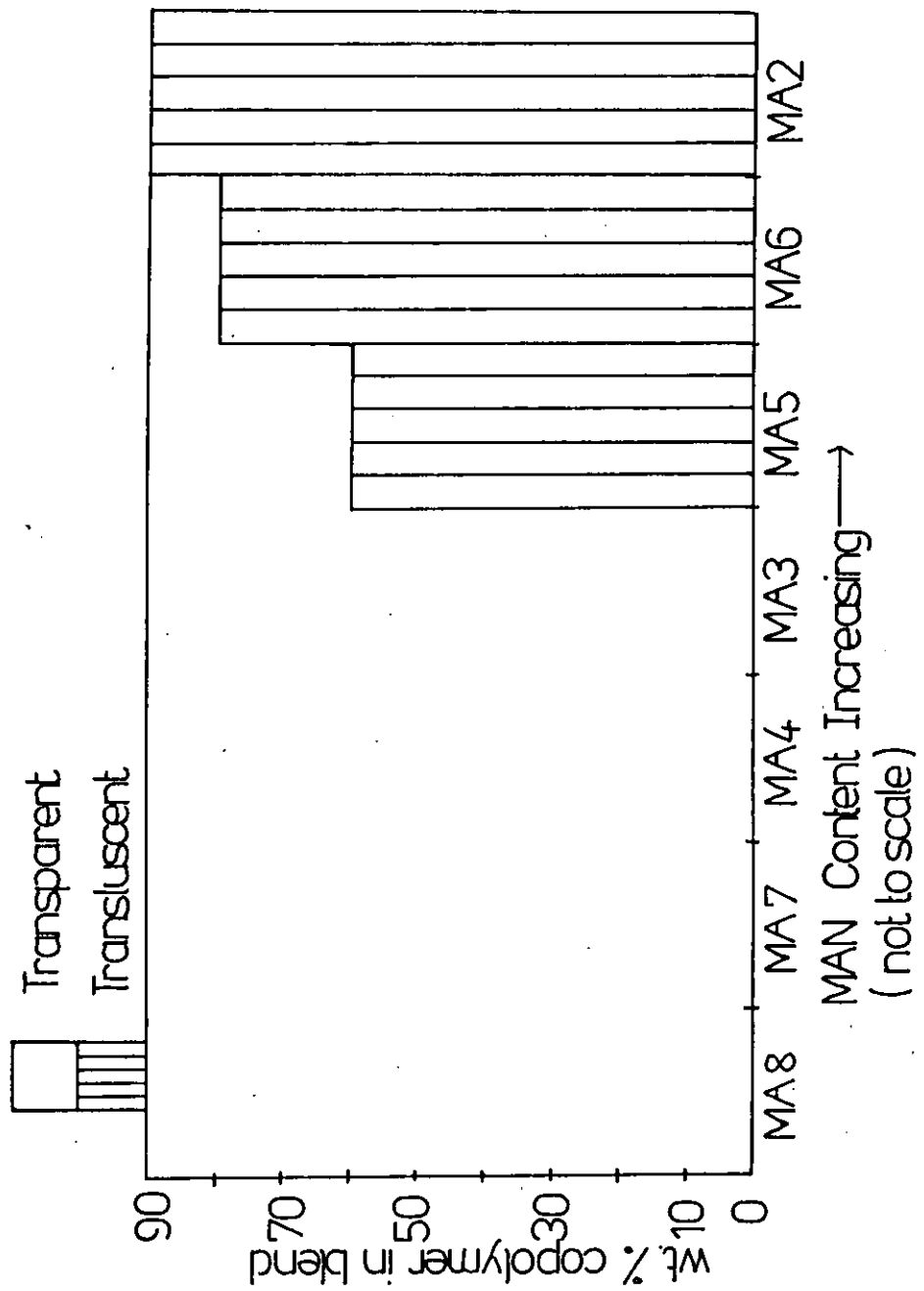
The glass transition temperatures of the various copolymers are plotted against composition in Figure (5.64). The maximum deviation from the value predicted by the Fox relationship was 1.5°C. The thermograms measured for blends of the various copolymers with PEPC are reproduced to demonstrate the essential features in Figures (5.65)-(5.70). Classifying the results in terms of the three categories defined in section (5.2.3), type (A) behaviour was demonstrated by MA6, MA2 and PMMA. Type (B) behaviour was only observed in blends of MA4, leaving blends of the remaining four copolymers to reside in category (C). However these blends did not display identical characteristics and it appeared that some blends had features similar to those displayed by blends of types A and B. Thus blends of MA3 exhibited a clearly composition dependent, if somewhat broadened, glass transition whilst blends of MA8 displayed 2 transitions which were almost independent of composition but also contained a third transition of intermediate composition.

Table 5.7. Sequence Length Distributions of MA Copolymers

		MA8		MA7		MA4		MA3		MA5		MA6		MA2	
		MAN	MMA	MAN	MMA	MAN	MMA	MAN	MMA	MAN	MMA	MAN	MMA	MAN	MMA
Number Average Sequence Length - $\bar{n}$		1.17	3.83	1.22	3.14	1.29	2.65	1.38	2.03	1.68	1.72	1.83	1.58	2.01	1.48
Mole Percentage of Particular Repeat Unit in Sequences X Units Long	X														
	1	85.4	26.1	81.6	31.8	77.4	37.7	68.1	49.3	59.7	58.3	54.6	63.2	49.6	67.8
	2	12.5	19.3	15.0	21.7	17.5	23.5	21.7	25.0	24.1	24.3	24.8	23.2	25.0	21.8
	3	1.8	14.3	2.8	14.8	4.0	14.6	6.9	12.7	9.7	10.1	11.2	8.5	12.6	7.0
	4	0.3	10.5	0.5	10.1	0.9	9.1	2.2	6.4	3.9	4.2	5.1	3.1	6.3	2.3
	5	0.0	7.8	0.1	6.9	0.2	5.7	0.7	3.3	1.6	1.8	2.3	1.2	3.2	0.7
	6	0.0	5.8	0.0	4.7	0.0	3.5	0.2	1.7	0.6	0.7	1.1	0.4	1.6	0.2

Figure (5.63)

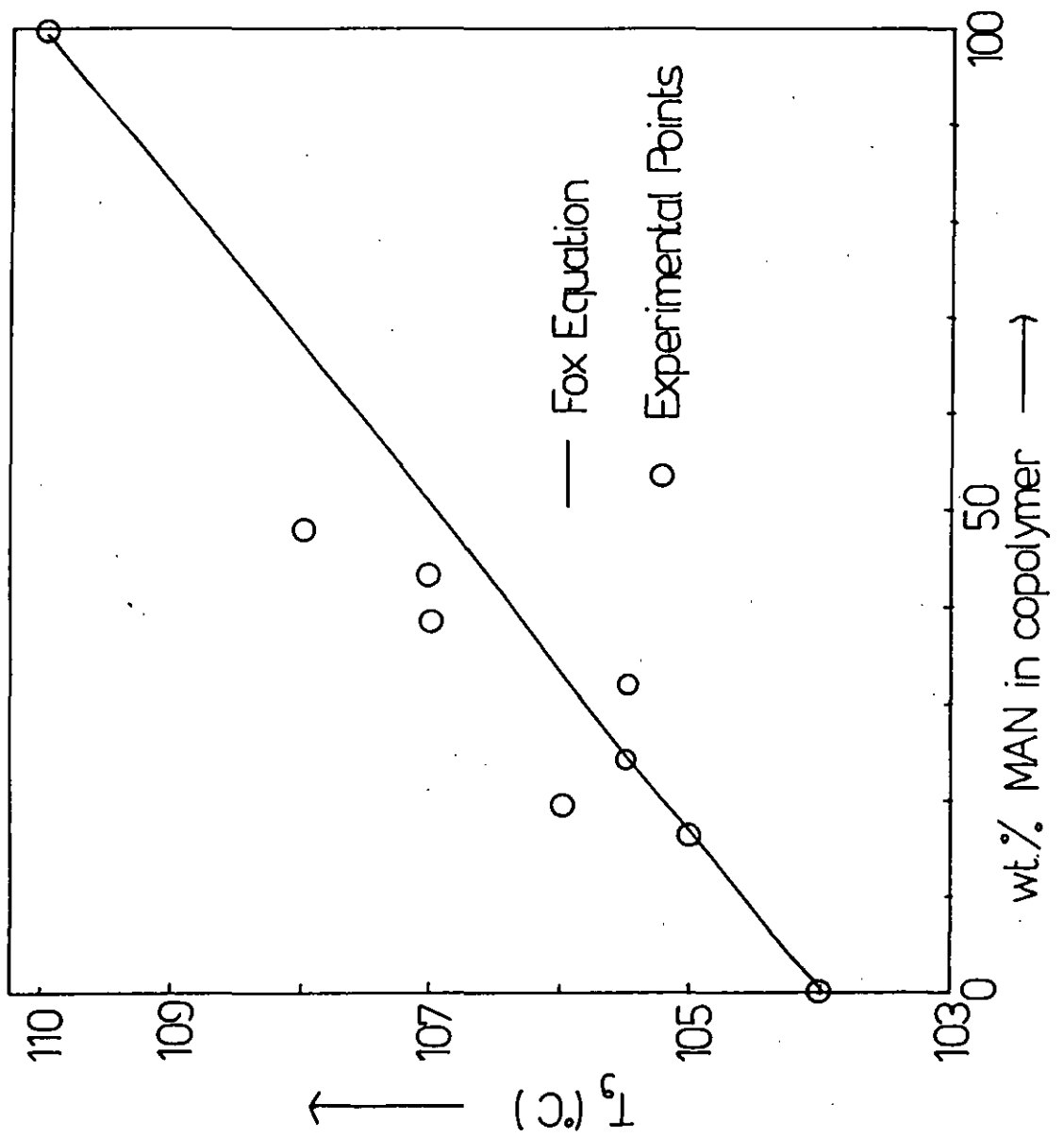
Variation of the Optical Properties of MA/PEPC Blends with Copolymer and Blend Composition





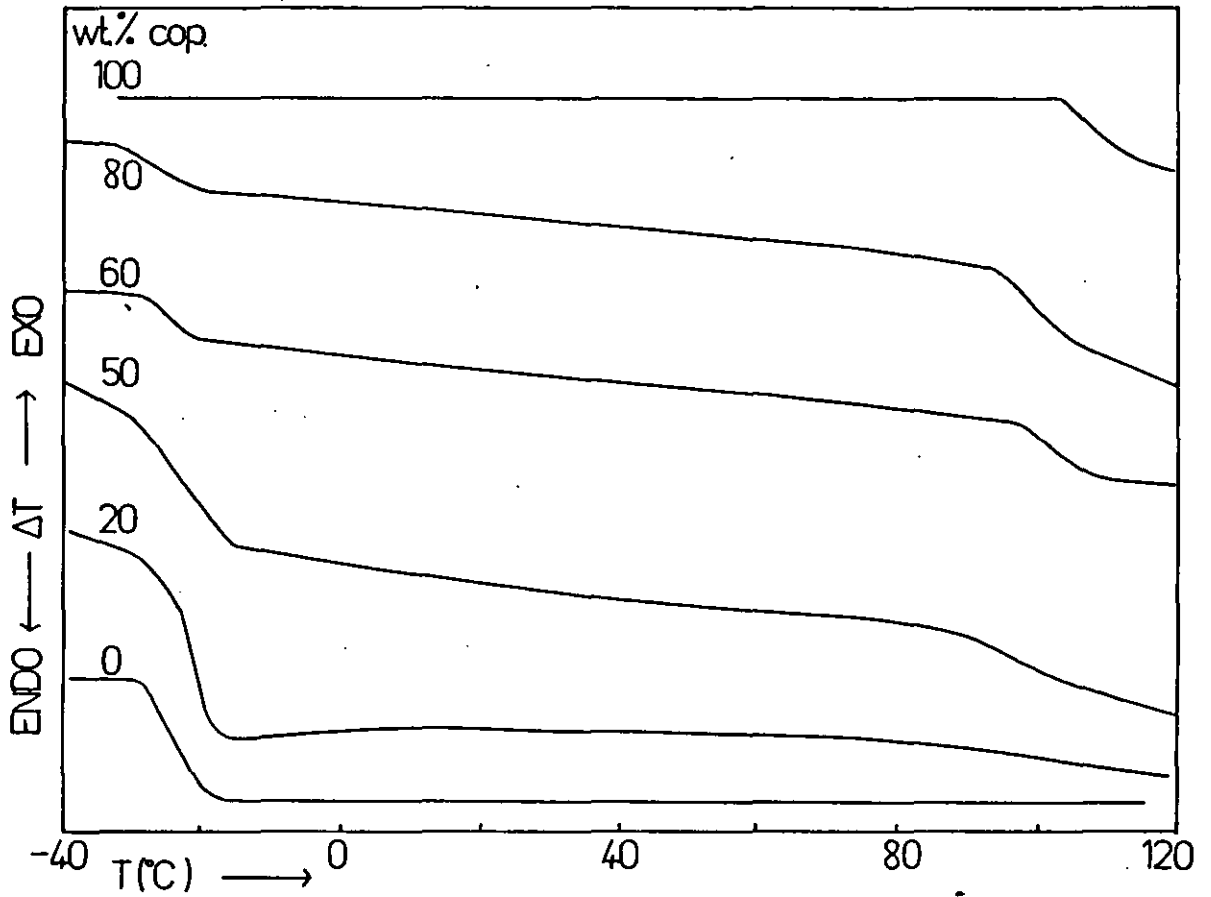
Figure(5.64)

Composition Dependence of  $T_g$  in MA Copolymers  
Measured by D.T.A.



Figure(5.65)

D.T.A. Thermograms for MA6/PEPC Blends



Figure(5.66)

D.T.A. Thermograms for MA4/PEPC Blends

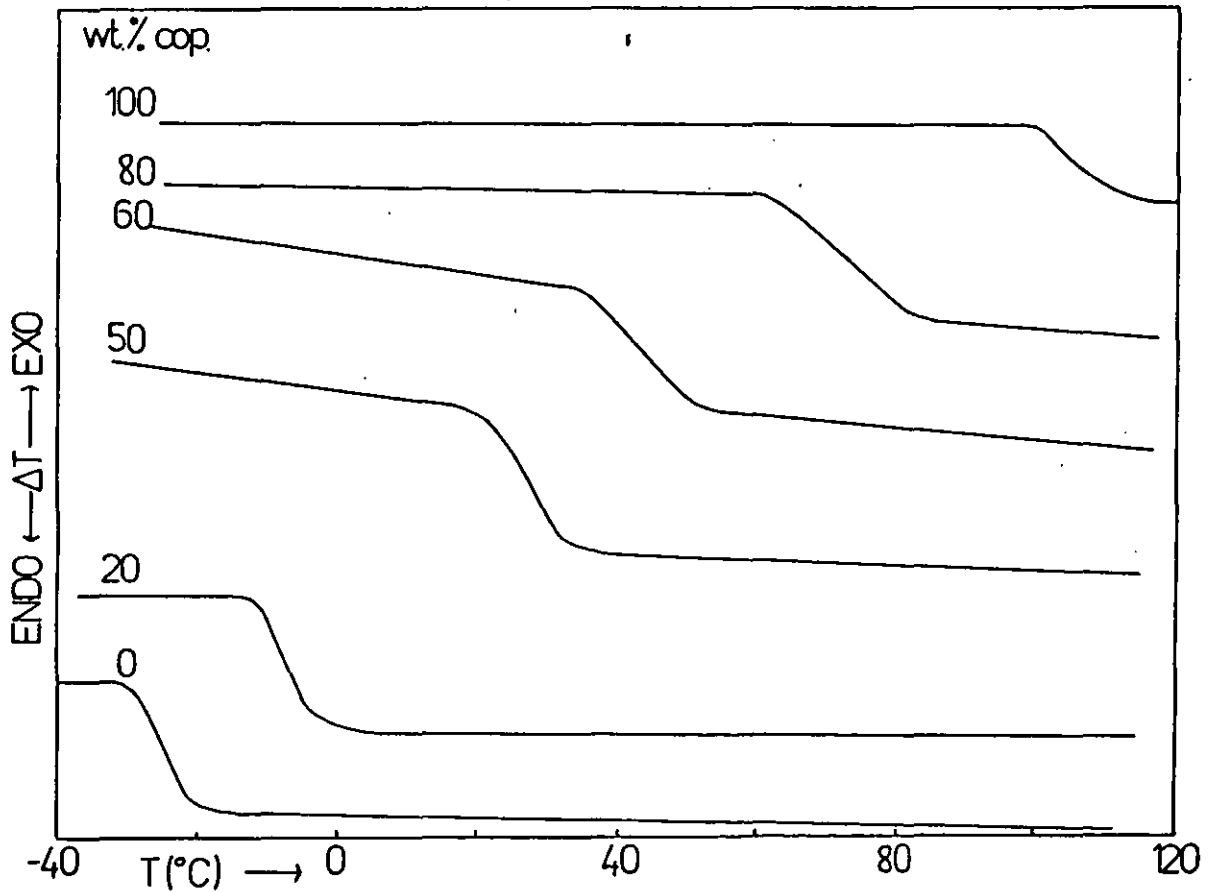
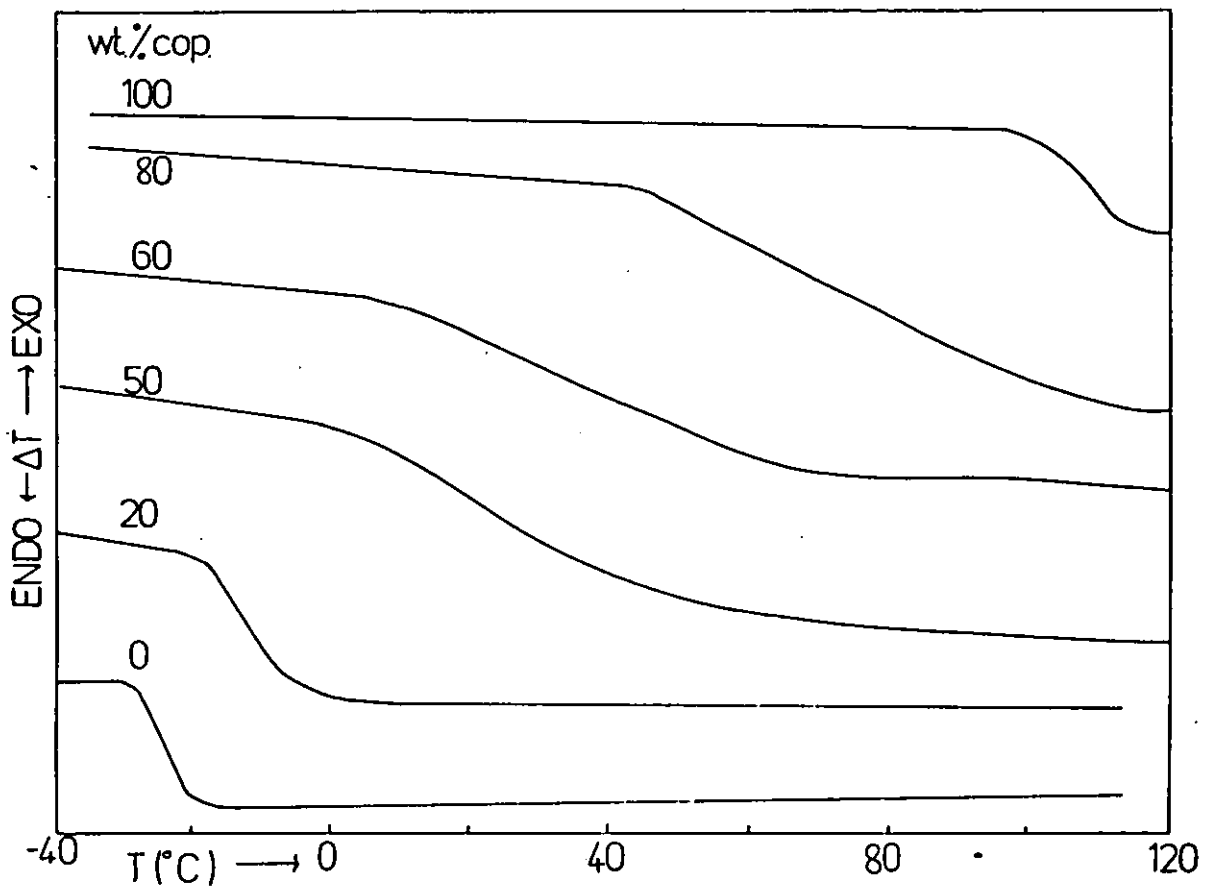


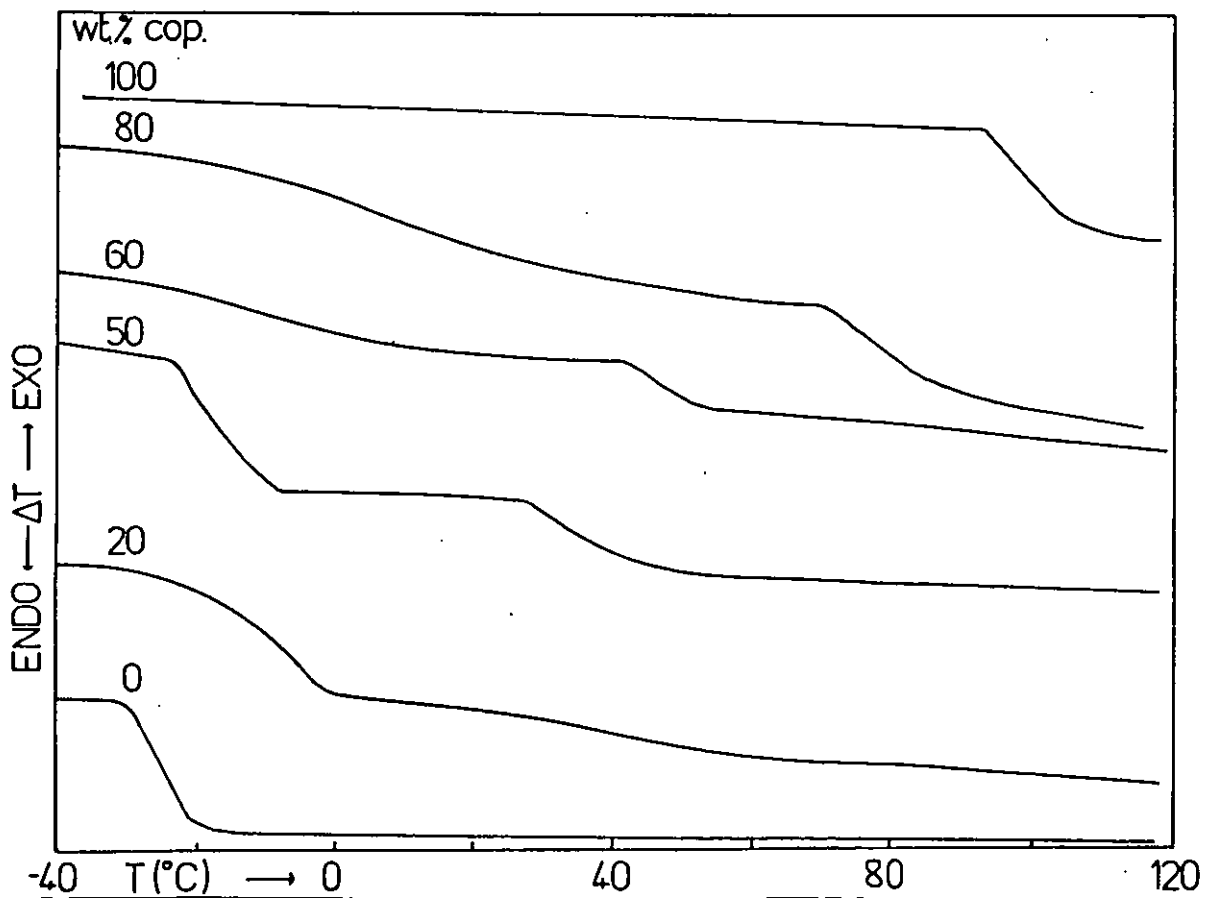
Figure (5.67)

D.T.A. Thermograms for MA3/PEPC Blends

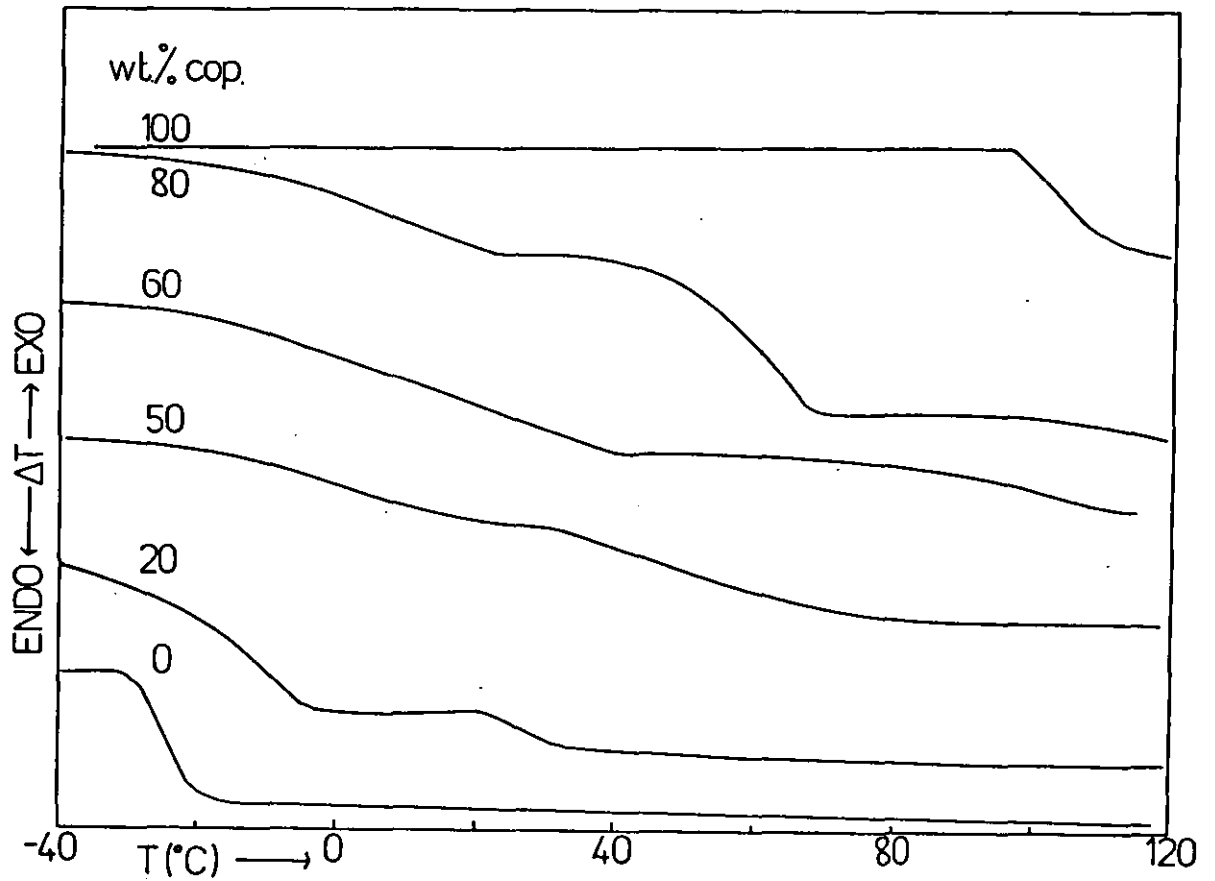


Figure(5.68)

D.T.A. Thermograms for MA8/PEPC Blends

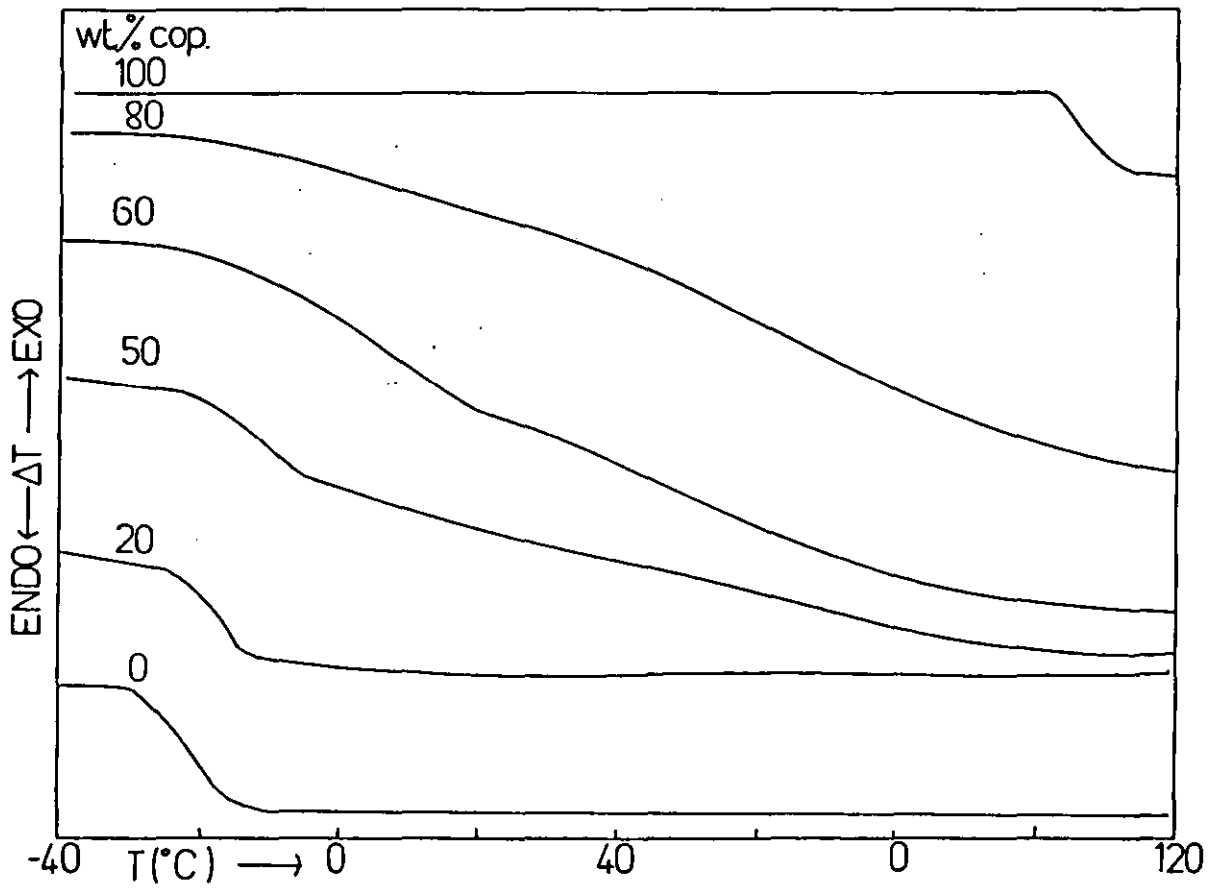


Figure(5.69)  
D.T.A. Thermograms for MA7/PEPC Blends



Figure(5.70)

D.T.A. Thermograms for MA5/PEPC Blends



### 5.3.4 Dynamic Mechanical Results

The pure copolymer glass transition temperatures lay between 111°-113° as indicated by the Fox equation. The classification of the glass transition behaviour of the blends (Figures (5.71)-(5.76)) approximately followed that found by DTA, save for a few notable exceptions. MA5 blends were clearly indicated by DMTA as being of category A rather than C, whilst MA3 blends appeared to be of category B, together with MA4. In the latter case however although the breadths of the loss tangent peaks were similar at equivalent compositions, as shown in Figure (5.77) the two blends exhibited a different composition dependence of  $T_g$  at loadings above 40 wt.% copolymer. The variation in glass transition behaviour with copolymer composition observed by DTA and DMTA is shown schematically in Figure (5.78).

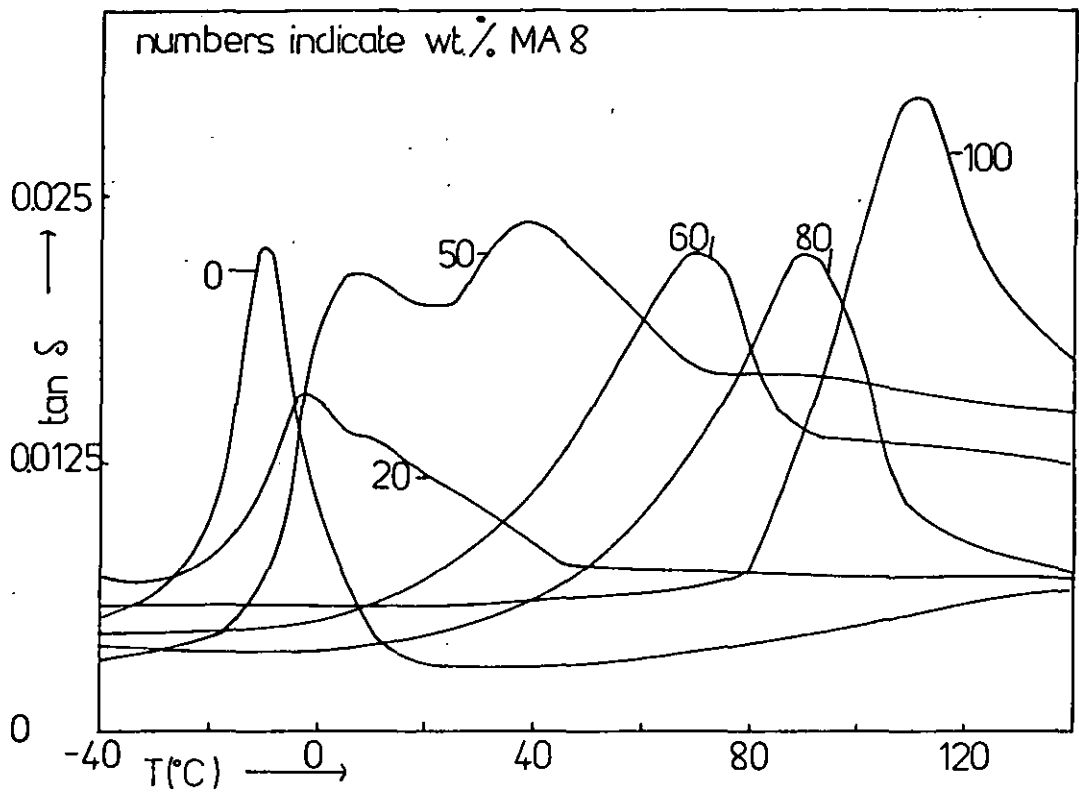
The influence of temperature on the mechanical behaviour of those films yielding a single, sharp relaxation (type B) was studied by annealing cast films of MA4 and MA3 blended with equal weights of PEPC at temperatures between 120-200°C. All samples had previously been annealed at 120°C under vacuum as described in chapter 3. The films were maintained at the elevated temperatures for thirty minutes and were subsequently quenched and analysed using the procedure described in section (4.4.4). Blends of both MA4 and MA3 exhibited loss tangent peaks whose position and breadth were independent of the quench temperature.

### 5.3.5 Dielectric Measurements on Selected MA/PEPC Blends

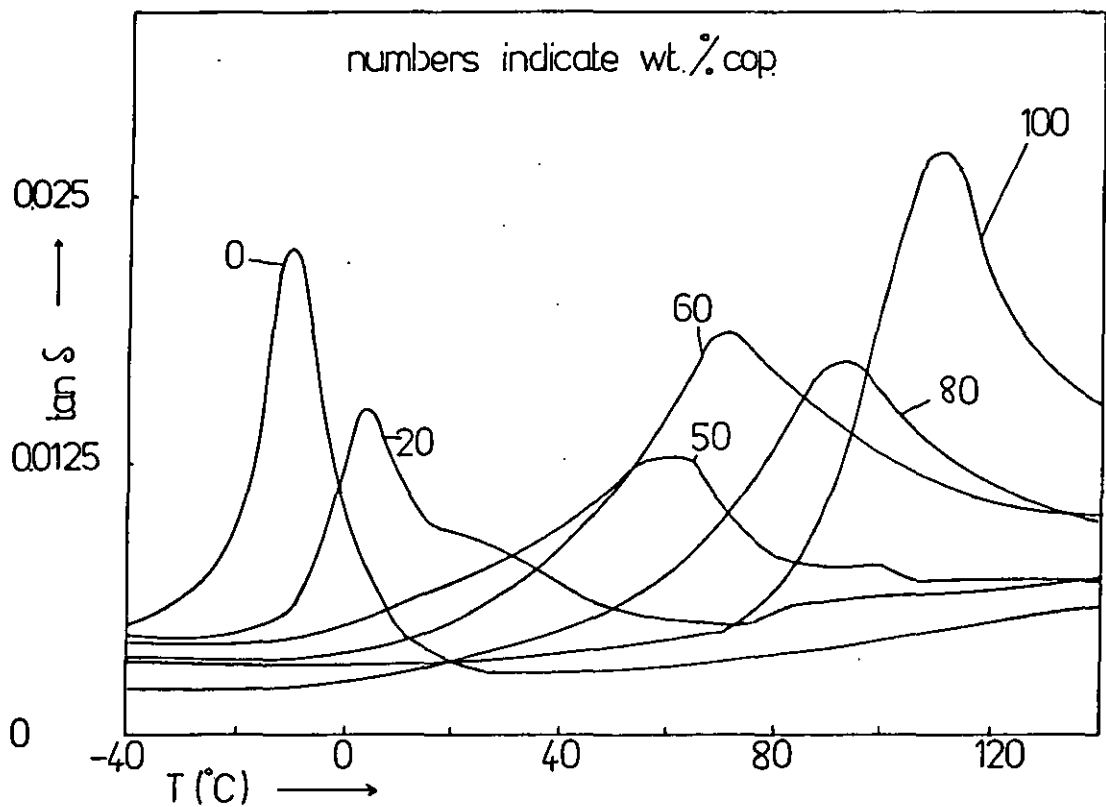
Measurements were made on a few blends, containing equal weights of copolymer and rubber, which represented the three types of miscibility behaviour defined previously.

MA2/PEPC, which has been shown to consist of two distinct phases

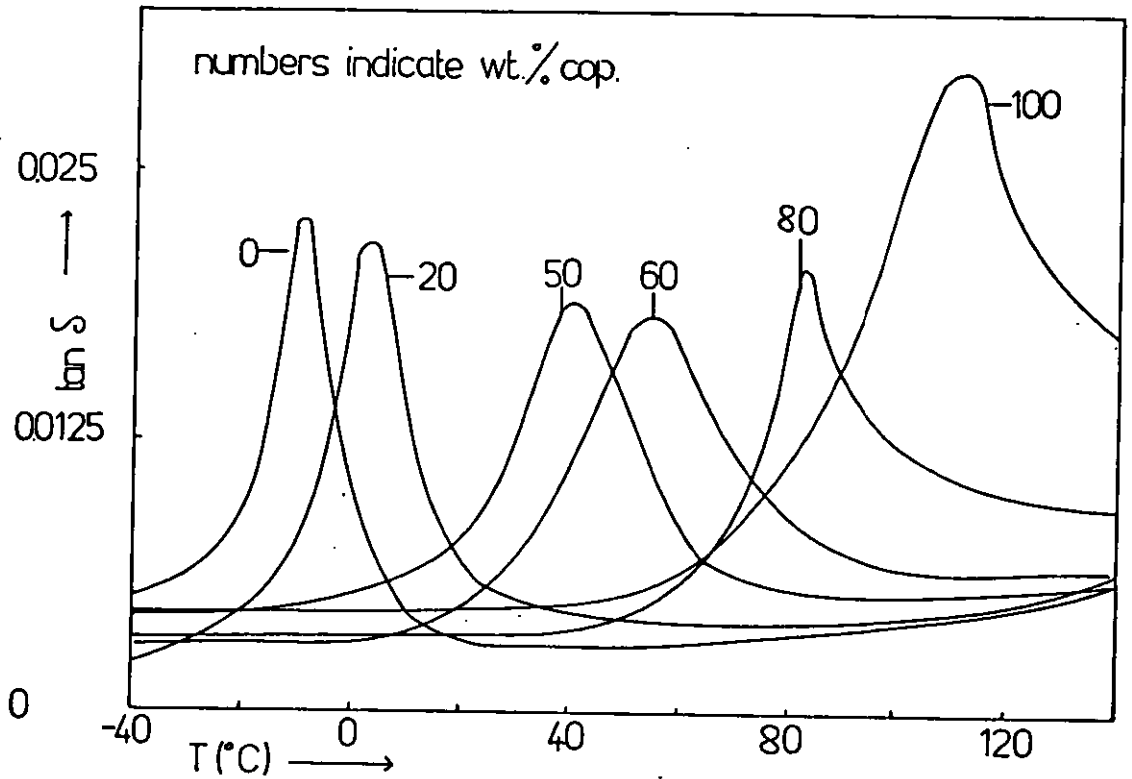
Figure(5.71)  
Loss Tangent vs. Temperature Curves for  
MA8/PEPC Blends



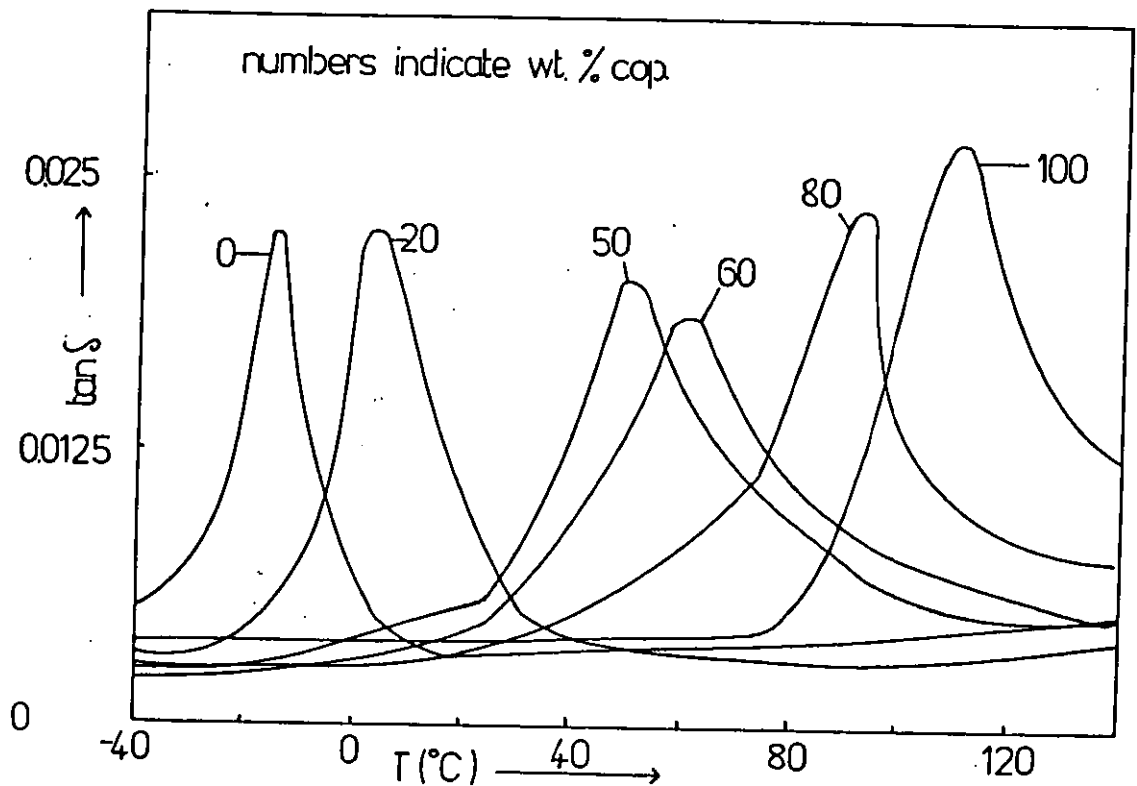
Figure(5.72)  
Loss Tangent vs. Temperature Curves for  
MA7/PEPC Blends



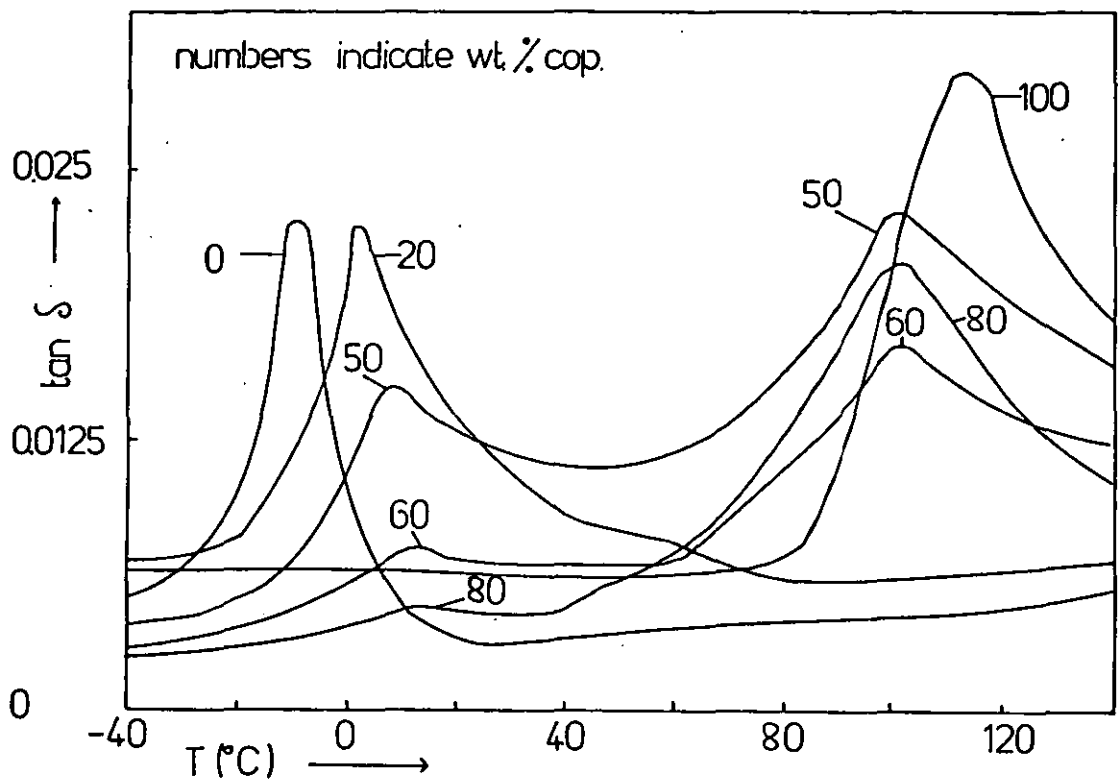
Figure(5.73)  
Loss Tangent vs. Temperature Curves for  
MA4/PEPC Blends



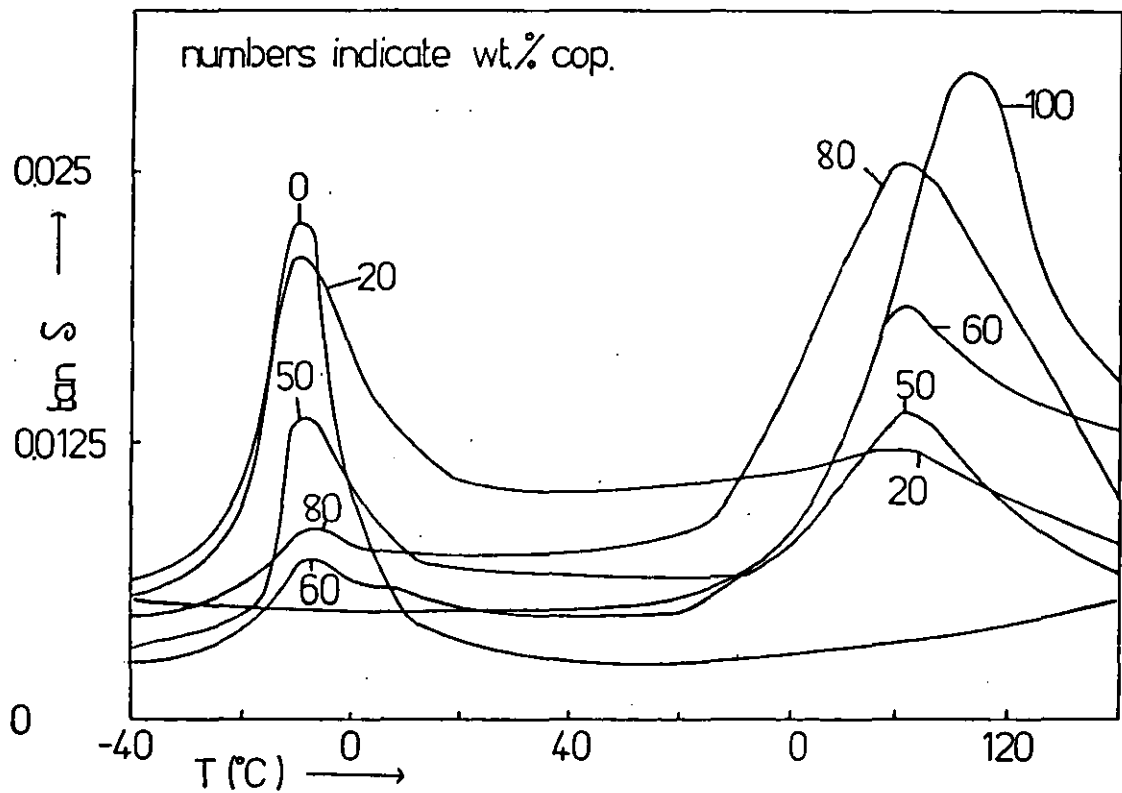
Figure(5.74)  
Loss Tangent vs. Temperature Curves for  
MA3/PEPC Blends



Figure(5.75)  
 Loss Tangent vs. Temperature Curves  
 for MA5/PEPC Blends



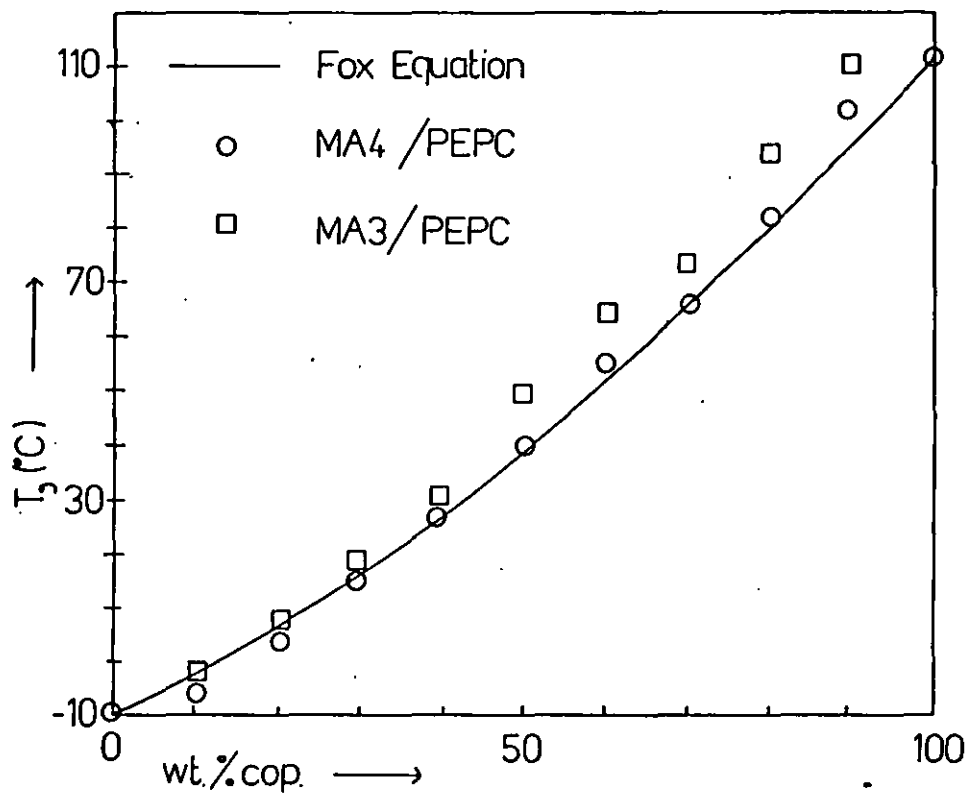
Figure(5.76)  
 Loss Tangent vs. Temperature Curves  
 for MA6/PEPC Blends





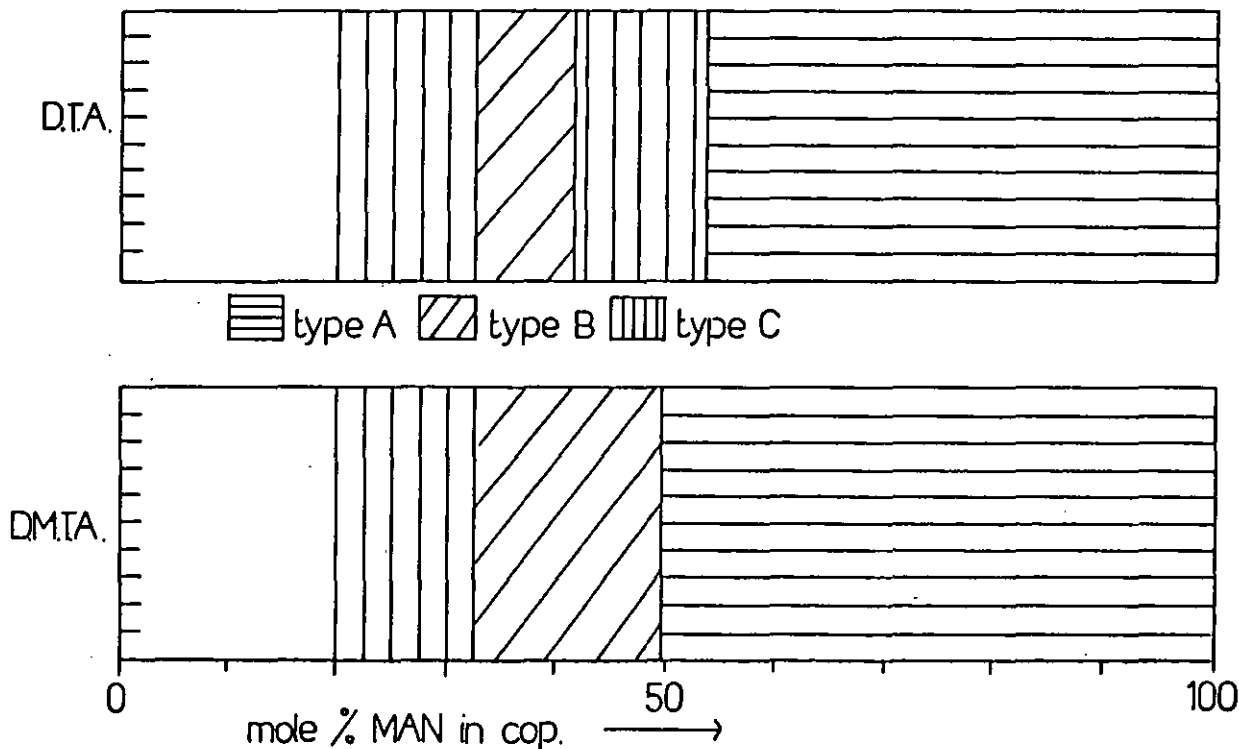
Figure(5.77)

Variation of Blend  $T_g$  with Composition for Blends of MA3 and MA4 with PEPC Measured by DMTA.



Figure(5.78)

Variation of  $T_g$  Behaviour with Copolymer Composition for MA/PEPC Blends



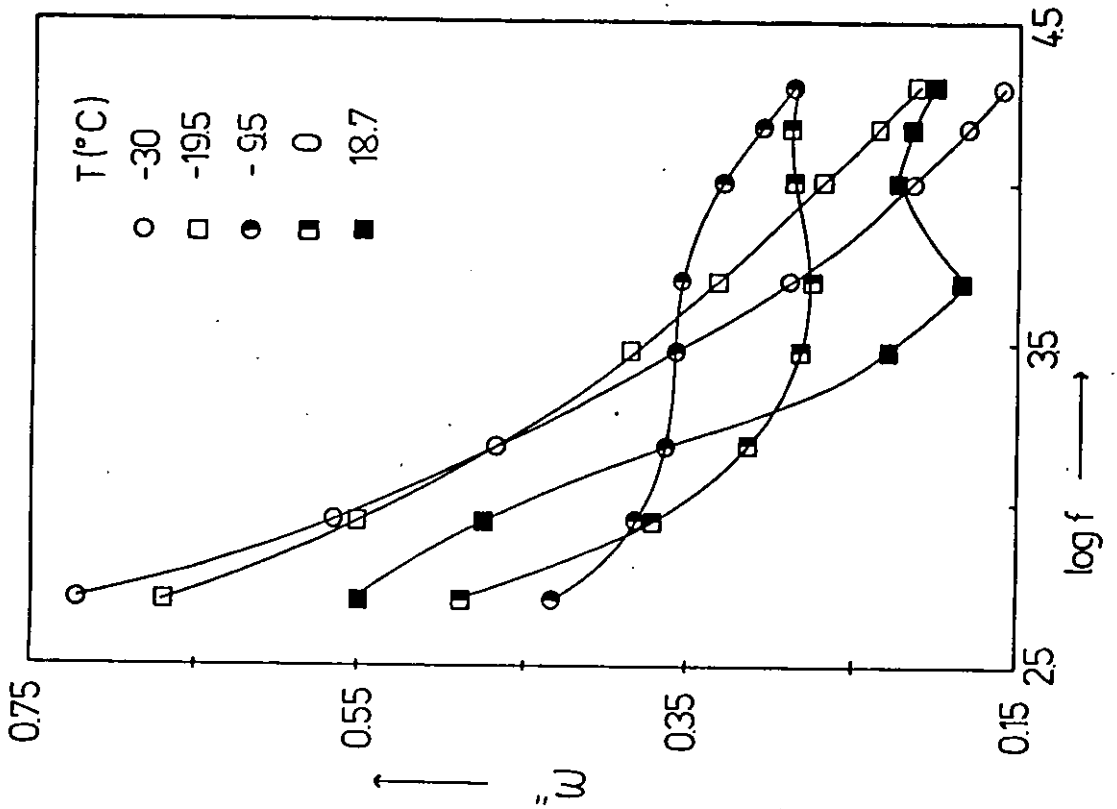
of almost pure copolymer and rubber, exhibited a peak in  $\epsilon''$  between -10 and 20°C as shown in Figures (5.79)-(5.80). This resulted in a loss tangent peak at about -10°C at 20 KHz (Figure (5.81)) as found for PEPC (Figure (5.51)).

MA4/PEPC, found to display a single composition dependent glass transition temperature by both DTA and DMTA, gave rise to dielectric loss plots whose shape did not change significantly with temperature (Figures (5.82)-(5.83)). The corresponding plot of the loss tangent (Figure (5.84)) similarly did not display any identifiable maxima but rose rapidly in the region 0-30°C.

MA5/PEPC (Figure (5.85)) behaved similarly to MA2/PEPC giving rise to a peak in the loss tangent curve (5.86) at 20 KHz, whose position was shifted upfield by some 10°C.

Figure(5.79)

Frequency Dependence of Dielectric Loss at Various Temperatures for MA2/PEPC



Figure(5.80)

Frequency Dependence of Dielectric Loss at Various Temperatures for MA2/PEPC

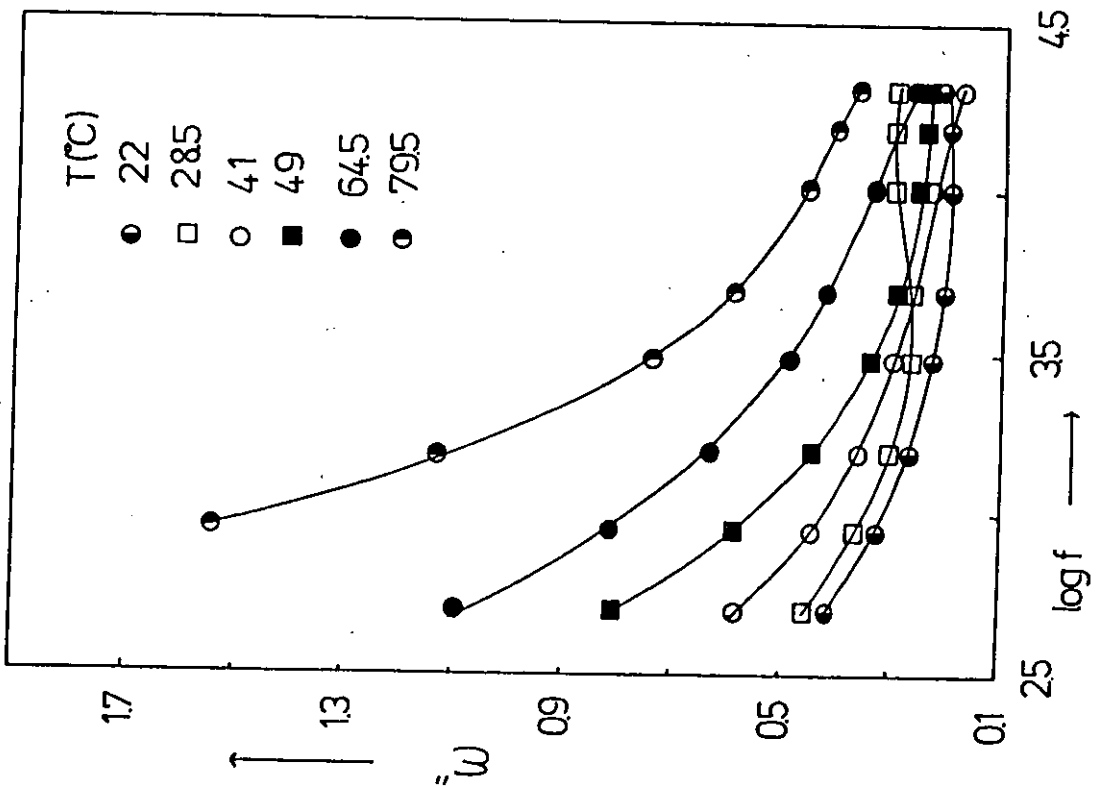
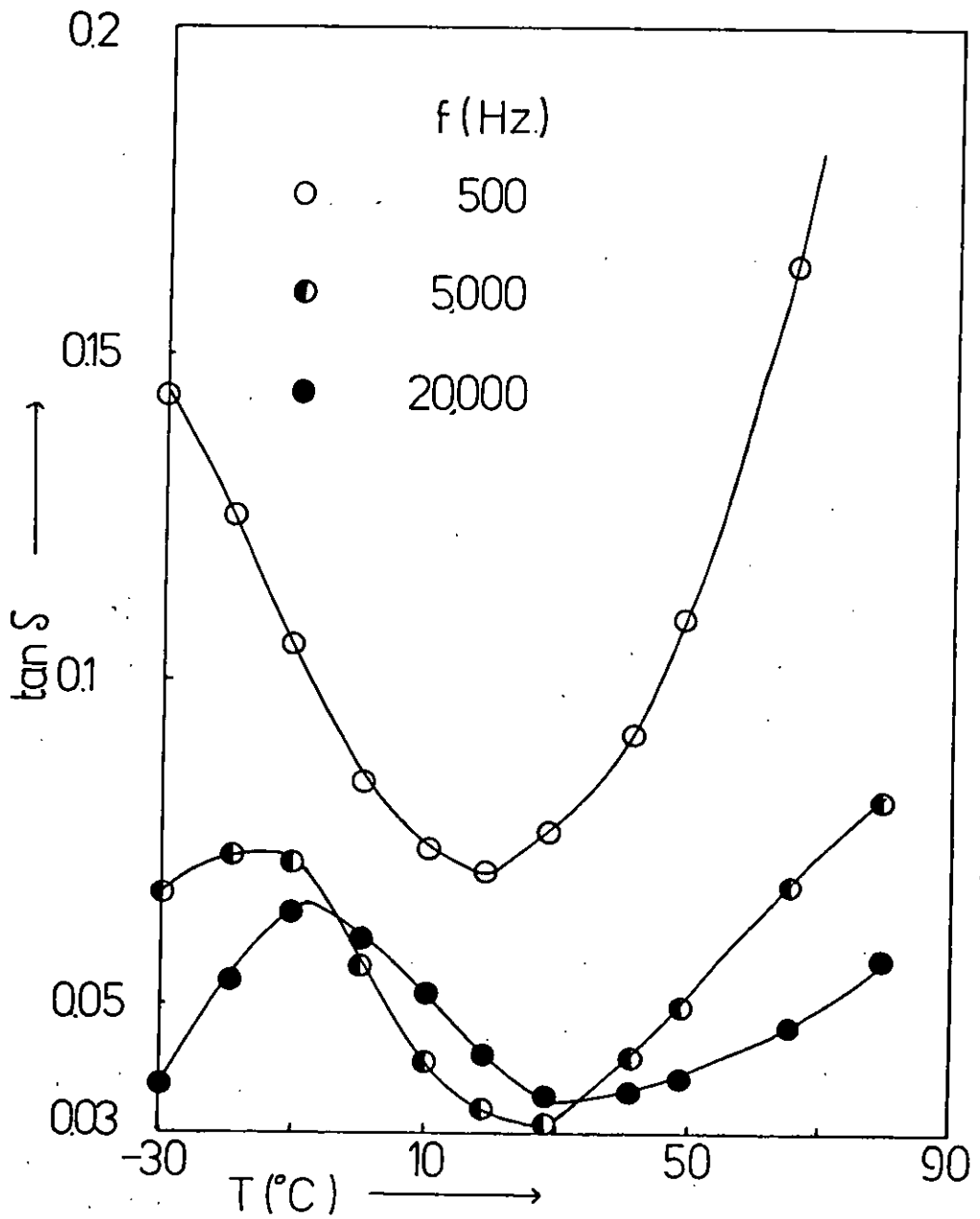


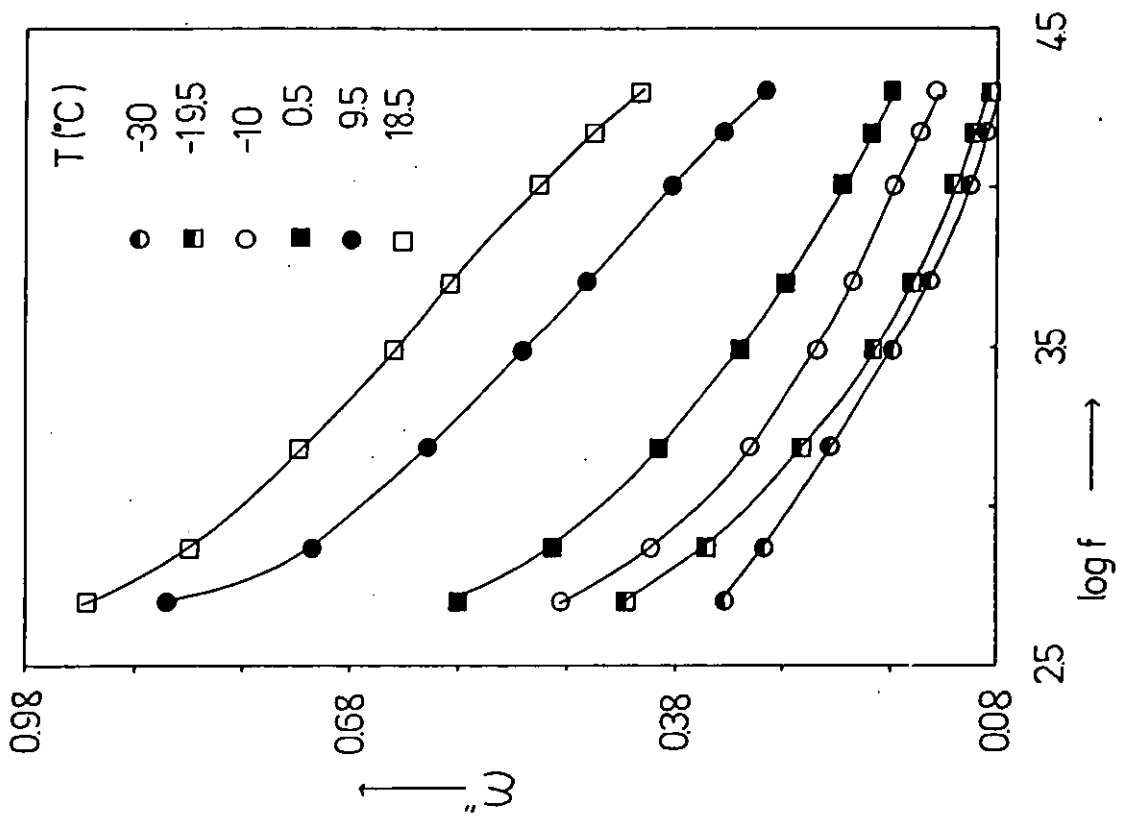
Figure (5.81)

Loss Tangent vs. Temperature Curves for  
MA2 / PEPC at Various Frequencies



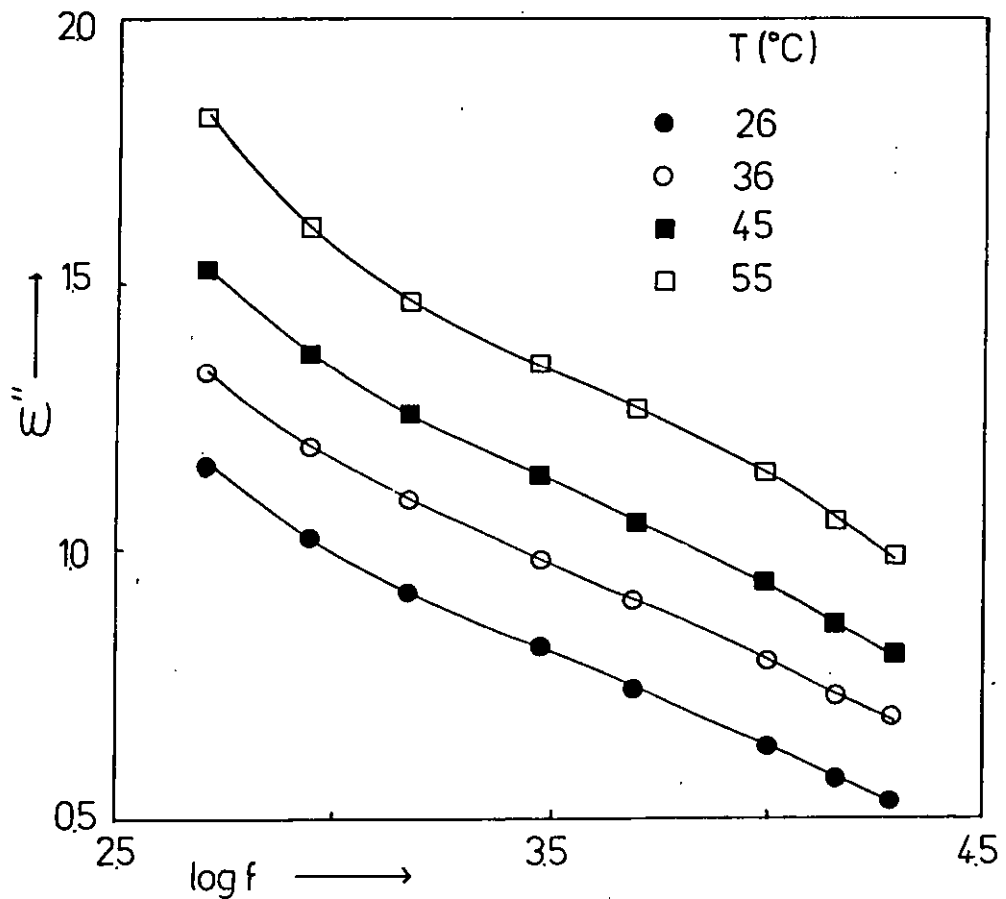
Figure(5.82)

Frequency Dependence of Dielectric Loss  
at Various Temperatures for MA4/PEPC



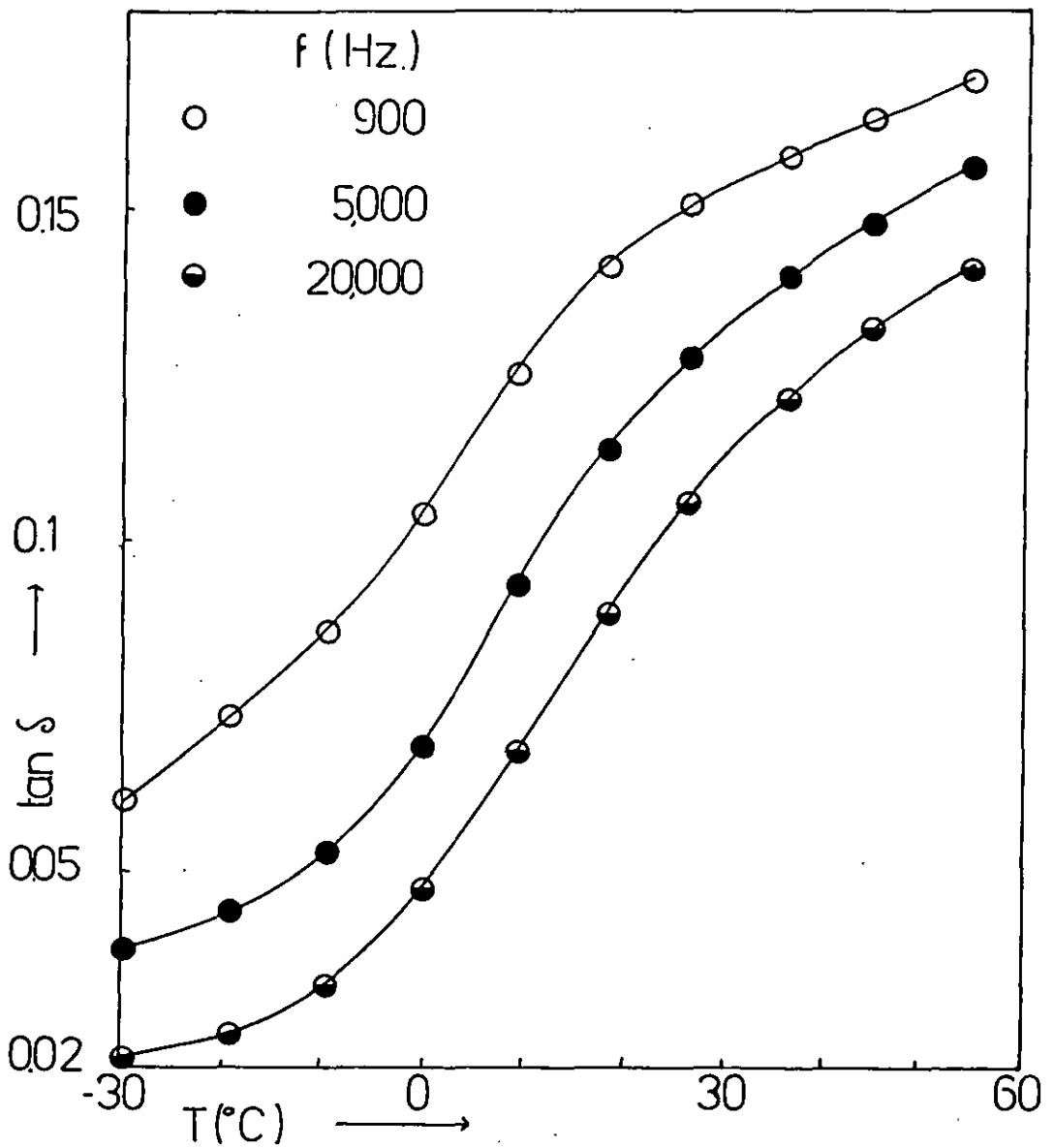
Figure(5.83)

Frequency Dependence of Dielectric Loss at  
Various Temperatures for MA4/PEPC



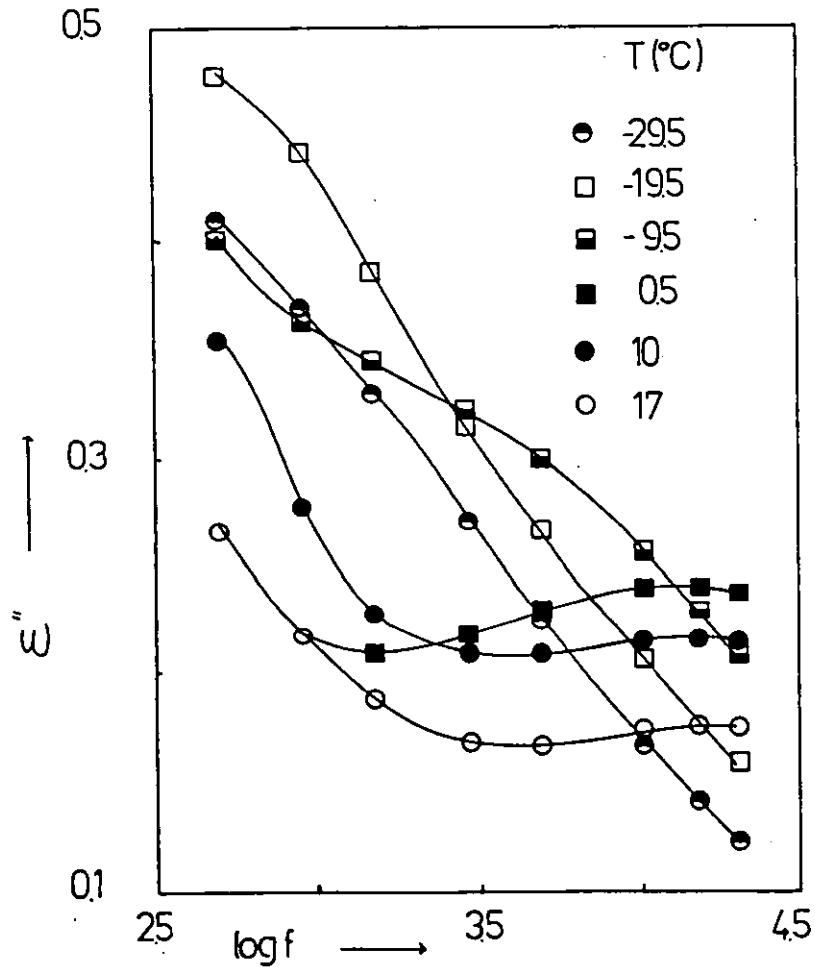
Figure(584 )

Loss Tangent vs. Temperature Curves for MA4 /  
PEPC at Various Frequencies



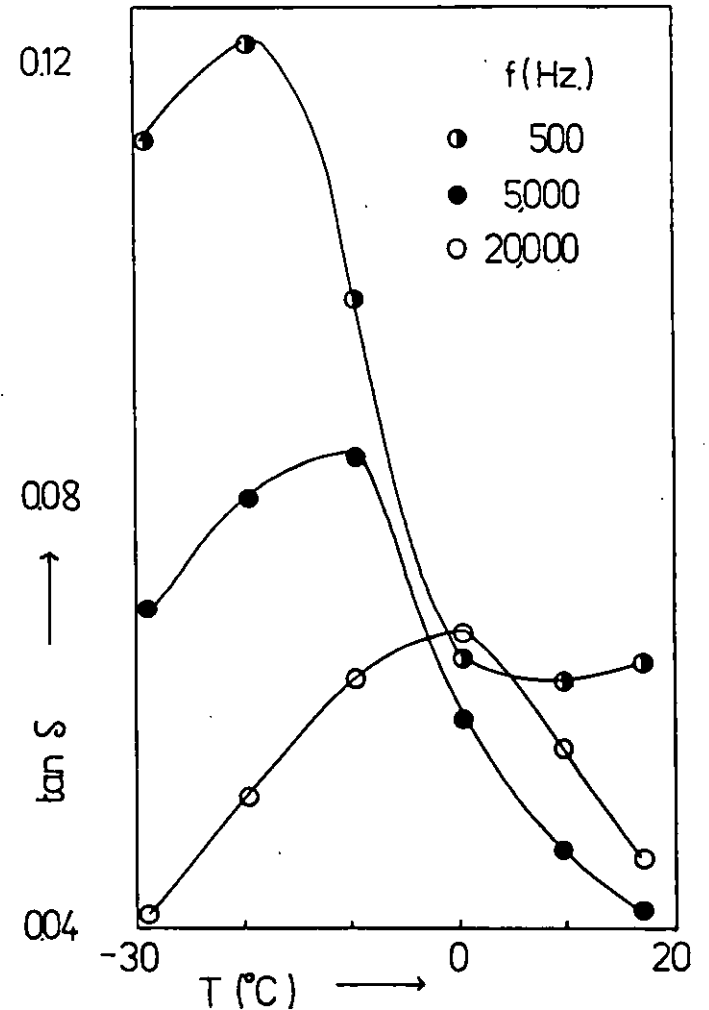
Figure(5.85)

Frequency Dependence of Dielectric Loss at Various Temperatures for MA5/PEPC



Figure(5.86)

Loss Tangent vs. Temperature Curves for MA5/PEPC at Various Frequencies



CHAPTER 6

DISCUSSION OF HOMOPOLYMER/HOMOPOLYMER BLENDS



## 6.1 THE INFLUENCE OF SOLVENT ON THE MISCIBILITY OF BLENDS CAST FROM SOLUTION

When polymer blends are prepared by dissolution in a common solvent followed by casting, the influence of the solvent on the resultant phase structure of the blend is often neglected. However a number of cases have been cited in the literature in which a change of solvent has caused a blend which was previously two-phase to become miscible. Poly(styrene)/poly(vinyl methyl ether) have been found to be miscible when cast from toluene<sup>(64)</sup>, benzene<sup>(69)</sup> and tetrachloroethylene<sup>(69)</sup> but immiscible when the solvent was chloroform<sup>(64)</sup>, trichloroethylene<sup>(75)</sup>, ethyl acetate<sup>(187)</sup> or methylene chloride<sup>(69)</sup>. Robard<sup>(69)</sup> and co-workers measured the interaction parameters between the two homopolymers and the above solvents and found that for miscibility the difference between the two parameters had to be less than 0.2. Gashgari and Frank<sup>(188)</sup> have discussed the influence of casting temperature on the morphology of a miscible blend. If the casting temperature ( $T_c$ ) is greater than that of the blend glass transition temperature ( $T_g^b$ ) there should be sufficient molecular mobility after removal of all the solvent for the blend to achieve thermodynamic equilibrium. However if  $T_c < T_g^b$  then a point will be reached during the casting process at which  $T_c$  is below the glass transition temperature of the ternary blend-solvent mixture. Solvent will continue to evaporate slowly from the glass formed at this point but there will be insufficient mobility for further large-scale motion of the polymer chains. Therefore the morphology of such a glass is characteristic not of the binary polymer blend but of the ternary mixture.

To minimise the effects of dissimilarities in the polymer/solvent interaction parameters preliminary studies were conducted on the miscibility of each blend in a range of solvents of varying solubility

parameter. The results presented in chapter 4 refer to the most favourable miscibility situation found in this way. Consequently it is expected that these results are independent of casting solvent. All samples were annealed at elevated temperature prior to measurement, as detailed in section (3.4), to facilitate complete removal of all solvent and the achievement of thermodynamic equilibrium. This was necessary as one component in all cases had a  $T_g$  above ambient temperature ( $T_c$ ).

## 6.2 POLY(METHYL METHACRYLATE)/POLY(EPICHLOROHYDRIN) BLENDS

This blend was studied by Peterson *et al.* <sup>(189)</sup> in their early paper on the behaviour of various polymer blends. The state of miscibility was ascertained on the basis of the behaviour of a ternary solution in cyclohexanone containing 15% (by weight) polymer. The solution was found to phase separate and a film cast from it was not transparent.

The DTA and DMTA results (Figures (4.1)-(4.2)) are consistent and show that the blend exhibits two glass transition temperatures, whose positions are slightly shifted towards one another with respect to the pure component transition temperatures. The blend  $T_g$ 's are independent of the overall composition, although the minor phase  $T_g$  is not sensed by DTA and lacks resolution by DMTA at the extremes of the overall composition range. The glass transition temperatures measured as the maximum of the  $\tan \delta$  peak appear some  $10^\circ\text{C}$  above the corresponding  $T_g$ 's determined by DTA. This difference is quite common when the frequency of oscillation is 1 Hz, but as shown in Figure (2.15) if  $T_g$  had been defined in terms of the maximum in  $E''$ , the DMTA  $T_g$  would have been lower.

Strictly speaking, as this blend exhibits two shifted  $T_g$ 's with

respect to the pure components it should be classified as partially miscible. However when the compositions of the two phases are analysed using the Fox expression (equation (2.98)) they contain approximately 8% and 97% PMMA by weight. This indicates such limited mutual solubility that the blend can be more usefully regarded as immiscible.

These results imply that the free energy of mixing ( $\Delta G_m$ ) varies qualitatively with composition in the manner shown in Figure (6.1). Examining the enthalpy of mixing ( $\Delta H_m$ ) in terms of the binary interaction energy density (B) quoted in section (2.4)

$$\frac{\Delta H_m}{V} = B\phi_1(1 - \phi_1) \quad (6.1)$$

if B is positive  $\Delta H_m/V$  will vary with composition as shown in Figure (6.2). In this plot composition has been converted from volume fractions to weight fractions ( $w_i$ ) using the relationship

$$\phi_1 = (w_1/\rho_1)/(w_1/\rho_1 + w_2/\rho_2) \quad (6.2)$$

where  $\rho_i$  is the density of polymer i. This expression assumes that the specific volume of the mixture is the sum total of the fractional contribution on a weight basis as pointed out by Koningsveld<sup>(11)</sup>.

It is apparent that at the extremes of the concentration range  $\Delta H_m/V$  falls towards zero whilst reaching a maximum at intermediate values.

The enthalpy curve in Figure (6.2) has been calculated using Hildebrand's<sup>(105)</sup> relation for B in terms of solubility parameters (equation (2.75)). The solubility parameters were calculated using group contribution tables and density values were extracted from the text of van Krevelen<sup>(111)</sup>. If  $\Delta H_m$  was of the same magnitude

Figure (6.1)  
Qualitative Variation of  $\Delta G_m$  with  
Composition for PMMA / PEPC

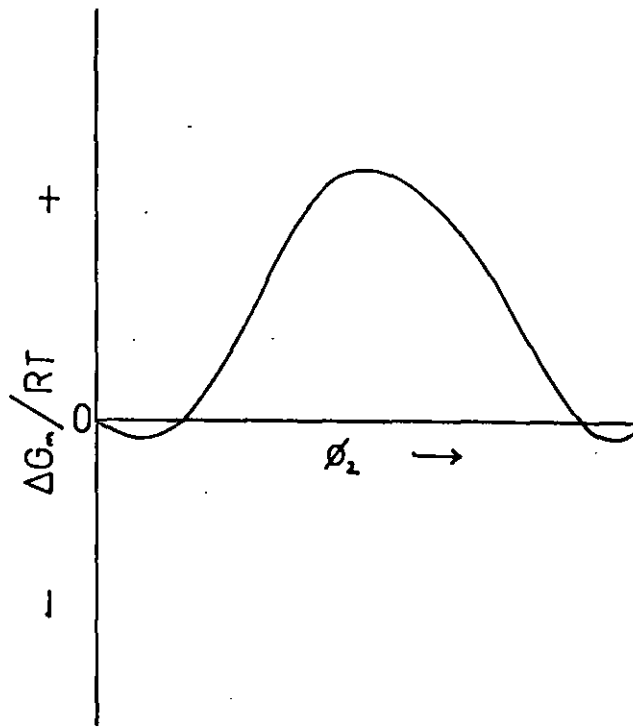
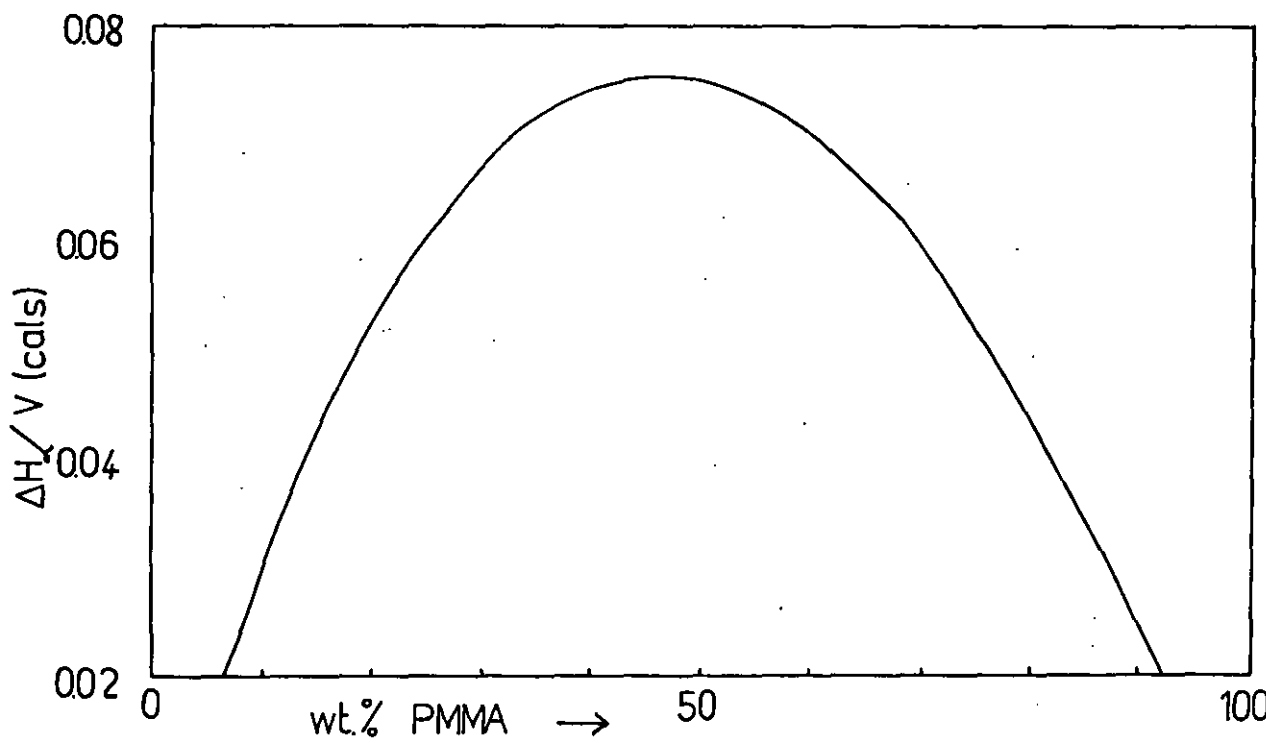


Figure (6.2)  
Variation of Calculated Enthalpy of Mixing  
with Composition for PMMA / PEPC



but negative, the curve of  $\Delta H_m/V$  against composition would be reflected in the x axis. In this situation the enthalpy of mixing would be most favourable for miscibility at intermediate compositions.

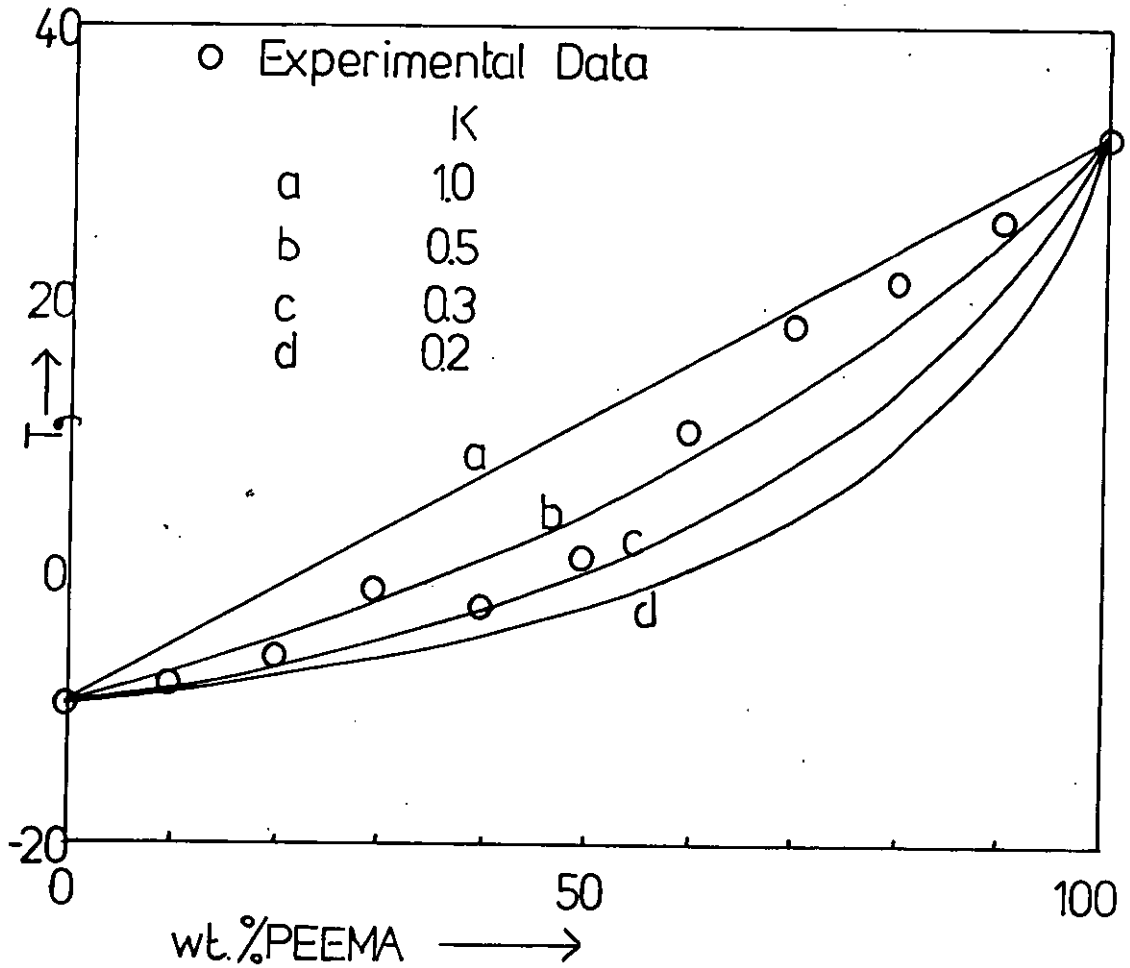
Given that PMMA and PEPC show only limited mutual solubility at the extremes of the composition range it is apparent that  $\Delta H_m$  is positive for this polymer pair indicating the absence of a specific interaction between the dissimilar species. The difference in the respective solubility parameters is  $0.55 \text{ cal}^{1/2}/\text{cm}^{3/2}$  which is well outside the critical limit of 0.1 at a degree of polymerisation of 100 for the two components at room temperature. In fact using the predictive scheme of Krause<sup>(114)</sup>, which is based on a comparison of the Flory-Huggins expression for  $(X_{12})_{CR}$  with the Hildebrand relationship (equations (2.43) and (2.75)), the degree of polymerisation would have to be below 40 for miscibility under ambient conditions. Consequently the dispersion forces of the two polymers are too disparate to facilitate miscibility at the molecular weights studied.

### 6.3 POLY(ETHOXY ETHYL METHACRYLATE)/POLY(EPICHLOROHYDRIN) BLENDS

The glass transition behaviour of blends of PEEMA/PEPC as measured by both DTA and DMTA (Figures (4.3) and (4.6)) demonstrates a single transition at all compositions. The composition dependence of  $T_g$  (Figures (4.4) and (4.7)) lies within 1-2°C of that predicted by the Fox relationship at loadings of PEEMA of 70 wt.% and above. At higher elastomer contents there is a negative deviation from the predicted values which reaches a maximum at a composition of 50 wt.%. Employing the Gordon-Taylor relationship (equation (2.96)) the data can be better fitted to the curve at 10-50 wt.% PEEMA by using K as an empirical parameter, as shown in Figure (6.3). However, at higher concentrations a threefold increase in K is necessary to fit

Figure (6.3)

$T_g$  Data for PEEMA/PEPC Measured by DMTA. Superimposed on Composition Dependences of  $T_g$  Calculated Using the Gordon-Taylor Eqn. with Various Values of K



the curve to the data.

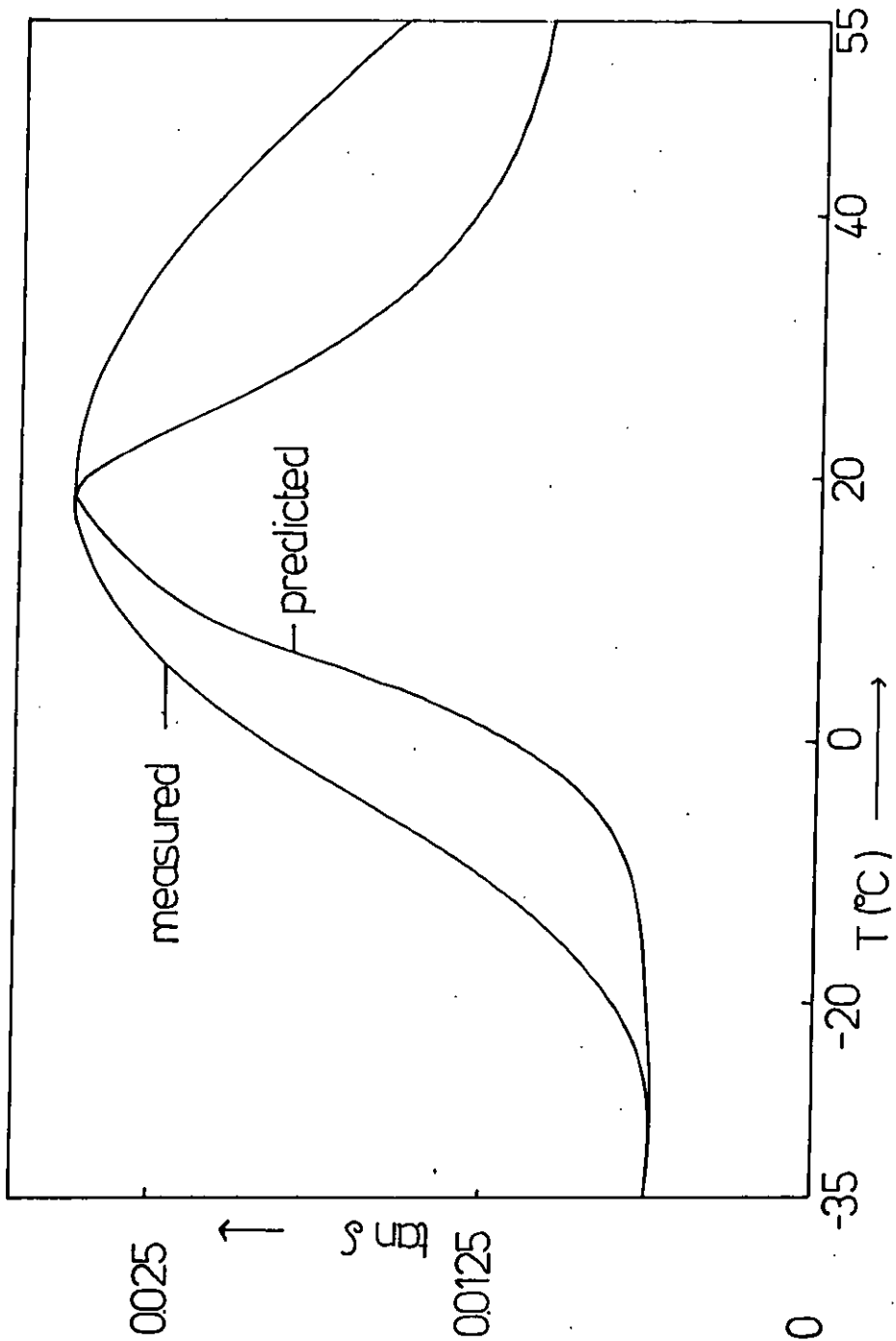
There are several examples of this type of compositional dependence of  $T_g$  in the literature. Bank *et al.*<sup>(64)</sup> in their study of poly-(styrene) blends with poly(vinyl methyl ether) by D.S.C. found that  $T_g$  followed the Fox line at compositions containing 80 wt.% PST and above. At lower PST concentrations there was a negative deviation from the calculated values of the order of 15-38°C, the maximum drift being at the mid-point of the composition range. Similar results were obtained by Fried *et al.* for a series of plasticized PVC<sup>(190)</sup> samples and for blends of poly(2,6-dimethyl 1,4-phenylene oxide) (PPO) with a copolymer of styrene and maleic anhydride. Xie *et al.*<sup>(192)</sup> have recently found an even more exaggerated deviation from the predicted  $T_g$  relationship for blends of PST with carboxylated PPO.  $T_g$  was found to vary sigmoidally with composition and at 20 wt.% carboxylated PPO exhibited a  $T_g$  10°C below that of PST, which one would expect to form the limiting minimum value for the blend.

The aforementioned systems fulfil some of the criteria for miscibility in that they have transparent films and exhibit a single composition dependent  $T_g$ . However, the transition width was found to be greater for the blends than for the pure components and attained a maximum value at intermediate compositions. Examination of the transition widths for PEEMA/PEPC in Figure (4.5) indicates that this system behaves similarly. In Figure (6.4) the measured loss tangent peak of a blend containing 70 wt.% PEEMA is contrasted with that which would be expected if the blend were miscible. The breadth of the measured transition is approximately twice that of the predicted transition.

The broadening of the glass transition process reflects heterogeneity within the blends at a level below that giving rise to a

Figure (64)

Comparison of the Measured Loss Tangent Peak for PEE/MA/PEPC (70 wt.% PEE/MA) with that Predicted for a Miscible Mixture





characteristic  $T_g$  ( $150 \text{ \AA}^{(4)}$ ). This notion of microheterogeneity is supported by the observation of film clarity at all compositions. The difference in the refractive indices of the two polymers ( $0.03^{(111)}$ ) is such that phases of  $1,000 \text{ \AA}^{(7)}$  and over would have been apparent had they been present. Consequently the glass transition behaviour observed does not relate to a single homogeneous phase but rather to distribution of microphases so that, for example, the value of  $T_g$  taken from the  $\tan \delta$  curve reflects the behaviour of the most commonly occurring composition. Why this composition should be below that of the overall composition in the range 10-60 wt.% PEEMA is not immediately apparent and has not received attention in the literature cited above.

Further examples of microheterogeneity include an interesting study by Wang and Cooper<sup>(193)</sup> on blends of PVC with a poly(urethane) which contained soft segments of poly(tetramethylene oxide) and hard segments of 4,4'-diphenylmethane diisocyanate. PVC was found to mix with the soft segments to form microphases, characterised by broad glass transition processes. However the hard segments remained unmixed and formed pure microphases. The shape of the  $T_g$  vs. composition plot is unique in that a Fox type relationship was followed at PVC concentrations up to 30% beyond which positive deviations from the predicted values were found. Savard *et al.*<sup>(194)</sup> in their study of blends of cellulose with poly(acrylonitrile) found that the amorphous phase was microheterogeneous as evidenced by a broadening of the  $\tan \delta$  relaxations, however the data did not allow precise allocation of glass transition temperatures so the composition dependence of  $T_g$  is not known. Hubbell and Cooper<sup>(195)</sup> only measured broadening in  $\tan \delta$  at compositions above 50% nitrocellulose in its blends with poly(caprolactone), they claim that the blend is miscible

at lower concentrations and then passes to the microheterogeneous state.

The difference in the solubility parameters of PEEMA and PEPC, calculated by the group contribution tables is  $0.69 \text{ cal}^{1/2}/\text{cm}^{3/2}$ . Using the Krause<sup>(114)</sup> scheme, for miscibility at 300K both components would need to have a degree of polymerisation below 25. As the actual degrees of polymerisation for PEEMA and PEPC are 700 and 3,900 respectively it is obvious that on the basis of dispersive forces alone this blend should be completely immiscible. Consequently the observation that the blend is partially miscible (microheterogeneous) implies that there is a greater affinity between PEEMA and PEPC than between PMMA and PEPC.

#### 6.4 POLY(TETRAHYDROFURFURYL METHACRYLATE)/POLY(EPICHLOROHYDRIN) BLENDS

Blends of PTHFMA with PEPC measured by thermal analysis (Figure (4.8)) exhibited two distinct transitions in the concentration range 30-90 wt.% PTHFMA. The plot of glass transition temperature against composition (Figure (4.9)) reveals that the elastomer rich phase incorporates increasing amounts of PTHFMA as the overall content of this constituent rises. Evaluation of the phase composition using the Fox relationship demonstrates that the amount of PTHFMA in this phase rises from 10-30 wt.% in the above range of overall concentration. By comparison the  $T_g$  of the PTHFMA rich phase is fairly constant and relates to a phase composition of about 80 wt.% of the dominant component.

Examination of the blends by DMTA (Figures (4.11) and (4.12)) reveals a similar phase distribution in many respects. In the range 10-40 wt.% PTHFMA a single transition was observed whose  $T_g$  increased steadily with composition, reflecting the incorporation of more PTHFMA

into the phase. However the variation of  $T_g$  was much less marked than that expected of a miscible blend. At 60 and 70 wt.% PTHFMA the major transition is rich in PTHFMA and the composition of this phase corresponds to that found by DTA (80 wt.%). A minor, low temperature transition also occurs at these compositions at positions reflecting a similar composition of the minor phase as that determined previously. At 50 wt.% PTHFMA a single, very broad transition occurs, the positions of the shoulders on this peak suggesting it arises from the overlap of transitions. The major difference between the results obtained by the two techniques is found at 80-90 wt.% PTHFMA where a clear elevation of the  $T_g$  of the major phase is found by DMTA but not by DTA.

The breadths of the glass transition processes, measured as defined in sections (4.2.3)-(4.2.4) for the two techniques are given in Figure (4.10). The breadth plotted, in those cases where two transitions occur, is that of the major transition. So, for example by DMTA, in the range 0-40 wt.% PTHFMA this refers to the elastomer rich phase whilst at 60-100 wt.% PTHFMA it is the breadth of the PTHFMA rich phase which is presented. The plots for DTA and DMTA are not strictly comparable because at 50 wt.% PTHFMA two transitions are apparent by DTA (major one PEPC rich) whilst a single broad transition was measured mechanically. Nevertheless the basic features of the two plots are similar in that at overall compositions other than at 50-60 wt.% PTHFMA the transition breadth is approximately a weighted average of the breadth of the two pure components. The weighting factor corresponding to overall blend composition. The sharp rise in transition breadth observed at 50 wt.% suggests that this peak in  $\tan \delta$  results from the overlap of several processes. As mentioned above clear shoulders to this peak correspond to elastomer

rich and elastomer poor phases, however the shape of the transition can only be accounted for by postulating the presence of a third phase of intermediate composition. This type of behaviour was reported by Huelck *et al.*<sup>(5)</sup> in a study of the dynamic mechanical properties of a series of interpenetrating networks of poly(ethyl acrylate) (PEA) with a random copolymer of styrene and methyl methacrylate. The blend composition was kept constant and the proportion of MMA in the copolymer was increased gradually. At low proportions of MMA a PEA rich and a PEA poor phase were formed. As the MMA content rose, a third intermediate transition became increasingly apparent, until finally the three relaxation peaks merged. However it seems probable that this cross-over from partial miscibility to microheterogeneity is due at least in part to the fact that segregation of the dissimilar polymer segments is restricted by their being linked covalently. In the case of PTHFMA/PEPC, at 50 wt.% the composition difference between the elastomer rich and PTHFMA rich phases (as indicated by the shoulders in  $\tan \delta$ ) is at a minimum. Consequently it is likely that the intermediate relaxation is due to a partial mixing of the two phases. Although a continuous transition was not observed by DTA at 50 wt.%, the PEPC rich transition was markedly broadened and the shallow slope of the high temperature part of this transition suggests a lack of sensitivity to the transition of the mixed phase.

The difference in the refractive indices of the pure components of the blend is only 0.015<sup>(111)</sup>, however the transparency observed at overall concentrations up to 60 wt.% PTHFMA cannot be attributed to this. The reasoning behind this assertion is that in the range 10-40 wt.% PTHFMA the difference in composition between the two phases is greater than at 60-90 wt.% PTHFMA. As the difference in composition between the two phases diminishes then so will the refractive index

difference, yet it was in the upper range of PTHFMA concentration that optical heterogeneity was observed. Consequently the optical properties of the blends are best explained in terms of phase size. The transparent samples must have phases which lie below the  $1,000 \text{ \AA}$  range, taken as the limit of resolution of natural light. Following this line of reasoning phase size must increase at compositions above 60 wt.% PTHFMA to a level within the resolution range. The fact that these films appear only slightly translucent and their detailed morphology cannot be observed is either due to the fact that the phase size is only slightly larger than the detection limit, the proximity of the refractive indices of the two phases or perhaps a combination of the two.

In terms of a classification of the type of miscibility exhibited by this blend it appears to lie within a sub-category of partial miscibility. As defined in section (1.2), partially miscible blends are taken to exhibit two glass transitions at temperatures intermediate between those of the pure components. Combining this definition with the thermodynamic view of partial miscibility depicted in Figure (2.2), one would not expect the composition of either phase to change with overall blend composition. However this was found to be characteristic of the elastomer rich phase and was also observed at high glass loadings for the PTHFMA rich phase by DMTA.

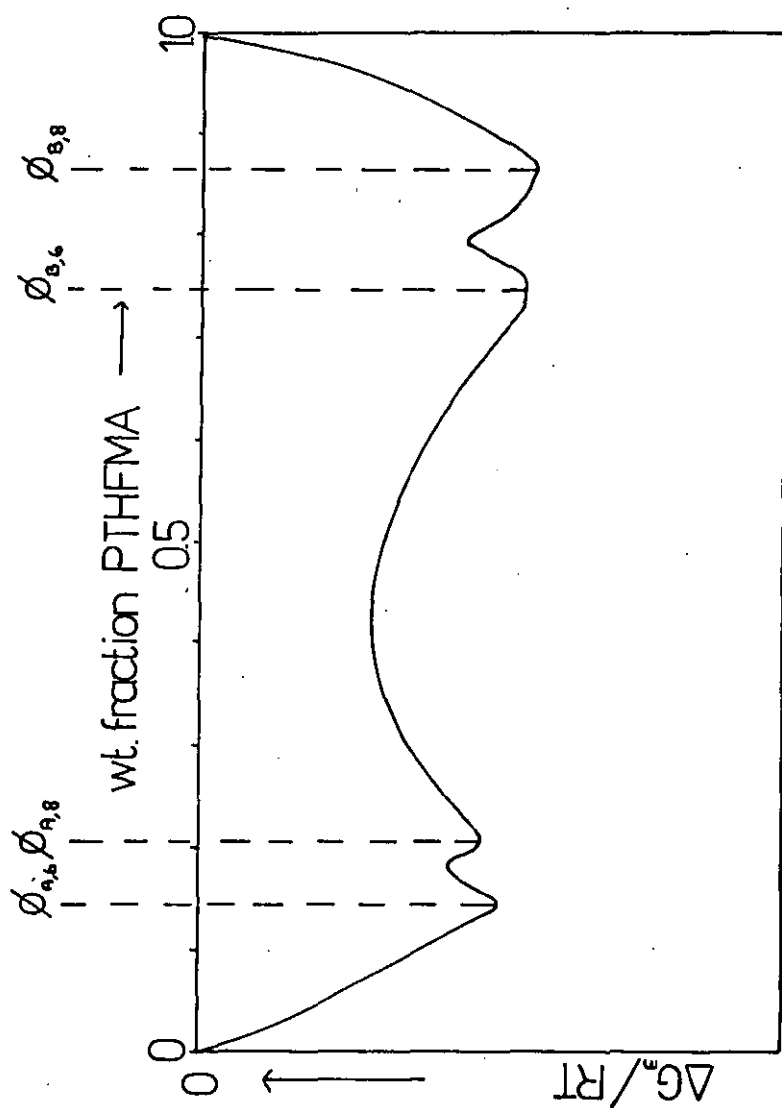
Gardlund<sup>(196)</sup> examined blends of poly(methyl methacrylate) with poly(carbonate) (PC) by DMTA and DSC and found that the mixture exhibited two glass transitions corresponding to a PC rich and a PMMA rich phase. The  $T_g$ 's of both phases were found to alter with the overall composition of the blend. Gardlund also noticed that using DSC the PC rich transition was apparent down to 35% PC whilst using DMTA this phase was only apparent down to 50 wt.% PC.

Wahrmund *et al.*<sup>(197)</sup>, in their study of bisphenol A poly(carbonate) blended with poly(butylene terephthalate) found that the amorphous region consisted of a virtually pure poly(carbonate) phase and a mixed phase rich in the poly(ester). This latter phase also displayed a variation of  $T_g$  with overall composition. The paper of Fried and Hanna<sup>(191)</sup> was quoted in section (6.2) with regard to microheterogeneous blends of PPO with a copolymer of styrene and maleic anhydride containing 8% maleic anhydride. When the proportion of anhydride was increased to 14% 2 glass transitions were observed, reflecting partial miscibility and in this example it was only the phase richer in the higher  $T_g$  component (PPO) which displayed a composition dependent  $T_g$ . Similarly Xie *et al.*<sup>(192)</sup> found that increasing the degree of carboxylation of PPO caused its blends with PST to change from being microheterogeneous to partially miscible. The partially miscible blends consisted of a pure PST phase and a phase rich in modified PPO which changed its composition with the overall constitution of the mixture.

The preceding examples from the literature all exhibit to some degree deviations from the behaviour expected of a partially miscible blend. In fact there appear to be no blend studies conducted to date which have found partially miscible polymer mixtures in which the composition of both phases remained constant as overall concentration varied. This implies that the free energy of mixing varies with concentration in a manner other than was shown in Figure (2.2). In Figure (6.5) the free energy of mixing has been plotted against blend composition. The curve has been deduced for simplicity only on the basis of the phases apparent at concentrations of 60 and 80 wt.% PTHFMA,  $\Delta G_m$  being at minima at these phase compositions. The compositions marked  $\phi_{A,6}$  and  $\phi_{B,6}$  represent the PTHFMA poor and PTHFMA rich

Figure (6.5)

Qualitative Variation of  $\Delta G_m$  with Overall Composition Using Phase Compositions Measured at 60 and 80 wt.% PTHFMA



phases respectively found in blends containing 60 wt.% PTHFMA. Similarly  $\phi_{A,8}$  and  $\phi_{B,8}$  relate to the phase compositions apparent in blends containing 80 wt.% PTHFMA. The type of  $\Delta G_m$  curve which links these points explains the observed behaviour for PTHFMA rich phases in that the phase formed corresponds to the minimum in the curve which lies nearest to the original blend composition. However this does not hold for the PTHFMA poor phase, where for example in blends containing 60 wt.% copolymer formation of this phase requires the passage from one well of minimum free energy to another. This cannot be explained in terms of one minimum lying at lower free energy than the other as this would require that the composition of the PTHFMA poor phase be constant at this point. When the phase compositions measured at overall concentrations across the range 10-90 wt.% PTHFMA are plotted as minima of a projected free energy of mixing curve it becomes impossible to consistently satisfy the requirements of either phase with a single function irrespective of the complexity introduced. It would appear therefore that the treatment of this system using the approach of equilibrium thermodynamics is not valid. The possibility of non-equilibrium phase separation is discussed in section (7.3).

The cause of the enhanced miscibility of this blend in comparison with the immiscible PMMA/PEPC cannot be attributed to the dispersion forces of the components being better matched. The solubility parameter difference between the species is  $0.9^{(111)}$ , indicating that at 300K the maximum degree of polymerisation tolerable for miscibility is about  $15^{(114)}$  for both components. This suggests that the system is even more immiscible than PMMA/PEPC where the maximum degree of polymerisation tolerable was found to be 40. Consequently in this system as with PEEMA/PEPC dispersion forces are not the sole factor influencing the state of mixing.



## 6.5 POLY(GLYCIDYL METHACRYLATE)/POLY(EPICHLOROHYDRIN) BLENDS

The unusual step at the high molecular side of the elution profile of PGMA was found on investigating the dissolution behaviour of the highest molecular weight fraction to result from the presence of a small amount of cross-linked material. Network formation was also found to occur in the solution polymerisation of GMA in butanone by D'Alelio *et al.* (213). The reason why this material is insoluble in the fractionated sample but soluble in the original form could be due to the influence of the lower molecular weight species, which are not present of course to the same degree in fraction f1. There is a slight shoulder on the high molecular weight side of fraction f1, whose blends with PEPC the data in section (4.4) refers to. However, as the lower molecular weight fractions yielded symmetrical elution curves but gave similar results, it would appear that the effect of this feature on miscibility is negligible.

The DTA and DMTA results immediately lead one to believe that this blend is miscible. The glass transition temperatures are clearly composition dependent and as distinct from microheterogeneous blends the breadth of the glass transitions for the mixtures are similar to those of the pure components. The composition dependence of the blend glass transition temperatures measured by the two techniques are very similar (Figures (4.16) and (4.18)) and correspond closely to the values predicted by the Fox equation at compositions of 60-90 wt.% PGMA. At lower concentrations there is a negative deviation from the predicted values which varies from 4-9°C. Using any of the alternative expressions for calculating  $T_g$  at a given blend composition, listed in section(2.5.4), one finds that they can only fit the data over a limited concentration range. The data can be fitted by using a value of K in the Gordon-Taylor equation which decreases continuously

from 3 to 1.8 in the range 10-60 wt.% PGMA but is constant thereafter. Given the definition of  $K$  (equation (2.97)) its basis in reality is destroyed if it is made dependent on composition in this manner. It is interesting to note however that if the Fox expression is rewritten in terms of mole fractions of repeat units, the measured  $T_g$ 's correspond to the predicted values to within  $2^\circ\text{C}$  in the range 10-40 wt.% PGMA but thereafter reveal a positive deviation of  $5.5$ - $8.5^\circ\text{C}$ .

The optical clarity of the blends at all compositions lends some support to the notion of miscibility. However the refractive indices of the two components are within  $0.0002^{(111)}$  of one another so that it is probable that even had the blends been immiscible they would have appeared to be transparent.

The number of miscible blends reported has increased rapidly in the last 20 years<sup>(9,10,32)</sup> and as the database has expanded it has become apparent that the compositional dependence of  $T_g$  in a miscible blend can take many forms. Blends of nitrocellulose and poly(methyl acrylate)<sup>(198)</sup> and natural rubber and poly(butadiene)<sup>(199)</sup> have been reported to exhibit a linear variation of  $T_g$  with composition. However in the former example measurements were not made at compositions above 30 wt.% poly(methyl acrylate) which has the lower  $T_g$  of the pair. Furthermore in the latter example  $T_g$  was determined by dilatometry and composition was expressed in terms of volume fractions rather than weight fractions. These two methods of expressing concentration are only equivalent when the densities of the two components are equal, which in this case they are not<sup>(205)</sup>. Blends of PVC-butadiene/acrylonitrile<sup>(200)</sup> random copolymers and PVC with a random terpolymer of ethylene, vinyl acetate and sulphur dioxide<sup>(201)</sup> have been cited as systems which follow a Fox type dependence of  $T_g$ . However once again measurements were not conducted on samples containing more

than 50 wt.% of the constituent with the lower  $T_g$ . Blends of poly-(butadiene) with a random copolymer of styrene/butadiene<sup>(202)</sup> show a negative deviation from the weight average value of  $T_g$  in a manner which is well approximated by the Gordon-Taylor equation using a value of  $K$  calculated from thermal expansion data. Kwei and co-workers<sup>(203,204)</sup> have investigated systems which contain a significant degree of hydrogen bonding and have found  $T_g$  to be elevated above the values predicted using a weight average value of the blend  $T_g$ . This effect was rationalised in terms of the strong specific interactions causing either steric hindrance or densification, thereby restricting molecular motion. There are very few instances in the literature of blends which show different types of deviation from the weight average values of  $T_g$  depending upon which constituent is in excess as displayed by PGMA/PEPC. One blend whose glass transition behaviour varied in a somewhat similar fashion consisted of poly(caprolactone) (PCL) mixed with a series of poly(ethylene) samples<sup>(206)</sup> which had been chlorinated to varying degrees. The variation is not as systematic as found in PGMA/PEPC but there is a general tendency for  $T_g$  to show a positive deviation from the weighted average values at low glass concentrations and a negative deviation at high compositions of PCL.

The preceding examples serve to show that the shape of the composition dependence of the glass transition temperature is of little use in distinguishing miscible and microheterogeneous blends. The examples of microheterogeneity listed in section (6.3) show a similar  $T_g$  dependence to PGMA/PEPC, although the negative deviations from the Fox equation are much greater in the former case. However it is clear that a much more reliable criterion for blend classification is the breadth of the glass transition process compared to that expected from measurements of the transition breadths of the pure components. On

this basis PGMA/PEPC blends are miscible.

It is apparent that the precise nature of the compositional variation of  $T_g$  in a miscible blend is dependent upon the physical properties of the two components and the nature of their intermolecular interaction. However the form of the relationship between these factors has yet to be formulated to provide a generally applicable expression.

The influence of temperature on PGMA/PEPC blends was illustrated in Figure (4.19). The shapes of the loss tangent curves of the samples annealed at 200°C are virtually identical and reveal the presence of a number of mixed phases. There are three distinct relaxation peaks corresponding to phase compositions of  $\approx$  22%; 47% and 65 wt.% PGMA (calculated using the experimental  $T_g$  vs. composition curve). This result signifies that PGMA and PEPC blends exhibit lower critical type miscibility. The fact that no change in optical clarity was observed on heating reflects the small difference in the refractive indices of the two components mentioned earlier. Obviously the refractive index difference between mixed phases would be smaller still.

The equivalence of the loss tangent curves of the quenched and slowly cooled samples reveal that the phase separation process is not reversible. Jager *et al.*<sup>(207)</sup> found that there was a kinetic barrier to re-entry to the one phase region in blends of PMMA/PVC due to the high viscosity of the system. However given that the PGMA blends were cooled slowly from a point about 180°C above the  $T_g$ 's of the miscible mixtures of intermediate composition, this does not provide an adequate explanation. The observation of network formation, both in the blends and the PGMA homopolymer following annealing at temperatures above 120°C, provides a more likely cause for irreversible phase separation. The network will restrict molecular mobility and as the cross-linking process is initiated at a temperature some 30°C below

that at which phase separation is first observed it is possible that entry to the two-phase region is also inhibited. This provides one explanation of the fact that three phases were observed, one of which corresponded quite closely to the composition of the original miscible mixture.

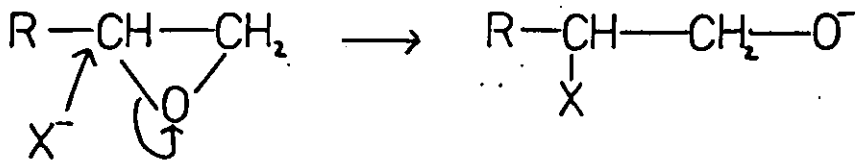
The initiation of the cross-linking process can only be conceived as involving the opening of the highly strained epoxy group in PGMA. Trace amounts of acid or base are sufficient to catalyse the cleavage process leading to the formation of poly(ether) linkages between the main chains (Figure (6.6)). As the figure shows, in the blend the propagation process can be conceived as involving either both components or PGMA alone.

The phase separation process being undetectable by a change in the blends optical clarity, it is proposed that the cloud point curve for the system can be approximated by the plot of loss tangent broadening temperature against composition (Figure (4.20)). The difference between the two phase boundaries will depend firstly on the level of heterogeneity required to show a detectable shift in the loss tangent peak width as compared with the level causing a change in optical properties. A further possible cause of disagreement concerns the fact that the equilibrium cloud point curve is determined by comparison of the data obtained on both heating and cooling. The difference between the two sets of data was explained by McMaster<sup>(25)</sup> in terms of a nucleation barrier for compositions other than at the critical point. McMaster<sup>(25)</sup> outlined a procedure to obtain the equilibrium cloud point curve using the value of the minimum temperature gap between the curves obtained on heating and cooling to correct the data. Phase separation in PGMA/PEPC is however not reversible so that only the heating curve can be measured. For these reasons the plots of peak broadening temperature

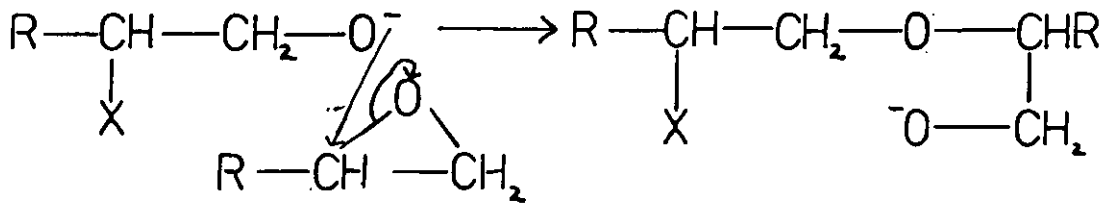
Figure (6.6)

Possible Steps Involved in Network Formation

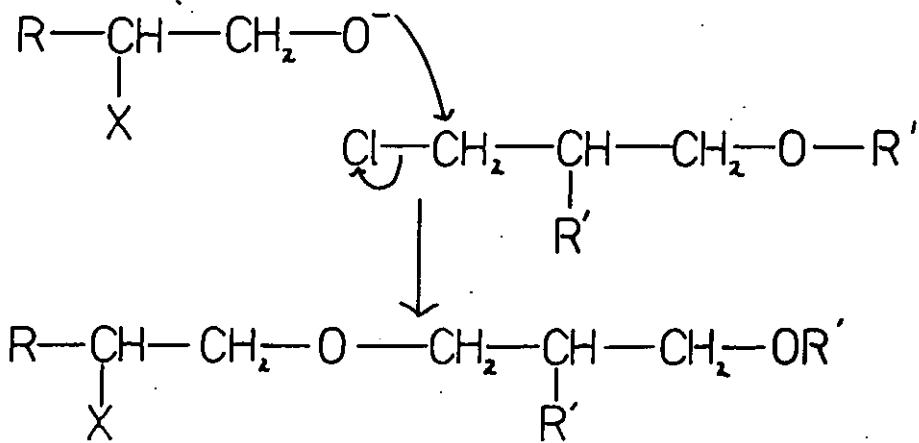
a) Base Catalysed Cleavage of Epoxy



b) Network Propagation Via GMA Only



c) Network Propagation Via PEPC



R — PGMA Chain

R' — PEPC Chain

are best described as pseudo-cloud point curves.

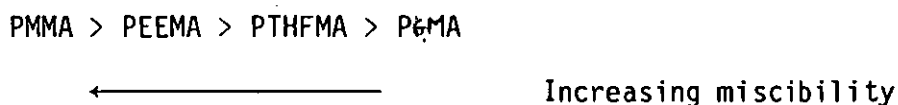
The molecular weight dependence of the pseudo-cloud point curves, exhibiting a shift to higher temperatures with decreasing molecular weights of PGMA, is in accord with the behaviour predicted by the equation of state theory. The shape of the boundaries is similar to that of cloud-point curves measured in a number of high polymer blends exhibiting lower critical miscibility<sup>(26,92)</sup>. The measured boundaries in all cases being much flatter than those predicted using McMaster's base parameter technique outlined in section (2.2.4). The phase boundaries measured by ZhiKuan *et al.*<sup>(92)</sup> in blends of chlorinated poly(ethylene) with poly(methyl methacrylate) samples of various molecular weights showed similar temperature shifts to those measured for PGMA/PEPC. They found that spinodals of similar shape to the measured phase boundaries could be generated if the interaction entropy parameter ( $Q_{12}$ ) in the equation of state model was assigned a negative value. This negative value of  $Q_{12}$  implies a higher degree of order in the blend than in the pure components, presumably resulting from specific interactions between the components.

Phase separation in PGMA/PEPC blends could be due to the equation of state parameters of the two components reaching a critical level of disparity having been closely matched at lower temperatures. However given that the dispersion forces of the polymers are not well matched, the solubility parameters differing by  $1.04 \text{ cal}^{\frac{1}{2}}/\text{cm}^{\frac{3}{2}}$ , one can only rationalise the observed miscibility behaviour by postulating the existence of a specific interaction between the species. Phase separation can be thought of in terms of the increased mobility of the chain segments on heating tending to disrupt the required alignment of the participating functional groups. Whilst the irreversibility of the process results from the inability of the chain segments to reassume their

favoured steric arrangement throughout the sample due to network formation.

## 6.6 SUMMARY

The homopolymer solubility parameters and the difference in constituent parameters for each blend are presented in Table (6.1). If the only relevant determinants of miscibility were dispersion forces then at constant temperature and molecular weight miscibility with PEPC should correspond to the following series



The data presented in chapter (4) has clearly shown that PGMA forms the most miscible blend with PEPC, PMMA the least miscible whilst both PEEMA and PTHFMA form blends of intermediate miscibility. This hierarchy of miscibility being the opposite of that predicted on the basis of solubility parameters leads one to conclude that favourable mixing is due to the presence of specific interactions which must consequently increase on going from PMMA to PGMA in the above series.

Given that the constituent with the greater  $T_g$  is a poly(methacrylate) derivative in each blend and that molecular weight is fairly constant along the series then the relevant portion of each which governs the miscibility with PEPC is the ester side chain. The dipole moments of hydrogenated methyl methacrylate and the small molecule equivalents of the various ester side groups and PEPC are listed in Table (6.2)<sup>(208)</sup>. All measurements had been conducted in benzene ( $\mu = 0$ ) at 20°C. As the methacrylate portion of each homopolymer segment has the same dipole moment, then the moment of the ester side-chain increases from a value of 0 for MMA to 1.9-2.0 for GMA. The




Table 6.1. Homopolymer Solubility Parameters

Polymer	$\delta(\text{cal}^{\frac{1}{2}}/\text{cm}^{\frac{3}{2}})$	$\Delta^1\delta$
PEPC	9.85	0.00
PMMA	9.30	0.55
PEEMA	9.16	0.69
PTHFMA	8.97	0.88
PGMA	8.81	1.04

1)  $\Delta = (\delta_{\text{PEPC}} - \delta_x)$

Table 6.2. Dipole Moments of Molecules Corresponding to Homopolymer Repeat Units or Parts Thereof

Molecule	Structure	$\mu$ (D)
Methyl isobutyrate	$  \begin{array}{c}  \text{CH}_3 \quad \text{O} \\    \quad // \\  \text{CH}_3 - \text{C} - \text{C} \\    \quad \backslash \\  \text{H} \quad \text{OCH}_3  \end{array}  $	1.98
Di-ethyl ether	$\text{CH}_3 - \text{CH}_2 - \text{O} - \text{CH}_2 - \text{CH}_3$	1.23-1.28
THF		1.69
Propylene oxide	$  \begin{array}{c}  \text{CH}_3 \text{CHCH}_2 \\  \quad \backslash \quad / \\  \quad \quad \text{O}  \end{array}  $	1.9-2.0
1-Chloroethyl ether	$  \begin{array}{c}  \text{CH}_2 - \text{CH}_2 - \text{O} - \text{CH}_2 \text{CH}_3 \\    \\  \text{Cl}  \end{array}  $	1.8

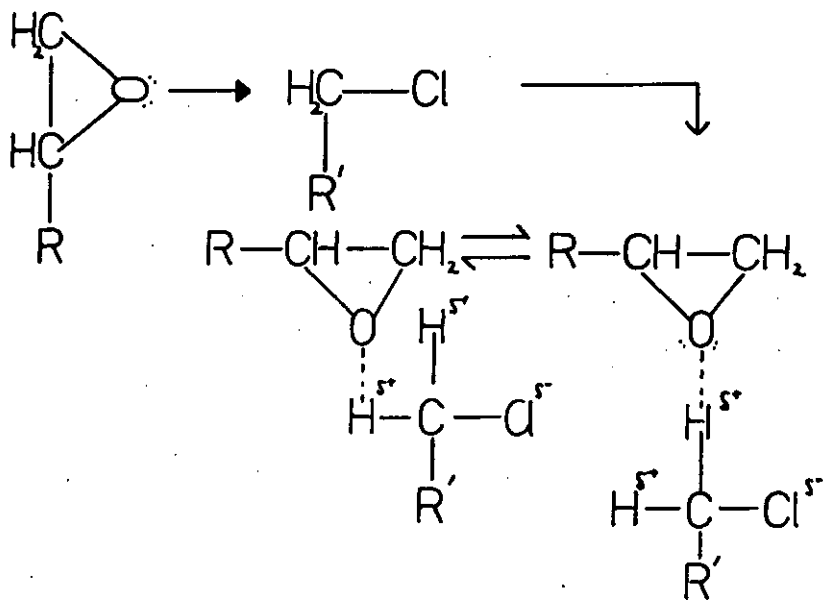
increasing electronegativity along the series corresponds to the order of increasing miscibility with PEPC. The nature of the specific interaction between the species can be envisaged as arising from two types of alignment. The  $\text{CH}_2\text{Cl}$  group of PEPC can interact with the methacrylate carboxyl group and the various forms of oxygen held in the esters side chains. This is illustrated for PGMA/PEPC in Figure (6.7). Similar types of interaction have been found in blends of PVC/poly( $\epsilon$ -caprolactone)<sup>(85)</sup> (PCL), PCL/PEPC<sup>(209)</sup> and PVC with a terpolymer of ethylene, vinyl acetate and carbon monoxide<sup>(210)</sup>.

Chiou. *et al.*<sup>(212)</sup> have recently found blends of poly(methyl acrylate) and poly(epichlorohydrin) to be miscible. However they concluded that on the basis of the additivity of the specific volumes of the components, the specific interaction between them was very weak. Obviously in this instance the only probable interaction is between the carboxyl and  $\text{CH}_2\text{Cl}$  groups. The interaction between the methacrylate carboxyl group and  $\text{CH}_2\text{Cl}$  would be of similar strength in all the blends investigated if present and consequently it cannot be responsible for the differences in miscibility observed. Therefore the latter interaction, which becomes stronger as the electronegativity of the ester side group increases can be regarded as the major factor influencing miscibility.

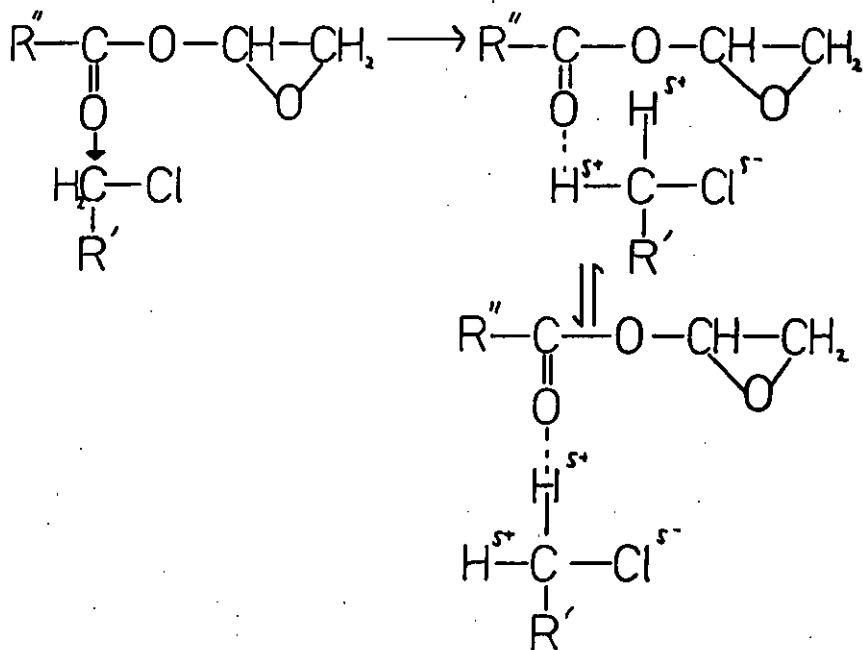
The interaction between  $\text{CH}_2\text{Cl}$  and the side group oxygen in blends of PEPC with PEEMA, PTHFMA and PGMA is akin to a hydrogen bond. However even in the case of PGMA/PEPC the interaction is very weak compared to that of a conventional hydrogen bond such as is found in water. This is due to the fact that the hydrogen atoms attached to the chlorine bearing carbon in PEPC are not markedly electropositive, the electron clouds of each being equally displaced towards the chlorine. The effect is somewhat greater in PVC for example where the carbon bearing the halogen has only one hydrogen attached to it. Consequently one would

Figure (6.7)  
Possible Specific Interactions Between  
PGMA and PEPC

a)



b)



expect a stronger interaction between PGMA and PVC than between PGMA and PEPC. However the former pair are immiscible in all proportions<sup>(211)</sup> possibly due to the greater flexibility of the pendant halogen bearing carbon atom in PEPC in comparison with CHCl group in PVC which forms part of the polymer backbone. Obviously this greater flexibility could facilitate co-ordination with the glycidyl methacrylate side-group. Additionally the polymer chain in PVC is more rigid than in PEPC, again facilitating inter-group attraction in blends of the poly-(ether).

The comparative weakness of the specific interaction is further evidenced by the fact that the glass transition temperatures of PGMA/PEPC blends were not found to be consistently elevated above the predicted values due to densification as found by Kwei *et al.*<sup>(203,204)</sup>. Consequently it is apparent that slight changes in polymer structure which alter the strength of interaction with a second component can significantly effect miscibility.

It is clear from the homopolymer blend studies conducted here and examination of comparable literature that when the experimental probe used is the glass transition behaviour, the assignment of a blend to a category of miscibility requires caution. Firstly in order to distinguish between miscible, partially miscible and microheterogeneous blends, measurements need to be performed across the complete range of composition. For example, if measurements were conducted only at the extremes of concentration then a single transition would have been apparent in blends of PEEMA, PTHFMA and PGMA with PEPC. Due to the relative volumes of the phases the partial miscibility of PTHFMA/PEPC was only clearly discernible in the intermediate composition range. Blends with PEPC of PGMA and PEEMA displayed a single composition dependent  $T_g$  and it was found that the miscible blend showed a smaller

degree of deviation from the Fox expression than the microheterogeneous blend. However as detailed earlier a number of miscible systems exhibit a composition dependence which can be more accurately represented by an expression such as the Gordon-Taylor. Application of this equation to the two systems using suitable values of K reveals that both sets of data display wide variations from the predicted values. Consequently assignment of miscibility or microheterogeneity to a mixture on the basis of the proximity of the glass transition data to that predicted using one of the relationships listed in section (2.5.4) can depend on the relationship chosen. It has been shown that a much less ambiguous method of differentiating between these two categories of mixing is to measure the breadth of the glass transition process, particularly at intermediate compositions.

## CHAPTER 7

### DISCUSSION OF HOMOPOLYMER/COPOLYMER BLENDS

## 7.1 COPOLYMER PREPARATION

The Fineman-Ross and Kelen-Tudos plots for copolymers of glycidyl methacrylate and methyl methacrylate (Figures (5.1) and (5.2)) exhibit linearity up to feed compositions of 80 mole% GMA. However a feed of 90 mole% GMA produces a copolymer containing less GMA than expected. Using the values of the reactivity ratios calculated for those copolymers having feed compositions up to 80 mole% GMA the copolymerisation equation (equation (2.133)) predicts that a feed of 90 mole% GMA will produce a copolymer containing 83 mole% GMA, yet analysis of the product revealed a composition of only 76% GMA. The copolymerisations were taken to a conversion of 10%, although strictly speaking the copolymerisation equation is only valid instantaneously. Nevertheless the deviation in composition cannot be explained by composition drift in the monomer feed as the feed would become progressively richer in GMA as would the copolymers produced if this were the case. Consequently the observation can only be rationalised by postulating that the relative reactivities of the two species changes at very high feed ratios producing copolymers richer in GMA than one would expect on the basis of observations at feeds of 80 mole% GMA and below.

The preparation of random copolymers of GMA/MMA has been reported in the literature although not at feed ratios above 40 mole% GMA. Iwakura *et al.* (214) determined the reactivity ratios during bulk copolymerisation at 60°C and found  $r_{\text{GMA}}$  and  $r_{\text{MMA}}$  to be 0.88 and 0.76 respectively. Sorokin *et al.* (215) measured values of  $r_{\text{GMA}} = 0.94$  and  $r_{\text{MMA}} = 0.75$  for solution copolymerisations in toluene and cyclohexanol but did not specify the conditions employed. Similarly Gluckman *et al.* (216) quoted the ratios as  $r_{\text{GMA}} = 1.05$  and  $r_{\text{MMA}} = 0.8$  using an unspecified mode of radical polymerisation. No literature values are available for radical copolymerisation of the species at 79°C in MEK;



the method employed in this study. However the measured values of 0.44 and 0.31 for  $r_{\text{GMA}}$  and  $r_{\text{MMA}}$  respectively do agree with the literature values in that  $r_{\text{GMA}} > r_{\text{MMA}}$ .

Copolymers of both styrene/methacrylonitrile and methyl methacrylate/methacrylonitrile exhibited linear Fineman-Ross and Kelen-Tudos plots as shown in Figures (5.25)-(5.26) and (5.61)-(5.62) respectively. This indicates the applicability of the copolymerisation equation to these systems over the composition ranges investigated. Comparison is made in Table (7.1) between the measured and literature values of the reactivity ratios for the two systems. It is apparent that there is good agreement between the two sets of data.

In all copolymerisations undertaken the degree of conversion was limited to  $\leq 10\%$  in order to ensure the production of compositionally homogeneous copolymers. Given that the reactivities of the two species were different, in each case the monomer mixture would become richer in the less reactive component as the degree of polymerisation increased, leading to the formation of copolymers containing ever increasing proportions of this monomer. Compositional homogeneity is important here as there is a large body of evidence to suggest that phase separation can occur within heterogeneous random copolymers. Molau<sup>(221)</sup> determined the tolerance of blends of various pairs of styrene/acrylonitrile copolymers to compositional variation. It was found that a difference of 3.5-4.5 wt.% acrylonitrile content was sufficient to cause phase separation. Kollinsky and Markert<sup>(222)</sup> similarly blended pairs of homogeneous copolymers of methyl methacrylate/n-butyl acrylate and found that to form homogeneous mixtures the difference in composition had to be between 0-20 mole% MMA. Obviously when there is a drift in composition during copolymerisation a continuous range of copolymer compositions are formed rather than two homogeneous species.

Table 7.1. Reactivity Ratios for Methacrylonitrile Copolymers

Comonomer (2)	$r_{\text{MAN}}$	$r_2$	T(°C)	Remarks
Styrene	0.25	0.25	80°C	Bulk polymerisation, peroxide catalyst (0.1%) <sup>(217)</sup>
Styrene	0.26	0.38	80°C	Bulk polymerisation, peroxide catalyst <sup>(218)</sup>
Styrene	0.24	0.39	60°C	Determined in this study, details in Table (3.2)
MMA	0.70	0.74	80°C	Bulk polymerisation, peroxide catalyst (0.1%) <sup>(218)</sup>
MMA	0.65	0.67	60°C	Bulk polymerisation, peroxide catalyst <sup>(219)</sup>
MMA	0.80	0.68	80°C	Conditions not given <sup>(220)</sup>
MMA	0.68	0.71	60°C	Determined in this study, details in Table (3.2)

Kollinsky and Markert<sup>(222)</sup> found that in copolymers with broad continuous chemical distributions microphases were formed containing mutually miscible macromolecules. Zimmt<sup>(223)</sup> blended PMMA with chemically heterogeneous copolymers of methyl methacrylate/n-butyl acrylate and found that when the overall MMA content of the copolymer was 77 wt.% clear films were formed which exhibited two glass transition temperatures. The first phase corresponded to an MMA rich fraction of copolymer dissolving in PMMA, thereby introducing some butyl acrylate and reducing  $T_g$ . The second phase contained copolymer which was thus richer in butyl acrylate and exhibited a  $T_g$  below that of the unblended copolymer. When a homogeneous copolymer of the same composition was blended with PMMA opaque films were formed. This was taken to indicate the need for some copolymer species soluble in both phases in order to control the size of the dispersed phase.

## 7.2 GLYCIDYL METHACRYLATE-CO-METHYL METHACRYLATE/POLY(EPICHLOROHYDRIN) BLENDS

The thermal analysis results for this series of blends indicate a single transition up to 50 wt.% copolymer which is rich in PEPC and tends to broaden with increasing copolymer content. At higher overall copolymer loadings the breadth and shape of the transitions in nearly all cases makes assignment of a single glass transition temperature a rather arbitrary process using the double tangent technique. Consequently whilst acknowledging that the data indicates a series of blends whose state of mixing appears intermediate between partial miscibility and microheterogeneity detailed discussion will be limited to the data collected by the dynamic mechanical technique.

Inspection of Figure (5.23) reveals that for copolymers containing 50-72 mole% GMA blended with PEPC the mixtures appear to exhibit decreased

mutual solubility in the overall composition range of 40-80 wt.% copolymer. This is evidenced by the appearance of two relaxation peaks or a considerable increase in peak breadth. There is a tendency however for the range of minimum miscibility to shift to higher copolymer concentrations as the GMA content increases. At blend compositions which yield a single glass transition temperature,  $T_g$  exhibits negative deviations from the Fox predicted values when the mixture is rich in elastomer and positive deviations when the glassy component is in excess. This type of behaviour was also found for mixtures of PTHFMA/PEPC as discussed in section (6.4).

Observations of the optical clarity of the blends showed that the onset of optical heterogeneity corresponded quite closely with the composition region of minimum miscibility. An exception to this was found in blends of copolymer K, containing the minimum amount of GMA, which appeared transparent at all compositions, yet clearly displayed two transition processes in the overall composition region of 40-60 wt.% copolymer. The refractive indices of copolymer K and PEPC are quite closely matched such that phases of 22 and 59 mole% copolymer would be expected to have indices differing by about 0.004. However this difference is obviously sufficient to provide a visual contrast as the refractive indices of the two phases observed at 60 wt.% copolymer in blends of copolymer H/PEPC differ by the same amount yet the blend appears opaque. Consequently it appears that in the blends of copolymer K, the disperse phase must have a principal dimension in the region of 150-1,000 Å, such that it exhibits a glass transition but cannot be detected by natural light.

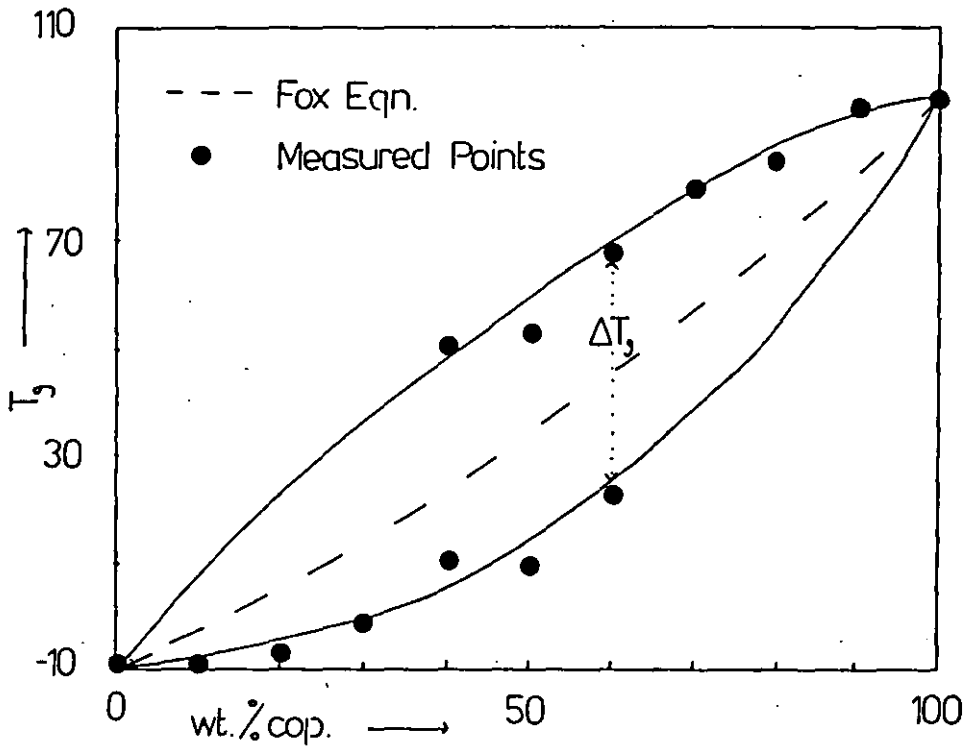
Disregarding the behaviour of blends containing the copolymer richest in GMA (copolymer J) for the present, what do the dynamic mechanical results tell us about the state of mixing in these systems?

Single glass transitions were observed in all blends at 10-30 and 90 wt.% copolymer, however as the overall difference in the quantities of the two components decreased transition width clearly increased. It was shown in chapter 6 that positive deviations from transition width additivity are good indicators of heterogeneity, so one can discount the possibility of miscibility at these compositions. Let us assume in the first instance that the blends are in fact made up of two phases whose glass transition temperatures vary with the overall blend composition. In Figure (7.1) the measured compositional variations of  $T_g$  are extrapolated to yield two curves lying above and below the line indicating the Fox predicted values of  $T_g$  for the system copolymer K/PEPC. The difference between the  $T_g$ 's of the two predicted phases ( $\Delta T_g$ ) is plotted against blend composition in Figure (7.2). This plot reveals that the greatest values of  $\Delta T_g$  are found in the intermediate composition range where there is clear evidence in fact of two processes occurring in this system. Extending this argument it is possible to interpret the apparently broadened unitary glass transitions observed as being due to the overlap of two processes. In the case of overall compositions rich in PEPC this would be expected to produce  $\tan \delta$  curves which rose quite steeply on the low temperature side but became increasingly diffuse on the high temperature side of the peak as  $\Delta T_g$  increased.  $\Delta T_g$  being  $> 20^\circ\text{C}$  at all compositions measured, the value of  $\tan \delta_{\text{max}}$  representing the major phase would not be expected to be influenced by this overlap process. The argument can be similarly extended to copolymer rich compositions and in both cases seems to fit the experimental observations. The effect of increasing  $\Delta T_g$  on the shapes of the loss peaks formed by overlap is illustrated in Figure (7.3).

Blends of PEPC with copolymers C, H and F behave similarly, however

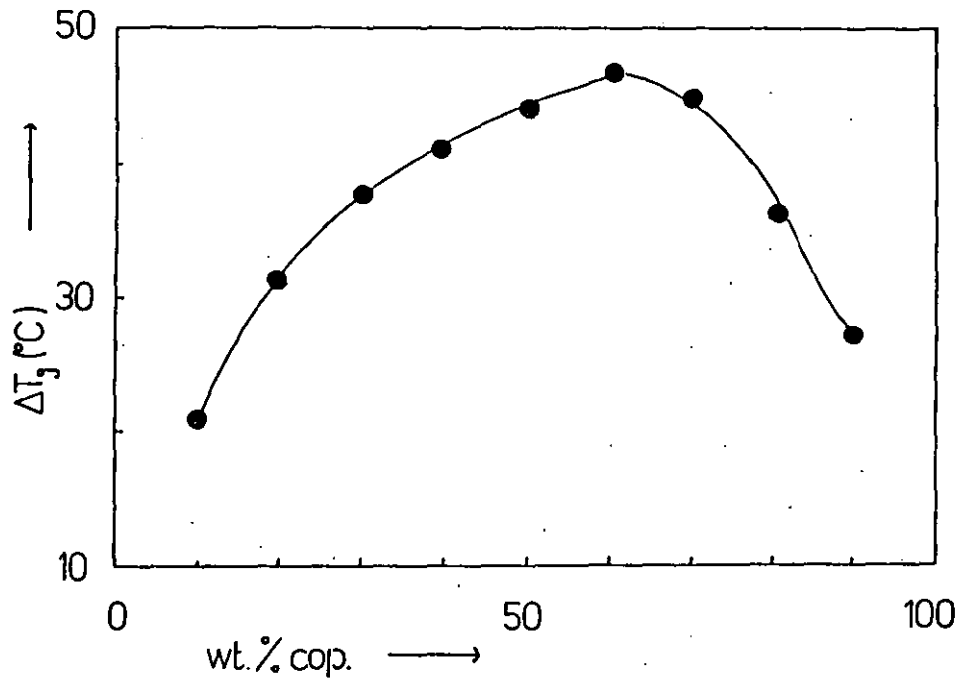
Figure(7.1)

Variation of  $T_g$  with Overall Blend Composition for Copolymer Rich and Copolymer Poor Phases in Copolymer K / PEPC Blends

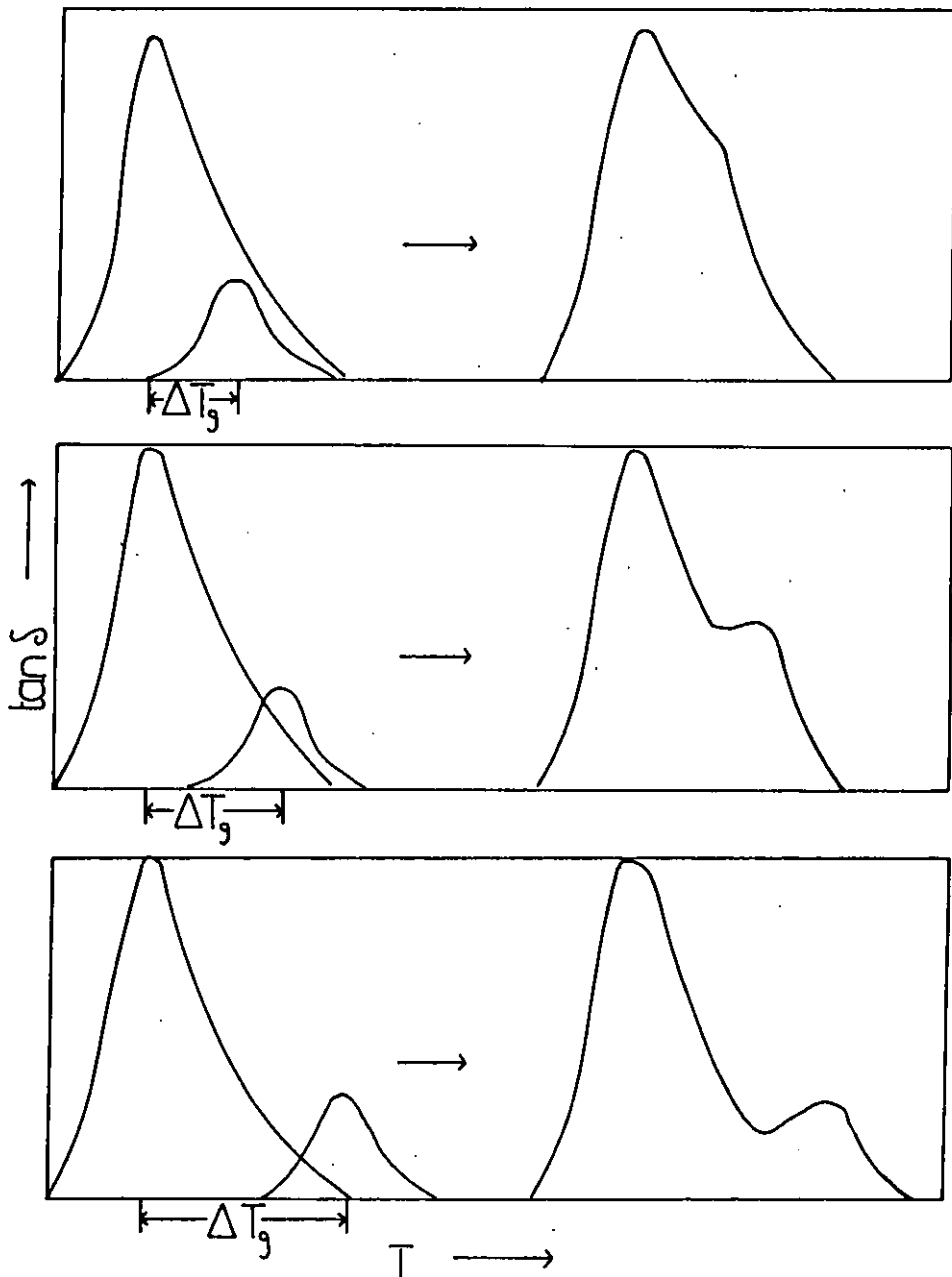


Figure(7.2)

Plot of Predicted  $\Delta T_g$  Values for Copolymer K / PEPC Against Blend Composition



Figure(7.3)  
Examples of Peak Broadening due to  
Transition Overlap



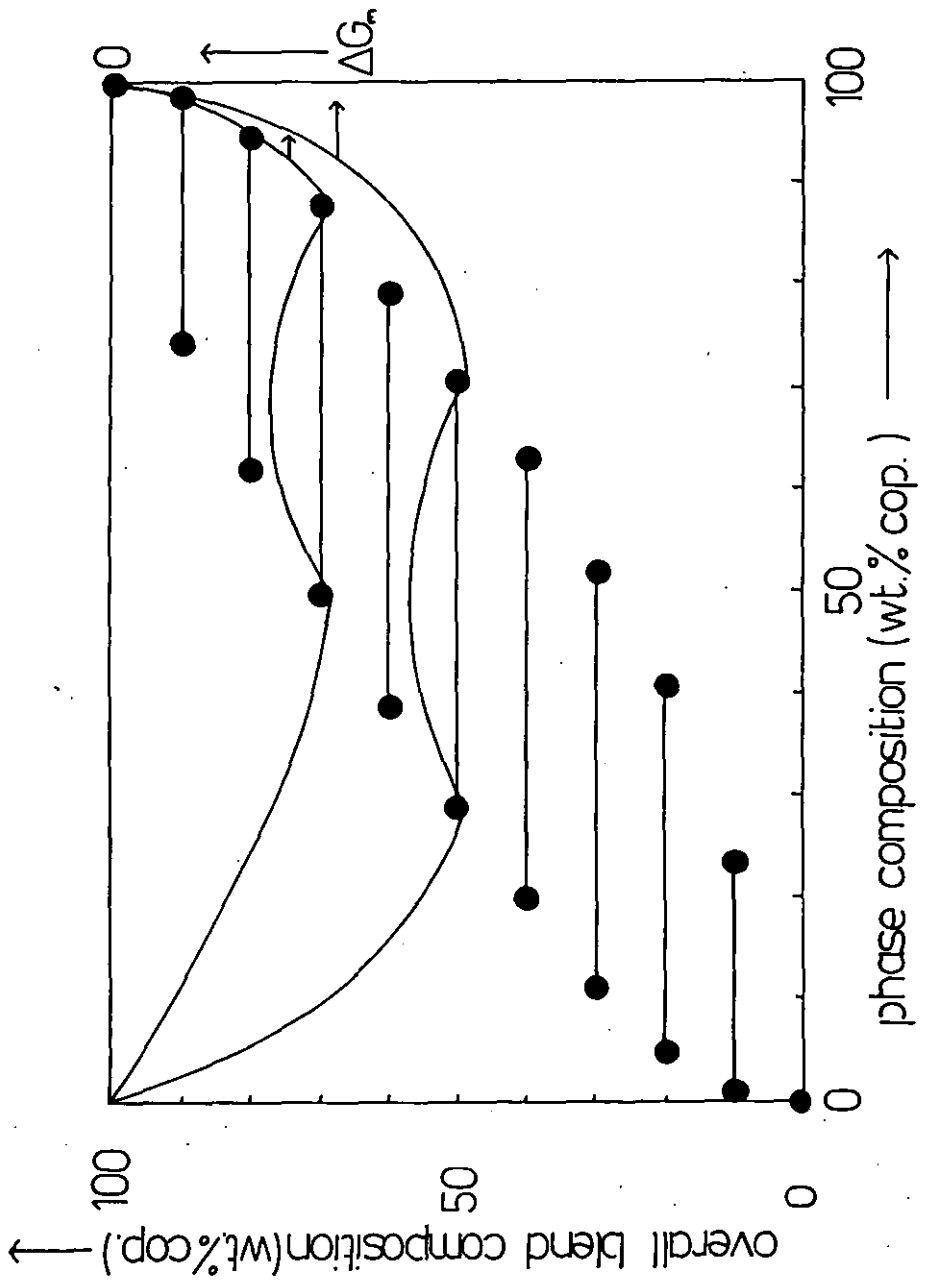
the shape of the composition vs. phase  $T_g$  curves alters with increasing copolymer GMA content such that the  $\Delta T_g$  maxima gradually shift to higher overall contents of copolymer. Consequently it appears that blends of copolymers containing 50-72 mole% GMA with PEPC are partially miscible but as with PTHFMA/PEPC phase composition alters with overall blend composition. The only alternative explanation is that the blends are microheterogeneous at the extremes of overall composition, but partially miscible in the intermediate range. This type of behaviour has not been reported previously and cannot be supported by any credible explanation.

In chapter 6 it was proposed that the composition dependent partial miscibility observed in blends of PTHFMA/PEPC could result from the complex shape of the free energy of mixing vs. composition curve. However closer examination of this proposition reveals that this type of miscibility behaviour cannot be described by a single  $\Delta G_m$  function which is valid at all compositions. The only way in which the data can be expressed in this context is by assuming that the  $\Delta G_m$  composition function varies with overall composition. This is depicted in Figure (7.4) where overall composition is plotted against phase composition for copolymer K/PEPC blends. Phase composition has been calculated from the measured and inferred phase glass transition temperatures using the Fox equation. Phase compositions correspond to the minima in the free energy curve and on this basis a number of possible  $\Delta G_m$  functions have been included in the figure. Although this approach describes the data one can only justify the assignment of a separate  $\Delta G_m$  curve to each composition if the temperature at which the phase relationship is established varies continuously with overall blend composition. Prior to measurement all samples were annealed at a temperature  $10^\circ\text{C}$  above the copolymer  $T_g$ . In terms of the conventional



Figure(74 )

Phase Composition vs. Overall Blend Composition  
for Copolymer K / PEPC Blends



view of partial miscibility, at this temperature ( $T_a$ ) two phases will be formed of different composition. All overall blend compositions lying between those of the two phases will phase separate in the same way such that the overall composition will be reflected in the relative volumes of the two phases but not in their composition. Prior to measurement samples were allowed to cool naturally to ambient temperature but given the small sample size ( $\approx 20$  mg.) in most cases this process could be expected to be rapid. Provided there was sufficient time, the composition of the two phases could change on cooling from  $T_a$  as in effect the mixture would pass from one tie line to the next. This process could continue until the mixture reached room temperature unless general translational mobility was halted in one phase at a higher temperature at which the copolymer rich phase entered the glassy state. Whether the measured phase composition is established at  $T_a$  or at a lower temperature, within this scheme one cannot explain composition dependent partial miscibility. Whilst overall blend composition should not influence phase composition, as the PEPC content rises so does the volume of the copolymer poor phase and hence the general level of translational mobility within the blend at any particular temperature above  $T_g$ . Therefore one could postulate that as the blend copolymer content decreases an increasing amount of PEPC diffuses from the copolymer poor phase and becomes associated with the copolymer rich phase although not intimately intermixed. This would result in the copolymer poor phase becoming relatively richer in copolymer and thus displaying a higher  $T_g$  and the copolymer rich phase becoming similarly richer in PEPC causing its  $T_g$  to be depressed and broadened assuming incomplete mixing. In fact the trend observed in the experimental data is for the proportion of PEPC present in each phase to rise as the overall PEPC content increases. The only way

in which these results can be explained is by assuming that at temperatures less than or equal to  $T_a$  the general level of translational mobility is such that the blends cannot achieve thermodynamic equilibrium within the time-scale allowed. Therefore the phases formed at each overall blend composition correspond to points only part-way along the tie-line. If the initial point on the tie-line is taken to correspond to the overall composition then the compositions of the non-equilibrium phases formed will shift with overall composition in the same manner. This explanation corresponds with the experimental findings for blends of copolymers K, C, H and F with PEPC.

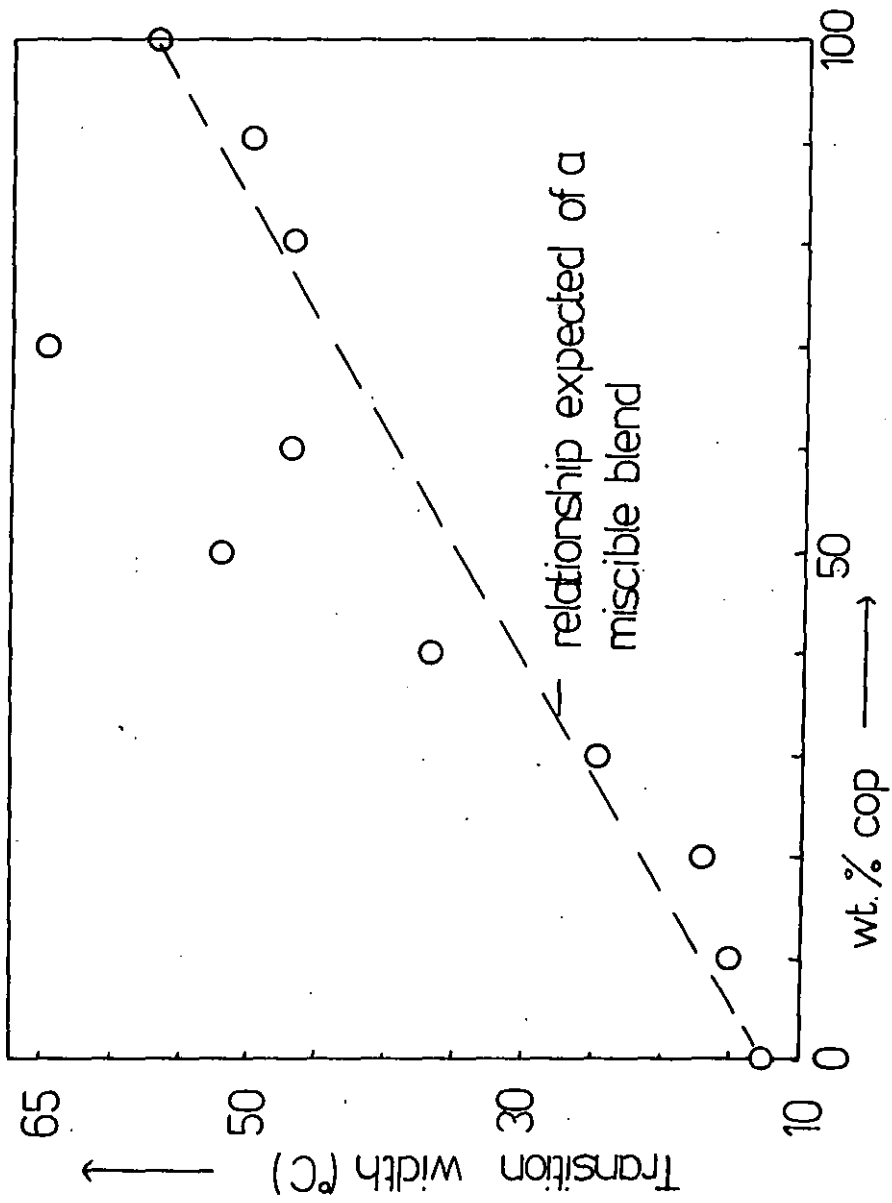
Blends of copolymer J/PEPC were found to behave somewhat differently. Single, broadened loss tangent peaks were observed at each composition and the shape of the  $T_g$  vs. concentration plot (Figure (5.22)) does not lend itself to the type of extrapolation performed in Figure (7.1). The shape of the compositional variation of  $T_g$ , the broadening of the glass transition process at intermediate compositions and the optical clarity observed independent of the relative quantities of the two components tend to indicate that this blend is microheterogeneous.

Generally blend miscibility tends as expected to increase as the content of the species (GMA) which interacts favourably with the homopolymer increases in the copolymer. Examination of the data measured on the microheterogeneous blend indicates that this mixture is on the threshold of miscibility. The transition widths, measured by DMTA, at half peak height are plotted against composition in Figure (7.5) and follow the pattern predicted on the basis of additivity except in the range 40-70 wt.% copolymer.

Using the classification of MacKnight *et al.*, discussed in section (2.3.1) these blends can be described as type (c) systems. This is because the homopolymer interacts favourably with one copolymer segment

Figure (7.5)

Composition Dependence of Transition Width for CopolymerJ /PEPC Blends



(GMA) but not with the other (MMA) as shown in chapter 6. Furthermore there is no specific interaction between the dissimilar copolymer segments. Some representative example of systems of this type are listed in Table (7.2), which is arranged so that it is comonomer 1 which interacts favourably with the homopolymer. Although the blends have been described as miscible in the copolymer composition ranges stated it should be noted that in the styrene-co-maleic anhydride/PP0<sup>(191)</sup> blends even at a concentration of 8 wt.% maleic anhydride the  $\tan \delta$  peaks were broadened. Similarly in the system styrene-co-p-chlorostyrene/PP0<sup>(225)</sup> it was found that the breadth of the glass transition process became gradually broader as the p-chlorostyrene concentration increased until at compositions  $> 67$  mole% 2 transitions were observed. It would appear therefore that although the composition at which two discrete phases are formed is easily measured division of the regions of microheterogeneity and miscibility is rather more difficult. Nevertheless it is clear that as the concentration of the interacting segment within the copolymer increases so does miscibility.

Using indirect methods of measurement ten Brinke *et al.*<sup>(99)</sup> have produced a list of the segmental interaction parameters present in blends of PP0 with copolymers of styrene-co-ortho or parahalogenated styrenes. Employing the approach of Krause, the range of copolymer composition giving rise to miscibility can be approximated by finding the region within which the effective interaction parameter ( $\chi_{\text{eff}}$ ) falls below the critical value of the interaction parameter ( $\chi_{\text{CR}}$ ) given by equation (2.43). As chain length increases  $\chi_{\text{CR}}$  will tend towards zero, so miscibility would be predicted at those compositions at which  $\chi_{\text{eff}} < 0$  in a blend of two high polymers. Inserting the tabulated segmental interaction parameters<sup>(99)</sup> into the expression for  $\chi_{\text{eff}}$  (equation (2.66)) set equal to zero yields a value of 28 mole% St. as

Table 7.2. Examples of Systems in Which the Homopolymer Interacts Favourably with One Copolymer Segment Type

Homopolymer	Comonomer 1	Comonomer 2	Range of Conc. of Comonomer 1 Over Which Miscibility Observed	Reference
Poly(2,6-dimethyl 1,4-phenylene oxide) (PPO)	Styrene	p-chlorostyrene	35-100 mole % St.	(224)
PPO	Styrene	p-chlorostyrene	33-100 mole % St.	(225)
PPO	Styrene	Maleic anhydride	92-100 wt. % St.	(191)
Poly(styrene)	PO	Brominated PO (1 bromine atom per segment on average)	13-100 wt. % PO	(226)

the limit of miscibility for the system PPO/poly(styrene-co-p-chloro-styrene). This compares quite favourably with the experimentally determined limit of 35 mole% St. However if instead of using experimentally deduced values of the segmental interaction parameters for the segments which interact unfavourably, one calculates them on the basis of solubility parameters, a limiting value of 36 mole% St. is reached. In this calculation  $\chi_{St/pClSt}$  and  $\chi_{PPO/pClSt}$  were determined using the form of Hildebrand's expression given in equation (2.75). However  $\chi_{PPO/St}$  being negative cannot be calculated in this way, consequently the measured value was used again. The success of this approach indicates that at the temperature at which phase behaviour was determined the so called free-volume terms have a negligible effect. Furthermore it is clear that  $\chi_{St/pClSt}$  and  $\chi_{PPO/pClSt}$  are only influenced by the relative dispersion forces of the dissimilar species.

If this same approach is applied to the system PPO/poly(styrene-co-maleic anhydride) the predicted range of miscibility is much greater than that found experimentally. Solubility parameter calculations indicate that the segmental interaction within the copolymer is extremely unfavourable and as this term makes a negative contribution to  $\chi_{eff}$  it results in the prediction that  $\chi_{eff}$  is negative in the range 50-100 mole% St. The experimentally measured range was 92-100 mole% St., therefore in order to arrive at a prediction within this range  $\chi_{St/MAL.ANH}$  has to be reduced. One can rationalise this reduction on the basis of there being a specific interaction between the species, which although not sufficient to make the interaction parameter negative serves to reduce the mutual antagonism of the two segment types. Given the miscibility of PST with PPO and poly(vinyl methyl ether) the existence of a slightly favourable interaction between styrene and an oxygen bearing species such as maleic anhydride is not beyond the

bounds of possibility.

The foregoing strategy was then applied to PEPC blends with GMA-co-MMA.  $X_{\text{GMA/MMA}}$  and  $X_{\text{MMA/PEPC}}$  were calculated using solubility parameters and  $X_{\text{GMA/PEPC}}$  was determined as a function of miscibility limit (Figure (7.6)). It is apparent that as the miscibility limit moves to higher GMA concentrations the cause of this is an increase in  $X_{\text{GMA/PEPC}}$ . The dynamic mechanical results have indicated that at a copolymer content of 76 mole% GMA the system is tending towards miscibility. Therefore, if one assumes that the actual miscibility limit is of the order of 80 mole% GMA this implies that  $X_{\text{GMA/PEPC}}$  is in the region of -0.003. This value was read off from Figure (7.6), the miscibility limit having been first converted to a volume percentage.

It would therefore appear that although there is indeed a favourable specific interaction between glycidyl methacrylate and epichlorohydrin, it is very weak. By comparison ten Brinke *et al.*<sup>(99)</sup> have deduced that the interaction between PPO and PST is of the order of -0.1. However it should be borne in mind that this latter system is one of the most miscible yet determined in that phase separation does not occur at any accessible temperature.

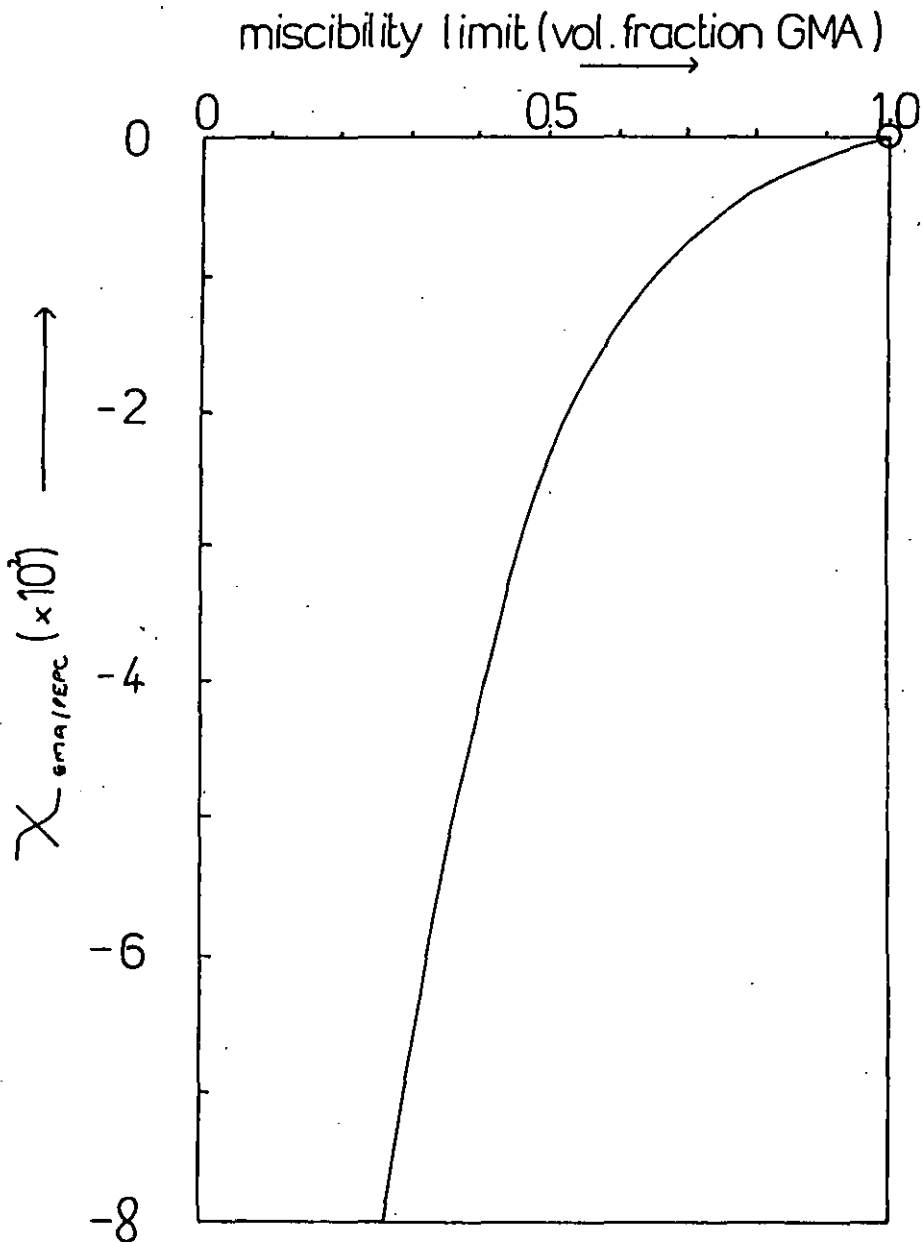
The small favourable interaction between PGMA and PEPC is very much in line with the results obtained on the miscibility behaviour of the homopolymer systems discussed previously. The relatively small changes in structure along the methacrylate series, although having a marked effect upon miscibility would not be expected to produce large changes in the segmental interaction parameter values.

Within the range of copolymer compositions studied miscibility was not quite attained. On account of the fact that miscibility invariably decreases in macromolecular mixtures with increasing temperature, detailed studies were not conducted on samples annealed above 105°C.



Figure(7.6)

Calculated Value of  $\chi_{GMA/PEPC}$  as a Function of the Limiting Concentration of GMA in Copolymers with MMA Necessary for Miscibility



Furthermore although quenching from elevated temperatures could in principle provide additional information on the nature of the phase diagram the observed tendency of the copolymers to crosslink on annealing above 120°C (as in PGMA) would make any such measurements strictly incomparable with those made on linear blends.

It has been shown that providing a specific interaction exists only between the homopolymer and one type of copolymer segment, the mean field approach can successfully predict the range of miscibility. Inspection of the expression for  $\chi_{\text{eff}}$  (equation (2.66)) shows that the only relevant concentration variable is the copolymer composition. Miscibility is not predicted to alter as the proportions of homopolymer to copolymer change. This provides further justification for the extrapolation of the  $T_g$  vs. composition plots, thus depicting partial miscibility over the complete range of overall blend composition.

### 7.3 STYRENE-CO-METHACRYLONITRILE/POLY(EPICHLOROHYDRIN) BLENDS

In chapter 5 it was shown that depending upon the composition of the copolymer, the miscibility behaviour of an SM copolymer with PEPC could be assigned to one of three general categories. Blends of PEPC with PST, PMAN and the copolymers richest in styrene and methacrylonitrile behaved similarly in that each blend exhibited 2 glass transition temperatures at positions close to those of the pure components. Analysis of the shift in glass transition temperatures within the blends using the Fox relationship indicated that the maximum content of component 2 in a phase rich in component 1 was about 7 wt.%. Consequently it is clear that in these systems mutual solubility is negligible. Table (7.3) lists the various solubility parameters and the maximum degrees of polymerisation which can be tolerated for miscibility according to the Krause scheme. Blends of SMI appear the most miscible.

Table 7.3. Calculated Degree of Polymerisation Tolerable for Miscibility in Measured 2 Phase Systems

Component (A)	$\delta(\text{cal s}^{\frac{1}{2}}/\text{cm.}^{\frac{3}{2}})$	$(\delta_A - \delta_{\text{PEPC}})$	$X_{\text{A/PEPC}}^*$	Maximum Degree of Polymerisation ( $x_1 = x_2$ ) at 373K
PEPC	9.85	-	-	-
PMAN	11.17	1.32	0.236	8.5
PST	9.36	-0.49	0.032	62.0
SM1	9.71	-0.14	0.003	667.0
SM4	10.30	0.45	0.027	74.0

$$* X_{\text{A/PEPC}} = V_R/RT(\delta_A - \delta_{\text{PEPC}})^2$$

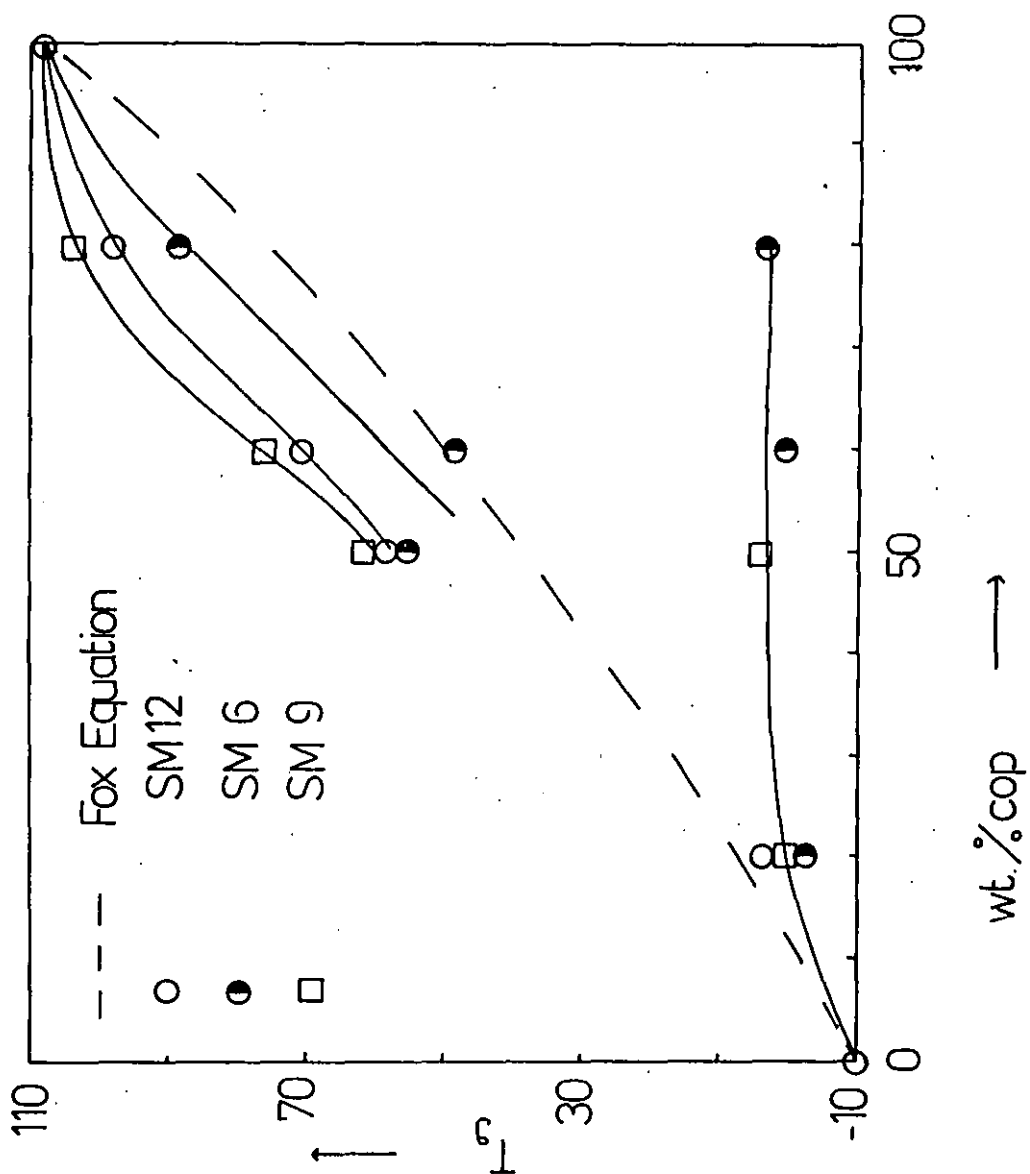
$$X_{\text{CR}} = \frac{1}{2}(x_A^{-\frac{1}{2}} + x_{\text{PEPC}}^{-\frac{1}{2}})^2$$

on this basis, however the actual degrees of polymerisation of the copolymer and PEPC are about 3 and 6 times respectively above the predicted limit for miscibility. The observed immiscibility of these systems is therefore to be expected due to the mismatch of the dispersion forces of the various blend pairs. Furthermore the chemical structures of the components do not readily suggest the possibility of specific interactions. Literature reports of the miscibility of PEPC with various other polymers do not abound, however in a fairly comprehensive but rudimentary study Peterson *et al.* (189) found that PEPC and PST phase separated in solution and produced opaque films.

Given the immiscibility of the aforementioned systems one can reasonably assume that copolymers richer in styrene than SM1 and richer in methacrylonitrile than SM4 are also immiscible. Blends containing copolymers of compositions between those of SM1 and SM4 were found to display increased mutual solubility. Copolymers in the ranges  $37.5 \leq x \leq 47.0$  and  $54.3 \leq x \leq 57.8$  mole% MAN formed a further miscibility category termed type (c) in chapter 5. These blends generally exhibited a single major glass transition process which was considerably broadened with respect to the weighted average transition width. There was also, at overall compositions containing  $\geq 50$  wt.% copolymer, evidence of a small low temperature relaxation which was not particularly well resolved in most cases but whose position in the temperature plane was fairly constant.

In Figure (7.7) the glass transition temperatures determined by DMTA are plotted against composition for three of these systems. The line representing the predicted  $T_g$ 's according to the Fox equation should strictly be drawn in separately for each blend, however as the copolymers represented here differ in  $T_g$  by only  $2^\circ\text{C}$  the error involved is negligible. The general trend which this diagram indicates

Figure(7.7)  
 Composition Dependence of  $T_g$  for SM Copolymer  
 Blends with PEPC which Exhibit Partial Miscibility



is for the major transition to lie above the predicted line at  $\geq 50$  wt.% copolymer and below the line at  $< 50$  wt.% copolymer. It appears that the blends form two phases, the composition of the copolymer rich phase being dependent on the overall composition whilst the copolymer poor phase appears to be of constant composition. If the observed composition dependence of the copolymer rich phase is extrapolated, one can explain the fact that a relaxation corresponding to this phase was not observed at 20 wt.% copolymer due to the proximity of the glass transition temperatures. This would result in an overlap of the two processes producing a single peak whose maximum value corresponded to that of the PEPC rich transition, but which was considerably broadened at higher temperatures. This picture corresponds to the experimental data observed. At higher copolymer compositions  $\Delta T_g$  increases considerably so that transition overlap is not to be expected. The fact that the PEPC rich transition is not well defined in the blends at overall compositions  $\geq 50$  wt.%, and indeed cannot be distinguished in some cases, is indicative of the relative volumes of the two phases. Furthermore, the visual clarity of the blends indicates that the size of the disperse is such that it falls below the limit of detection of natural light. The breadth of the loss tangent curves corresponding to the copolymer rich transition is such that this phase seems to contain a range of blend compositions. The situation is elucidated further on inspection of the dynamic mechanical data obtained using solid bars of sample rather than supported films (Figures (5.44)-(5.45)). The loss tangent curves measured in the copolymer composition range under discussion, on samples containing equal weights of components, confirm the presence of a minor phase rich in PEPC. However the breadth of the major phase transition is twice that of the pure components lending credence to the view that there is a degree of heterogeneity

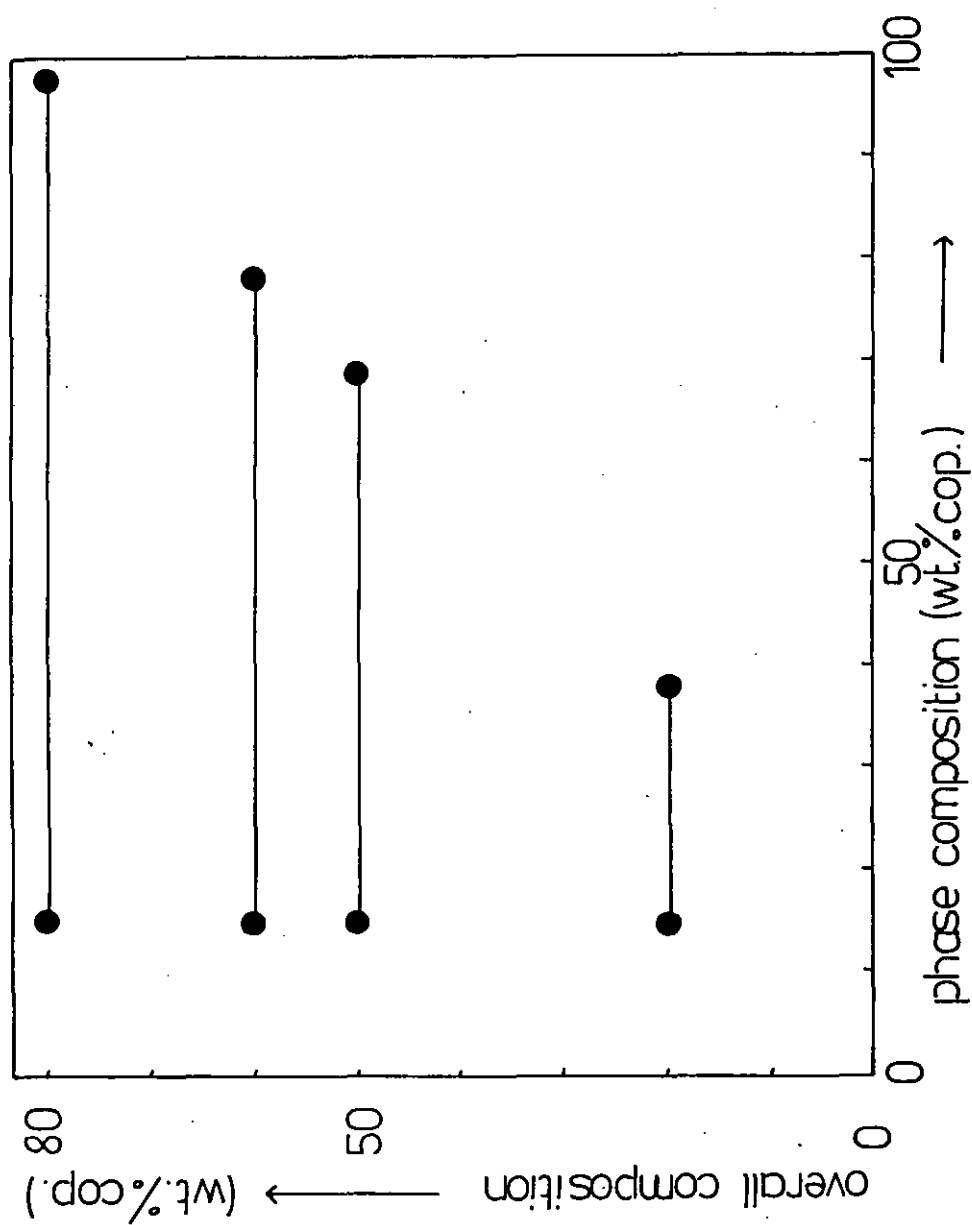
within this phase.

In Figure (7.8) phase composition is plotted against overall blend composition for SM9/PEPC mixtures. The independence of the elastomer rich phase of overall composition and the heterogeneity of the copolymer rich phase indicate that in this system the depression of the  $T_g$  of this latter phase with increasing PEPC content could result from diffusion of PEPC out of the PEPC rich phase. It is assumed that the quantity of PEPC which diffuses is a constant proportion of the volume of the copolymer poor phase. Therefore as the volume of this phase rises with the overall proportion of PEPC in the mixture so the  $T_g$  of the copolymer rich phase drops. Alternatively as with GMA-co-MMA/PEPC blends the observed phase behaviour could be due to there being a kinetic block to equilibrium phase separation. However in the SM/PEPC blends this block would only seem to restrict the attainment of the equilibrium phase composition in the case of the phase which is richer in copolymer.

The final category of blends had the properties of optical transparency; a single composition dependent  $T_g$  and little apparent broadening of the glass transition process. This mode of behaviour was only observed over a limited range of copolymer composition such that  $47.0 < n < 54.3$  mole% MAN. The composition dependence of the blend  $T_g$ 's showed slight deviations from the Fox predictions at the extremes of the overall concentration range. The deviations were consistently negative at low copolymer contents and similarly positive at high copolymer loadings so the data cannot be represented with any improvement by one of the alternative expressions to the Fox equation.

Dielectric relaxation studies performed on samples representing the immiscible (SM4/PEPC), partially miscible (SM9/PEPC) and miscible blends (SM3) were reported in section (5.2.5). Although PEPC homopolymer

Figure(7.8)  
Phase Composition vs. Overall Composition  
for SM9/PEPC Blends





gave rise to clear peaks in the plots of dielectric loss against frequency, this was generally not the case for the blend samples. It was therefore not feasible to assess blend heterogeneity by examination of the normalised dielectric loss plots. A further complication observed was that conductivity effects tended to obscure the relaxation processes as temperature was increased. In the case of PEPC this caused  $\tan \delta$  to rise steeply above 20°C at the lower end of the frequency range. In PEPC this effect can be attributed to the presence of impurities such as trace amounts of residual solvent. In multi-phase materials interfacial polarization can also contribute to conductivity effects if the dielectric constants of the phases are dissimilar. This latter process was considered by Maxwell, Wagner and Sillars and received attention in section (2.6.5).

The dielectric loss tangent vs. temperature plots provide the most suitable basis for comparison of the various samples. The frequency dependent  $\tan \delta$  peak observed for PEPC occurred over a temperature range characteristic of the  $\alpha$  relaxation process measured by DMTA and DTA. The structure of the polymer repeat unit indicates that one would expect to observe a  $\beta$  peak associated with the rotation of the  $\text{CH}_2\text{Cl}$  side group. However this type of process typically occurs at temperatures below about -60°C and was therefore outside the experimental temperature range.

SM4/PEPC exhibited a relaxation whose  $\tan \delta$  maximum was shifted 5°C upfield compared to that of PEPC at equivalent frequencies. This is indicative of a phase, the greater proportion of which consists of PEPC. This result compares with the dynamic mechanical data which revealed the presence of a phase whose  $T_g$  was 3°C above that of the pure elastomer. The shift relative to PEPC seen in SM9/PEPC of about 20°C is similarly comparable to that observed for the copolymer poor

phase by dynamic mechanical analysis. Whilst SM3/PEPC did not display a clear relaxation in the temperature region indicative of a PEPC rich phase the broad shoulder observed at  $-10 - 30^{\circ}$  does suggest a degree of heterogeneity in this system. The principal relaxation in this system, although somewhat obscured by conductivity effects can be related to the single glass transition process observed previously.

In conclusion it would appear that these results confirm the earlier miscibility classification of SM4/PEPC and SM9/PEPC, but tend to imply that the SM3/PEPC blend is not completely homogeneous. It should be noted however that the samples used for the dielectric work were compression moulded at a temperature some  $50^{\circ}\text{C}$  above the anneal temperature used for the dynamic mechanical film samples. Although samples were not quenched after moulding, it is possible that heterogeneous zones characteristic of the onset of phase separation were formed during the moulding process, and that equilibrium was not re-established on cooling prior to the formation of the glass. The applicability of this explanation can be tested by examination of the dynamic mechanical data measured on a similarly compression moulded sample (Figure (5.44)). The loss tangent curve exhibited by this sample has the breadth characteristic of a homogeneous phase, however there is a slight shoulder in the region  $-20 - 20^{\circ}\text{C}$  tending to support the notion of limited phase separation occurring at elevated temperatures.

The fact that no change in mechanical response was observed for films quenched from temperatures up to  $200^{\circ}\text{C}$  suggests that at this temperature the blend is still outside the spinodal. It is likely that the limited amount of phase separation observed in the moulded samples is beyond the detection limit of the instrument when the sample size is greatly reduced as in the case of cast films. Unfortunately measurements could not be performed at higher temperatures due to the

rapid degradation of the rubber.

The influence of copolymer composition on the miscibility of PEPC with SM copolymers was shown schematically in Figure (5.48). It appears that true miscibility occurs over a very limited composition range within the boundaries of the zone of partial miscibility. Let us now compare these results with those predicted on the basis of the mean field theory<sup>(98-100)</sup>. Assuming that dispersion forces dominate in this system as suggested earlier, the segmental interaction parameters calculated in Table (7.3) can be applied. On the same basis of calculation the interaction between the dissimilar copolymer segments is 0.44. The effective interaction parameter for the system is given by

$$\chi_{\text{eff}} = \chi_{\text{ST/PEPC}} \phi_{\text{ST}} + \chi_{\text{MAN/PEPC}} \phi_{\text{MAN}} - \chi_{\text{ST/MAN}} \phi_{\text{ST}} \phi_{\text{MAN}} \quad (7.1)$$

where the concentration terms refer to volume fractions of the respective species within the copolymer. If equation (7.1) is rewritten in terms of solubility parameters one obtains

$$\frac{RT\chi_{\text{eff}}}{V_R} = (\delta_{\text{ST}} - \delta_{\text{PEPC}})^2 \phi_{\text{ST}} + (\delta_{\text{MAN}} - \delta_{\text{PEPC}})^2 \phi_{\text{MAN}} - (\delta_{\text{ST}} - \delta_{\text{MAN}})^2 \phi_{\text{ST}} \phi_{\text{MAN}} \quad (7.2)$$

The copolymer solubility parameter ( $\delta_{\text{cop}}$ ) is defined as

$$\delta_{\text{cop}}^2 = \delta_{\text{ST}}^2 \phi_{\text{ST}} + \delta_{\text{MAN}}^2 \phi_{\text{MAN}} \quad (7.3)$$

Rewriting equation (7.2) in terms of  $\delta_{\text{cop}}$  one obtains

$$\frac{RTX_{\text{eff}}}{V_R} = (\delta_{\text{cop}} - \delta_{\text{PEPC}})^2 \quad (7.4)$$

Inspection of this expression reveals that using segmental interaction parameters which have all been calculated from solubility parameters  $X_{\text{eff}}$  cannot assume negative values.  $X_{\text{eff}}$  has been plotted against copolymer composition in Figure (7.9). The value of  $X_{\text{CR}}$  plotted in this diagram was determined from equation (2.43). The degree of polymerisation of the copolymer was calculated using the average value of  $\bar{M}_w$  assuming a repeat unit molecular weight intermediate between that of styrene and methacrylonitrile. Miscibility is predicted in the region of copolymer composition over which  $X_{\text{eff}} < X_{\text{CR}}$ . On this basis copolymers containing 69-77 volume% styrene fulfil the criteria for miscibility. This range corresponds to 33-43 mole% MAN, thereby underestimating the true range of miscibility by some 10 mole% MAN. In view of the simplistic assumptions which underpin solubility parameter theory this error is quite reasonable.

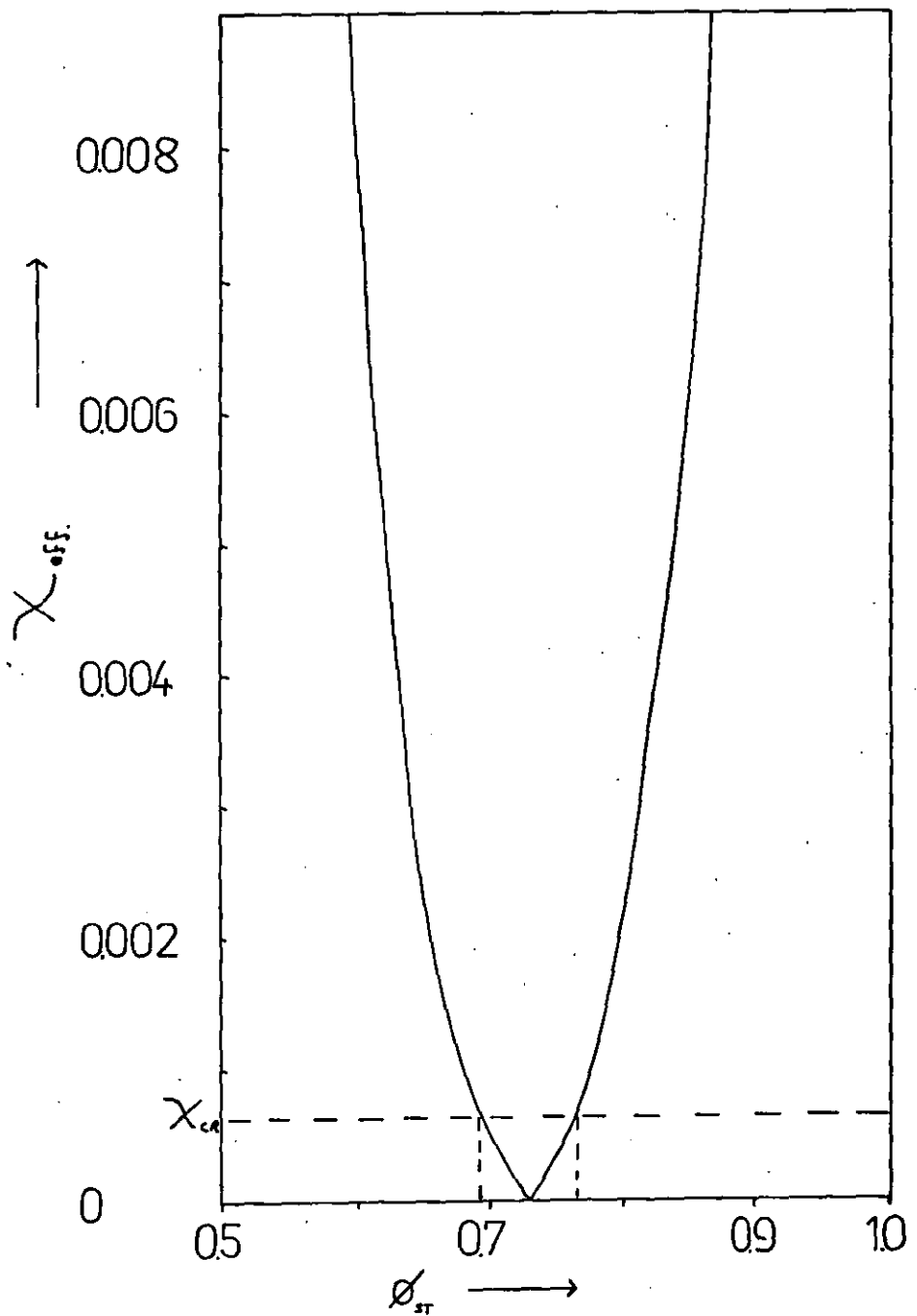
If one assumes that equation (7.1) is valid but that the individual segmental interaction parameters cannot be determined using solubility parameters, the relative  $X_{ij}$  values can be determined via the experimental miscibility limits. At the extremes of miscibility it is assumed that  $X_{\text{CR}} = X_{\text{eff}}$ . Substitution of the approximate copolymer compositions at the boundaries between the miscible and partially miscible zones yields two equations containing three unknowns. Simple manipulation yields the following equations

$$X_{\text{MAN/PEPC}} = X_{\text{CR}} + 0.377 X_{\text{MAN/ST}} \quad (7.5)$$

$$X_{\text{ST/PEPC}} = X_{\text{CR}} + 0.144 X_{\text{MAN/ST}} \quad (7.6)$$

Figure(7.9)

Variation of  $\chi_{\text{eff}}$  with Copolymer Composition for the System SM/PEPC



$$X_{\text{MAN/PEPC}} = 2.6 X_{\text{ST/PEPC}} \quad (7.7)$$

Therefore  $X_{\text{MAN/ST}} > X_{\text{MAN/PEPC}} > X_{\text{ST/PEPC}}$ . Whilst the segmental interaction parameters calculated using Hildebrand's relationship follow the same order of ranking the relative magnitudes of the three  $X_{ij}$  values do not correspond to equations (7.5)-(7.7). The most striking example of this can be shown by comparison of equation (7.7) with the equivalent expression determined using solubility parameters

$$X_{\text{MAN/PEPC}} = 7.3 X_{\text{ST/PEPC}} \quad (7.8)$$

A number of systems with the same general characteristics as SM/PEPC blends, in that an AB copolymer mixed with a homopolymer C displays miscibility over a limited range of copolymer composition, have been reported. A further property shared by these systems is that homopolymers A and B are immiscible with homopolymer C. Mixtures of poly(methyl methacrylate) and styrene/acrylonitrile copolymers (SAN) have been reported as miscible by a number of authors. Schmitt<sup>(227)</sup> has claimed that the system was miscible when the copolymer contained 10-39 wt.% acrylonitrile. Blends containing copolymers lying at the extremes of this range were found to phase separate on heating, whilst SAN samples containing 19 wt.% AN remained miscible up to at least 300°C. Miscible PMMA/SAN mixtures were investigated further by Naito *et al.*<sup>(228)</sup> who deduced the excess entropy and enthalpy of mixing of the system to be miniscule. Infra-red measurements showed the methacrylate carbonyl stretching frequency to have been shifted slightly downfield. This indicates the presence of a specific interaction, however the intensity of the displaced peak revealed that less than 3% of the methacrylate segments present were involved in this process. Naito

*et al.* (228) concluded that miscibility was due to the similarities of the physical properties of the two components. Miscibility is not predicted on the basis of calculated solubility parameters as  $\delta$  values for PMMA and PST are virtually identical.

Poly(2,6-dimethyl 1,4-phenylene oxide) (PPO) although miscible in all proportions with PST has been shown to be completely immiscible with all the ortho and para halogenated poly(styrenes). Copolymers of the various halogenated styrenes do in many cases however form miscible blends with PPO at certain compositions. Table (7.4) gives some examples of such systems reported in the literature. ten Brinke *et al.* (99) have deduced the values of the segmental interaction parameters for a number of these blends principally from the measured phase boundaries. The various  $\chi_{ij}$  values were all positive, providing further justification for the mean field theory. However if the measured interaction parameters are resolved into the component solubility parameters via Hildebrand's relationship the resulting equations are not consistent. Unfortunately group contribution tables do not allow for small structural changes, such as between ortho and para substituted styrenes, so that a true comparison between the predicted and measured range of miscibility is not possible.

The close proximity of the calculated solubility parameters relating to PST and PMMA was referred to earlier with respect to PMMA/SAN blends. It was on account of this apparent similarity in overall dispersion forces that following the relative success of the mean field theory in treating SM/PEPC blends similar experiments were conducted on MA/PEPC blends.

#### 7.4 METHYL METHACRYLATE-CO-METHACRYLONITRILE/POLY(EPICHLOROHYDRIN)

##### BLENDS

PMMA was found to be completely immiscible with PEPC thereby

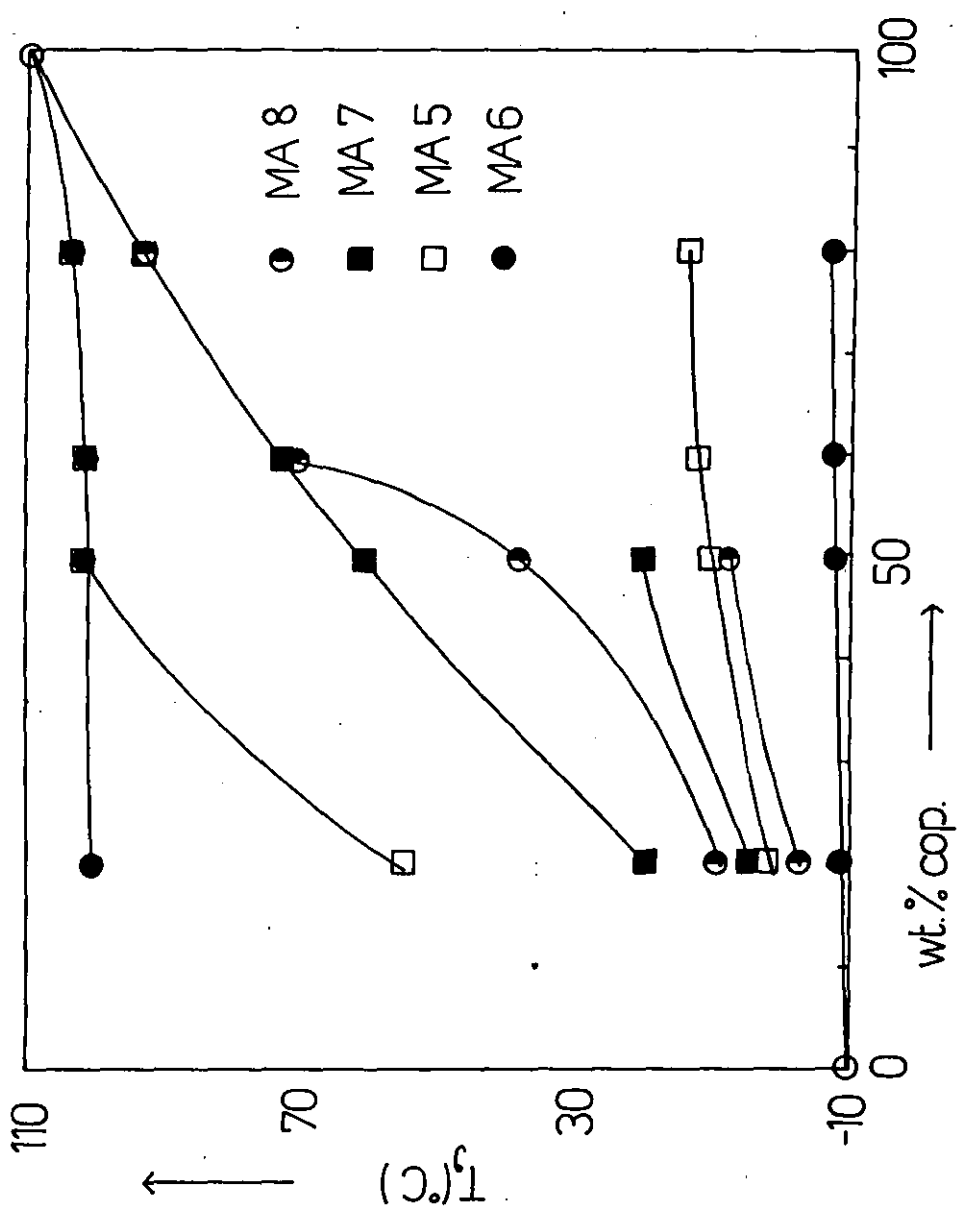
Table 7.4. Random Copolymers of Various Halogenated Styrenes Whose Blends with PPO Have Been Reported

Comonomer 1	Comonomer 2	Range of Copolymer Composition in Which Miscibility Observed	Reference
$\sigma$ -fluorostyrene	p-chlorostyrene	15-74 mole % p-chlorostyrene	(229)
$\sigma$ -fluorostyrene	$\sigma$ -chlorostyrene	15-36 mole % $\sigma$ -chlorostyrene	(229)
p-fluorostyrene	$\sigma$ -chlorostyrene	Immiscible at all compositions	(229)
p-fluorostyrene	p-chlorostyrene	Immiscible at all compositions	(229)
p-fluorostyrene	$\sigma$ -fluorostyrene	10-38 mole % p-fluorostyrene	(230)
$\sigma$ -chlorostyrene	p-chlorostyrene	68-98 mole % $\sigma$ -chlorostyrene	(231)



confirming the result of Petersen *et al.* (171) and providing a system of the same type as SM/PEPC. Copolymers containing  $\geq 55$  mole% MAN formed blends with PEPC which exhibited two distinct glass transition processes whose position in the temperature plane showed no dependence on overall blend composition. The blends were also found to appear translucent leaving no doubt as to their immiscibility. Blends containing MA5 (50 mole% MAN) behaved similarly, the principal differences being the depression of the  $T_g$ 's of both phases at high overall PEPC contents as shown in Figure (7.10) and the tendency of the blends to appear optically homogeneous at copolymer contents above 60 wt.%. The cause of the latter property change can only be due to a reduction in size of the disperse copolymer poor phase, as phase composition is virtually constant in the range over which blends pass from being translucent to transparent, meaning that in this range the refractive index difference is also constant. The observed immiscibility of PMMA with PEPC indicates that a range of MMA rich copolymer compositions will exist which form blends containing phases of virtually the pure components. This region was not identified experimentally but must occur at copolymer contents  $< 20$  mole% MAN. Copolymers MA8 and MA7 containing 20-25 mole% MAN formed blends with PEPC which when measured mechanically revealed the presence of two phases at compositions containing  $\leq 50$  wt.% copolymer. Although the loss tangent peaks associated with the two processes tend to overlap,  $\Delta T_g$  is such that the respective maximum values can be deduced. At higher copolymer contents a single transition process was observed whose composition dependence followed that of the copolymer rich phase observed at lower copolymer loadings (Figure (7.10)). The thermal analysis data generally reflected these trends, although at high copolymer concentrations there was some depression of the base line of the thermogram at the low temperature side

Figure (7.10)  
 Composition Dependence of  $T_g$  for Blends of  
 Various MA Copolymers with PEPC

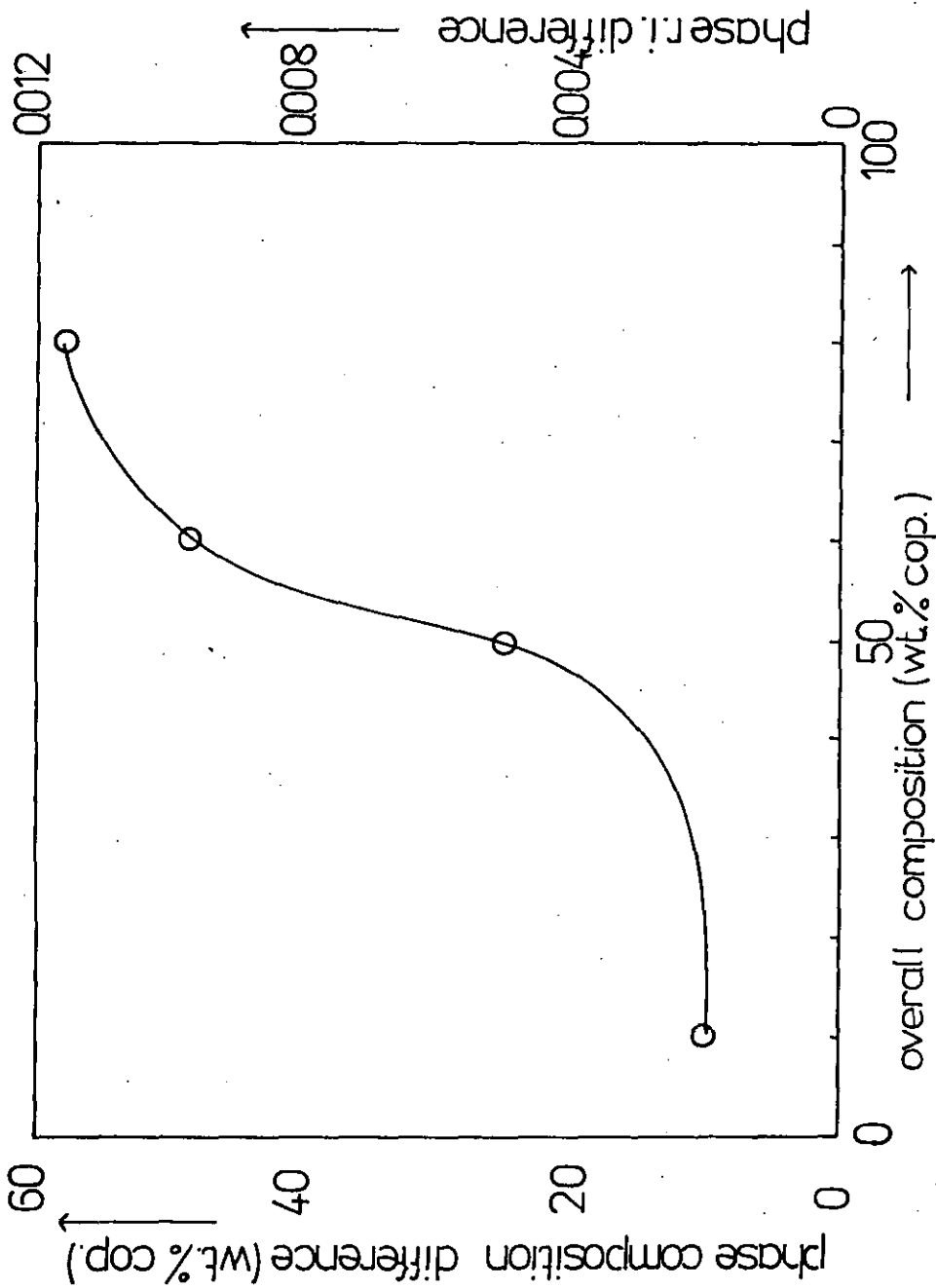


of the principal transition. In this instance the non-appearance of the copolymer poor transition cannot be justified in terms of peak overlap as  $\Delta T_g$ , based on the measurements at 20 and 50 wt.% copolymer, tends to increase with overall copolymer composition. At low  $\Delta T_g$  values the difference in composition of the two phases was such that their refractive indices differed by only 0.002, consequently irrespective of phase size the blends would appear transparent. However, as the difference in composition increases so does the mismatch between their refractive indices, and on the basis of the observed variations in phase composition with overall composition one would expect the contrast to be sufficient for visibility at overall compositions above about 50 wt.% copolymer. This is shown in Figure (7.11) and it is assumed, based upon the observations made on the homopolymer blends discussed in the previous chapter, that a refractive index difference greater than 0.005 is sufficient to show up phase separation given that the disperse phase is larger than the limit of detection. The observed transparency of the blends at all compositions tends to suggest therefore that although it seems probable that a copolymer poor phase does exist at high overall copolymer concentrations, the dimensions of this phase are such that it does not exhibit a clear glass transition process. This explains the thermal analysis observations and suggests that these phases give rise to such small variations in  $\tan \delta$  that the process is obscured by the low temperature tail of the peak due to the relaxation of the dominant phase.

Blends containing copolymers MA8 and MA7 with PEPC can be seen to exhibit composition dependent partial miscibility. The composition of both phases appears to change with the relative proportion of the blend constituents in the manner found for blends of PEPC with certain SM copolymers. Explanation of the observed behaviour in terms of non-

Figure(7.11)

Variation in the Differences in Phase Composition and Phase Refractive Index for MA8 /PEPC with Overall Composition



equilibrium phase separation is similarly applicable to this system.

At copolymer compositions between those giving rise to the above partially miscible blends and the previously discussed immiscible blends, a third type of miscibility behaviour was observed. Blends of MA3 and MA4 displayed transparent films and a single composition dependent glass transition temperature. Examination of the transition breadths reveals that MA4 blends fulfil the criterion for miscibility whilst MA3 blends display transitions that are rather more diffuse. The dependence of  $T_g$  on the overall blend concentration (Figure (5.77)) is such that it follows the Fox equation except at the extremes of concentration in MA4 blends, but shows larger deviations over a wider concentration range in MA3 blends. MA3/PEPC blends appear to demonstrate the properties of microheterogeneous quasi-binary mixtures whilst MA4/PEPC blends have properties associated with homogeneity, at least on the segmental level associated with the glass transition process.

The dielectric measurements made on this system follow a similar pattern to that found for SM/PEPC blends. MA2/PEPC previously classified as immiscible displayed loss tangent peaks at temperatures shifted only slightly upfield from those observed for PEPC at corresponding frequencies. MA5/PEPC had  $\tan \delta$  maxima at temperatures some 10°C higher than MA2/PEPC which reflects the differences observed by both DTA and DMTA between the blends. No clear transition was manifest in the apparently miscible MA4/PEPC sample due to the interference of conductivity processes. There is however no indication of the presence of a PEPC rich phase in this blend which confirms the greater homogeneity of this mixture. Furthermore it does not appear that the preparation of the sample has, due to phase separation, increased the heterogeneity as was found for SM3/PEPC.

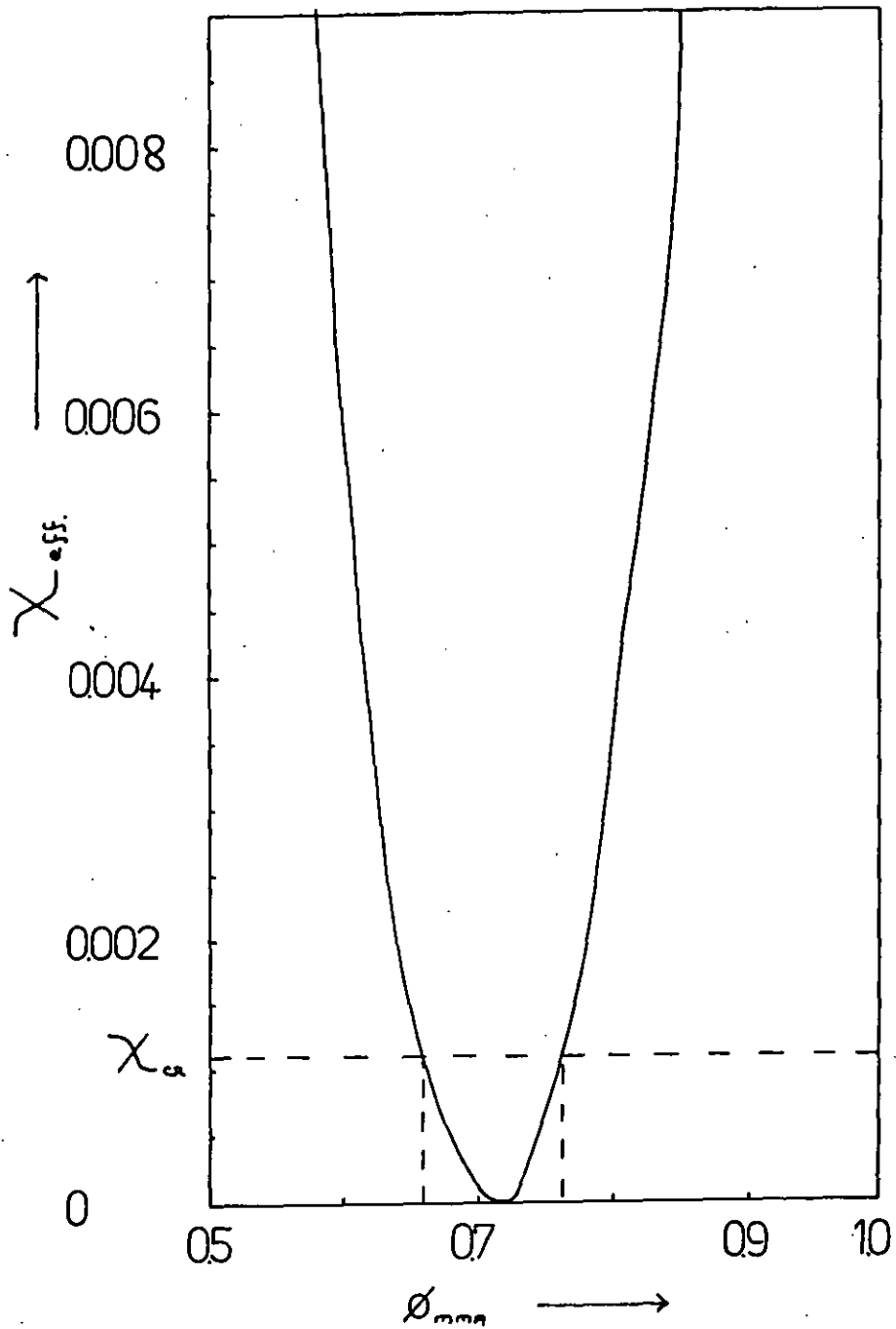
The variation of the effective interaction parameter with copolymer

composition determined using the appropriate form of equation (7.2) is shown in Figure (7.12).  $X_{\text{eff}}$  can be seen to vary in an almost identical fashion to that calculated for the SM/PEPC system. This is due to the proximity of the calculated solubility parameters for PST and PMMA ( $\delta_{\text{PST}} = 9.36$   $\delta_{\text{PMMA}} = 9.31$  cal<sup>1/2</sup>/cm.<sup>3/2</sup>).  $X_{\text{CR}}$ , the calculated limiting value of  $X_{\text{eff}}$  for miscibility, is however greater for MA/PEPC as the copolymers are of lower molecular weight than the SM series. Figure (7.12) shows that miscibility in the system is predicted in the range  $0.66 \leq \phi_{\text{MMA}} \leq 0.76$  which corresponds to 32-42 mole% MAN. This concentration range embraces copolymers MA4 and MA3 which formed blends with PEPC exhibiting miscibility and microheterogeneity respectively. This correspondence between the predicted and measured range of miscibility indicates that dispersion forces are the dominant factor in determining miscibility in this system and that solubility parameters are appropriate measures of the relative contribution made by each constituent. The disparity between the calculated and experimentally determined range of miscibility in SM/PEPC blends cannot be due to the  $\delta$  values of PMAN and PEPC on the basis of the previous statement. If one assumes therefore that  $\delta_{\text{PST}}$  is in error, the true value can be found by substitution of a copolymer concentration giving rise to a miscible blend into equation (7.2), given that  $X_{\text{eff}} < X_{\text{CR}}$ . This operation reveals that  $\delta_{\text{PST}} \approx 8.6$  cal<sup>1/2</sup>/cm.<sup>3/2</sup> as opposed to the value of 9.36 indicated by group contribution tables.

The inability of solubility parameters in the context of the mean-field approach to explain the observed miscibility in blends of PMMA/SAN was mentioned in section (7.3). However, using the calculated  $\delta$  values for PMMA and PAN together with the  $\delta_{\text{PST}}$  value inferred above,  $X_{\text{eff}}$  falls to zero at a copolymer composition of 20 wt.% AN. This is in excellent agreement with the results of Schmitt<sup>(227)</sup> who found that

Figure(7.12)

Variation of  $\chi_{eff}$  with Copolymer Composition for the System MA/PEPC



the most miscible blends were formed by copolymers containing 19 wt.% AN. Furthermore Naito *et al.*<sup>(228)</sup> showed that specific interactions were present in this system to such a small degree that it is most appropriate for miscibility to be discussed in terms of overall dispersion forces.

The range of copolymer compositions giving rise to miscible blends in the system poly(vinyl chloride)/butadiene-co-acrylonitrile calculated using the above approach corresponds to that found by Zakrzewski<sup>(200)</sup>. He attributed the miscibility determined using torsion pendulum measurements to a strong specific interaction between PVC and the acrylonitrile segments of the copolymer. In view of the success of the mean field theory in describing the behaviour of this blend this explanation appears extremely unlikely.

The mean-field theory does seem to break down in the case of blends of PVC with ethylene-co-vinyl acetate which was included in a listing of miscible systems by Olabisi *et al.*<sup>(10)</sup>. Application of equation (7.2) indicates that the minimum value of  $\chi_{\text{eff}}$  is attained when the copolymer contains less than 10 wt.% ethylene, whilst miscibility is claimed at a content of 35 wt.% ethylene in the aforementioned text. However examination of the original literature does provide some explanation of this inconsistency. Hammer<sup>(178)</sup> first reported the presence of single transition peak in the blend at copolymer contents of 30-35 wt.% ethylene as measured by torsion pendulum, but did not include any data on the respective transition widths of the components and the blend. In a later study Shur and Ranby<sup>(232,233)</sup> found that in this composition range there were in fact two transitions present. One corresponded to a mixed phase of copolymer and homopolymer, whilst the other was due to PVC alone. They also found that the proportion of PVC in the mixed phase could be increased by raising the temperature



at which the components were milled together, thereby increasing the break down of the particulate structure of the PVC. It is therefore apparent that at 30-35 wt.% ethylene the blend formed is only partially miscible and as complete immiscibility has been found at a copolymer content of 55 wt.% ethylene<sup>(178,234)</sup> it would seem that a truly miscible mixture would be formed at ethylene concentrations < 30 wt.%.

#### 7.5 GENERAL ASPECTS OF THE BEHAVIOUR OF COPOLYMER/HOMOPOLYMER BLENDS

The miscibility behaviour of the two homopolymer/copolymer systems which did not exhibit specific segmental interactions has been shown to correspond semi-quantitatively with predictions made on the basis of the mean field theory. Calculation of the various segmental interaction parameters on the basis of solubility parameters proved to be most appropriate to blends of MA copolymers with PEPC. Furthermore it was shown that the behaviour of PVC/butadiene-co-acrylonitrile could be similarly explained. The inability of the theory to properly account for the observed range of miscibility in blends of SAN/PMMA and SM/PEPC could be considered as being indicative of the limitations of the overall approach. The disparity between the calculated and observed behaviour increased as the cohesive energy densities (C.E.D.) of the copolymer segments diverged. This was shown by the fact that SM copolymers ( $\delta_{MAN} - \delta_{ST} = 1.81 \text{ cal}^{1/2}/\text{cm}^{3/2}$ ) were predicted to achieve miscibility with PEPC at a copolymer composition 10 mole% below that observed whilst SAN copolymers were ( $\delta_{AN} - \delta_{ST} = 3.2 \text{ cal}^{1/2}/\text{cm}^{3/2}$ ) not predicted to form any miscible mixtures with PMMA. The empirical observation that a reduction in  $\delta_{ST}$  improved the correspondence between the measured and predicted behaviour tends to imply that the C.E.D. of styrene is influenced in its copolymers by the C.E.D. of the other segment. The

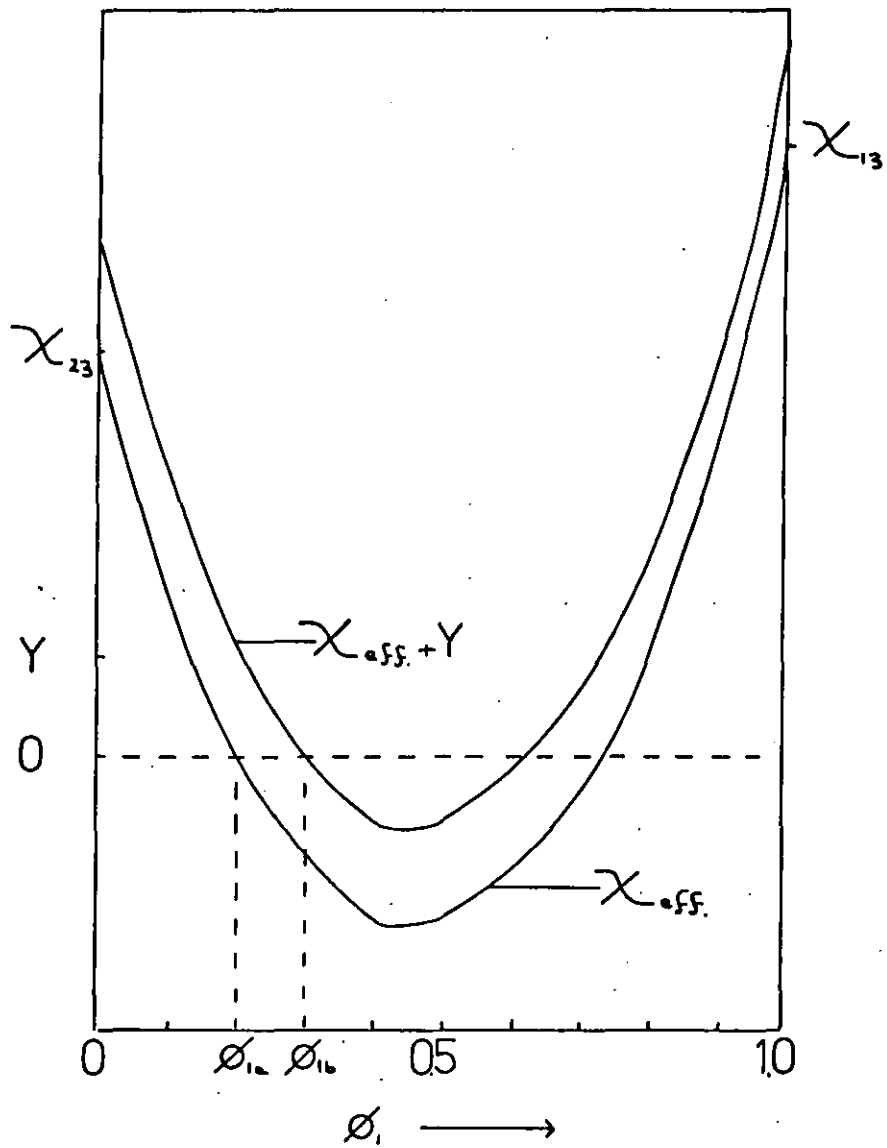
very high C.E.D. values of both acrylonitrile and methacrylonitrile would thus maximise this effect. One cannot however envisage a molecular process which could account for this behaviour. It was mentioned in section (2.3) that miscibility depends on the free volume terms as well as the effective interaction parameter. It has previously been assumed that the influence of the former term was negligible at the temperatures at which the blends were annealed. If this was not the case in the SM and SAN systems the positive contribution of the free volume terms would tend to move the onset of miscibility to higher compositions of the copolymer segment with the larger segmental interaction with the homopolymer. This is illustrated in Figure (7.13) for a system at constant temperature where the limit of miscibility moves from  $\phi_{1a}$  to  $\phi_{1b}$  as the free volume contribution increases from 0 to  $Y$ . The hypothesis is concordant with the behaviour of the above systems in that the observed miscibility was found at higher contents of acrylonitrile and methacrylonitrile than predicted.

Application of the concept of an effective interaction parameter being the determinant of miscibility to GMA-co-MMA/PEPC blends indicated that there was a small specific segmental interaction between GMA and epichlorohydrin. The small size of this interaction and the relatively small size of the interaction parameter between the copolymer segments, which tends to decrease  $\chi_{eff}$ , meant that miscibility was expected only at high copolymer contents of GMA. Furthermore the miscibility of PGMA and PEPC and the observed phase separation which resulted from relatively minor changes in the structure of the methacrylate homopolymer corresponds with the small negative value of  $\chi_{GMA/PEPC}$ .

In the homopolymer/copolymer systems not exhibiting specific segmental interactions miscibility can be regarded as being due to the dilution of the repulsive forces between the dissimilar copolymer

Figure (7.13)

Influence of Free Volume Terms ( $\gamma$ ) on the Range of Miscibility



segments by the addition of a homopolymer. The homopolymer of course must interact more favourably with each copolymer segment than they do with each other. If the validity of Hildebrand's relationship between segmental interaction parameters and solubility parameters is assumed, miscibility occurs at copolymer compositions at which the overall cohesive energy densities of the two components are matched. It has been shown that application of this concept can result in the formation of miscible blends at least on a level of mixing corresponding to the glass transition process. However, as miscibility results from an overall balance of forces and not from the alignment of segments of the two species in a regular fashion, as in the case of specific interactions, one would not expect homogeneity to extend to a sub- $T_g$  level. This view can be supported by a number of examples in the literature. Inoue<sup>(235)</sup> examined blends of PVC with acrylonitrile/butadiene copolymers, previously reported as miscible by Zakrzewski<sup>(200)</sup> using techniques sensitive to  $T_g$ , using X-ray Diffraction. He concluded that the blend appeared two-phase by this technique. Matsuo *et al.* performed electron microscopy examinations of the same blend and discovered the presence of microphases whose diameters were in the region of  $100\text{\AA}$ . Similarly McBrierty *et al.*<sup>(236)</sup> found that pulsed N.M.R. measurements indicated the presence of inhomogeneities of the order of  $20\text{-}150\text{\AA}$  in the PMMA/SAN system declared miscible by Naito *et al.*<sup>(228)</sup>

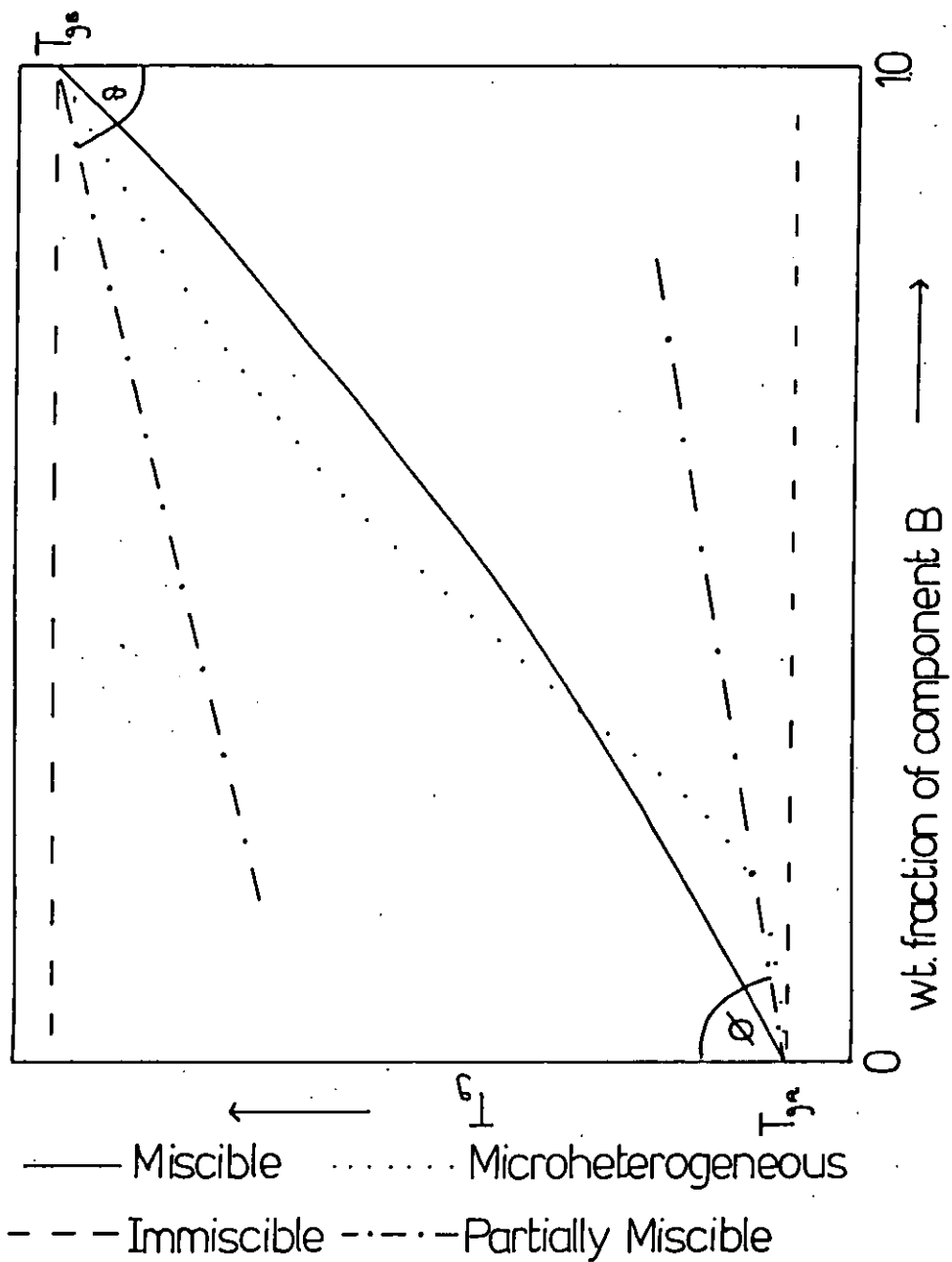
Throughout this study it has been apparent that the miscibility of a two component system can be assessed in many cases by examination of the plot of blend  $T_g(s)$  against overall composition. Immiscible mixtures display essentially two horizontal lines in such a plot, lying close to the  $T_g$ 's of the pure components. As the degree of miscibility rises one or both phases tend to incorporate increasing

amounts of the other component such that the angles  $\phi$  and  $\theta$  in Figure (7.14) decrease. It was generally found in this study that the compositions of both phases in the partially miscible systems varied with overall blend content. Due to the dimensions of the minor phase or the proximity of the two glass transition processes it was found that the  $T_g$ 's of both phases could usually only be detected at intermediate compositions. Both miscible and microheterogeneous blends gave rise to a single transition process. Whilst no system was found whose glass transition behaviour precisely followed the equations of Fox, Gordon-Taylor or Couchman-Karasz, the deviation was found to be somewhat greater in the microheterogeneous mixtures. Nevertheless as pointed out in chapter 6 a more sensitive indicator of microheterogeneity is the deviation of the transition breadth from additivity.

A number of authors have claimed improved correlation between observed and predicted values of  $T_g$  in random copolymers by the use of increasingly complex relationships. These relationships have in turn been applied to blends with the exception of the equations of Couchman and Karasz which were derived specifically. The miscible blends which were found in this work most nearly matched the  $T_g$  dependence corresponding to the Fox equation, further indicating the lack of a generally applicable relationship. A generalised equation would in addition to the terms relating the concentration and  $T_g$  of each component have to contain a factor relating the interaction between unlike segments and the proportion of interacting species.

The tendency of the effective interaction parameter and the free volume contribution to increase with temperature explains the tendency of certain miscible blends to phase separate on heating. PGMA/PEPC mixtures were found to behave in this manner, although the tendency of the system to cross-link made it impossible to establish the

Figure(7.14)  
Possible Variation of  $T_g$  vs. Composition Plots  
with Blend Miscibility



equilibrium cloud-point curve. Miscible SM/PEPC blends measured in the form of thin films appeared to remain homogeneous up to 200°C, although there was some indication of the formation of a PEPC rich phase at about 180°C when the sample size was increased. In the miscible MA/PEPC blend there was no such indication of heterogeneity at elevated temperatures. This difference between the systems provides further evidence that at equivalent temperatures the free volume contribution is larger for SM blends than MA blends.

It was shown in chapter 6 that the dependence of phase composition on overall concentration in partially miscible blends has been well established in the literature. The phenomenon has not received any explanation however. Whilst the hypothesis of non-equilibrium phase separation does appear to explain the observed properties of such mixtures, the behaviour of immiscible mixtures is apparently anomalous. In immiscible blends there seems to be no kinetic block to phase separation and it is only phase volume and not phase composition which varies with concentration. This apparent inconsistency can be explained however when one recalls that the blends were initially cast from solution. The initial solution concentration was of the order of 2% (by weight) and as solvent evaporated thus concentration naturally increased. The casting solution, when prepared, appeared homogeneous in all cases, however Peterson<sup>(189)</sup> observed phase separation in solutions containing PST/PEPC and PMMA/PEPC at overall polymer concentrations of 20%. At this concentration even at ambient temperature the species would not be lacking in mobility so that the equilibrium phase relationship was formed very early on in the casting process in immiscible systems. In partially miscible systems the mutual antagonism between the components was greatly reduced so that the ternary solution remained homogeneous at much higher overall concentrations. If the glass

transition temperature of the ternary mixture lay above the casting temperature, at the solution concentration at which phase separation started then there would be insufficient mobility for the mixture to achieve equilibrium. Upon annealing at higher temperatures ( $T_a$ ) the bulk of the remaining solvent would be lost rapidly so that the initial concentration of the blend at  $T_a$  would correspond quite closely to that of the initial relative concentration of the two components in solution. Non-equilibrium phase separation could then occur over time as indicated previously.

#### 7.6 SUMMARY

It was shown in chapter 2 that the Equation of State Theory provides a theoretical basis for the observed behaviour of polymer blends. However it does not provide a practical tool for predicting the behaviour of quasi-binary polymer systems even when the equation of state parameters for the two components are known.

The treatment of homopolymer blends by the simple solubility parameter approach has been shown to be similarly inadequate when a small specific interaction occurs between the species. As the vast majority of miscible homopolymer systems owe their relative homogeneity to the presence of a specific interaction between the species, the approach is fundamentally flawed as a predictive tool. However in the realm of homopolymer/random copolymer blends the use of solubility parameters has proved useful in the construction of miscible systems. Furthermore in the context of the mean field approach, miscibility limits can be predicted to a reasonable degree of accuracy. This is particularly so when the free volume terms are relatively insignificant at the temperature of phase formation.

A non-equilibrium phase separation process has been proposed to



account for the phenomenon of composition dependent partial miscibility. This type of behaviour has been observed both in this work and in the literature on polymer blends. Furthermore the established criterion for miscibility of a single, composition dependent glass transition has been shown to be necessary but not sufficient. Data on the breadths of the transitions is also required, across the complete composition range, to make a correct classification of blend miscibility.

## REFERENCES

- 1) Emmett, R. A., *Ind. Eng. Chem.*, 36, 730 (1944).
- 2) Pittenger, G. E. and Cohan, F., *Mod. Plast.*, 25, 81 (1947).
- 3) Cizek, E. P., U.S. Patent, 3, 383, 435 (1968).
- 4) Kaplan, D. S., *J. Appl. Pol. Sci.*, 20, 2615 (1976).
- 5) Huelch, V., Thomas, D. A. and Sperling, L. H., *Macromols.*, 5, 340 (1972).
- 6) Matsuo, M., Nozaki, C. and Jyo, Y., *Pol. Eng. Sci.*, 9, 197 (1969).
- 7) Rosen, S. L., *Pol. Eng. Sci.*, 7, 115 (1967).
- 8) Bohn, L. in "Polymer Handbook", 2nd Edition, Wiley, N.Y. (1975).
- 9) Paul, D. R. and Newman, S., "Polymer Blends, Vol. 1", Academic, N.Y. (1978).
- 10) Olabisi, O., Robeson, L. M. and Shaw, M. T., "Polymer-Polymer Miscibility", Academic, N.Y. (1979).
- 11) Koningsveld, R., Ph.D. Thesis, Leiden (1967).
- 12) Coleman, M. M. *et al.*, *Polymer*, 24, 1410 (1983).
- 13) Cruz, C. A., Barlow, J. W. and Paul, D. R., *Macromols.*, 12, 726 (1979).
- 14) Walsh, D. J. and Zhikuan, C., *Eur. Pol. J.*, 19, 519 (1983).
- 16) Flory, P. J., *J. Chem. Phys.*, 10, 51 (1942).
- 17) Flory, P. J., *J. Chem. Phys.*, 12, 425 (1944).
- 18) Flory, P. J., "Principles of Polymer Chemistry", Cornell University, N.Y. (1953).
- 19) Huggins, M. L., *Ann. N.Y. Acad. Sci.*, 41, 1 (1942).
- 20) Huggins, M. L., "Physical Chemistry of High Polymers", Wiley, N.Y. (1958).
- 21) Flory, P. J., Orwoll, R. A. and Vrij, A., *J. Am. Chem. Soc.*, 86, 3515 (1964).
- 22) Flory, P. J., *J. Am. Chem. Soc.*, 87, 1833 (1965).
- 23) Eichinger, B. E. and Flory, P. J., *Trans. Faraday Soc.*, 64, 2035 (1968).
- 24) Flory, P. J., *Discuss. Faraday Soc.*, 49, 7 (1970).

- 25) McMaster, L. P., *Macromols.*, 6, 760 (1973).
- 26) Bank, M., Leffingwell, J. and Thies, C., *J. Pol. Sci., A-2*, 10, 1097 (1972).
- 27) Wagner, E. and Robeson, L. M., *Rubb. Chem. Tech.*, 43, 1129 (1970).
- 28) Bohn, L., *Adv. Chem. Ser.*, 142, 66 (1975).
- 29) Dearin, R. D. and Crugnola, A. M., *Adv. Chem. Ser.*, 154, 22 (1976).
- 30) Noel, O. F. and Carley, J. F., *Pol. Eng. Sci.*, 15, 117 (1975).
- 31) Corish, P. J. and Powell, B. D., *Rubb. Chem. Tech.*, 47, 481 (1974).
- 32) Robeson, L. M., *Pol. Eng. Sci.*, 24, 587 (1984).
- 33) Battaerd, H. A., *J. Pol. Sci., C*, 49, 149 (1975).
- 34) Eastmond, G. C., *Pol. Eng. Sci.*, 24, 541 (1984).
- 35) Scott, R. L., *J. Chem. Phys.*, 17, 279 (1949).
- 36) Tompa, H., *Trans. Faraday Soc.*, 45, 1142 (1949).
- 37) van der Waals, J. D. and Kohnstamm, P. L., "Lehrbuch der Thermodynamik, Vol. 2", Barth, Leipzig (1912).
- 38) Guggenheim, E. A., *Trans. Faraday Soc.*, 44, 1007 (1948).
- 39) Maron, S. H., *J. Pol. Sci.*, 38, 329 (1959).
- 40) Miller, A. R., *Proc. Camb. Phil. Soc.*, 39, 54 (1943).
- 41) Orr, W. J., *Trans. Faraday Soc.*, 40, 320 (1944).
- 42) Guggenheim, E. A., *Proc. Royal Soc., A*, 183, 203 (1944).
- 43) Koningsveld, R., *Br. Pol. J.*, 7, 435 (1975).
- 44) Koningsveld, R., Kleintjens, L. A. and Schoffeleers, H. M., *Pure Appl. Chem.*, 39, 1 (1974).
- 45) Powers, P. O., *Pol. Prep. Am. Chem. Soc. Div. Pol. Chem.*, 13, 528 (1973).
- 46) Koningsveld, R. and Kleintjens, L. A., *Pure Appl. Chem. Macromol. Suppl.*, 8, 197 (1973).
- 47) Schmitt, B. J., *Br. Pol. J.*, 6, 181 (1974).
- 48) Nishi, T. and Kwei, T. K., *Polymer*, 16, 285 (1975).
- 49) Solc, K., "Polymer Compatibility and Incompatibility", Harwood, N.Y. (1982).
- 50) Allen, G., Gee, G. and Nicholson, J. P., *Polymer*, 2, 8 (1961).

- 51) McIntyre, D., Rounds, M. and Campos-Lopez, E., Pol. Prep. Am. Chem. Soc. Div. Pol. Chem., 10, 531 (1969).
- 52) Koningsveld, R. and Kleintjens, L. A., Br. Pol. J., 9, 212 (1977).
- 53) Staverman, A. J., Rec. Trav. Chem., 56, 885 (1937).
- 54) Huggins, M. L., J. Phys. Chem., 74, 371 (1970).
- 55) Huggins, M. L., J. Phys. Chem., 75, 1255 (1971).
- 56) Koningsveld, R., Adv. Pol. Sci., 7, 1 (1970).
- 57) Roe, R. J. et al., Macromols., 17, 189 (1984).
- 58) Bernstein, R. E., Cruz, C. A., Paul, D. R. and Barlow, J. W., Macromols., 10, 681 (1977).
- 59) ten Brinke, G., Eshuis, A., Roerdink, E. and Challa, G., Macromols., 14, 867 (1981).
- 60) Jager, H. et al., Pol. Comm., 24, 290 (1983).
- 61) Zhikuan, C. and Ruona, S., Polymer, 24, 1279 (1983).
- 62) Rostami, S. and Walsh, D. J., Macromols., 17, 315 (1984).
- 63) Bank, M. et al., Pol. Prep. Am. Chem. Soc. Div. Pol. Chem., 10, 622 (1969).
- 64) Bank, M., Leffingwell, J. and Thies, C., Macromols., 4, 43 (1971).
- 65) Kwei, T. K., Nishi, T. and Roberts, R. F., Macromols., 7, 667 (1974).
- 66) Nishi, T., Wang, T. T. and Kwei, T. K., Macromols., 8, 227 (1975).
- 68) Nishi, T., J. Macromol. Sci., B, 17, 517 (1980).
- 69) Robard, A., Patterson, D. and Delmas, G., Macromols., 10, 706 (1977).
- 70) Robard, A. and Patterson, D., Macromols., 10, 1021 (1977).
- 71) Su, C. S. and Patterson, D., Macromols., 10, 708 (1978).
- 72) Hourston, D. J. and Hughes, I. D., Polymer, 19, 1181 (1978).
- 73) Reich, S. and Gordon, J. M., J. Pol. Sci., A-2, 17, 371 (1979).
- 74) Reich, S. and Cohen, Y., J. Pol. Sci., A-2, 19, 1255 (1981).
- 75) Davis, D. D. and Kwei, T. K., J. Pol. Sci., A-2, 18, 2337 (1980).
- 76) Gelles, R. and Frank, C. W., Macromols., 16, 1448 (1983).
- 77) Sanchez, I. C. and Lacombe, R. H., J. Phys. Chem., 80, 2352, 2568 (1976).

- 78) Sanchez, I. C. and Lacombe, R. H., *Macromols.*, 11, 1145 (1978).
- 79) Sanchez, I. C., *J. Macromol. Sci.*, B, 17, 565 (1980).
- 80) Prigogine, I., "The Molecular Theory of Solutions", North Holland, Amsterdam (1957).
- 81) Hildebrand, J. H., Prausnitz, J. M. and Scott, R. L., "Regular and Related Solutions", Van Nostrand, N.Y. (1970).
- 82) Lin, P. H., Ph.D. Thesis, Washington (1970).
- 83) Koningsveld, R., Chermin, H. and Gordon, M., *Proc. Royal Soc., A*, 319, 331 (1970).
- 84) Hocker, H., Blake, G. J. and Flory, P. J., *Trans. Faraday Soc.*, 67, 2251 (1971).
- 85) Olabisi, O., *Macromols.*, 8, 316 (1975).
- 86) Bondi, A., *J. Phys. Chem.*, 70, 530 (1966).
- 87) Bondi, A., *J. Phys. Chem.*, 68, 441 (1964).
- 90) Roerdink, E. and Challa, G., *Polymer*, 19, 173 (1978).
- 91) Roerdink, E. and Challa, G., *Polymer*, 21, 509, 1161 (1980).
- 92) Zhikuan, C., Ruona, S., Walsh, D. J. and Higgins, J. S., *Polymer*, 24, 263 (1983).
- 93) Zhikuan, C. and Walsh, D. J., *Makromol. Chem.*, 184, 1459 (1983).
- 95) Patterson, D. and Robard, A., *Macromols.*, 11, 690 (1978).
- 97) Doubé, P. and Walsh, D. J., *Polymer*, 20, 1115 (1975).
- 98) Kambour, R. P., Bendler, J. T. and Bopp, R. C., *Macromols.*, 16, 753 (1983).
- 99) ten Brinke, G., Karasz, F. E. and MacKnight, W. J., *Macromols.*, 16, 1827 (1983).
- 100) Paul, D. R. and Barlow, J. W., *Polymer*, 25, 487 (1984).
- 101) Stein, V. D. J., Jung, R. H., Illers, K. H. and Hendus, H., *Ang. Makromol. Chem.*, 36, 89 (1974).
- 102) Chious, J. S., Paul, D. R. and Barlow, J. W., *Polymer*, 23, 1543 (1982).
- 103) Alexandrovitch, P. R., Karasz, F. E. and MacKnight, W. J., *Polymer*, 18, 1022 (1977).
- 104) MacKnight, W. J. *et al.*, *Thermochim. Acta*, 54, 349 (1982).
- 105) Hildebrand, J. H. and Scott, R. L., "The Solubility of Non-Electrolytes", Reinhold, N.Y. (1949).

- 106) Scatchard, G., Chem. Revs., 8, 32 (1931).
- 107) Bohn, L., Rubb. Chem. Tech., 41, 495 (1968).
- 108) Di Benedetto, A. T., J. Pol. Sci., A, 1, 3459 (1963).
- 109) Feodors, R. F., Pol. Eng. Sci., 14, 147 (1974).
- 110) Hayes, R. A., J. Appl. Pol. Sci., 18, 61 (1961).
- 111) van Krevelen, D. W., "Properties of Polymers", Elsevier, Amsterdam (1976).
- 112) Small, P. A., J. Appl. Chem., 3, 71 (1953).
- 113) Hoy, K. L., J. Paint Tech., 42, 76 (1970).
- 114) Krause, S., J. Macromol. Sci., C, 7, 251 (1972).
- 115) Haward, R. N., "The Physics of Glassy Polymers", Applied Science, London (1973).
- 116) Ledwith, A. and North, A., "Molecular Behaviour and the Development of Polymer Materials", Chapman and Hall, London (1975).
- 117) Bueche, F., "Physical Properties of Polymers", Wiley, N.Y. (1962).
- 118) Ferry, J. D., "Viscoelastic Properties of Polymers", Wiley, N.Y. (1961).
- 119) Fox, T. G. and Flory, P. J., J. Am. Chem. Soc., 70, 2384 (1948).
- 120) Fox, T. G. and Flory, P. J., J. Appl. Phys., 21, 581 (1950).
- 121) Doolittle, A. K., J. Appl. Phys., 22, 1471 (1951).
- 122) Doolittle, A. K., J. Appl. Phys., 23, 236 (1952).
- 123) Williams, M. L., Landel, R. F. and Ferry, J. D., J. Am. Chem. Soc., 77, 3701 (1955).
- 124) Kauzmann, W., Chem. Rev., 43, 219 (1948).
- 125) Gibbs, J. H., J. Chem. Phys., 25, 185 (1956).
- 126) Gibbs, J. H. and DiMarzio, E. A., J. Chem. Phys., 28, 373 (1958).
- 127) Gibbs, J. H. and DiMarzio, E. A., J. Pol. Sci., A, 1, 1417 (1963).
- 128) Gibbs, J. H. and DiMarzio, E. A., J. Res. Nat. Bur. Stds., 68A, 611 (1964).
- 129) Adam, G. and Gibbs, J. H., J. Chem. Phys., 43, 139 (1965).
- 130) Nielsen, L., "Mechanical Properties of Polymers", Reinhold, N.Y. (1962).

- 131) Nielsen, L., J. Macromol. Sci., C, 3, 69 (1969).
- 132) Nielsen, L., "Mechanical Properties of Polymers and Composites", Marcel Dekker, N.Y. (1974).
- 133) Wood, L. A., J. Pol. Sci., 28, 319 (1958).
- 134) Gordon, M. and Taylor, J. S., J. Appl. Chem., 2, 493 (1952).
- 135) Mandelkern, L., Martin, G. M. and Quinn, F. A., J. Res. Nat. Bur. Stds., 58, 137 (1957).
- 136) Fox, T. G., Bull. Am. Phys. Soc., 1, 123 (1956).
- 137) Kelley, F. N. and Bueche, F., J. Pol. Sci., 50, 549 (1961).
- 138) Gibbs, J. H. and DiMarzio, E. A., J. Pol. Sci., 40, 121 (1959).
- 139) Illers, K. A., Kolloid Z., 190, 16 (1963).
- 140) Kanig, G., Kolloid Z., 190, 1 (1963).
- 141) Johnston, N. W., Pol. Prep. Am. Chem. Soc. Div. Pol. Chem., 10, 609 (1969).
- 142) Johnston, N. W., J. Macromol. Sci., C, 14, 215 (1976).
- 143) Couchman, P. R. and Karasz, F. E., Macromols., 11, 117 (1978).
- 144) Couchman, P. R., Macromols., 11, 1156 (1978).
- 145) Couchman, P. R., Pol. Eng. Sci., 24, 135 (1984).
- 146) Debye, P., "Polar Molecules", Dover, N.Y. (1929).
- 147) Davies, R. A. and Lamb, J., Quart. Revs., 11, 134 (1957).
- 148) Cole, K. S. and Cole, R. H., J. Chem. Phys., 9, 341 (1941).
- 149) Fuoss, R. M. and Kirkwood, J. G., J. Am. Chem. Soc., 63, 385 (1941).
- 150) Davidson, D. W. and Cole, R. H., J. Chem. Phys., 18, 1417 (1950).
- 151) Davidson, D. W. and Cole, R. H., J. Chem. Phys., 19, 1484 (1951).
- 152) Goldstein, M., Macromols., 18, 277 (1985).
- 154) Busch, K. C., J. Macromol. Sci., B, 2, 179 (1968).
- 156) Schatzki, T., J. Pol. Sci., 57, 496 (1962).
- 157) Seitz, F. and Turnbull, D., "Solid State Physics", Academic, N.Y. (1963).
- 158) Hoff, A. W., Robinson, D. W. and Wilbourn, A. H., J. Pol. Sci., 18, 161 (1955).

- 159) Maxwell, J. C., "Electricity and Magnetism", Clarendon, London (1892).
- 160) Wagner, K. W., Arch. Electrotech., 2, 271 (1914).
- 161) Sillars, R. W., Proc. Royal Soc., A, 169, 66 (1939).
- 162) Feldman, D. and Rusu, M., Eur. Pol. J., 10, 41 (1974).
- 163) Akiyama, S., Konatsu, J. and Kaneko, R., Pol. J., 7, 172 (1975).
- 164) Fujimoto, K. and Yoshimiya, N., Rubb. Chem. Tech., 41, 669 (1968).
- 165) MacKnight, W. J., Stoelting, J. and Karasz, F. E., Adv. Chem. Ser., 99, 29 (1971).
- 166) Wetton, R. E., MacKnight, W. J., Fried, J. R. and Karasz, F. E., Macromols., 11, 158 (1978).
- 167) Alexandrovitch, P. S., Karasz, F. E. and MacKnight, W. J., J. Macromol. Sci., B, 17, 501 (1980).
- 168) Ferry, J. D., Fitzgerald, E. R., Johnson, M. F. and Grandine, L. D., J. Appl. Phys., 22, 717 (1951).
- 169) Nielsen, L., J. Am. Chem. Soc., 75, 1435 (1953).
- 170) Wolfe, K., Kunststoffe, 41, 89 (1951).
- 171) Peterson, R. J. et al., Pol. Prep. Am. Chem. Soc. Div. Pol. Chem., 10, 385 (1969).
- 172) Scheider, I. A. and Vasile, C., Eur. Pol. J., 6, 687 (1970).
- 173) Friedman, D. W. and Sperling, L. H., J. Pol. Sci., A, 7, 425 (1969).
- 174) Koleske, J. V. and Lundberg, R. D., J. Pol. Sci., A, 7, 795 (1969).
- 176) Manson, J. A. and Sperling, L. H., "Polymer Blends and Composites", Plenum, N.Y. (1976).
- 177) Koleske, J. V. and Lundberg, R. D., J. Pol. Sci., B, 7, 795 (1969).
- 178) Hammer, C. F., Macromols., 4, 69 (1971).
- 179) Alfrey, T. and Goldfinger, G., J. Chem. Phys., 12, 205 (1944).
- 180) Mayo, F. R. and Lewis, F. M., J. Am. Chem. Soc., 66, 1594 (1944).
- 181) Walling, C., "Free Radicals in Solution", Wiley, N.Y. (1957).
- 182) Fineman, M. and Ross, S. D., J. Pol. Sci., 5, 259 (1950).
- 183) Kelen, T. and Tudos, F., J. Macromol. Sci., A, 9, 1 (1975).
- 184) Kennedy, J., Kelen, T. and Tudos, F., J. Pol. Sci., A-1, 13, 2277 (1975).
- 185) Randall, J. C., "Polymer Sequence Determination", Academic, N.Y. (1977).



- 186) Harrison, E., Ph.D. Thesis, Loughborough (1984).
- 187) Williams, P. W., Unpublished Results.
- 188) Gashgari, M. A. and Frank, C. W., *Macromols.*, 14, 1558 (1981).
- 189) Peterson, R. J., Corneliussen, R. D. and Rozelle, L. T., *Pol. Prep. Am. Chem. Soc. Div. Pol. Chem.*, 10, 385 (1969).
- 190) Fried, J. R., Lai, S. Y., Kleiner, L. W. and Wheeler, M. E., *J. Appl. Pol. Sci.*, 27, 2869 (1982).
- 191) Fried, J. R. and Hanna, G. A., *Pol. Eng. Sci.*, 22, 705 (1982).
- 192) Xie, S., MacKnight, W. J. and Karasz, F. E., *J. Appl. Pol. Sci.*, 29, 2679 (1984).
- 193) Wang, C. B. and Cooper, S. L., *J. Appl. Pol. Sci.*, 26, 2989 (1981).
- 194) Savard, S., Levesque, D. and Prud'Homme, R. E., *J. Appl. Pol. Sci.*, 23, 1943 (1979).
- 195) Hubbell, D. S. and Cooper, S. L., *J. Appl. Pol. Sci.*, 21, 3035 (1977).
- 196) Gardlund, Z. G., *Adv. Chem. Ser.*, 206, 129 (1984).
- 197) Wahrmond, D. C., Paul, D. R. and Barlow, J. W., *J. Appl. Pol. Sci.*, 22, 2155 (1978).
- 198) Kargin, V. A., *J. Pol. Sci., C*, 4, 1601 (1963).
- 199) Bartenev, G. M. and Kongarov, G. S., *Rubb. Chem. Tech.*, 36, 668 (1968).
- 200) Zakrewski, G. A., *Polymer*, 14, 348 (1973).
- 201) Hickman, J. J. and Ikeda, R. M., *J. Pol. Sci., A-2*, 11, 1713 (1973).
- 202) Zlatkevich, L. Y. and Nikolskii, V., *Rubb. Chem. Tech.*, 46, 1210 (1973).
- 203) Fahrenholtz, S. R. and Kwei, T. K., *Macromols.*, 14, 1076 (1981).
- 204) Min, B. Y., Pearce, E. M. and Kwei, T. K., *Pol. Prep. Am. Chem. Soc. Div. Pol. Chem.*, 24, 441 (1983).
- 205) Brydson, J. A., "Rubber Chemistry", Applied Science, London (1978).
- 206) Belorgey, G. and Prud'Homme, R. E., *J. Pol. Sci., A-2*, 20, 191 (1982).
- 207) Jager, H., Vorenkamp, E. and Challa, G., *Pol. Comm.*, 24, 290 (1983).
- 208) McClellan, A. L., "Tables of Experimental Dipole Moments", Freeman, London (1963).
- 209) Brode, G. L. and Koleske, J. V., *J. Macromol. Sci.*, 6, 1109 (1972).

- 210) Robeson, L. M. and McGrath, J. E., *Pol. Eng. Sci.*, 17, 300 (1977).
- 211) Williams, P. W., Unpublished Results.
- 212) Chiou, J. S., Barlow, J. W. and Paul, D. R., *J. Appl. Pol. Sci.*, 30, 1173 (1985).
- 213) D'Alelio, G., Hofman, E. and Strazik, W. F., *J. Macromol. Sci.*, A, 6, 513 (1972).
- 214) Iwakura, Y., Kurosaki, T., Arigu, N. and Ito, T., *Makromol. Chem.*, 97, 128 (1966).
- 215) Sorokin, M. F. *et al.*, *Plast. Massy*, 3, 3 (1963).
- 216) Gluckman, M. S., Kampf, M. J., O'Brien, J. L. and Fox, T. G., *J. Pol. Sci.*, 37, 411 (1959).
- 217) Fordyce, R. G., Chapin, E. C. and Ham, G. E., *J. Am. Chem. Soc.*, 70, 2489 (1948).
- 218) Cameron, G. G., Grant, D. H., Grassie, N., Lamb, J. E. and McNeill, I. C., *J. Pol. Sci.*, 36, 179 (1959).
- 219) Lewis, F. M., Walling, C., Cummings, W., Briggs, E. R. and Wenisch, W. J., *J. Am. Chem. Soc.*, 70, 1527 (1948).
- 220) Young, L. J., *J. Pol. Sci.*, 54, 411 (1961).
- 221) Molau, G. E., *J. Pol. Sci. Pol. Lett.*, 3, 1007 (1965).
- 222) Kollinsky, F. and Markert, G., *Makromol. Chem.*, 121, 117 (1969).
- 223) Zimmt, W. S., *Ind. Eng. Chem. Prod. Res. Dev.*, 18, 91 (1979).
- 224) Shultz, A. R. and Beach, B. M., *Macromols.*, 7, 902 (1974).
- 225) Fried, J. R., Karasz, F. E. and MacKnight, W. J., *Macromols.*, 11, 150 (1978).
- 226) Kambour, R., Bopp, R., Maconnachie, A. and MacKnight, W. J. *Polymer*, 21, 133 (1980).
- 227) Schmitt, B. J., *Angew. Chem.*, 18, 273 (1979).
- 228) Naito, K., Johnson, G. E., Allara, D. L. and Kwei, T. K., *Macromols.*, 11, 1260 (1978).
- 229) Vukovic, R., Kuresevic, V., Segudovic, N., Karasz, F. E. and MacKnight, W. J., *J. Appl. Pol. Sci.*, 28, 1379 (1983).
- 230) Vukovic, R., Karasz, F. E. and MacKnight, W. J., *Polymer*, 24, 529 (1983).
- 231) ten Brinke, G., Karasz, F. E. and MacKnight, W. J., *J. Appl. Pol. Sci.*, 29, 3131 (1984).

- 232) Shur, Y. J. and Ranby, B., J. Appl. Pol. Sci., 19, 1337 (1975).
- 233) Ranby, B., J. Pol. Sci. Pol. Symp., 51, 89 (1975).
- 234) Marcinin, K., Romanov, A. and Pollak, V., J. Appl. Pol. Sci.,  
16, 2239 (1972).
- 235) Inoue, T., Pol. Comm., 25, 148 (1984).
- 236) McBrierty, V. J., Douglass, D. C. and Kwei, T. K., Macromols.,  
11, 1265 (1978).

